Digital computer models for the clinical interpretation of arterial blood pressure and flow.

Bourne, P R

DIGITAL COMPUTER MODELS FOR THE CLINICAL

INTERPRETATION OF ARTERIAL BLOOD PRESSURE AND FLOW

BY

PETER ROBIN BOURNE

CHELSEA COLLEGE

UNIVERSITY OF LONDON

Presented for the degree
of Doctor of Philosophy
of the University of London.

ABSTRACT

Digital computer models for the clinical interpretation of arterial blood pressure and flow

P. R. BOURNE

Simultaneous measurements of arterial blood pressure and flow contain information about the static and dynamic properties of the arteries. These properties can be represented by elements in a model of the circulation which can be adjusted so that the model variables match corresponding measurements in a patient. Then the adjusted elements are an estimate of the arterial properties of the particular individual. The techniques required to implement this method of analysis, using a digital computer, have been examined.

A suitable model was designed and its ability to match patient measurements was compared with that of three published models. From the results it has been possible to show the general effect of differences in model structure and detail on matching accuracy.

A simple algorithm is described which will efficiently match the new model to measured data. It is compared with more complex search methods and shown to be faster and equally accurate.

The new model has been matched to several recordings of femoral artery pressure and ascending aortic flow and the results of this are presented. Some areas of application of the model to clinical research in cardiology have been considered and the particular field of vasodilator therapy is discussed in detail.

CONTENTS

APPENDICES

FIGURES

TABLES

ACKNOWLEDGEMENTS

The experimental work for this research was carried out in the Bioengineering Department of the Rayne Institute, St. Thomas' Hospital. I am grateful to the Research Endowments Committee of St. Thomas' who have supported me financially and to the Rayne Foundation.

I wish to thank the Head of the Bioengineering Department, Mr. T. K. Cowell and my other colleagues for their support and useful discussions on many aspects of this work.

Many members of the staff of the Cardiac Department at St. Thomas' have generously helped and advised me in addition to giving access to their measurement data. In particular Drs. M. M. Webb-Peploe, S. Jenkins, D. Thompson and Miss J. Morice have given me considerable assistance.

I must express special thanks to Dr. R. I. Kitney, my supervisor, for the help and guidance that he has given.

Mrs. J. McNamara has expertly typed the final manuscript and given valuable advice on the general presentation. Finally I must thank my wife, Christine, who in addition to typing the draft manuscript has helped and encouraged me throughout the work.

CHAPTER 1

INTRODUCTION

The role of engineers and physicists, working in the field of physiological measurement in hospitals, has changed significantly over the last ten years. Prior to this, in the 1960's, advances in electronic technology had provided great opportunities for the development of new instrumentation. Much of this work was done in the medical institutions where the clinical needs could be assessed and equipment trials carried out. As a result many instruments and transducers were designed and developed by hospital groups and subsequently produced by industrial companies. During the 1970's commercial firms have established a range of products which satisfy most of the present needs for making routine measurements. In addition, the larger companies now have their own research and development groups able to produce new equipment designs to meet well defined requirements for medical electronic apparatus. Hospital based design is now only necessary in areas where the development of an instrument must evolve with the clinical requirement. Within this new context many hospital groups have turned their attention to the problems of the presentation and further analysis of data that is being routinely produced by commerical instruments. The reducing cost of small digital computers and the general availability of cheap microprocessor based machines, has encouraged an interest in signal analysis.

In 1973 the cardiac department at St. Thomas' hospital purchased a Varian minicomputer to assist with the analysis of measurements made during cardiac catheterisation. The main proposal was to automate

some of the methods of analysis which had previously been carried out manually on recordings made on photographic paper. The intention was to connect the computer directly to the electrical signals produced by the transducer amplifiers, digitise them, and determine the required numerical results. The aim of the work described in this thesis was to examine alternative ways of interpreting the measured data which had not been practical using manual techniques. The specific objective was to investigate methods of analysing simultaneous measurements of arterial blood pressure and flow using mathematical models of the circulation. This approach is particularly relevant because the accurate estimation of physical variables plays an important part in cardiology. The action of the control mechanisms, and the interactive nature of the different elements of the cardiovascular system, makes it difficult to deduce precise physiological values of cardiac or circulation function. Quantities such as mean blood flow or maximum rate of change of pressure are frequently used as diagnostic indicators on the basis of experience with large numbers of patients. The assumed relationships between these quantities and the condition of the circulation are equivalent to a simple cardiovascular model. Much of the information contained in continuous records of blood pressure and flow cannot be extracted by these forms of manual calculation. Computers are likely to be used increasingly to collect and analyse the data from cardiological investigations because of the quantity of data involved. They can greatly help the investigation by providing the results of simple analysis at the time of measurement. These machines also make it possible to develop better methods of analysis using more realistic models of the circulation to provide quantitative values for physiological parameters.

In this research project the techniques required to apply published models of the arterial circulation to the analysis of blood pressure and flow are developed. By the use of simple parameter estimation techniques it has been possible to calculate values for the overall compliance of the major arteries and the inertial effect of the blood; the total peripheral resistance is also determined. These parameters are of importance because they represent the physiological components of the load against which the left ventricle ejects blood. If the ventricle is failing then modification of this load by drugs or other means may assist the heart to perform adequately. At present the most common way of characterising the arterial system is to compute the hydraulic input impedance from simultaneous measurements of aortic pressure and flow. The method of model analysis is complimentary to that of impedance determination, which characterises the load but does not directly reveal the factors which determine it.

Simultaneous measurements of pressure and flow are already being carried out at St. Thomas' on patients who have had heart surgery. In this case only the femoral or radial artery pressure is normally available. There is considerable interest in making both measurements in the ascending aorta to determine the input properties of the arterial system. Some data of this type has been obtained using two separate catheters but routine measurements await the availability of a combined pressure-flow catheter. For this work the femoral pressure results have been used to investigate the design of models and to develop mathematical and computing techniques. A small study illustrating how the method can be used to aid research into the effect of drugs is presented using the ascending aortic pressure recordings. The model developed for this work has also been used to simulate

changes in the arterial system. The results have been compared with published work to test some of the current hypotheses about the changes that take place in arteries in disease states.

CHAPTER 2

THE MEASUREMENT AND ANALYSIS OF ARTERIAL BLOOD PRESSURE AND FLOW

2.1 NORMAL DIAGNOSTIC MEASUREMENTS

Cardiological investigation is mainly carried out to determine what defects are present in a particular heart. A variety of possible conditions will need to be considered. For example, holes in the walls of the heart chambers may prevent the blood circulating correctly. The blood supply to the myocardium may be insufficient, or deficiencies in the past may have permanently damaged the heart muscle. Enlargement (hypertrophy) of the ventricles, especially the left ventricle, can cause obstruction of the inflow and outflow tracts - hypertrophic obstructive cardiomyopathy (HOCM). Valve defects can affect cardiac performance by obstructing flow when they should be open, stenosis, or failing to close properly, incompetence. The heart is controlled by its own conduction pathways and damage to these may cause irregular rhythms which reduce the heart's efficiency.

In summary, there are four principal aspects of heart pathology which can require investigation.

1. Failure of the heart muscle to contract effectively.
2. Mechanical inhibition of the blood flow through the heart by defective valves or hypertrophy.
3. Conduction defects.
4. Shunt blood flow paths.

The main purpose of diagnosis is to decide what treatment may be possible to improve the patient's condition. Some aspects of the investigation will be directly related to decisions about such therapy. In particular the vascular system affects the performance of the heart's pumping function. It may be possible to alter some vascular properties with drugs to optimise the load on a failing heart and improve its performance. Tests on the behaviour of the vasculature, and the effect of specific drugs on it, may therefore be carried out during the diagnostic procedures.

Initial investigation is usually made by non-invasive techniques. Heart sounds may indicate irregularities in ventricular contraction and the flow of blood. These can be examined with the stethoscope and the phonocardiograph. Ultrasound echocardiography may reveal abnormal ventricular wall movement or valve defects. The electrocardiograph (ECG) detects the electric field produced by conduction through the myocardium and can be used to examine a variety of conduction defects.

If these tests show that a serious malfunction may exist, especially one which would require surgical correction, then invasive procedures are normally employed to make more direct and accurate measurements. These commonly involve the insertion of catheters into the blood vessels and heart chambers. They can then be used for the injection of radiopaque dyes to allow X-ray examination of the heart, termed angiocardiography. Catheters are also used for measuring blood pressure, flow, taking blood samples or introducing indicators into the blood flow (Verel and Grainger, 1973). Pressure and flow measurements are the special interest of this project and will be considered in more detail.

By attaching an external transducer to the end of a fluid filled catheter introduced into a blood vessel, it is possible to measure the blood pressure at the tip of the catheter. These techniques were pioneered by Cournand and others in the 1940's and are now routine procedures. Pressure measurements are used to quantify valve defects, in terms of pressure gradients, and the pumping action of the heart chambers.

Mean flow can be estimated by injecting an indicator and measuring its concentration in the blood stream using the Stewart - Hamilton indicator dilution technique (Bloomfield, 1974). Mean aortic flow, termed cardiac output, taken with arterial pressure gives some indication of the load against which the left ventricle pumps. Further examination of left ventricular pressures can provide insight into the contraction efficiency of the ventricle, sometimes termed contractility.

Accurate measurements on the circulation of the living patient are difficult. Cardiac catheterisation, which is employed where precision is considered necessary, is relatively hazardous. Various complications have been reported (Braunwald and Swan, 1968). It is possible inadvertently to knot catheters which requires special techniques to remove them. Guide wires, used to aid the catheter insertion, can be bent, broken or jammed in the end of the catheter. Both catheters and guide wires can damage the heart or the blood vessels. Blood clots can be produced which block blood vessels - thrombosis - or more seriously produce floating particles - emboli - which may lodge in the brain or lung. Irregularities in heart rhythm may be produced by the introduction of catheters into the heart chambers.

Because of these difficulties and hazards there is a great incentive to extract the maximum possible information from a given set of measurement

procedures. Both higher quality measuring instruments and more detailed analysis have their part to play in this. There is equally a reluctance to make extra measurements especially if this involves additional insertion sites for catheters, so that clinical research is often based on a critical analysis of the routine data.

2.2 IMPROVEMENTS IN THE MEASUREMENT OF PRESSURE AND FLOW

Invasive blood pressure measurement is usually made by fitting a strain gauge pressure transducer, connected to an amplifier, to the external end of a fluid filled catheter. This arrangement is limited by the resonant frequency of the catheter-transducer system (Gabe, 1972) which is of the order of 10 - 30Hz. Some increase in the frequency range can be made using semiconductor strain gauge transducers which have a lower compliance. Transducers have been designed which are small enough to fit the end of a catheter (Gauer and Gienapp, 1950), one of the most recent using semiconductor elements (Millar and Baker, 1973). These give a very much higher resonant frequency of up to 1 or 2KHz. Similar miniature transducers can also be used to advantage directly on the end of a needle or catheter. By avoiding the use of a long connecting catheter, which is necessary with larger transducers to get them clear of the insertion site, resonant frequencies up to 100Hz can be achieved.

More recently blood flow has been measured invasively by electromagnetic flowmeters (Patel, Austen and Greenfield, 1964). By encircling a blood vessel with a probe containing two coils and a pair of electrodes it is possible to measure the instantaneous volume flow rate in the vessel. These "cuff" probes can only be applied during surgery when the vessel is exposed. Williams, Barefoot and Shenk (1969) have deve-

loped a flexible cuff probe which is applied to the ascending aorta during open chest surgery and can subsequently be withdrawn through a small hole in the chest wall, in the same way as a chest drain. This procedure enables measurement of aortic blood flow to be made for several days after surgery. Mills (1966) designed an inverted version of the cuff probe which allows the velocity of blood around the outside of the probe to be measured. Mounted in the end of a catheter, the device permits the instantaneous blood velocity to be measured by catheterisation. The frequency response of these electromagnetic flowmeters can be limited to about 15 Hz because of the isolation circuitry required for safety and the small size of the electrical signals.

Cardiologists have recently become interested in analysing simultaneous measurements of arterial pressure and flow so as to characterise the arterial system in ways that are useful clinically (Noble, 1979). The physical principles of this subject have been discussed in detail by McDonald (1974) and others. The following sections will be concerned only with the techniques of input impedance analysis and the use of models.

2.3 STRUCTURE AND PROPERTIES OF THE ARTERIAL SYSTEM

From the diagram of fig. 2.1 it can be seen that the systemic arterial system is a highly irregular branched structure. The individual sections of artery are tapered compliant tubes filled with blood, which is a substantially incompressible fluid. Pressure waves can be propagated through this blood and, at the frequencies of physiological interest, the wavelength is comparable with the length of the arteries. Fig. 2.2 shows the arterial pressure time course at different points

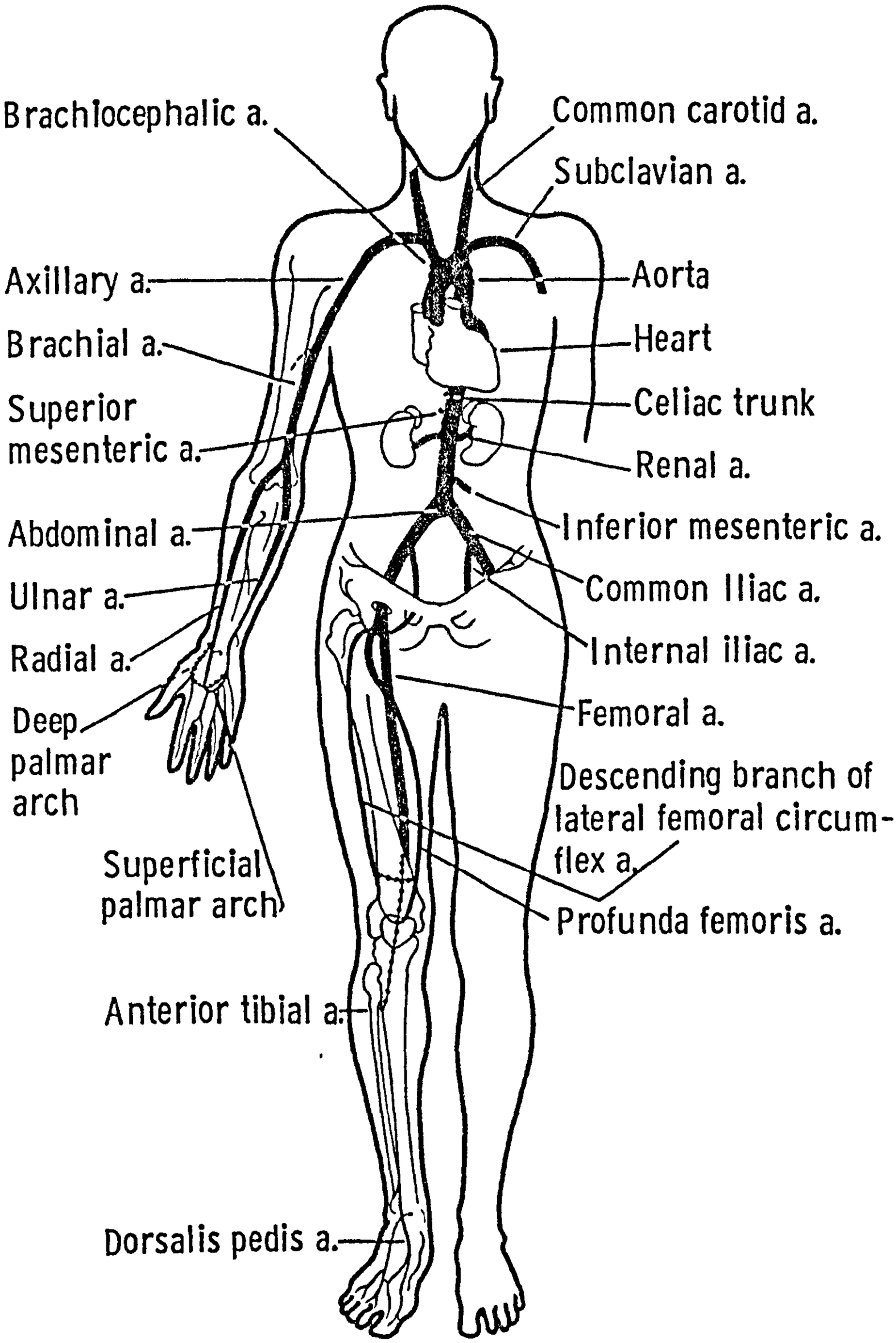

Fig 2.1 MAJOR ARTERIES OF THE BODY

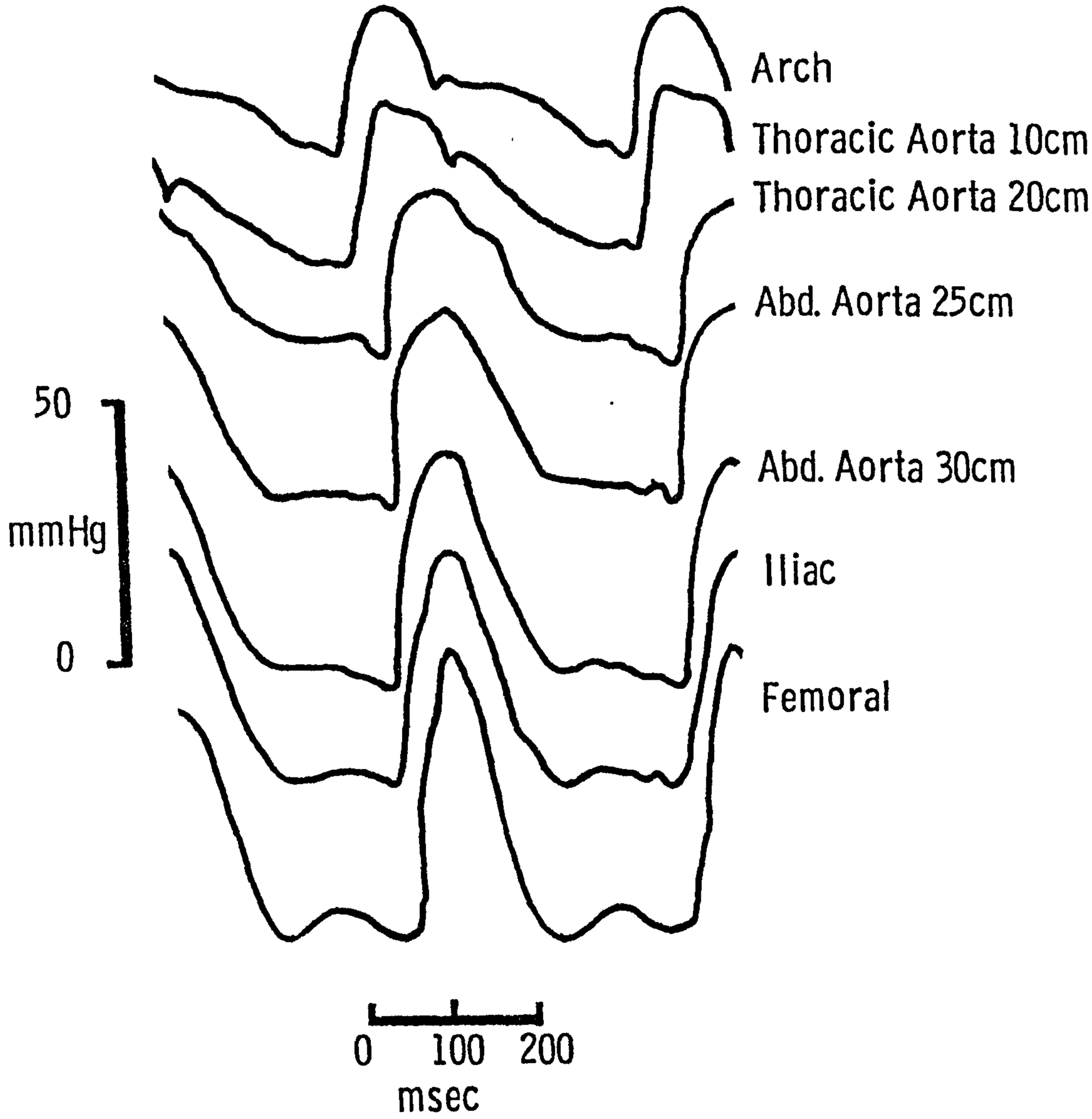

Fig 2.2 CHANGES IN THE ARTERIAL PRESSURE PULSE SHAPE IN THE DOG FROM McDONALD (1974).

along a dog aorta (McDonald, 1974) from which it can be seen that the pulse height of the pressure wave clearly increases towards the periphery. Aortic and femoral artery pressures from a cardiac catheter patient, fig. 2.3, show a similar relationship. The usual explanation of this phenomenon is that it is the result of the reinforcement of the forward travelling pressure wave by waves reflected from the arteriolar beds. This has been argued in detail by McDonald (1974) for the dog who has calculated that the reflecting site is in the region of the pelvic and thigh muscle beds. However Defares and Van der Waal (1969) maintain that reflection effects are small and that pulse amplification can be explained by the effect of geometric and elastic taper of the aorta.

Blood is pumped along the systemic arteries by the pulsating action of the left ventricle. The driving pressure function is not sinusoidal and consists of harmonics mainly in the range 0 - 10 Hz. The frequency spectrum of the ascending aorta and femoral artery pressures in one of the patients studied is shown in fig. 2.4. Pulse amplification is indicated by the increase in the amplitude of the harmonics in the femoral artery.

The compliance of the aorta is the property by which it stores blood during systole and gradually constricts in diastole maintaining blood pressure and flow. The arteries are thick walled tubes and the pressure-volume relationship for them is non linear. However, considering the accuracy with which human circulatory measurements can be made, it is often considered adequate to represent the compliance C as a linear function of pressure P and volume V,

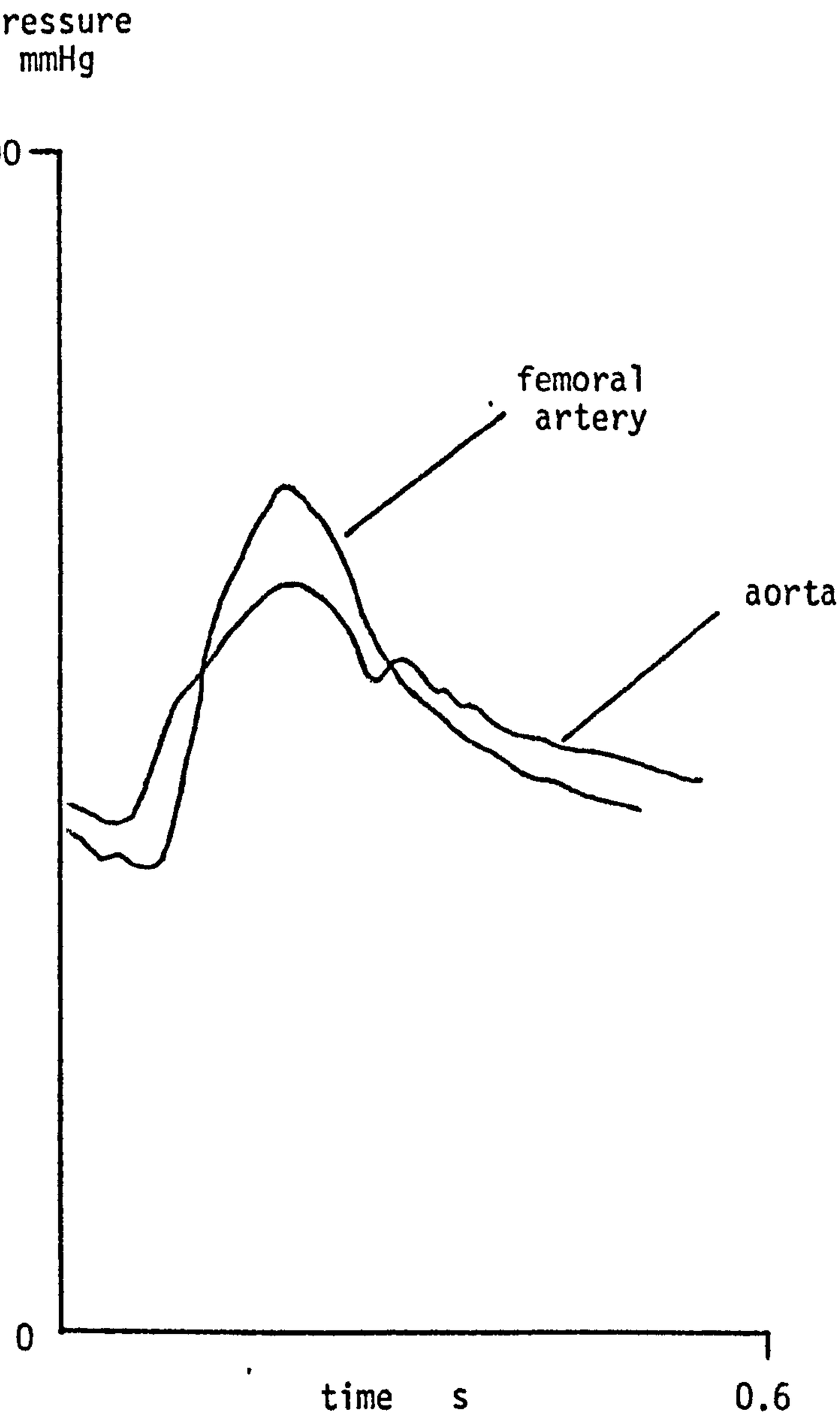

Fig. 2.3

Aortic and femoral artery pressures for the same patient shown over one heart beat.

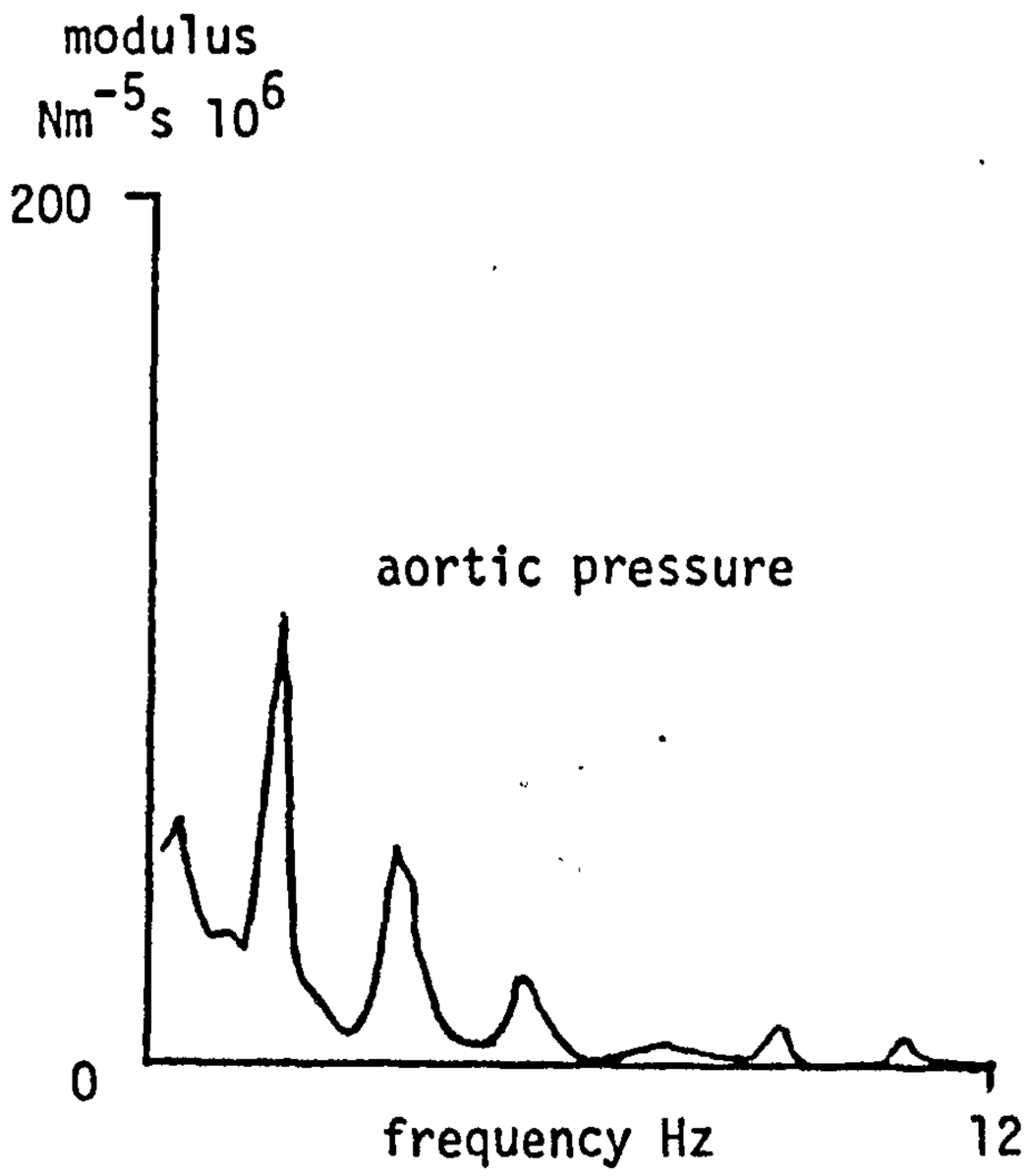

Fig. 2.4

Modulus spectra of the arterial pressures shown in fig. 2.3

$$C = \frac{dV}{dP} \qquad \text{..... (2.1)}$$

If the arteries were rigid then pressure waves would be propagated at the velocity of sound in blood. In compliant arteries however, the velocity approximates to,

$$v = \sqrt{\frac{E\ h}{2rp}} \qquad \text{..... (2.2)}$$

where p is the density of blood, E the Youngs modulus for the artery, h its thickness and r the mean radius. This is the Moens-Korteweg equation for wave propagation along a thin-walled tube (McDonald, 1974, p.254). Arterial compliance is therefore a major determinant of the pressure-flow relationships in the large arteries. It determines both the volume storage effects and strongly influences wave reflection. This suggests that dynamic pressure-flow relationships should give an indication of arterial compliance. In clinical terms arterial compliance is significant in that it is altered by some pathological conditions and by ageing. There is evidence that it may be affected by drugs through their effect on vascular smooth muscle (Dobrin and Rovick, 1969) and by sodium content in heart failure (Zelis, Delea, Coleman and Mason, 1970).

It is well established that there are energy losses in arterial walls when stretched, that is they are viscoelastic. Arterial wall properties have been subject to considerable investigation and it has been shown that these viscoelastic qualities are significant in their effect on the haemodynamics (Westerhof and Noordergraaf, 1970).

The acceleration of blood in the arteries results in a pressure drop ΔP_I along the artery. If blood velocity, v, were uniform in a radial

direction then for a length of artery L, radius r

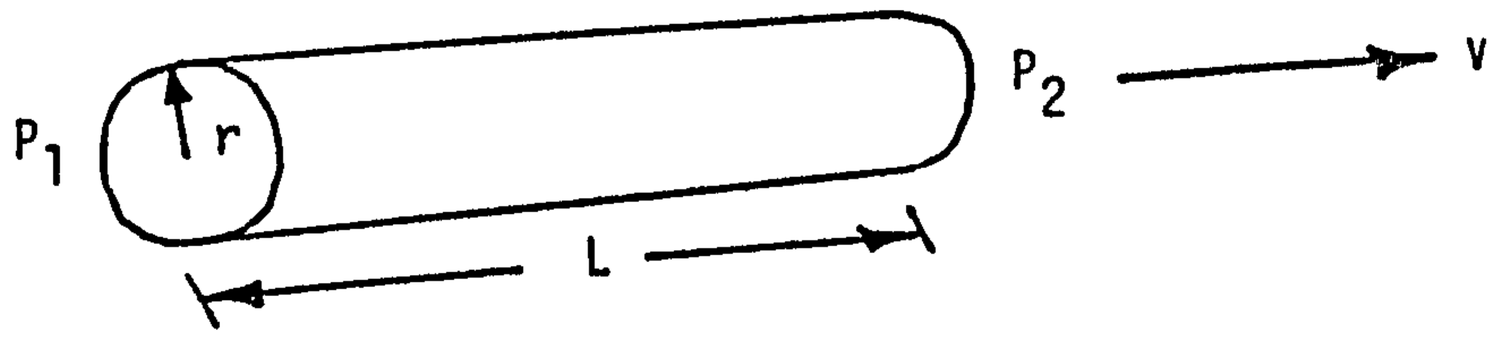

$$\pi r^2(P_1 - P_2) = (\pi r^2 \; L)p \; \frac{dv}{dt}$$

$$\Delta P_I = P_1 - P_2 = \dot{p} \; L \; \frac{dv}{dt}$$

in terms of volume flow F

$$F = \pi r^2 v$$

$$\Delta P_I = \frac{p \; L}{\pi r^2} \; \frac{dF}{dt} \qquad \ldots\ldots\ldots\ldots\ldots\ldots \quad (2.3)$$

The term $\frac{p \; l}{\pi r^2}$ is the inertance, I, of the blood. Friction between the blood and the vessel walls results in the actual blood velocity falling to zero at the walls and the resulting flow profile, in the large arteries, is characteristically that shown in fig. 2.5. Equation 2.3 is a useful approximation for this relatively flat profile whereas it would be quite inaccurate for the parabolic profile characteristic of a fully developed laminar flow.

Friction between the blood and the vessel walls results in a resistance to steady flow, R. Poiseuilles equation relates ΔP_R, F and R for a viscous fluid in a uniform circular tube,

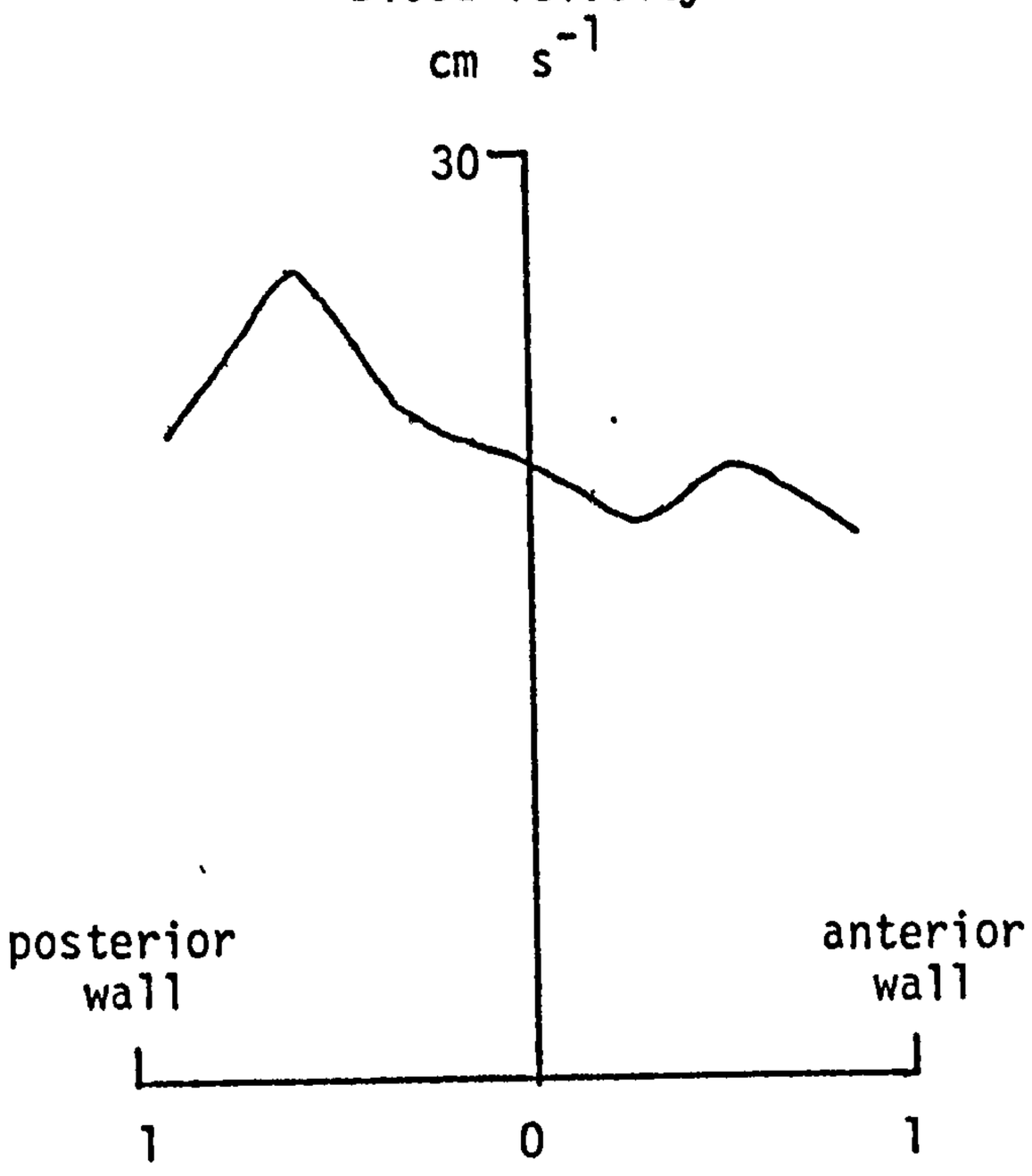

Fig. 2.5

Time averaged velocity profile of the blood flow in the acending aorta of man. After Shultz (1972), p 295.

$$\Delta P_R = \frac{8\mu L}{\pi r^4} F \qquad \text{..... (2.4)}$$

where μ is the viscosity of the fluid and $\frac{8\mu L}{\pi r^4}$ the fluid resistance R. Blick and Stein (1972) discuss deviations from this equation which occur for blood flow. In the aorta these result mainly from turbulent flow and the influence of the ventricular reservoir on the development of the flow profile. In a fully developed "Poiseuille" flow the radial flow profile is parabolic. The effect of the large protein molecules in blood only alters its effective viscosity in small blood vessels less than about 0.5 mm in diameter.

2.4 TIME DOMAIN ANALYSIS OF THE CIRCULATION USING MODELS

The simple linear equations 2.1, 2.3 and 2.4 represent approximations to the basic properties of blood vessels. It has already been noted that the distribution of such properties along the vessels is of importance in determining blood flow. The Navier - Stokes equations describe laminar flow for a Newtonian fluid. Wormersley (1957) gives a simplified frequency domain solution of these equations for fluid flow in an elastic tube which could be applied to a section of artery. Rideout and Dick (1967) have shown that time domain solutions of the Navier - Stokes equations applied to flow in tubes are possible which can be used in the construction of simulation models of the whole circulation. They first linearise the equations and then produce a difference equation solution in the radial and axial spacial directions. Radially the tube is split up into N concentric rings, axially it is divided into lengths L. For the simplest approximation where $N = 2$ the fluid resistance R and inertance I are found to be,

$$R = \frac{8l\mu L}{8\pi r^4} \qquad \text{..... (2.5)}$$

$$I = \frac{9p\ L}{4\pi r^2} \qquad \text{..... (2.6)}$$

Equation 2.5 compared with Poiseuille's equation 2.4 gives a resistance 1.26 greater. Fry (1959), assuming a nearly flat velocity profile, gives,

$$R = 1.6\ \frac{8\mu L}{\pi r^4} \qquad \text{..... (2.7)}$$

that is 1.6 times the Poiseuille figure. This is likely to be more accurate than either the Poiseuille or the Rideout and Dick relation for the proximal aorta as both of these formulae are based on a fully developed laminar flow. Equation 2.6 gives an inertia of 2.25 greater than equation 2.3 which is for a completely flat velocity profile. Fry (1959) gives,

$$I = \frac{1.1pL}{\pi r^2} \qquad \text{..... (2.8)}$$

which is only 1.1 greater.

Any linear treatment of the arterial wall is approximate and consequently formulae abound for the effective compliance. Rideout and Dick give,

$$C = \frac{3\pi r^3 L}{2Eh} \qquad \text{..... (2.9)}$$

which may be compared with the formula of Westerhof, Bosman, deVries and Noordergraaf (1969),

$$C = \frac{3\pi r^2 (a + 1)^2 L}{E(2a + 1)} \quad \ldots\ldots\ldots\ldots\ldots\ldots \quad (2.10)$$

where h = wall thickness

a = r/h .

and E = Youngs modulus of elasticity for arterial wall.

The total pressure drop, ΔP, along the axis of an artery segment of length L, is obtained by adding equations 2.3 and 2.4,

$$\Delta P = RF + I \frac{dF}{dt} \quad \ldots\ldots\ldots\ldots\ldots\ldots \quad (2.11)$$

For continuity of flow the pressure at the mid-point of the segment, P, must obey the relationship,

$$P = \frac{1}{C} \int \Delta F dt \quad \ldots\ldots\ldots\ldots\ldots\ldots \quad (2.12)$$

where ΔF is the net flow into the segment and C the segment compliance. Equation 2.11 can be conveniently written for the nth segment as,

$$\frac{dF_n}{dt} = (P_{n-1} - P_n - F_n R_n)/I_n \quad \ldots\ldots\ldots\ldots \quad (2.13)$$

where P_n is the outlet pressure of the segment. Equation 2.12 relates the mid-point pressure and the total segment compliance. By shifting it half a segment to the outlet it may be expressed in the same form,

$$\frac{dP_n}{dt} = \frac{1}{\frac{1}{2}(C_n + C_{n+1})} (F_n - F_{n+1}) \quad \ldots\ldots \quad (2.14)$$

To simulate the arterial circulation the arteries may then be divided up into segments to which the equations 2.13 and 2.14 may be applied. The shorter these segments are the better the approximation will be to a distributed system and wave propagation effects will be represented up to higher frequencies. It is convenient to make branching points in the circulation coincide with the ends of such segments. The equations may then be solved with analogue or digital computer techniques to produce the simulation.

Models of this type can be used to characterise the arterial system of a patient from measurements of arterial pressure and flow. If the measured pressure and flow are compared to the corresponding variables in a model then matching errors can be determined and the model adjusted to minimise these errors. The optimum values of the parameters which were adjusted can then be used as the best estimate of the corresponding physiological parameters in the patient. This type of analysis extracts information about the mechanical properties of the arterial system from complex pressure and flow waveforms. In this respect it has more potential than simple deductions made from mean and peak values of the variables. On the other hand it does not help to determine an index of the load which the systemic circulation presents to the left ventricle.

Arterial modelling cannot be used as a clinical tool until the reliability and significance of the predictions that are made can be established. The technique is suitable for application to clinical research

studies in which changes in arterial properties are of interest. It may assist in interpreting the effects of vascular drugs used to modify ventricular afterload and also be useful in determining the effects of ageing on the major arteries. Further application may be to the assessment of arterial defects prior to vascular surgery.

A major advantage of modelling for analysis is flexibility. It is relatively easy to use a model for different sets of measurements by examining the corresponding outputs from the model. This is of value in cardiology where it may not be possible, for example, to measure flow and pressure in the same locations during diagnosis and after surgery. Another practical benefit is that model matching algorithms can work on the basis of minimising matching error. This makes it possible to deal objectively with measurement errors when estimating physiological parameters.

Many models of the circulation have been produced and the subject was reviewed by Beneken in 1972. Very little progress has taken place since that time in the design principles of circulation models despite a proliferation of new models. Beneken (ibid.) classifies models by their application and in the present context it is important to distinguish simulation models from those used to characterise a system. Most of the earlier models were used to simulate the circulation and used to test hypotheses relating to its behaviour. Beneken's (1965) model, later elaborated (Beneken and de Wit, 1967), was one of the most significant attemts to model the whole circulation including the heart. The work of Noordergraaf (1956) and Westerhof et al. (1969) is the starting point of most later workers for modelling the systemic arterial system in detail. Noordergraaf's anatomical data for the arteries is some of

the most extensive published. Most of the subsequent vascular models (e.g. Snyder, Rideout and Hillestad, 1968, Tewari and Sundaram, 1971, Ohley, Birtwell, Braun, Bicker and Soroff, 1976 and Laxminarayan, Sipkema and Westerhof, 1978) have used simpler models of arteries. These have been compared qualitatively with physiological measurements, usually from dogs.

There has been significant progress in using models to characterise the individual circulation. Defares and Van der Waal (1969) designed a single compartment model for estimating human arterial compliance from arterial pressure. Rothe and Nash (1968) estimated five dog renal artery parameters with their model. Sims (1972) has shown that it is possible to estimate as many as 13 parameters in the experimental animal preparation when enough measurements are made. Simple arterial models have been used to match a single human pressure (Watt and Burrus, 1976, Wesseling, Purschke, Smith, Wust, de Wit and Weber, 1976). Aaslid (1974) and Brubakk and Aaslid (1978) have produced one of the few detailed models of the whole circulation which has been matched to human data available in the normal clinical situation.

Developments in parameter estimation have largely been with animal data. The work that has been done with human data involves, in most cases, simple arterial models that do not represent the distribution of arterial properties along the direction of blood flow. This is partly because with animals it is possible to make more simultaneous measurements than is acceptable in man. In the clinical situation the modeller will not often be able to choose the measurements that are made and the quality of measurement will be a compromise with the cost and safety of the procedures used. It seems appropriate at this time to

accept these compromises and try to gain clinical benefit from the more realistic arterial models that are currently available.

2.5 FREQUENCY DOMAIN ANALYSIS

The systemic circulation is the load into which the left ventricle pumps blood. In the terminology of muscle mechanics this represents the afterload. The preload is the inital muscle stretch which is related to the end-diastolic-volume. Unfortunately, there is no simple measure of ventricular afterload. It is clear from aortic pressure and flow waveforms that they are not related by a simple linear function as the time courses are very different. The ratio of peak pressure to peak flow is of no value in determining the pressure in diastole, for example. The ratio of mean pressure to mean flow gives a useful measure of steady state conditions but has no significance in describing the arterial dynamics.

In Fourier analysis any periodic function X(t) may be represented by a series of sine functions of time,

$$X(t) = \sum_{n=1}^{\infty} a_n \sin(\omega_n t + \phi_n) \quad \ldots\ldots\ldots\ldots \quad (2.15)$$

where a_n is the amplitude and ϕ_n the phase angle of the component frequency ω_n. The aortic input pressure and flow can therefore be resolved into sinusoidal components of different frequencies if they are considered to be periodic. The analysis of Rideout and Dick (1967) shows that the pressure flow relationship may be approximated by a series of linear differential equations. On this assumption the ratio of the amplitudes of pressure and flow, for each Fourier frequency, will be

constant. These ratios are usually termed the aortic impedance amplitude, by analogy with electrical circuits. The difference in phase between the pressure and flow for each frequency is the impedance phase. Impedance defined in this way is a complex quantity having both a modulus and phase at each frequency. A plot of impedance amplitude against frequency gives a description of the input characteristics of the aorta. As any periodic input function can be subjected to Fourier analysis the input impedance spectrum is the same for any such input if the condition of linearity described is reasonable.

If the time functions are considered to be resolved into an infinite number of frequencies then the input impedance-frequency function becomes a continuous curve. The frequency components of the pressure and flow functions themselves can then be considered as continuous amplitude-density functions of frequency.

Aortic input impedance spectra have a distinctive shape (Fig. 2.6) with a large component at zero frequency which is equal to the mean pressure/mean flow quotient. The impedance falls rapidly up to about 2 Hz. This region represents the volume storage effect of the aorta being mainly determined by aortic compliance. The subsequent oscillations in impedance are the result of reflections from the various branches. Above about 10 Hz the impedance fluctuations die out. The standard analysis of electrical transmission lines gives a constant impedance for the case of no reflections termed the characteristic impedance. This concept is equally applicable to the linearised equations for fluid flow in arteries and in this case its modulus is given by Z_o, if any energy losses are neglected, where,

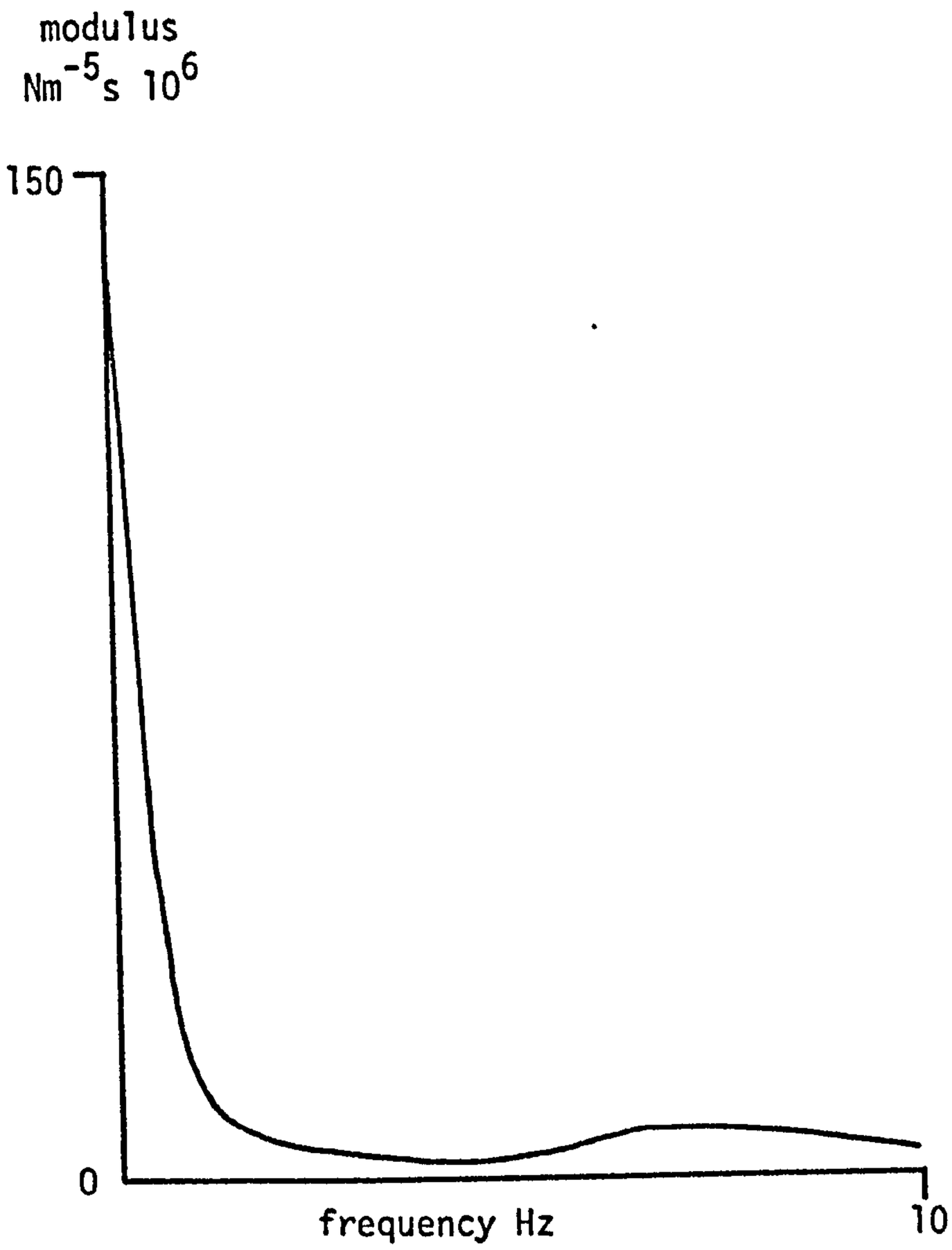

Fig. 2.6

Typical aortic input impedance for a normal adult. Based on the data of Nichols et al. (1977).

$$Z_o = \sqrt{\frac{I}{C}} \qquad \ldots\ldots\ldots\ldots\ldots\ldots \quad (2.16)$$

The phase angle of Z_o is zero, that is with no reflections the pressure and flow time courses would be linearly related or the same shape. Where there are reflections, Z_o is applicable to the forward and reflected waves individually. At high frequencies the reflection sites are many wavelengths away and the reflections are strongly attenuated. For this reason the impedance above 10 Hz tends towards Z_o. At these frequencies the input impedance then indicates the ratio of inertial to compliant properties of the aorta, if losses are neglected.

The circulation offers a different impedance to sinusoidal flows of different frequencies. As arterial flow is not sinusoidal it is necessary to carry out a frequency analysis of the pressure and flow measurements and to represent the input impedance by an impedance spectrum. A spectrum has the disadvantage that it does not give a single parameter which could be readily correlated with pathological conditions (Milnor, 1975). For this reason it has become normal practice to average the impedance over a specified frequency range. Unfortunately this average impedance has been termed the characteristic impedance by some authors (Nichols, Conti, Walker and Milnor, 1977) although it is not equal to this quantity as normally defined in electrical engineering. Many papers have been published on the measurement of aortic input impedance (e.g. Westerhof, Elzinga and Van den Bos, 1973) and discussed the factors which affect it. As yet there is relatively little evidence of any diagnostic value although it is an area of growing interest (Noble, 1979). With the success of cardiac surgery in correcting valve defects and congenital malformation other factors influencing heart failure have become more important (Webb-Peploe, 1979) including

arterial impedance. O'Rourke (1970) indicated changes in arterial parameters that result from hypertension. More recently Nichols et al. (1977) and Pepine, Nichols and Conti (1978) have studied aortic impedance in heart failure. Impedance has a special significance in vasodilator drug therapy (Mason, 1978) in which the peripheral resistance is reduced with drugs such as hydrallazine. Any alteration of the aortic compliance may increase the input impedance in such a way as to increase the dynamic load on the left ventricle. Similarly it may be possible to find drugs which beneficially alter the compliance while preserving the peripheral resistance and thus mean blood pressure. The same analysis may be relevant to quantifying the effect of fatty deposition in the major arteries and other forms of arterial degeneration termed collectively arteriosclerosis.

2.6 SCOPE OF THE RESEARCH

Beneken in his review (1972) of cardiovascular modelling writes,

"It is a little disappointing to observe that many good model studies have thus far been applied in few situations ....

The majority of models published so far serve mainly to improve understanding. In the near future it is believed that models will be used with more direct relation to patient diagnosis and care."

The literature indicates that with a few exceptions cardiovascular models have still not been applied to human clinical data or been used to aid diagnosis or care. The aim of this research was to advance the clinical application of cardiovascular modelling techniques. For this reason the work was allied to specific clinical measurements that were being made for independent reasons, because of the hazard of all invasive cardiovascular measurements it is not realistic to ask for

extra measurements. Simultaneous arterial pressure - flow measurements are being made already as has been indicated. Modelling is an attractive alternative to frequency analysis for this data. A model has been developed which uses ascending aortic flow as a driving function or input. Arterial pressure either in the ascending aorta or the femoral artery can be matched by adjusting the model. In practice ascending aortic pressure is measured during investigation but femoral pressure for long term monitoring. This flexibility is a special virtue of model based analysis. It would not be easy to directly estimate the aortic input impedance using the femoral artery pressure for example.

Special emphasis has been placed on designing a practical model system. Digital computer programs are used and no special electronics is involved. The programs will run on an average mini-computer such as are used increasingly for laboratory data analysis. With analogue computer models specialised equipment, not generally available in a hospital, is required so that the methods developed in one institution cannot readily be used in another centre. Using a digital computer also makes modifications to the model very easy. Computer control of the matching procedure avoids the need for any special skills on the part of the operator. The results can be printed out using the normal facilities available on a computer.

Modelling in general can make heavy demands on a small computer. For this reason some effort has been directed towards finding the complexity of model which is justified by the quality of the data which is produced clinically. A comparison has been made between four different models for this purpose.

CHAPTER 3

EXPERIMENTAL TECHNIQUES

3.1 PRESSURE AND FLOW MEASUREMENT APPARATUS

In cardiology measurement techniques have to combine an adequate degree of safety for the patient and an acceptable cost. This research has been based on the use of currently available standard equipment designed for clinical application with these criteria in mind. Measurements have been made both after cardiac surgery and during diagnostic cardiac catheterisation. However, the procedures used for the latter are not satisfactory for application outside research and a combined pressure - flow catheter will be needed for routine application. At present catheters of this type are not readily available and those made to special order are extremely expensive.

Pressure Transducers

The two types of transducer most frequently used at St. Thomas' for measuring pressure are strain gauge and inductance manometers. In both types one side of a diaphragm is exposed to the blood pressure and the other to a reference, usually atmospheric pressure. The diaphragm deflects with changing blood pressure and this deflection is converted into an electrical signal. In the strain gauge manometer a conductor is strained by the diaphragm and the resulting resistance change measured using a bridge arrangement and an amplifier. One or more of the bridge arms can be active strain gauge elements. The classic version of this type of transducer is the unbonded wire strain gauge mano-

meter of which the Statham P23 series are examples. Semiconductor strain gauge elements are also used now that the initial problems of light and temperature sensitivity have been overcome. The doping can be arranged so that the substrate forms an insulated diaphragm with the semiconducting elements on the back. This gives electrical isolation between the patient and the instrumentation. Semiconductor manometers can be made small enough to be fitted to the end of a catheter to be in direct contact with the circulating blood. The Micro-tip transducer made by Millar Instruments Inc. (Millar & Baker, 1973) is of this type. Also available is a miniature semiconductor transducer made by Gaeltec Ltd. fitted in the end of a luer connector. Both types can be connected direct to the end of a catheter, avoiding the use of connecting catheters required with standard transducers. The catheter tip inductance manometer made by Thompson Telco has a diaphragm fitted with a plunger which forms the core of an inductor. Deflection of the diaphragm causes changes in the inductance of the winding of the inductor which in turn alters the frequency of an L-C oscillator in the amplifier. The frequency changes are demodulated to give an electrical voltage output proportional to pressure. The system was developed from the design of Gauer and Gienapp (1950).

Modern transducers used with appropriate catheters and amplifiers have two main limitations to their accuracy, zero offset and limited frequency response. As a result of the zero offset of transducers and amplifiers some zero pressure reference must be used. With an external transducer a tap can be arranged to switch the transducer from blood pressure to atmospheric pressure. With a catheter tip transducer some other reference must be used. In the cardiac department at St. Thomas' an external transducer with a fluid filled

catheter is normally employed for this purpose.

Catheter Transducer Frequency Response

The classical method of accurate blood pressure measurement is to use a fluid filled catheter whose tip is inserted to the point where pressure is to be measured. A transducer is attached to the end of the catheter which contains a diaphragm one side of which is exposed to the catheter and the other side to the atmosphere. The diaphragm deflects with changing blood pressure and this deflection is converted into an electrical signal. The frequency response of this system is limited by the interaction of the fluid in the catheter, the catheter itself and the stiffness of the transducer diaphragm. Considering the fluid and the diaphragm as a simple mass-spring arrangement it can be analysed as a second order damped system. A simplified solution of the describing equation is presented here to relate the results to the catheter-manometer properties. A rigorous solution can be found in most standard texts on control theory (e.g. D'Azzo and Houpis, 1966).

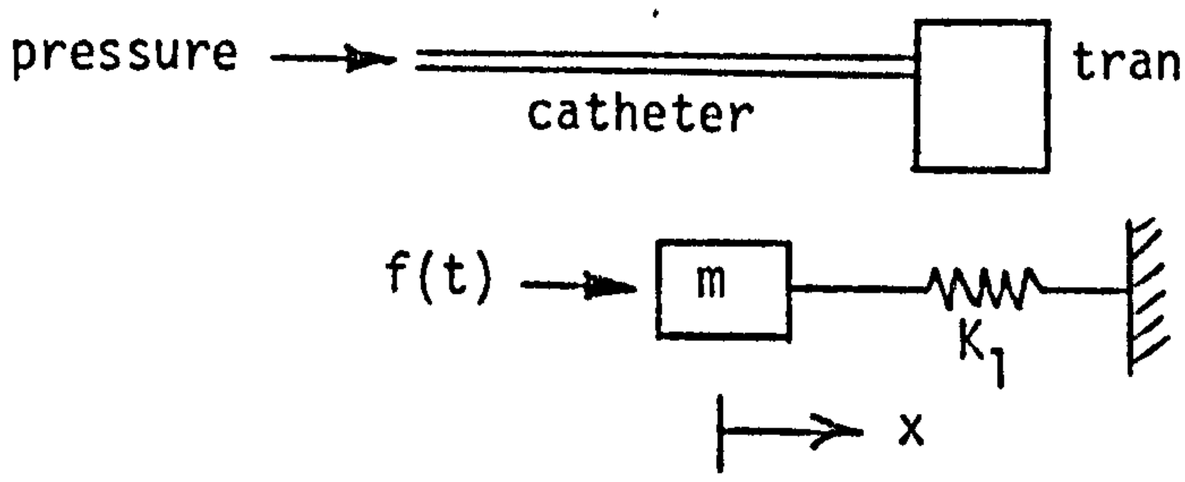

simple representation of catheter-transducer system.

The equation of motion of the diaphragm is,

$$\frac{d^2x}{dt^2} = \frac{-k_1x}{m} \quad \frac{-k_2}{m} \quad \frac{dx}{dt} + f(t) \quad \ldots\ldots\ldots\ldots \quad (3.1)$$

assuming the fluid in the catheter is incompressible so that the diaphragm and fluid have the same displacement.

x = diaphragm displacement

m = mass of fluid in catheter

f(t) = (force on fluid due to pressure)/m

k_1 = diaphragm stiffness

k_2 = viscous damping

Transforming equation 3.1 using the Laplace operator, s and rearranging gives,

$$s^2X(s) + \frac{sk_2}{m} X(s) + \frac{k_1}{m} X(s) = F(s)$$

giving the transfer function,

$$\frac{X(s)}{F(s)} = \frac{1}{s^2 + \frac{sk_2}{m} + \frac{k_1}{m}} \quad \ldots\ldots\ldots\ldots \quad (3.2)$$

Substituting s = jw in equation 3.2 the steady state frequency response θ (w) is given by,

$$\Theta(w) = \frac{X(jw)}{F(jw)} = \frac{1}{\frac{k_1}{m} - w^2 + \frac{jwk_2}{m}} \quad \ldots\ldots\ldots \quad (3.3)$$

If the damping factor, k_2, is zero then the frequency response is infinite at an angular frequency w_o given by,

$$\frac{k_1}{m} = w_o^2$$

$$\text{or} \quad w_o = \sqrt{\frac{k_1}{m}}$$

It can be shown from the roots of equation 3.2 that w_o is also the undamped natural frequency of the system.

Equation 3.3 can be written,

$$\Theta(w) = \frac{1 / w_o^2}{1 - \left(\frac{w}{w_o}\right)^2 + j2\xi \left(\frac{w}{w_o}\right)} \quad \ldots\ldots\ldots\ldots \quad (3.4)$$

where $\xi = \frac{k_2 / m}{2w_o}$, which is termed the damping ratio.

If the catheter-transducer is calibrated at low frequencies ($w << w_o$) then $1/w_o^2$ is part of the calibration factor. The frequency dependent sensitivity factor then becomes,

$$A(w) = \frac{1}{1 - \left(\frac{w}{w_o}\right)^2 + j2\xi \left(\frac{w}{w_o}\right)} \quad \ldots\ldots\ldots\ldots \quad (3.5)$$

Differentiating equation 3.5 with respect to w and equating to zero gives the maximum response to a forcing function of the damped system to be at a frequency w_d where,

$$w_d = w_o\sqrt{(1 - 2\xi^2)} \quad \text{.....} \quad (3.6)$$

It should be noted that this is not equal to the damped natural frequency, w_D which is given by,

$$w_D = w_o\sqrt{(1 - \xi^2)} \quad \text{.....} \quad (3.7)$$

for $0<\xi<1$

The undamped natural frequency, w_o, is a measure of the useful frequency response of the system. Relating this to the catheter dimensions,

$$m = pL\pi r^2$$

and

$$k_1 = \frac{f}{x} = \frac{P\pi r^2}{V/\pi r^2}$$

$$w_o = \sqrt{\frac{k_1}{m}} = \sqrt{\frac{1}{c}\pi\frac{r^2}{pL}} \quad \text{.....} \quad (3.8)$$

where,

p = density of fluid

L = catheter length

r = catheter internal radius

c = diaphragm volume compliance

P = pressure

V = diaphragm volume displacement

This analysis is accurate only in as far as the catheter walls are much stiffer than the diaphragm. With miniature semiconductor transducers the catheter compliance may be dominant. Equation 3.8 shows that a stiff transducer diaphragm and a short, large bore, catheter will give the highest frequency response.

Two pressure transducer arrangements have been used in this work. For post surgical measurements a 2 inch long 18G catheter was used connected to either a Millar PC 350 catheter tip transducer or Gaeltec 3EA luer transducer with a 3 way tap, fig. 3.1. The frequency response of this system was measured using a sinusoidal pressure generator whose output was constant to within $\pm$ 1dB (12%) up to 100Hz. A Gaeltec transducer was used with an S8 carrier amplifier. The signal was filtered at 100Hz to remove traces of the 2kHz carrier. The system was found to have a constant output to within $\pm$ 0.5dB from 0 to 70Hz and a time delay of less than 1 ms from 1 - 100Hz after allowing for the filter. A pressure zero was obtained before each measurement by turning the tap to give an atmospheric pressure reading. During cardiac catheterisation pressure was measured with a Millar PC350 catheter tip transducer introduced into the ascending aorta. This device has a quoted frequency response up to 20kHz. Pressure zero reference was established using an external transducer connected to the sheath used to introduce the catheter.

Calibration in each of these cases was carried out using a mercury column.

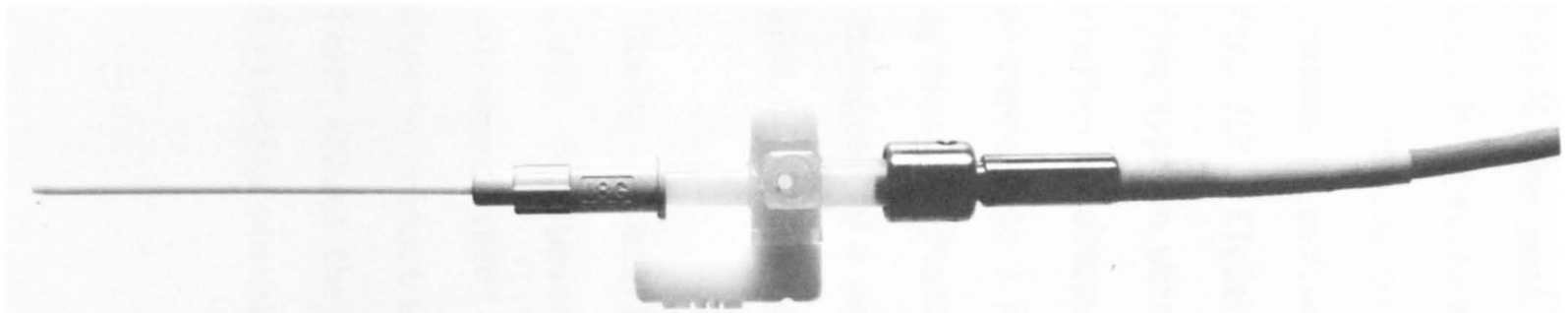

Fig. 3.1

Gaeltec luer fit 3EA transducer connected to a 2 inch long 18G catheter with a 3 way tap.

Flow Measurement

In the project blood flow has been measured using Carolina Medical Electronics 601D flowmeters. For post surgical measurements an extractible flow probe type 900 (Williams, Barefoot and Shenk, 1969) was used placed around the ascending aorta. The probe is held in place by a suture which passes in medical rubber tubing through the chest wall as shown in fig. 3.2. Electrically the probe is a conventional electromagnetic flow type in which two coils are energised with a square wave current creating an alternating magnetic field in the blood vessel. The blood represents a moving conductor in this field and so has an alternating electric field induced in it at right angles to the field. This is detected by a pair of silver electrodes held in contact with the outside of the blood vessel.

Blood flow was measured during catheterisation with a catheter tip mounted probe type 1008, fig. 3.3, which is an inverted form of the cuff probe (Spencer and Barefoot, 1968) with the field produced around the catheter and electrodes in contact with the blood. This transducer measures the flow in a layer around the catheter independent of the vessel size giving blood velocity whereas the cuff probe will measure volume flow rate.

Accuracy

The major defects and errors in the electromagnetic measurement of blood flow are described by Mills (1972). Many of these relate to flowmeter design and are not discussed here. The amplitude-frequency response of the flowmeters, shown in fig. 3.4, is flat within $\pm$ 1dB to 10Hz.

Fig. 3.2

Carolina Medical type 900 extractible aortic flow probe shown with suture, passing through tubing, to hold it in place around the aorta.

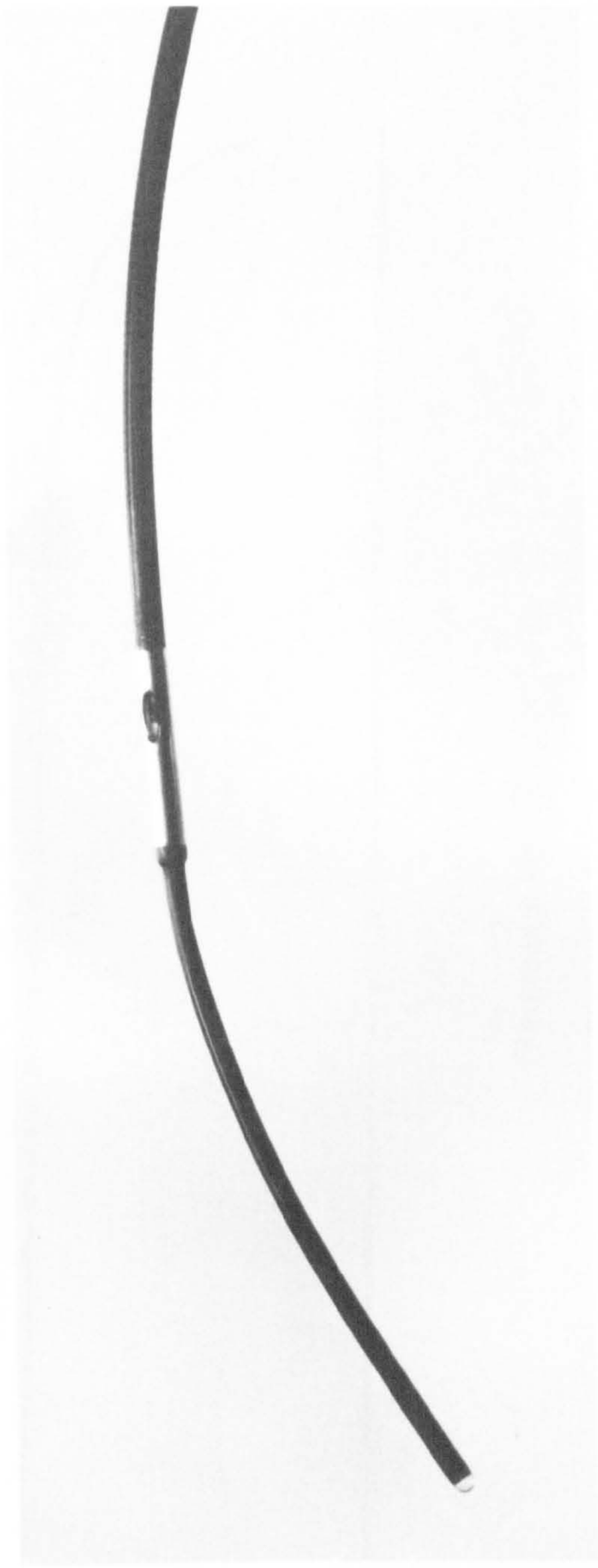

Fig. 3.3
Carolina Medical type 1008 catheter tip blood velocity transducer.

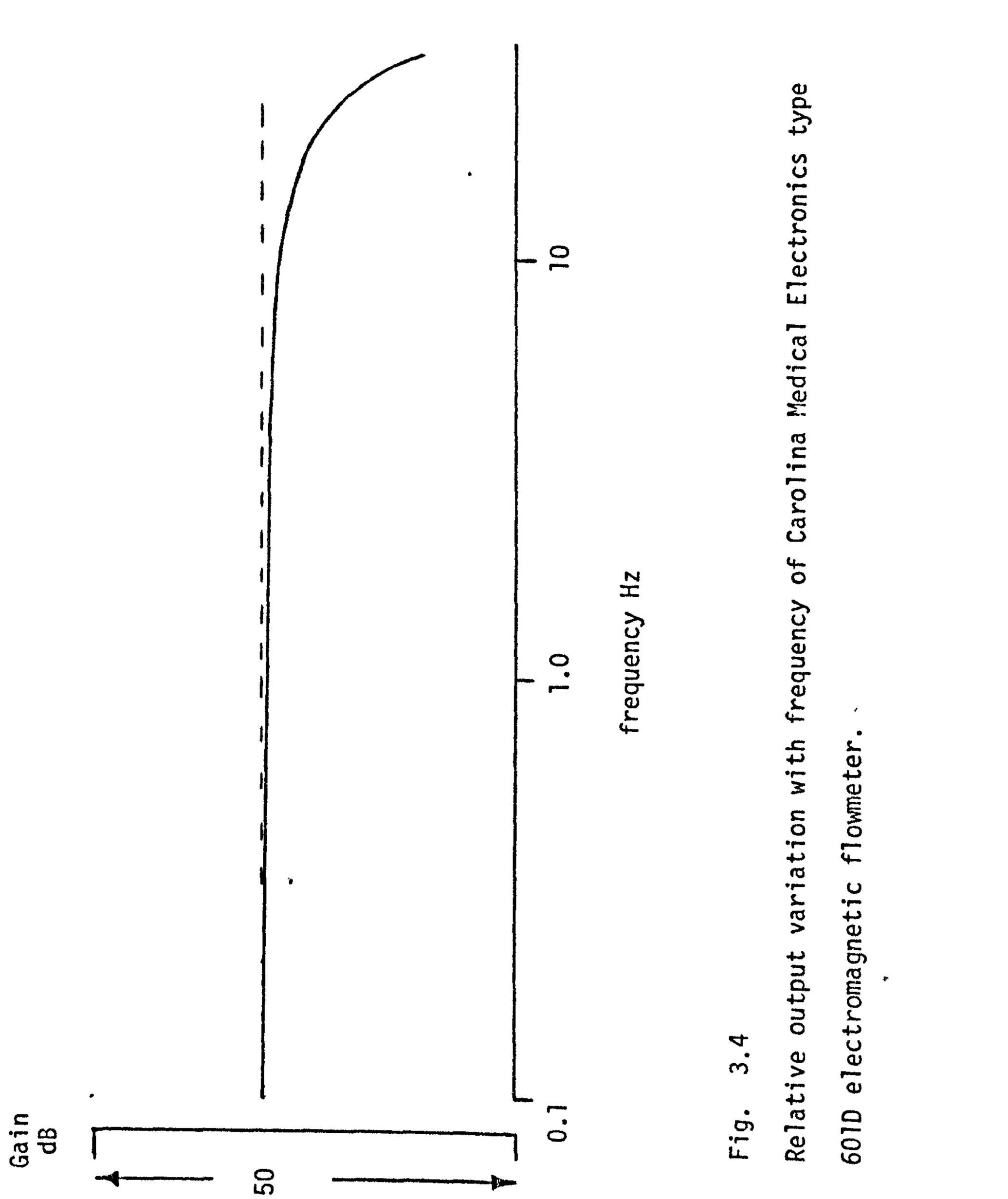

Fig. 3.4
Relative output variation with frequency of Carolina Medical Electronics type 601D electromagnetic flowmeter.

The phase response, fig. 3.5, shows a constant time delay of 35 - 40 ms between 1 and 10Hz. Although this performance is not very good it is adequate for diagnostic purposes. What little clinical data exists indicates that the input impedance of the arterial system is small and fairly constant beyond about 10Hz as it tends towards the hydraulic characteristic impedance. So frequencies beyond 10Hz will not provide any further diagnostic information. At the lower end most of the useful information is probably contained within one heartbeat, that is within a record no longer than 1 s normally, which is equivalent to a frequency resolution of 1Hz. As there is no phase factor associated with the steady component of flow the phase accuracy of the flowmeter between 0 and 1Hz is of little significance. The most serious limitation of the Carolina 601D flowmeters is their noise output, the manufacturers claimed noise figure is equivalent to less than 0.1 l/min RMS for the cuff probe or 1 cm/s RMS for the velocity probe. It has been found that much of this noise is residual high frequency components that can be removed by a 12Hz low pass filter without substantially affecting the overall frequency response.

Calibration

Cuff probes are difficult to calibrate as a section of blood vessel must be used to simulate the real working conditions. Carolina Medical supply the cuff probes complete with a calibration factor and this has been used. Unfortunately the post surgical measurements were made by several clinicians at different times and with various size probes and it was not possible to confirm the calibration factors used. The velocity probes were not supplied calibrated and the calibration factors were determined using a constant flow apparatus filled with

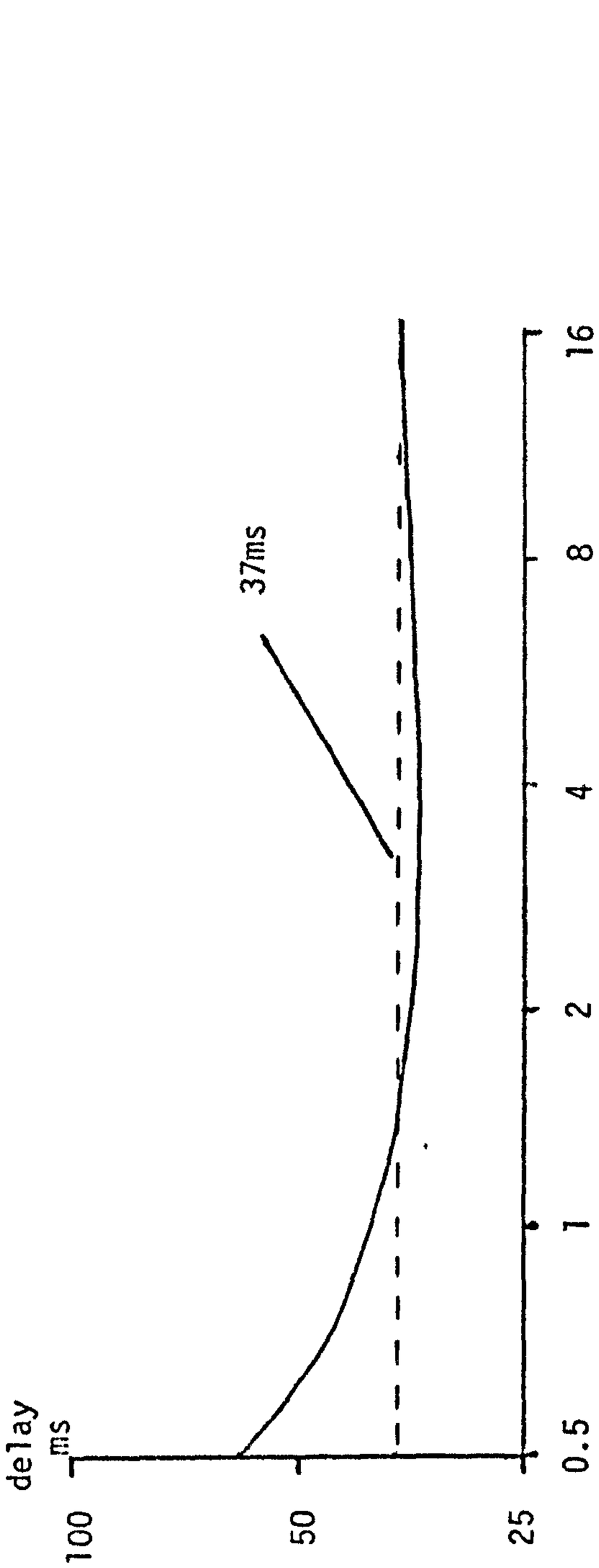

Fig. 3.5
Delay time of Carolina Medical Electronics type 601D electromagnetic flowmeter.

saline and a rotameter flowmeter used as a standard. True zero flow for electromagnetic flowmeters can be difficult to determine accurately. In these applications zero flow was taken to be the flow during the second half of diastole. The technique used for this is described in section 3.5.

3.2 CLINICAL TECHNIQUES

Post-operative Monitoring

The extractible flow probe was fitted around the ascending aorta immediately prior to chest closure after heart surgery. The probe was led out through the chest wall between the ribs and sealed with sticky plaster. A 2 inch long 18G catheter was inserted into the femoral artery using an introducer and then secured to the leg with plaster. The Gaeltec or Millar miniature transducer was fitted to the needle with a three way tap, care being taken to exclude air.

From an ethical point of view the flow probe is equivalent to a chest drain and does not present a significant hazard. There are no reported cases of difficulty in withdrawing the probe. Some probes have failed to give a recognisable flow signal after a period of use and some of these have functioned correctly after withdrawal. It must therefore be assumed that the probe electrodes can fail to sustain good electrical contact with the aortic vessel walls. To assess left ventricular load an aortic pressure measurement would be preferred. However it is not wise to leave an indwelling catheter so far upstream near to the coronary and carotid arteries. Blood clots form on any foreign body in the blood stream including heparinised catheters and

any fragment of clot entering the coronary or carotid arteries could have serious consequences. For this reason the femoral or radial artery sites are preferred. In these studies only femoral artery records are used. These arterial measurements would normally be made to monitor the patient and do not therefore constitute an additional hazard. The only deviation from normal practice is in using a micro-manometer rather than a fluid filled catheter.

Cardiac Catheterisation

The measurements with the catheter tip flow probe were made during normal diagnostic cardiac catheterisation on one patient having coronary artery disease but with a normal left ventricular function. Beta blocker therapy was stopped 24 hours before catheterisation to restore normal haemodynamic conditions. Prior to investigation the patient was given 0.3 mg atropine and 10 mg diazepan as a mild sedative. The CME flow catheter was introduced into the aorta from an incision in the femoral artery. Using the modified Seldinger technique (Brooksby, Swanton, Jenkins and Webb-Peploe, 1974), a needle was inserted into the artery through the skin, a guide wire pushed through the needle and the needle removed. A hollow catheter with a sheath on it was then pushed over the wire and into the artery. The wire was removed and the catheter and sheath pushed into the aorta. The hollow catheter was then withdrawn and replaced by the flow probe. A Millar PC350 catheter tip manometer was then introduced into the ascending aorta, by the same method, from the other femoral artery. This technique using separate catheters for flow and pressure, is not satisfactory for routine use as the normal investigations only require a single catheter and one insertion site. In the future flow probes with a

built-in catheter tip pressure transducer may be used. The ones currently available are very expensive at around £1000 each and difficult to obtain.

3.3 DATA COLLECTION

In the post operative situation the measurements were recorded using a special purpose monitoring system, (Bourne and Williams, 1975). An R-wave marker pulse is generated from the patient's ECG using a trigger circuit and this pulse can be moved in relation to the heart cycle by a variable delay. The R-wave marker is positioned in the diastolic (ventricular filling) period and identifies a period of zero arotic blood flow. The unfiltered ECG, femoral artery pressure and aortic flow were recorded on a Phillips Analog 7 FM tape recorder at 3.75 inches s^{-1}. At this speed the frequency response of the recorder is 1250Hz $\pm$ 3dB and the signal to noise ratio 41 dB. When the tape is replayed to retrieve the data the R-wave marker is triggered by the recorded ECG. This marker was used by the computer editing system to identify individual heart beats. The R-wave marker, femoral artery pressure and aortic flow were then subjected to preliminary editing and re-recorded onto a Phillips Minilog 4FM cassette recorder run at 7.5 inches s^{-1}. This recorder has a frequency response of 13500 Hz $\pm$ 3dB with a signal to noise ratio of 42 dB. This further stage of recording was necessary because only limited access to the monitoring system was available. The pressure was calibrated using a mercury manometer initially to set up an electrical calibration in the pressure amplifier. During patient measurements a pressure zero was recorded using the 3 way tap on the transducer and the electrical calibration was also recorded. Flow zero was established approximately using the

display oscilloscope but this was not used for final calibration of the results. The flow sensitivity was determined by adjusting the "standby zero" to set the flowmeter to read some convenient flow on its digital meter and recording the change in flowmeter output. The calibration factor used with the flowmeter was that which gave accurate reading on this meter.

For the cardiac catheterisation measurements the flowmeter and Millar pressure transducer were connected to a monitoring system (Bourne, 1979). The signals were connected to a Varian computer based analysis system (Waldron and Stoate, 1979) and stored digitally on magnetic tape. The pressure signal was unfiltered but the flow signal was filtered to remove noise. A 12Hz active filter was used based on a design by Bronzite (1970) adapted to give a constant time delay characteristic with a transfer function derived by Thompson (1952). This gave an amplitude response flat to $\pm$ 1dB to 10Hz, -3dB at 12Hz, with a time delay 33ms $\pm$ 2ms from 1 - 30Hz.

The computer analysis system program collected 9.6 second records of pressure and flow. In the terminology of the system each record was a "file" and the set of files forming a particular patient investigation a "catheter". Each catheter has a unique number for the working year and within the catheter the files are numbered in chronological order starting at 1. The catheter for this particular study was transferred to a specific reel of magnetic tape. Each pressure-flow file consisted of a continuous record with each flow sample followed by two pressure samples. The sampling rates were 100Hz for the flow and 200Hz for the pressure. R-wave markers are embedded in the file as out-of-range pressure values. The tapes were transferred to the

Bioengineering computer for the subsequent analysis. This system has the advantage that no further filtering or noise is imposed on the signals after sampling on-line by the computer. In particular, no analog tape recording which has relatively low signal to noise ratio, is necessary. The pressure was calibrated with a mercury manometer and the results and atmospheric zero stored numerically in the header to the catheter files. The flow calibration was done in the same way as in the post operative studies, the results again being stored in the catheter files.

3.4 DIGITAL COMPUTER EQUIPMENT

Two computers were used in this project, both manufactured by Varian Data Machines and of similar specification. The Cardiac department system is based on a 620/L-100 processor with 28K words of memory and the Bioengineering department one on a V72 with 32K. As the Cardiac laboratory system was only used for data collection it will not be described further but can, in all important aspects, be taken to be the same as the Bioengineering machine. The V72 is a 16 bit word computer with capabilities and performance much the same as other machines in hospital and laboratory use such as the Data General Nova and the Digital Equipment PDP 11 series. For modelling, arithmetic speed is important and our machine is at the slow end of current technology with 1200 ns cycle time core memory. It has no enhancements for floating point arithmetic such as a floating point processor or writeable control store routines. All floating point arithmetic is carried out by the integer arithmetic unit of the central processor using software (program) algorithms.

Current machines of this type have features which would give a speed increase of four or five times for model simulation. Modern semiconductor core memory with fast "cache" buffer store could give a speed increase of a factor of two more. So an overall reduction in the model program running times of a factor of ten is well within current technology and represents additions actually available for the now obsolete Varian V72. The type of computer installation associated with on-line clinical signal acquisition, analysis and result production involves a substantial investment in expensive peripherals such as a hard disc, printer-plotter and display equipment. With the reducing cost of electronics these predictions of increased speed are based on systems designed to make efficient use of the peripherals. This point has been laboured because digital modelling is relatively slow compared with analogue simulation.

The Bioengineering computer is equipped with an analogue to digital converter (ADC) sampling the output from a sixteen channel multiplexer. Input to four of these channels is made via switchable constant delay active filters. For the post surgical measurements these filters were set for a 3dB frequency at 30Hz, to filter the tape recorded signals. At this setting they have a response of $\pm$ 1dB from 0 - 25Hz and a time delay of 13 ms $\pm$ 1 ms from 1 - 30Hz. The sampling rate used for all this work was 100Hz giving a theoretical bandwidth of 50Hz. At 50Hz the filters have an attenuation of 30dB, i.e. a transmission of approximately 3%. With reasonable recordings the total signal plus noise at 50Hz should be less than 10% so that aliasing (Bendat and Piersol, 1971) should not produce more than 0.3% spurious signal generation.

The catheter laboratory data was collected and digitised without further

filtering. Pressure was sampled at 200Hz and flow at 100Hz. The recorded data with range and calibration information was stored on standard ½" computer tape at 800 BPI using the IBM standard recording format.

A Tektronix storage oscilloscope type 613 was used to display graphical information for editing data and for the analysis studies. Permanent paper copy was obtained from it using a Tektronix 4631 photographic hard copy unit. A Centronics matrix printer was used for program listing and numerical results.

The computer was operated under the Varian BETA disc based system modified by myself and colleagues for our set of peripherals. The operating system modifications were made in the Varian assembly language and all the analysis programs written in Fortran IV.

3.5 DATA EDITING AND CALIBRATION

All the computer programs used in this project are listed in Appendix 3 together with appropriate references where they were not written by myself. Two programs were written to put the pressure-flow measurements into a suitable form for model matching and impedance determination. One deals with the analogue recordings from post-surgical monitoring, the other with the digital recordings from the catheter laboratory.

Analogue Recordings

The program HTDAT1 (appendix 2) digitises the R-wave marker, arterial

pressure and aortic flow at 100Hz and stores them in three separate arrays. The recordings include zero and calibration levels for the pressure and flow. The arrays were split up into single heart beats by reference to the R-wave marker so that each beat began and ended in diastole. The flow signal was corrected for zero error by fitting a straight line by the method of least squares to the first and last three samples of the flow signal for each beat and subtracting it from the whole of the flow for that beat. The pressure was corrected by subtracting the recorded initial zero pressure value. The flow record was shifted to compensate for the relative time delay between it and the pressure record. Pressure and flow were calibrated by reference to the calibration recordings. Each beat of pressure and flow was then displayed on the computer oscilloscope. Suitable individual beats were selected by eye and subsequently punched onto standard 8 hole paper tape for input to the circulation models. Two criteria were used to select beats, first that the traces were similar to preceding beats and second that the pressure started and ended the beat at the same value. The models use a recorded beat repetitively to simulate a stable haemodynamic state. Both criteria ensure that the patient is physiologically stable and also that the pressure, when repeated, did not have a sudden change in value at the end of each beat. Visual editing was considered adequate as unsuitable beats are usually caused by ectopic heart beats or substantial patient or catheter movements whose effects are clearly visible on the traces.

Digital Recordings

The catheter laboratory data is stored digitally on magnetic tape with range and calibration information. Initial calibration and processing

of the data is carried out by the routines AOIMP and AOIMP1 (appendix 2). The pairs of pressure samples were averaged so as to give a common sampling rate of 100Hz for flow and pressure. Continuous flow and pressure records were then formed with beat to beat intervals stored separately, the flow record being shifted as before to correct for relative time delays. Because of the poor quality of the flow signal in the recordings made so far, an ensemble average flow and pressure for one heart beat was generated. This was done by averaging all the points in each beat for every time interval measured from the ECG R-wave. A record of maximum length of 512 10 ms samples was then constructed by repeating the average waveforms as many times as possible within this length. Calibration was carried out as before with the flow zero correction being carried out for each individual beat before averaging. This helps to remove respiratory and other slowly changing zero errors from the signal. A single average beat is then punched on paper tape in the same format as before using the visual editing procedure.

These recordings were also subjected to frequency analysis to compute the aortic input impedance. For this purpose AOIMP1 first tailors the pressure record by subtracting a least squares fit line to the first and last three values of the pressure recording with the same routine used for flow baseline correction. The record comprises only complete beats so that the pressure starts and finishes at the same point on the heart cycle. The effect therefore is similar to removing the mean pressure component except that the pressure record starts and finishes at zero. The flow record is zero at both ends as the record starts in diastole. This procedure helps to reduce the effect of the finite record length which introduces "leakage" (Bendat and Piersol, 1971) into the frequency spectrum. The two records are then "padded out" to 512 (2^9) samples

by adding zeros to the end of the records.

3.6 SUMMARY OF EQUIPMENT PERFORMANCE

Catheter laboratory measurements

Fig. 3.6 shows the complete arrangement for the measurements made during cardiac catheterisation using the catheter-tip flow probe and Millar pressure transducer. The flow system has a time delay of nominally 37 ms over the range 1 - 15Hz and the flow filter 33 ms, giving a total flow delay of 70 ms with reference to the unfiltered pressure signal. This has been corrected for in the data calibration programs for both frequency analysis and modelling. The characteristics of the filter results in an overall amplitude response -3dB at 10Hz and -8dB at 15Hz.

Post surgical measurements

Fig. 3.7 shows the system used for the measurements made in the intensive care ward after surgery. The flowmeter output has a response -3dB at 15Hz and a nominal time delay of 37 ms. The pressure system has a constant amplitude response in the main region of interest of 0 - 15Hz with no significant time delay. The 30Hz filters have the same effect on both signals and so cause no relative frequency or phase distortion of significance.

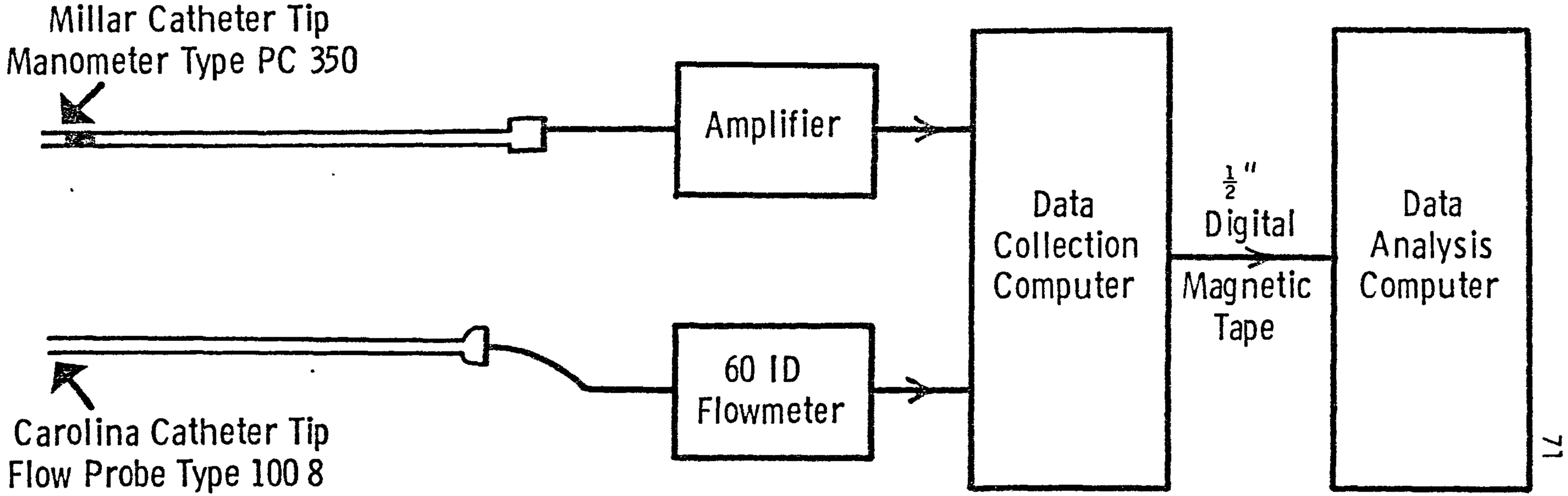

Fig 3.6 CATHETER LABORATORY PRESSURE - FLOW MEASUREMENTS WITH CATHETER TIP TRANSDUCERS.

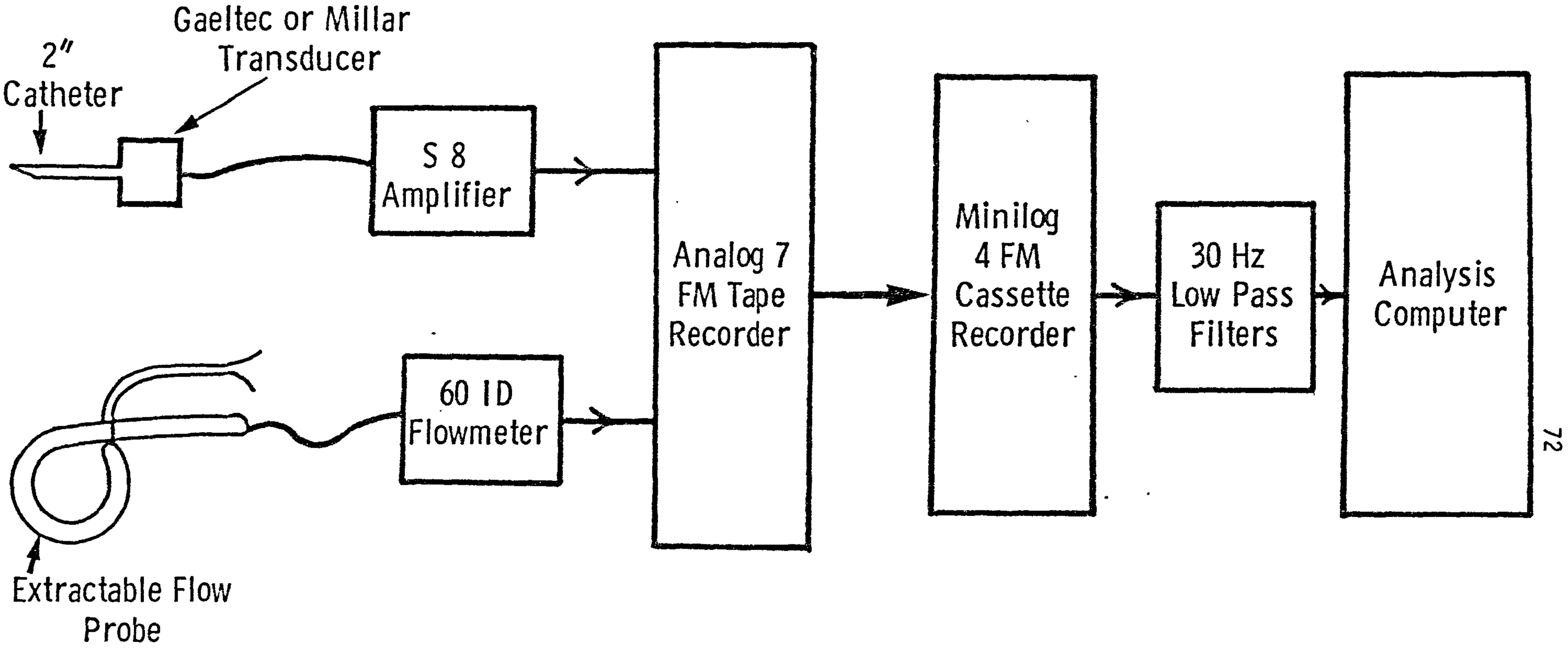

Fig 3.7 ARRANGEMENT FOR POST SURGICAL PRESSURE - FLOW MEASUREMENTS.

CHAPTER 4

THE DESIGN OF SUITABLE MODELS

4.1 SPECIFICATION

Digital computer simulation of the circulation has been used in preference to analogue models. This gives considerable flexibility in the choice of matching algorithms and has also enabled the performance of four different models to be studied. This would not have been possible using analogue techniques because of the time that it would have taken to construct each model and test it. However, digital models of any complexity are slow running so that the most detailed model has only been run on a limited number of patient recordings. The nature of the clinical measurements determined that a model of the arterial system was required which started at the ascending aorta and terminated in the peripheral vascular bed and able to simulate conditions in both the aorta and the femoral artery. The choices then left were the number of branches to be represented and the number and size of the segments which represented those branches.

An initial examination was made of the Beneken (1965) circulation model to gain some experience of the behaviour of models. Hyndman (1973) developed a digital version of this model and a Fortran program listing was available (Kitney, 1974). From this experience a model was designed using the anatomical data of Noordergraaf (1956) and subsequently revised (Westerhof et al., 1969), which is the basis for many other circulation models including those studied here. Two further models were examined, those of Aaslid (1974) and Snyder et al., (1968), both of which were

developed as analogue simulations. For these studies they have been converted to digital form represented by Fortran programs, of the same basic structure as that developed for the new model. Aaslid's version was specifically designed for clinical use and had been tested with the data from a substantial number of patients. It is a model of the complete circulation including the heart and pulmonary system and in this respect is similar to Beneken's with more detail in the vascular system. The model of Snyder et al. is of the arterial system only with more segmentation and branches than Aaslid's.

4.2 PRELIMINARY STUDY OF THE BENEKEN/HYNDMAN (1973) MODEL

In this model the circulation is divided into the compartments shown in fig. 4.1. The ventricles are simulated by generators in the Hyndman version which produce parabolic stiffness functions of time during systole. Periodic stiffness generators under steady conditions in a closed loop system of constant volume, eject the volume of blood that enters them, and so obey Starlings Law (Rothe, 1966). The systemic arterial section consists of two compartments each containing compliance and resistance, only the extra-thoracic region has an inertial term. None of Hyndman's nervous or humoral control system additions were used.

Some adjustable factors were added to the model so that it could be matched to patient measurements. Left ventricular force of contraction is controlled by a scaling factor for the systolic stiffness factor and the compliance of the two arterial segments are modified by a compliance scaling factor and similarly the peripheral resistance. The heart rate was controlled by adjusting the interbeat interval. The only other changes made to Hyndman's original program were those required to work with the particular input and output devices available on the Varian

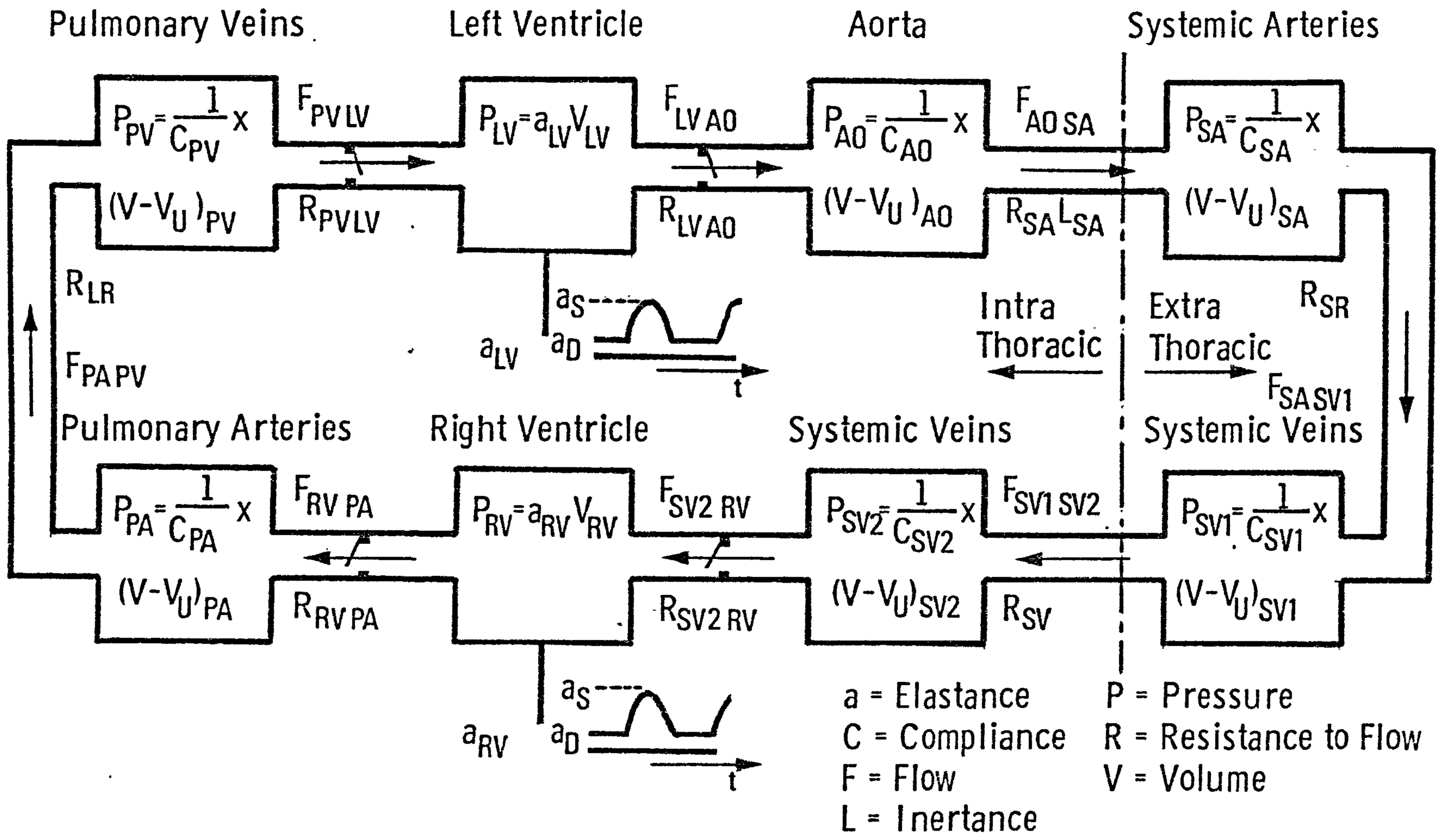

Fig 4.1 BENEKENS (1965) CIRCULATION MODEL.

computer. The resulting model was denoted HT03.

Steady state pressure and flow time - graphs, with the adjustable scaling factors set to 1.0, are shown in fig. 4.2. These appear to be the same as those published for the model confirming the validity of the program used. Some basic defects are immediately apparent by comparison with normal measurement (fig. 4.3). The left ventricular pressure has an abnormally high initial rate of rise and the peak is distorted apparently in association with the very high peak flow. These features indicate either that the left ventricular stiffness function is unrealistic or that the vascular load on the ventricle is abnormal. Examination of the aortic pressure shows that there is no dicrotic notch. This feature has usually been ascribed to the aortic valve being pushed back into the ventricle although there is some evidence that it may be partly the result of reflected pressure waves (Wemple, 1972). Neither effect would be represented by this model. The femoral artery pressure has a lower pulse, or peak to peak, amplitude than the aortic pressure, this only occurs in humans if there is a gross obstruction of the aorta. In any other case the femoral artery pulse pressure is markedly greater than that in the aorta, because of pressure wave reflections.

The model was next compared with recordings from a patient, P, who had triple vessel coronary artery disease. Catheters has been introduced into both femoral arteries permitting the simultaneous measurement of aortic pressure,with a Millar catheter tip manometer, and flow, with the catheter tip flow probe. Measurements were also made of left ventricular pressure alone, using the Millar manometer, while the heart was paced at 93 to 172 beats per minute with an atrial pacing

Fig. 4.2

Digital computer simulation of the original Beneken circulation model.

LVP = left ventricular pressure
AOP = aortic pressure
AOF = aortic flow
FAP = femoral artery pressure

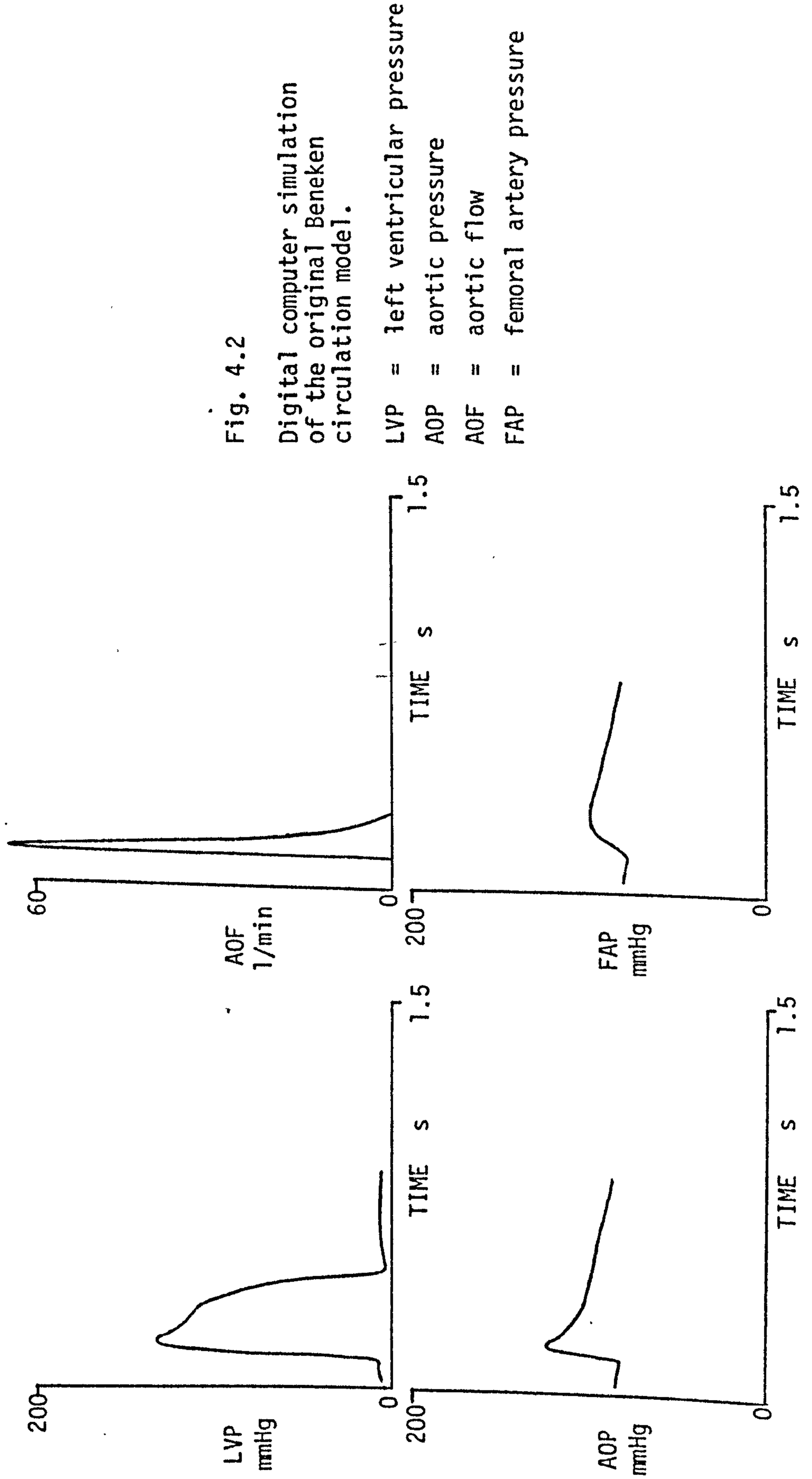

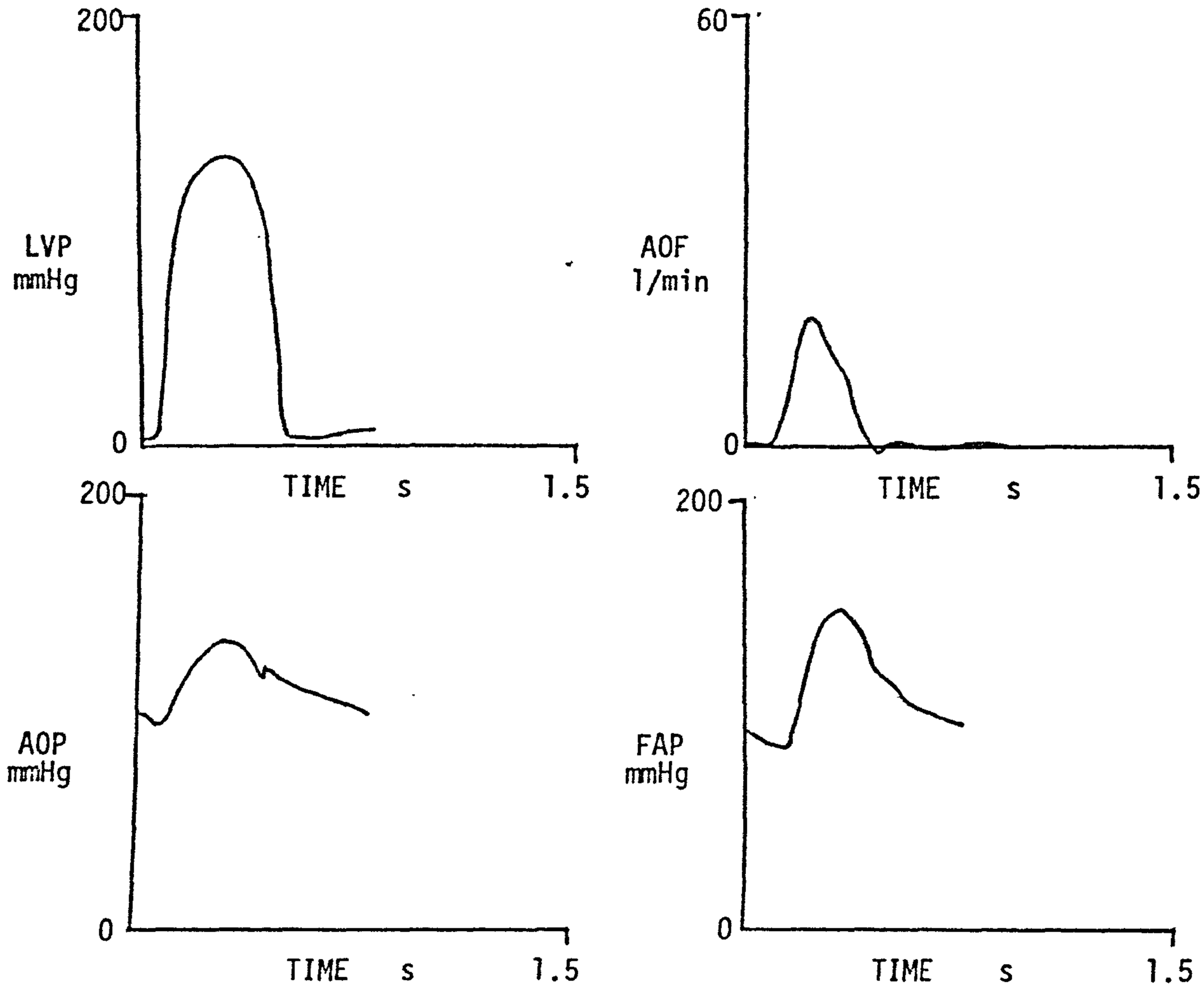

Fig. 4.3

Representative pressures and flows for a normal human constructed by reference to patient measurements.

LVP = left ventricular pressure

AOP = aortic pressure

AOF = aortic flow

FAP = femoral artery pressure

catheter. There were no signs of aortic valve defects in this patient. The pressure and flow time-courses were normal in appearance despite angiographic evidence that parts of the ventricle were not contracting properly (akinesia). The arterial measurements for one selected heart beat are shown in fig. 4.4 and the following values were calculated from them,

Patient P

beat to beat interval 0.849 s

stroke volume 67.1 ml

arterial pressures:

mean	118.0 mmHg	
systolic	162.5 mmHg	) pulse pressure 75.9 mmHg
diastolic	86.6 mmHg	)

The left ventricular stiffness generator in the Beneken model assumes a linear relationship between total mechanical systolic time, T_s, and the interbeat interval time, T_i of the form,

$$T_s = A\,T_i + B \quad \ldots\ldots\ldots\ldots\ldots\ldots \quad (4.1)$$

where A = 0.2 and B = 0.16 s. Mechanical systole is the time for which the ventricle is contracted and can be measured from the ventricular pressure as the time during which the pressure is elevated. From the pacing study on patient P the values for A and B in equation 4.1 were found to be 0.469 and 0.093 s respectively. This was further investigated by examining pacing studies on two more patients, M and G. Linear regression analysis of the results for the three

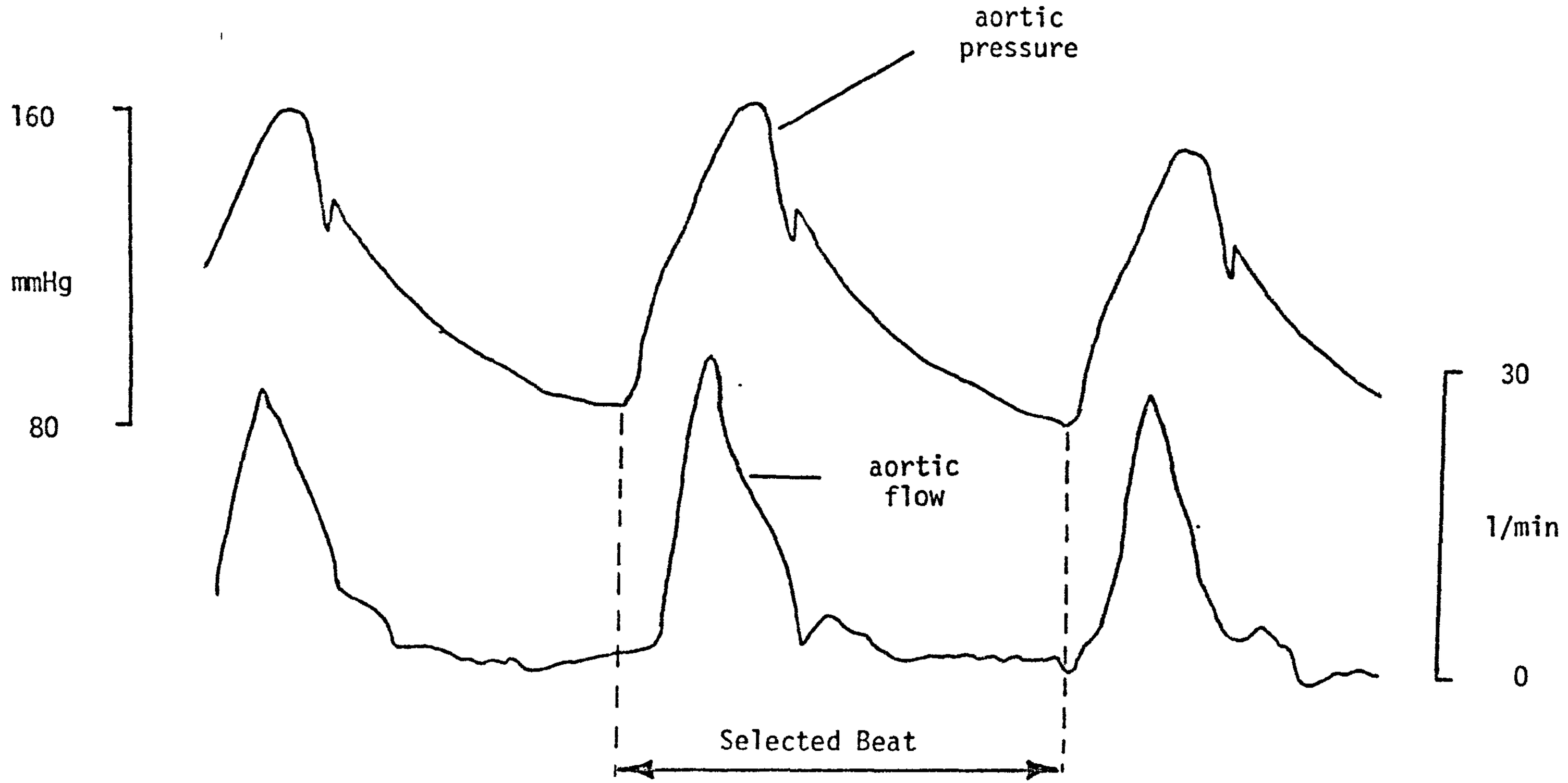

Fig. 4.4 Aortic pressure and flow recordings from patient P.

patients is shown in fig. 4.5. Fitting equation 4.1 the constant A ranges from 0.147 to 0.515 and B from 0.093 s to 0.258 s. These results indicate that a linear relationship as used by Beneken (1965) may be a valid representation for an individual patient at different heart rates. The variation in A and B between patients shows that there is little value in using this equation for single studies on different patients. For this reason the model was modified so that T_s was independently adjustable. For the recording of patient P pressure and flow T_s was calculated to be 0.491 s from the pacing study.

Tests on the model were carried out by adjusting arterial compliance, peripheral resistance and ventricular stiffness factor and attempting to match the results calculated from patient P. The model was run for five heart beats to achieve stable conditions after adjustment. The following criteria were applied in matching the model,

ventricular stiffness to match stroke volume

peripheral resistance to match mean aortic pressure

arterial compliance to match pulse aortic pressure.

Table 4.1 shows the results obtained from the best match that could be achieved, and are illustrated by the model outputs in fig. 4.6. Compared with the traces in fig. 4.4 the aortic pressure is clearly the wrong shape, with no dicrotic notch as was noted before. The femoral artery pulse pressure is slightly less than the aortic pulse pressure and the peak flow of 742 ml/s is much greater than the 481 ml/s measured in the patient. The aortic pressure and flow abnormalities indicate that the ventricular stiffness generator may be inadequate and

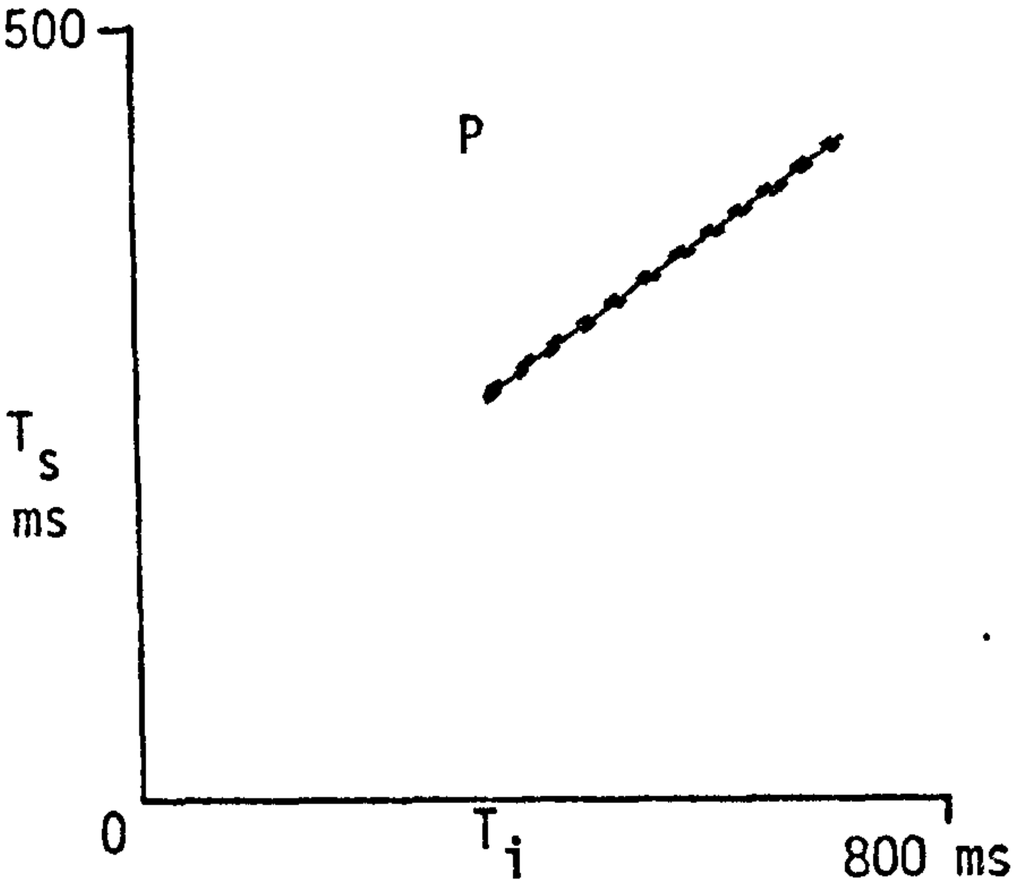

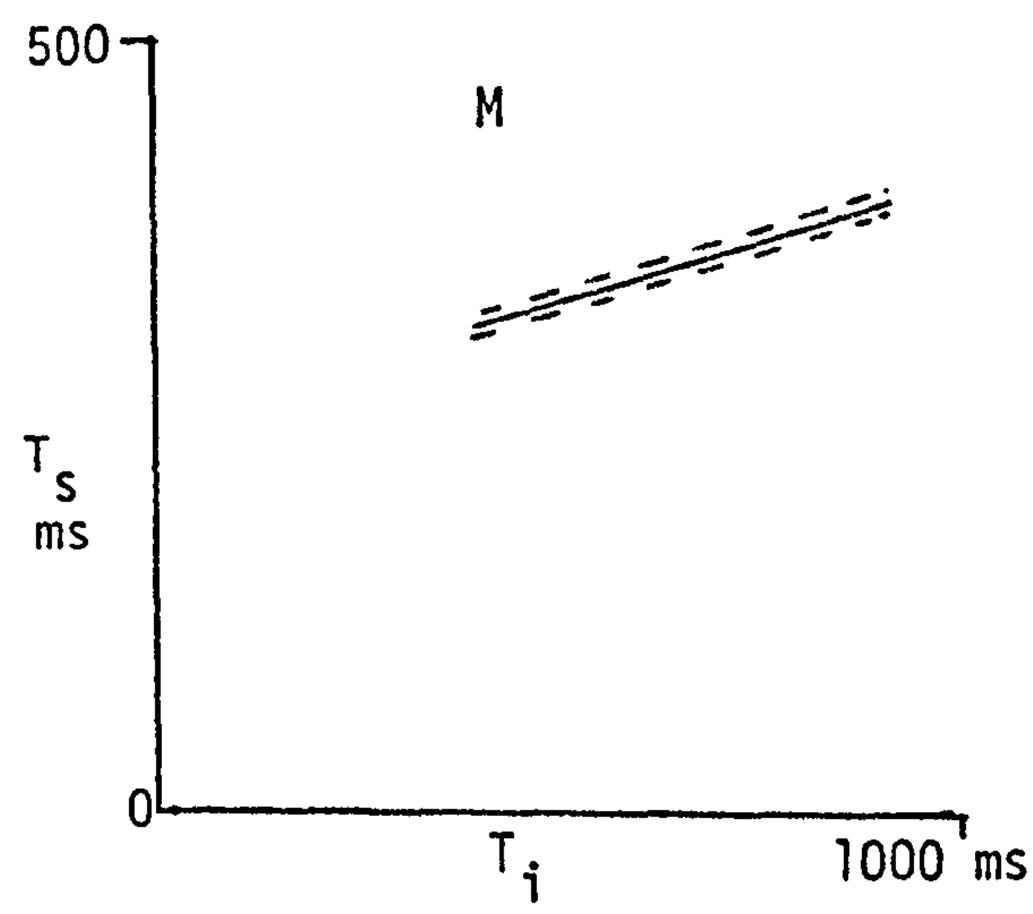

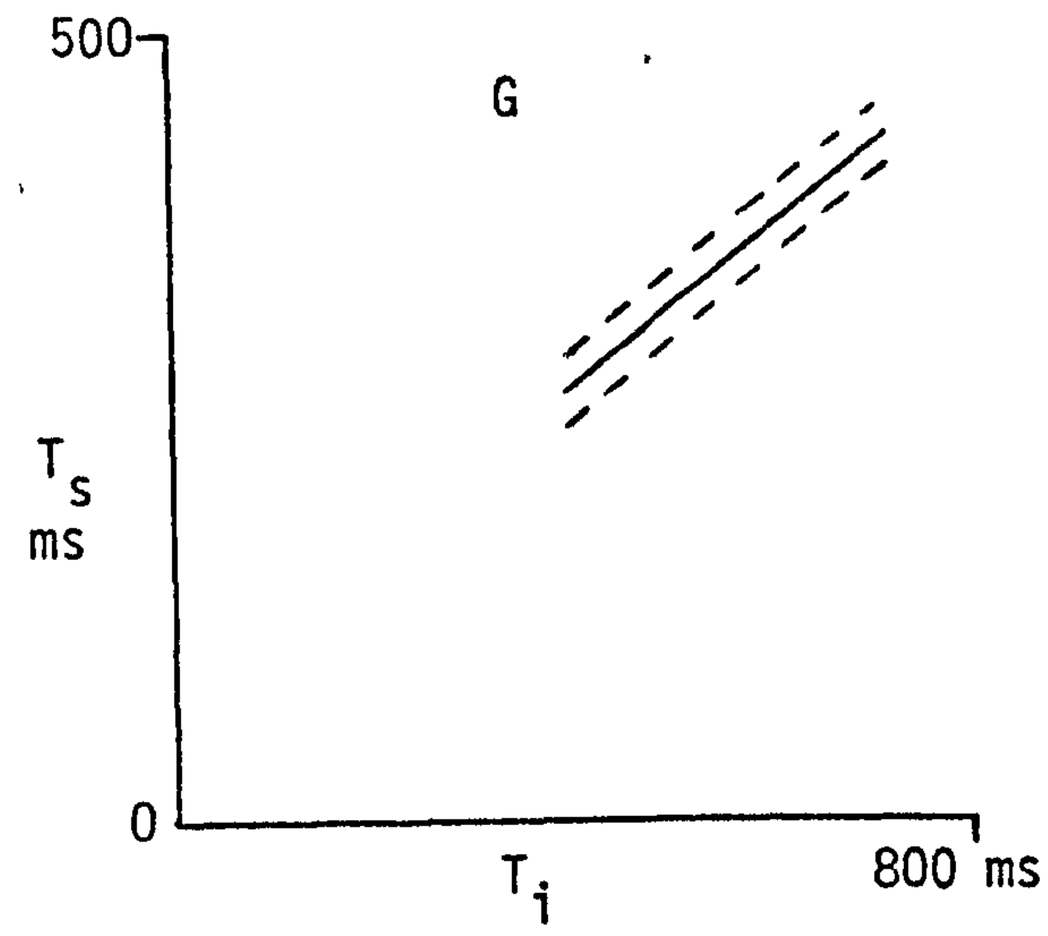

Fig. 4.5
Linear regression analysis of systolic time T_s against interbeat interval T_i. Dotted lines indicate $\pm$ 1 standard error.

	Aortic Pressures mmHg					
	Systolic	Diastolic	Mean	Pulse	Stroke Volume ml	Peak Flow ml/s
Patient P	162.5	86.6	118.0	75.9	67.1	481
Model	154.3	78.1	118.1	76.2	67.1	742

Table 4.1 Results from matching Benekens (1965) model to patient P.

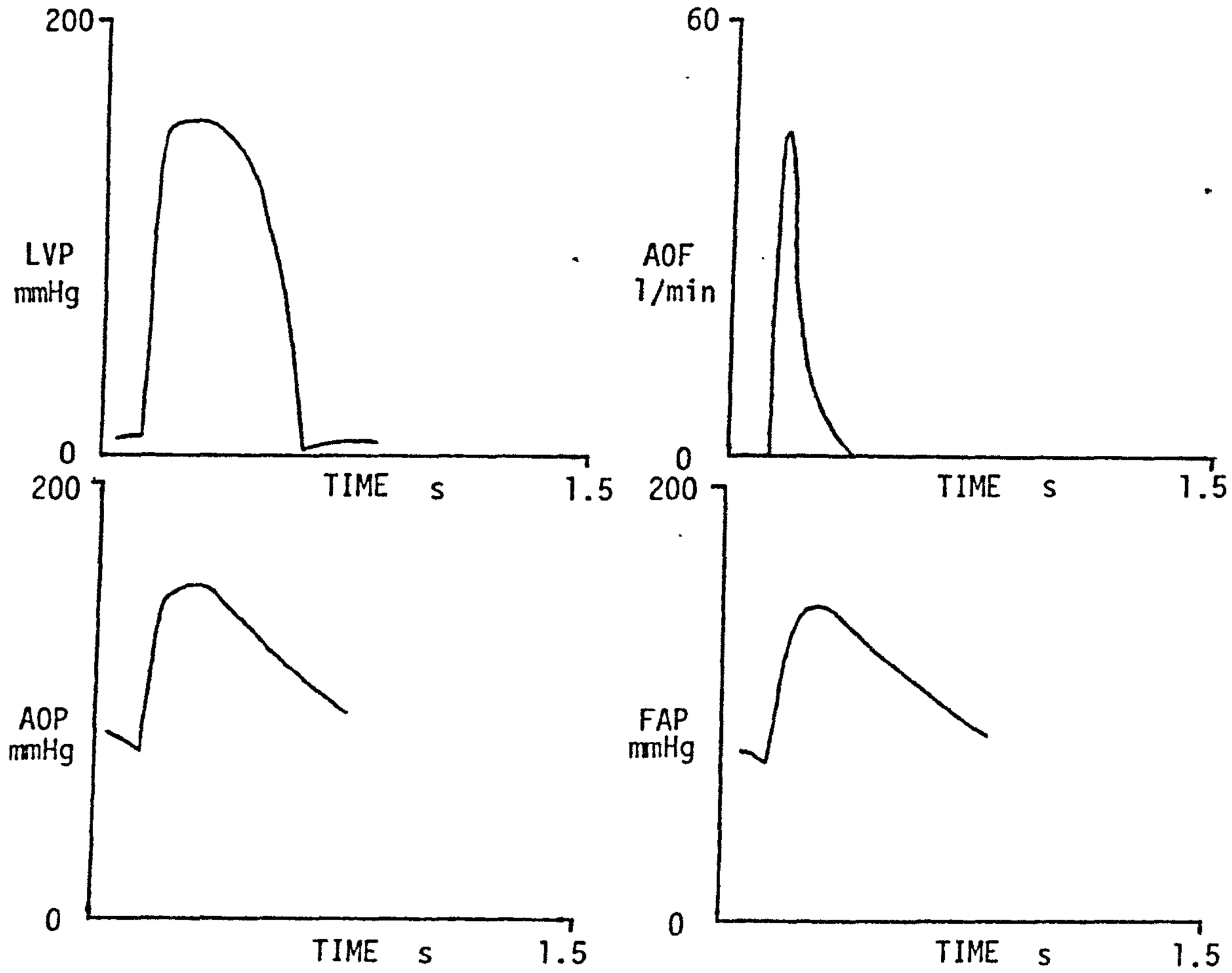

Fig. 4.6

Attempt to match the complete Beneken model to patient P by adjusting arterial compliance and peripheral resistance.

LVP = left ventricular pressure

AOP = aortic pressure

AOF = aortic flow

FAP = femoral artery pressure

it was therefore studied in more detail.

Cine-angiogram results from a patient J were used to examine ventricular stiffness. This patient was a 50 year old woman with trivial mitral valve disease and a normal left ventricular function. If the single plane cine-angiogram is assumed to be a section through an ellipsoidal ventricle the volume can be calculated (Greene, Carlisle, Grant and Bunnell, 1967). The graph shown in fig. 4.7 was produced on this basis by the cardiac laboratory cine-angiogram analysis system designed by Waldron (1974). From these results left ventricular stiffness, defined as pressure/volume, was plotted against time (fig. 4.8) and compared with the left ventricular pressure. The form of this stiffness function is very similar to the empirically determined relationship used by Snyder et al., fig. 4.9. An approximation to this was produced using exponential and cubic functions as shown in fig. 4.10 compared with the stiffness calculated for patient J. The function was incorporated into a modified form of Beneken's (1965) model with an improved version of the arterial model based on that of Aaslid (1974). The result shown in fig. 4.11 does not give a satisfactory left ventricular pressure. The stiffness generator approach was not further considered for three reasons.

1. Too many parameters are involved which would have to be adjusted to give a satisfactory function for each patient.

2. The stiffness function would have to be dependent on valve opening to give the characteristic shape shown in fig. 4.8. It would not be an independent driving function.

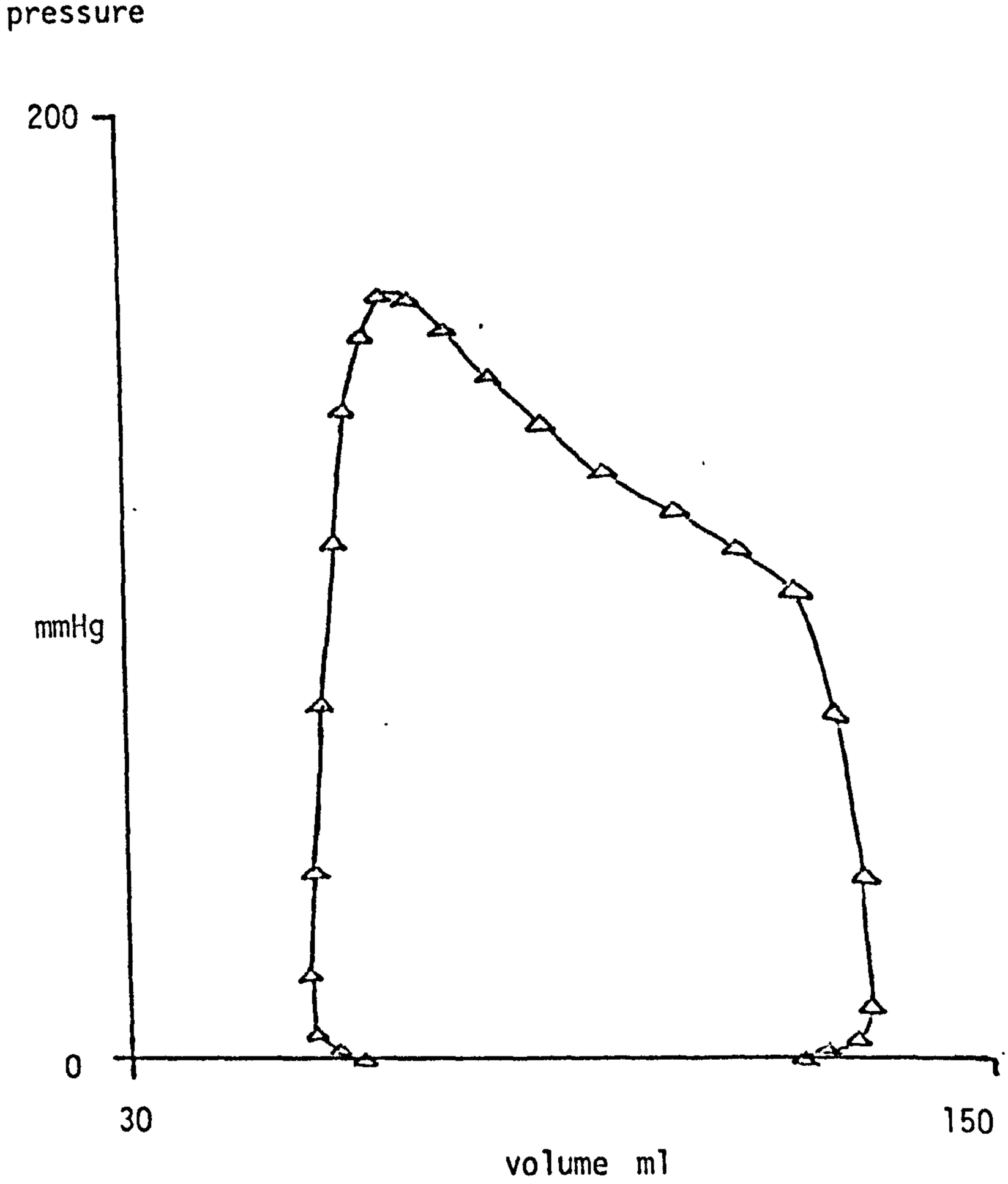

Fig. 4.7

The left ventricular pressure - volume relationship for patient J derived from a single plane cine-angiogram.

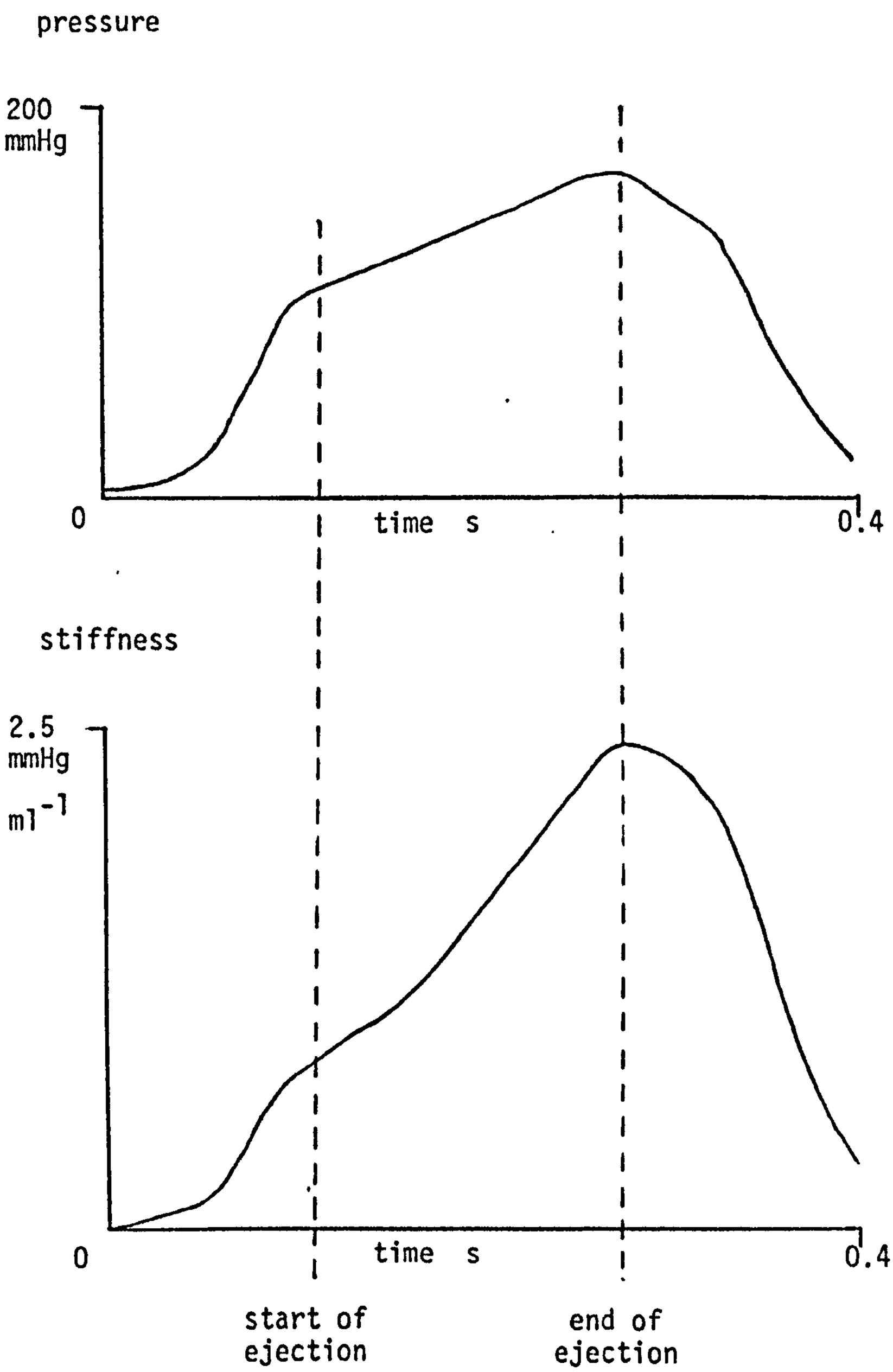

Fig. 4.8

The left ventricular stiffness function of patient J compared with the left ventricular pressure.

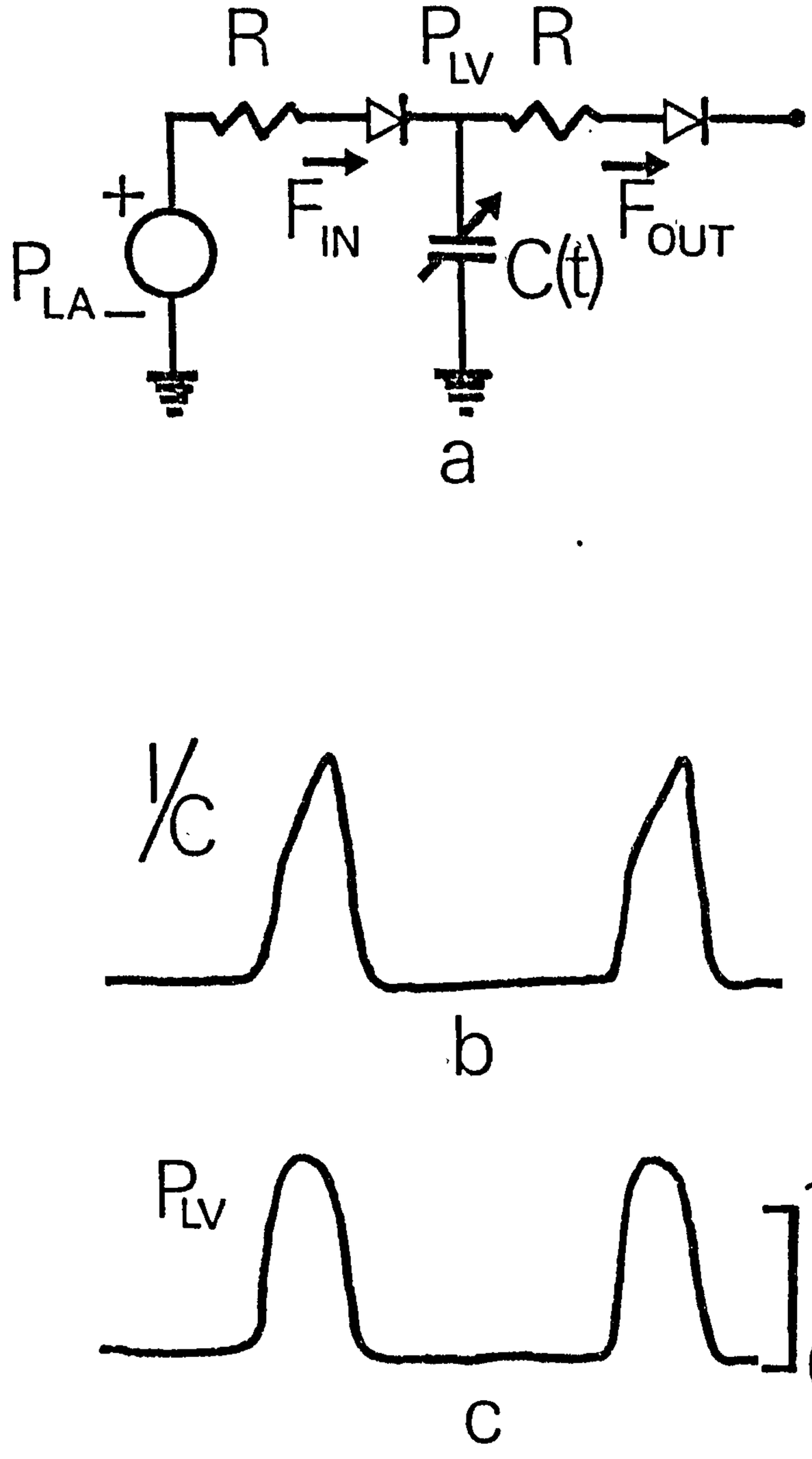

Fig 4.9 LEFT VENTRICLE SIMULATION OF SNYDER ET. AL. (1968) SHOWING (a) THE LEFT VENTRICLE MODEL INCORPORATING A COMPLANCE FUNCTION C, (b) THE STIFFNESS FUNCTION 1/C USED AND (c) THE RESULTING MODEL LEFT VENTRICULAR PRESSURE.

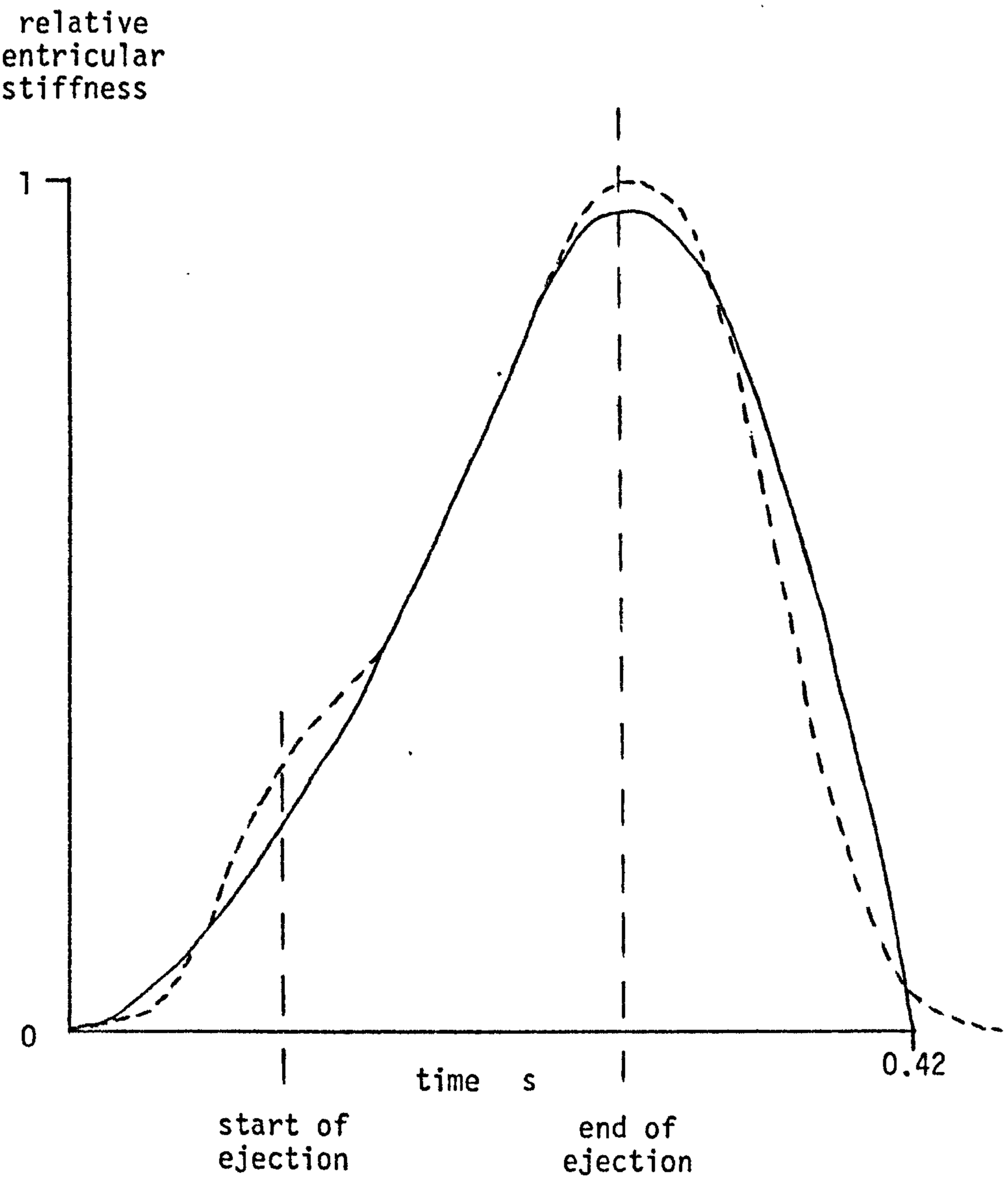

Fig. 4.10

Experimental ventricular stiffness - solid trace - compared with the angiographic measurements on patient J - dotted trace.

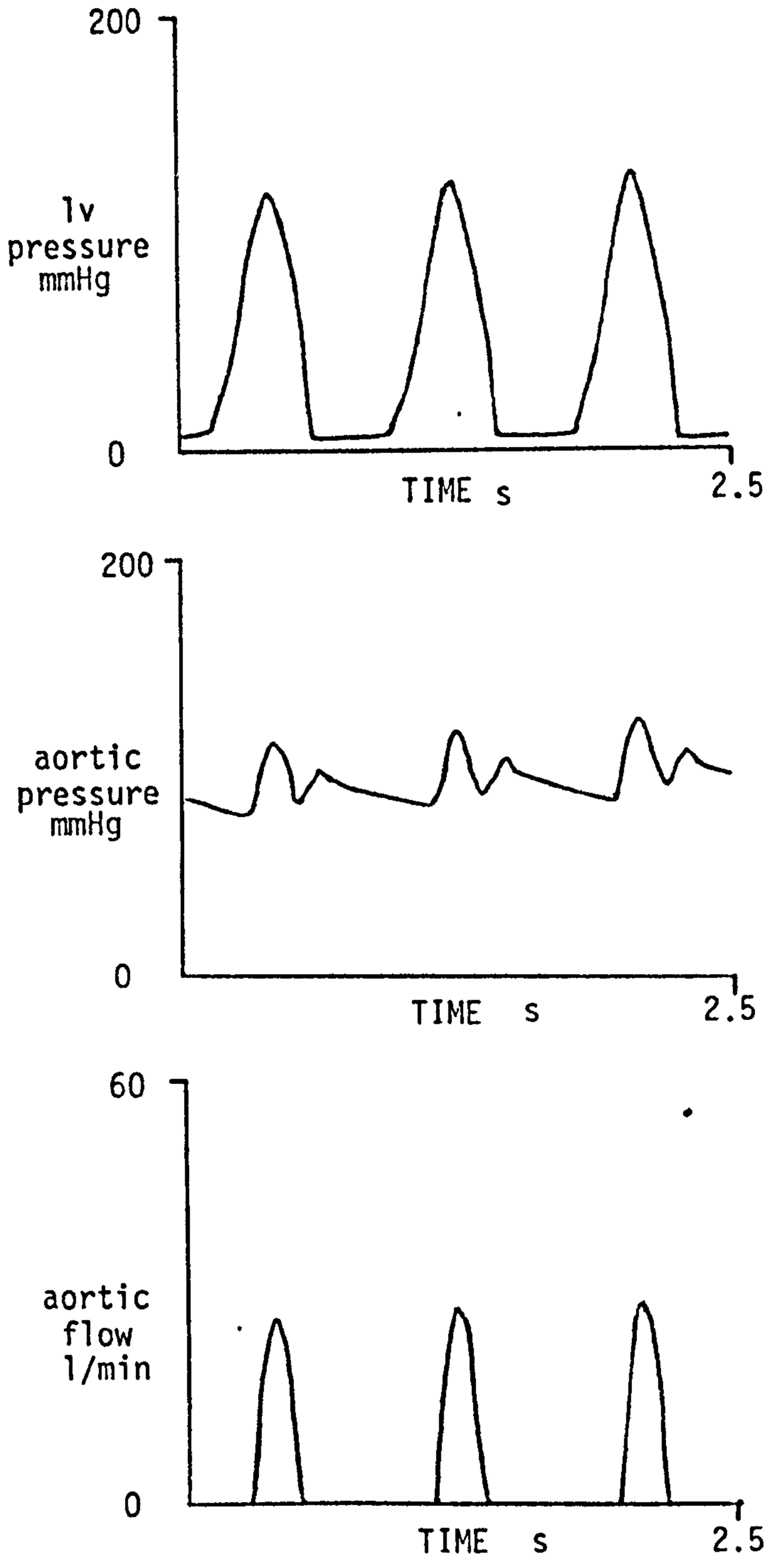

Fig. 4.11

The Beneken model with modified stiffness generator and arterial representation.

3. No simple relationship exists between volume stiffness and ventricular muscle properties hence stiffness does not give particular insight into ventricular physiology.

Possible defects in the Beneken (1965) arterial model were examined with a program using aortic flow, measured with the extractable flow probe, as a driving function. Only the systemic artery model was included, terminated by a peripheral resistance and a constant 10 mmHg venous pressure. The result is shown in fig. 4.12 for Beneken's original values of arterial compliance and peripheral resistance. An acceptable aortic pressure is now produced, compared with that shown in fig. 4.2, with a dicrotic notch, but there is no improvement in the femoral artery pulse pressure. This suggests that the input properties of the arterial model are satisfactory but that the requirement for pulse amplification down the artery cannot also be satisfied with so few compartments. The unusual left ventricular and aortic pressure shapes and the high peak aortic flow seem to be the result of defects in the ventricular model.

Summary

This study examined the suitability of Beneken's (1965) model for matching arterial pressure and flow measured in different patients. The model's deficiencies in this role can be summarised as follows;

1. the equation relating systolic time to interbeat interval does not allow for the variation between patients,

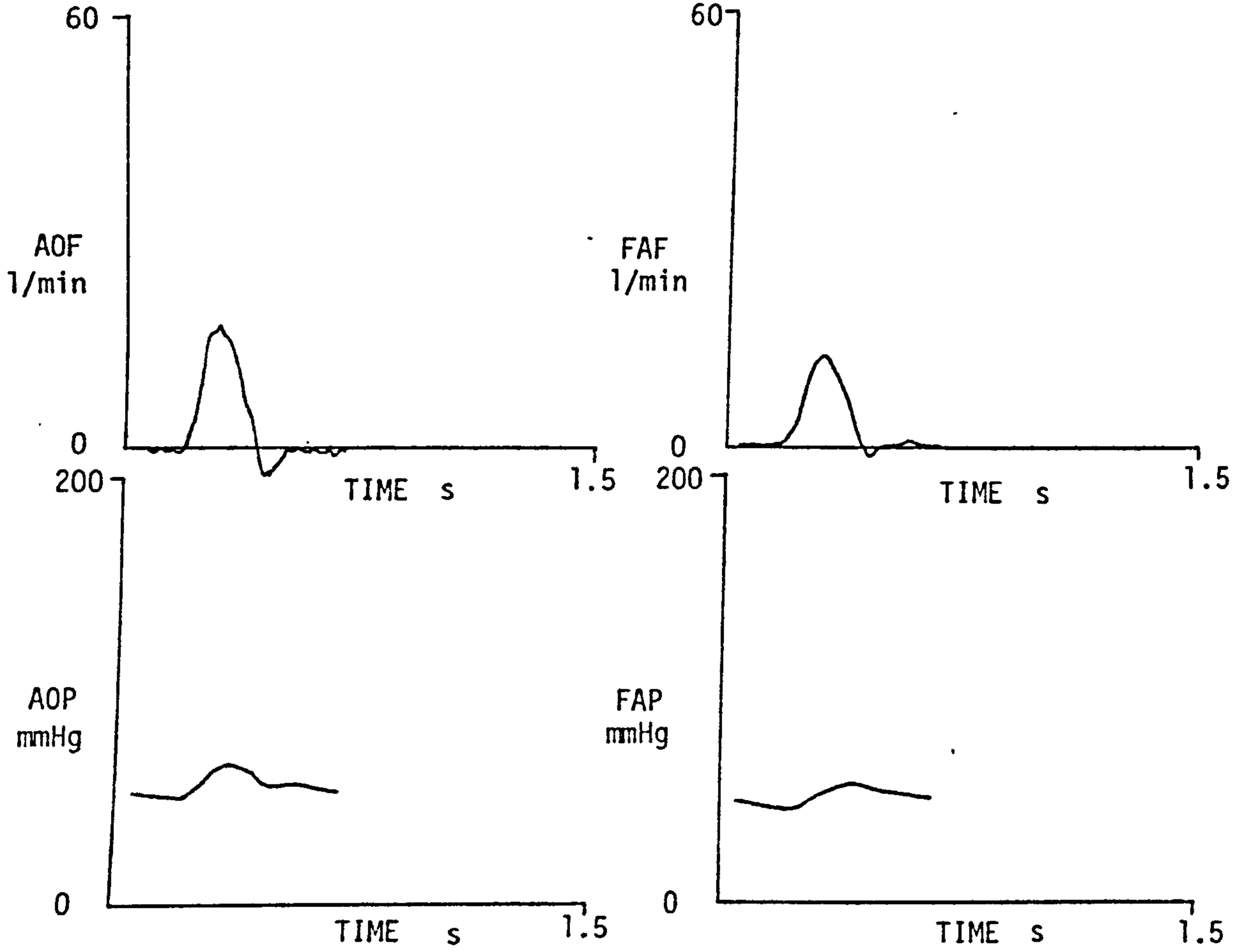

Fig. 4.12

The Beneken arterial model with a measured aortic flow as driving function.

AOF = aortic flow

AOP = aortic pressure

FAF = femoral artery flow

FAP = femoral artery pressure

2. a left ventricular simulation using a stiffness function would be complicated and not yield clinically significant information,

3. Beneken's two compartment arterial model may be satisfactory for aortic pressure and flow measured at the same site, it seems unlikely that this number of compartments would be able to reproduce the distribution of pressure down the artery.

The tests on the Beneken (1965) model in various forms have shown that, despite its limitations, the simple two compartment systemic arterial simulation may be a valid representation of the input properties of the aorta. This is relevant to the analysis of clinical data measured in the ascending aorta. There would be a considerable attraction in using a simple model of this type as the computational work involved in it is small. For this reason a digital version of the Beneken (ibid.) systemic arterial simulation was constructed based on the Hyndman (1973) program. No ventricular simulation was included, the model starts at the ascending aorta. The intra-thoracic and extra-thoracic arterial segments are used (fig. 4.1) together with the simple systemic vein simulation. Between the veins and arteries a peripheral resistance was included, R_S, which could be adjusted. The venous segment was terminated in a steady venous pressure P_{ven}. All the control mechanisms added by Hyndman (ibid.) were removed as before.

The model program was written in a form compatible with the overlay structure adopted for the analysis programs used with all the models and their variants. This required that the COMMON in the program and

its subroutines was written in a standard form. Appendix 1 gives a listing of the equation set for the model. The complete program was designated HT04 and its derivatives, given in appendix 3, HT041 etc.

In the remainder of this thesis the "Beneken model" will refer to this arterial simulation from the Beneken (1965) model, the "Aaslid model" to the arterial section of the Aaslid (1974) model and the "Snyder et al. model" to the simulation of Snyder et al. (1968).

4.3 A NEW MODEL DESIGN

The study of the Beneken model indicated the basic requirements for an arterial model for matching clinical measurements of aortic flow and aortic or femoral artery pressure. A useful ventricular model would have to be based on muscle physiology and be correspondingly complicated. The geometrical assumptions in the ventricle models of Beneken and Aaslid are not likely to hold in the presence of myocardial defects. It was concluded that such a model would increase the computational load without any diagnostic benefits. The simple stiffness generator used by Hyndman (1973) was rejected on the basis of the examination described in section 4.2. Instead it was decided to use the measured aortic flow itself as the input, or driving function, for the model.. The systemic venous system does not affect the pressure flow dynamics in the systemic arteries and as no dynamic venous measurements would be available clinically it was decided to terminate the arterial model with peripheral resistances and a steady venous pressure.

If no mean venous pressure measurement was made this was taken to be 10 mmHg.

The arterial part of the model designed by Aaslid seemed to be a good basis for a design to overcome the limitations of Beneken's original simulation. It is similar in some respects to the design of Beneken & de Wit(1967). Initially it was decided to simplify Aaslid's model by removing the damping factors as the basic improvement required was an increase in longitudinal detail, to give pressure pulse amplification. A model of this form was used for the test of the ventricular stiffness function described in the last section. However examination of the Aaslid model revealed that the derivation of the segment parameters from Noordergraaf's data was obscure so the segmentation was modified slightly and the parameters recalculated directly from the table of Westerhof et al. (1969). The segment compliances were taken directly from this table and the arterial resistances and inertia calculated using the equations 2.7 and 2.8 (Chapter 2) of Fry as used by Aaslid (1974). This model was designated HT11.

The systemic arteries were divided into the 11 segments shown in fig. 4.13 and each segment was described by equations of the form of 2.13 and 2.14, repeated here for convenience,

$$\frac{dF_n}{dt} = (P_{n-1} - P_n - F_n R_n)/I_n \quad \ldots\ldots\ldots\ldots \quad (2.13)$$

$$\frac{dP_n}{dt} = \frac{1}{\frac{1}{2}(C_n + C_{n+1})} (F_n - F_{n+1}) \quad \ldots\ldots\ldots \quad (2.14)$$

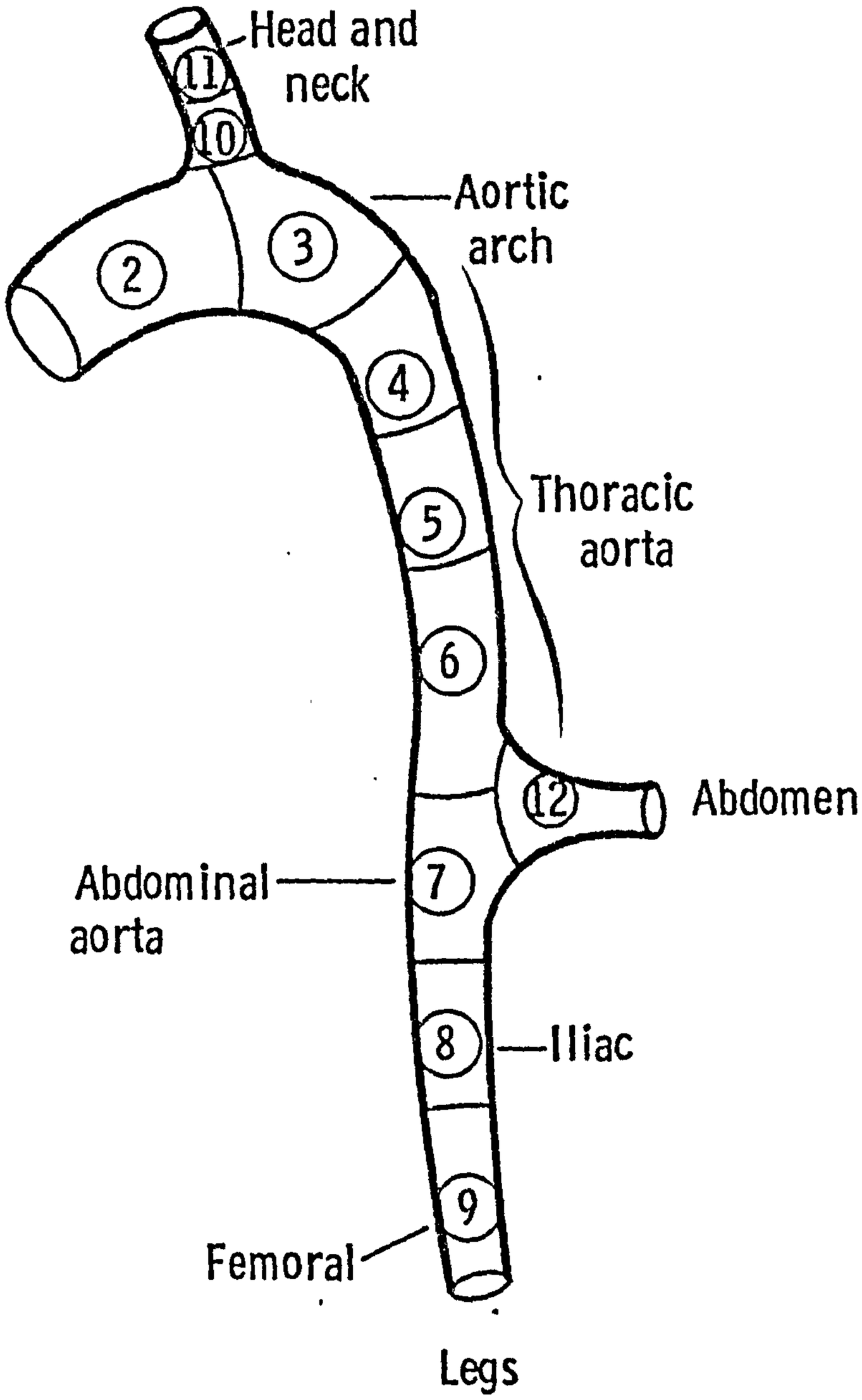

Fig 4.13 SEGMENTATION OF NEW ARTERIAL MODEL

where $\frac{1}{2}(C_n + C_{n+1})$ is the outlet compliance of segment n, C'_n .
For simplicity each segment incorporated a whole number of Westerhof et al. (1969) original segments as shown in Table 4.2. This makes it very easy to add extra detail from Westerhof et al. (ibid.) which might be required in any region to accept different measurements. Segment compliance resistance and blood inertia are shown in table 4.3 where I_A is the inertia scaling factor, one of the adjustable terms in the model, and has a nominal value of 1.0. Using the representation of equation 2.14, the compliances in this table are outlet compliances, that is the average of the compliance of the segment and of that following it. C_A is the compliance scaling factor, nominal value 1.0. The Fortran program for this model is given in appendix 1. Subroutine EQNS contains the equation for the arterial model and the following convention is used, for segment N,

X(1,N) = flow in segment

X(2,N) = outlet pressure

Z(1,N) = segment resistance

Z(2,N) = segment blood inertia

Z(3,N) = outlet compliance

The three branches of the model are terminated by three peripheral resistances,

R(1) = 11.2 R_s Legs

R(2) = 4.49 R_s Head

R(3) = 1.45 R_s Abdomen

where R_s is the overall scaling factor again with a nominal value of

Model Segment No.	Segment Length cm	Segments of Westerhof et al. (1969)
2	6	2A, 2B, 3A
3	3.9	3B
4	5.2	4A
5	5.2	4B
6	5.2	4C
7	15.9	5A, 5B, 5C
8	14.1	6A, 7A, 7B
9		8, 9
10		13A, 14A, 26, 27
11		14B, 15, 16, 17, 18, 19A
12		24A, 25AA, 20, 23, 25BA

Table 4.2 Composition of model segments.

Segment number	Resistance $\frac{mmHg}{ml^{-1}s^{-1}}$	Inertance $\frac{mmHg}{ml^{-1}s^{-2}}$	Compliance $\frac{ml}{mmHg^{-1}}$
2	0.302	0.964 I_A	0.133 C_A
3	0.365	0.942 I_A	0.0743 C_A
4	0.638	1.438 I_A	0.0564 C_A
5	3.071	3.156 I_A	0.317 C_A
6	3.684	3.457 I_A	0.0378 C_A
7	17.640	13.179 I_A	0.0302 C_A
8	91.322	19.573 I_A	0.0373 C_A
9	289.76	35.128 I_A	0.0207 C_A
10	2.187	1.464 I_A	0.0999 C_A
11	399.4	29.5 I_A	0.909 C_A
12	11.805	3.503 I_A	0.0093 C_A

Table 4.3 Arterial segment parameter values for the new arterial model HT11. C_A and I_A are nondimensional scaling factors with normal values of 1.

1.0. These resistances are based on those given by Beneken and de Wit (1967), normalised to give a total peripheral resistance of 1.0 for R_s = 1.0. This represents a reasonable base value giving a cardiac output of 100 ml/s (6 l/min) for an arterial-venous gradient of 100 mmHg. These resistances can vary a great deal in an individual patient as there can be considerable changes in the distribution of regional blood flow, the effects of this on the arterial haemodynamics are discussed in chapter 8.

C_A, R_s and I_A then form the model adjustments available for matching the model to records of patient measurements. Additional adjustments were incorporated in the version of the model used for input impedance studies to change the relative values of the three peripheral resistances.

Fig. 4.14 is a block diagram of the program. BEAT is a subroutine which runs the model for one heartbeat, calling DFSOLN to integrate the differential equations at steps of 2.5 ms. Four calls to DFSOLN provide the basic interval of 10 ms for the model. The program listed is one with a matching algorithm using the subroutine SEARCH. The driving function for the model is aortic flow which is input to the model from paper tape to array AOF.

4.4 THE AASLID MODEL

This model is also based on Noordergraaf's (1956) anatomical data, although it was not clear exactly how the arterial parameter values were arrived at, and incorporates wall damping and peripheral damping. Aaslid has shown that his model matches well with measurements of left

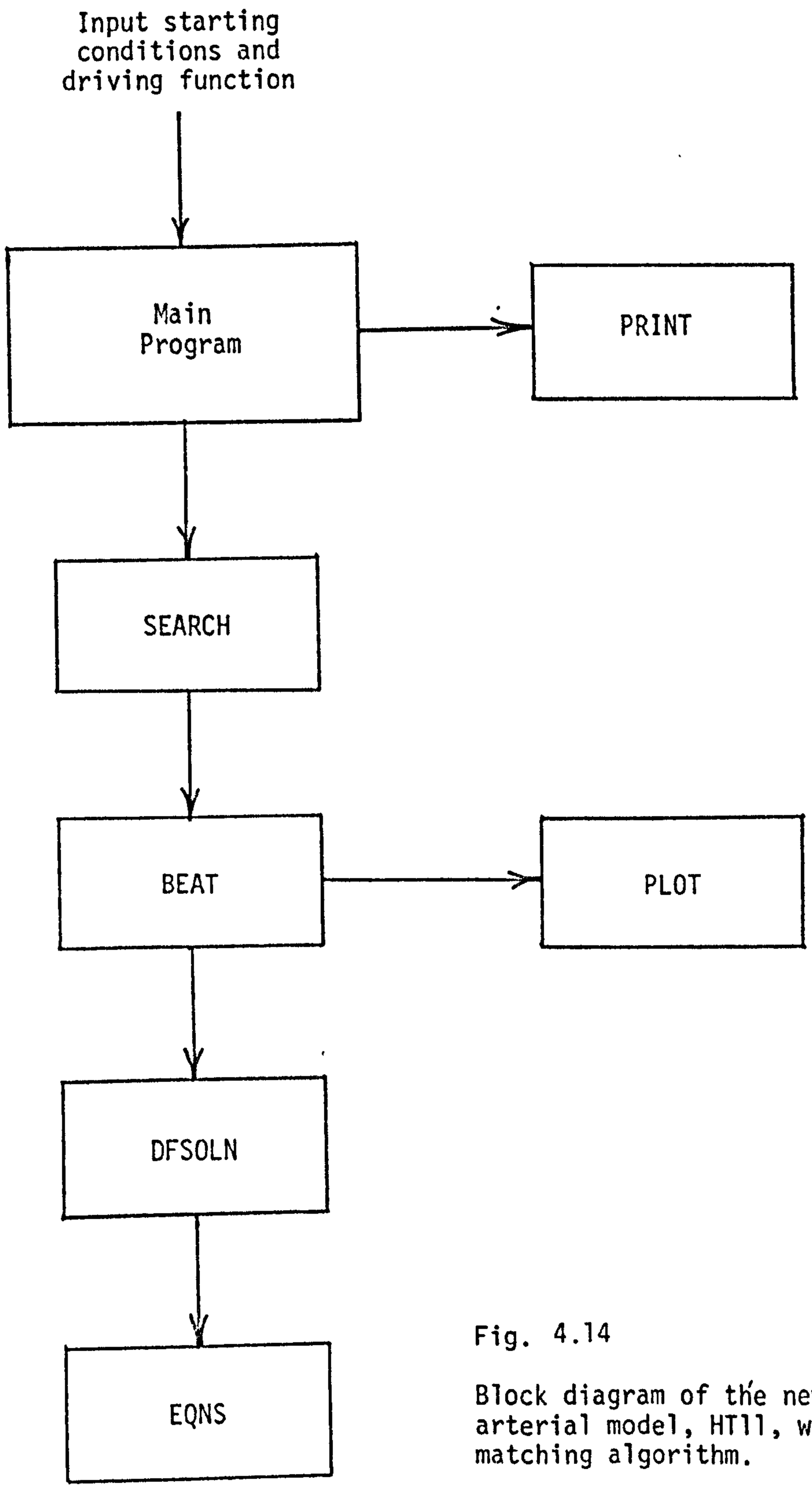

Fig. 4.14

Block diagram of the new arterial model, HT11, with matching algorithm.

ventricular and aortic pressure using a left ventricular model to generate flow. Only the arterial section of this model was used, with patient flow as an input and a constant venous pressure. The arterial segments are shown in fig. 4.15 and the arterial parameters in table 4.4. In addition to the adjustment to arterial compliance and peripheral damping provided by Aaslid, terms have been added to control blood inertia and arterial damping. The peripheral resistances for the models are given by,

$$R(1) = 10.0\ R_s \quad \text{legs}$$
$$R(2) = 4.0\ R_s \quad \text{head and neck}$$
$$R(3) = 1.62\ R_s \quad \text{abdomen}$$

Equation 2.14 has been modified to include the wall damping terms as follows,

$$\frac{dP_n}{dt} = \frac{1}{C'_n} \quad (F_n - F_{n+1}) + \left(\frac{dF_n}{dt} - \frac{dF_{n+1}}{dt}\right) D_n \qquad \text{..... (4.2)}$$

where D_n is the wall damping. This is equivalent to adding an additional pressure term P_d along the segment proportional to the rate of change of volume of the segment, $F_n - F_{n+1}$, so that,

$$P_d = (F_n - F_{n+1})\ D_n$$

giving,

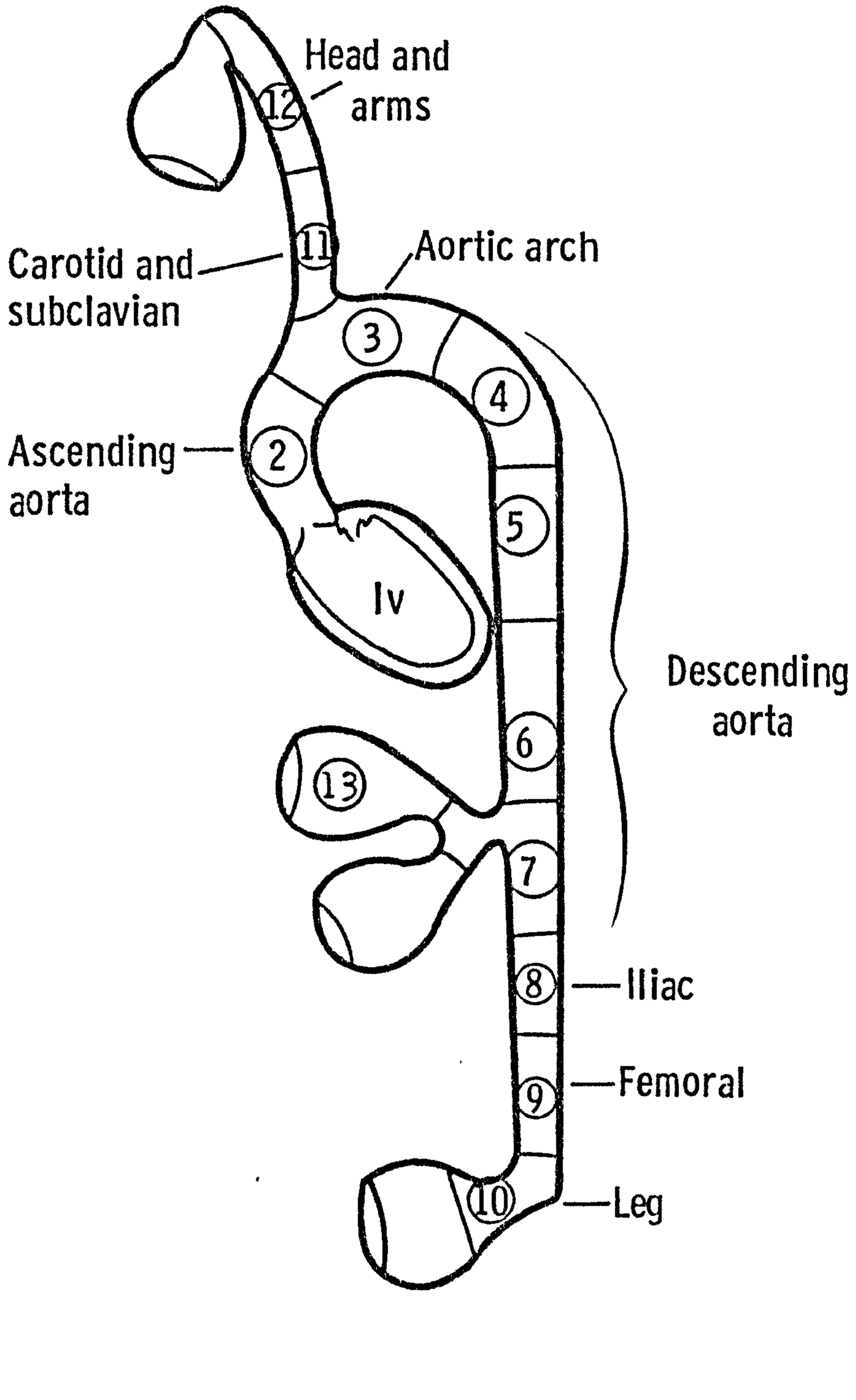

Fig 4.15 SEGMENTATION OF ARTERIAL MODEL OF AASLID (1974)

Segment number	Resistance mmHg $ml^{-1}s$	Inertance mmHg $ml^{-1}s^{2}$	Compliance ml $mmHg^{-1}$	Damping time constant s
2	0.0002	0.0006 I_A	0.23 C_A	0.01 T_A
3	0.0002	0.0008 I_A	0.23 C_A	0.007 T_A
4	0.0004	0.0013 I_A	0.17 C_A	0.005 T_A
5	0.0004	0.0013 I_A	0.17 C_A	0.005 T_A
6	0.0008	0.0021 I_A	0.12 C_A	0.005 T_A
7	0.0015	0.0027 I_A	0.08 C_A	0.005 T_A
8	0.006	0.005 I_A	0.032 C_A	0.005 T_A
9	0.02	0.009 I_A	0.03 C_A	0.01 T_A
10	0.04	0.013 I_A	0.1 + 0.11 C_A	0.15 T_P
11	0.01	0.006 I_A	0.04 C_A	0.01 T_A
12	0.04	0.013 I_A	0.15 + 0.17 C_A	0.33 T_P
13	0.01	0.006 I_A	0.10 + 0.11 C_A	0.1 T_P

Table 4.4

Arterial parameter values for Aaslid's (1974) model, HT13.

$$\frac{dP_d}{dt} = \left(\frac{dF_n}{dt} - \frac{dF_{n+1}}{dt}\right) D_n$$

A similar damping term in the last, or terminating, segment of each branch is incorporated. The damping terms are most conveniently expressed as time constants, $T_n = C'_n D_n$. The adjustment of arterial damping is additional to the variables used by Aaslid.

The complete equation set for this model is given in Appendix 1. The model was designated HT13.

4.5 THE SNYDER, RIDEOUT AND HILLESTAD MODEL

This is a model of the arterial system similar to that of Aaslid and including arterial but not peripheral damping. A small simplification was made, to reduce the number of equations, by lumping all the abdominal arteries together. The resulting segmentation, shown in fig. 4.16, has eight branches. The parameters for the main segments are given in table 4.5 and for the branches in table 4.6.

The arterial damping is given by the uniform time-constant $0.002\ T_A$. C_A, R_s, I_A and T_A are variables which have been introduced into the model to make it adjustable, when set to 1.0 the model parameters are those used by Snyder et al. (1968). The main arterial segments are represented by equations 2.13, 4.2 as for the previous model. The branches B1 to B8, which include no inertia term, each reduce to 2 resistances and a single compliance, fig. 4.17, where,

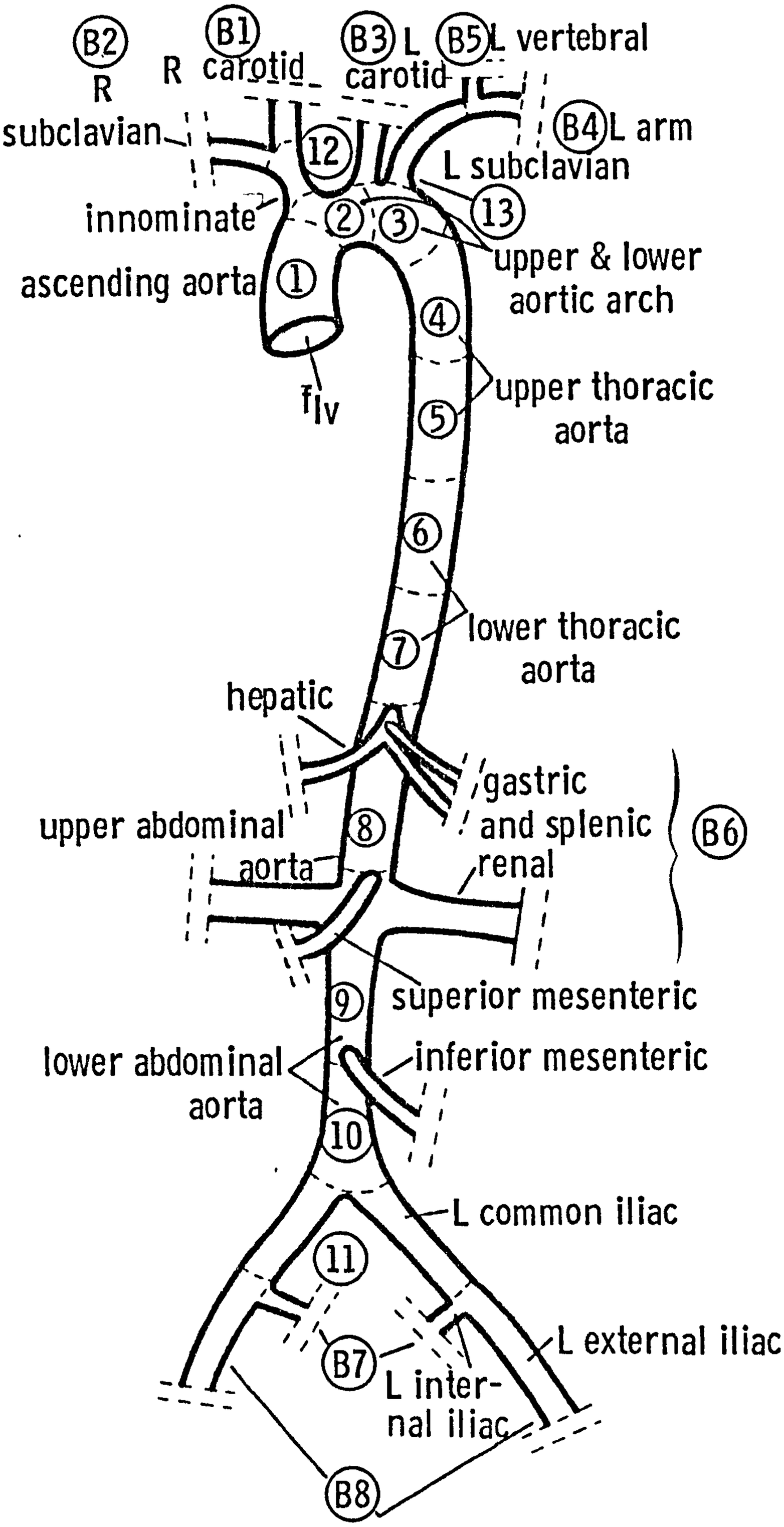

Fig 4.16 SEGMENTATION OF ARTERIAL MODEL OF SNYDER et al. (1968)

Segment number	Resistance mmHg $ml^{-1}s$	Inertance mmHg $ml^{-1}s^2$	Outlet Compliance ml $mmHg^{-1}$	Damping time constant s
1	0.000109	0.00159 I_A	0.0863 C_A	0.002 T_A
2	0.000034	0.000579 I_A	0.0613 C_A	"
3	0.000093	0.000986 I_A	0.0589 C_A	"
4	0.000185	0.00198 I_A	0.0744 C_A	"
5	0.000185	0.00198 I_A	0.0503 C_A	"
6	0.000262	0.00233 I_A	0.0262 C_A	"
7	0.000262	0.00233 I_A	0.0197 C_A	"
8	0.000278	0.00248 I_A	0.0764 C_A	"
9	0.000775	0.00415 I_A	0.00702 C_A	"
10	0.000775	0.00415 I_A	0.00697 C_A	"
11	0.00399	0.00625 I_A	0.0337 C_A	"
12	0.00275	0.00508 I_A	0.0411 C_A	"
13	0.0354	0.0474 I_A	0.0254 C_A	"

Table 4.5

Arterial segment parameter values for the model of Snyder et al., (1968) HT14.

Branch number	First segment resistance	Compliance	Second segment resistance
	mmHg $ml^{-1}s$	ml mmHg^{-1}	mmHg $ml^{-1}s$
1	1.51	0.0821	6.02 R_S
2	1.45	0.1599	5.79 R_S
3	1.51	0.0821	6.02 R_S
4	3.01	0.0657	12.0 R_S
5	2.75	0.0657	11.0 R_S
6	0.404	0.4431	1.62 R_S
7	3.76	0.0449	15.8 R_S
8	2.11	0.1948	8.28 R_S

Table 4.6

Branch parameter values for the model of Snyder et al. (1968) HT14.

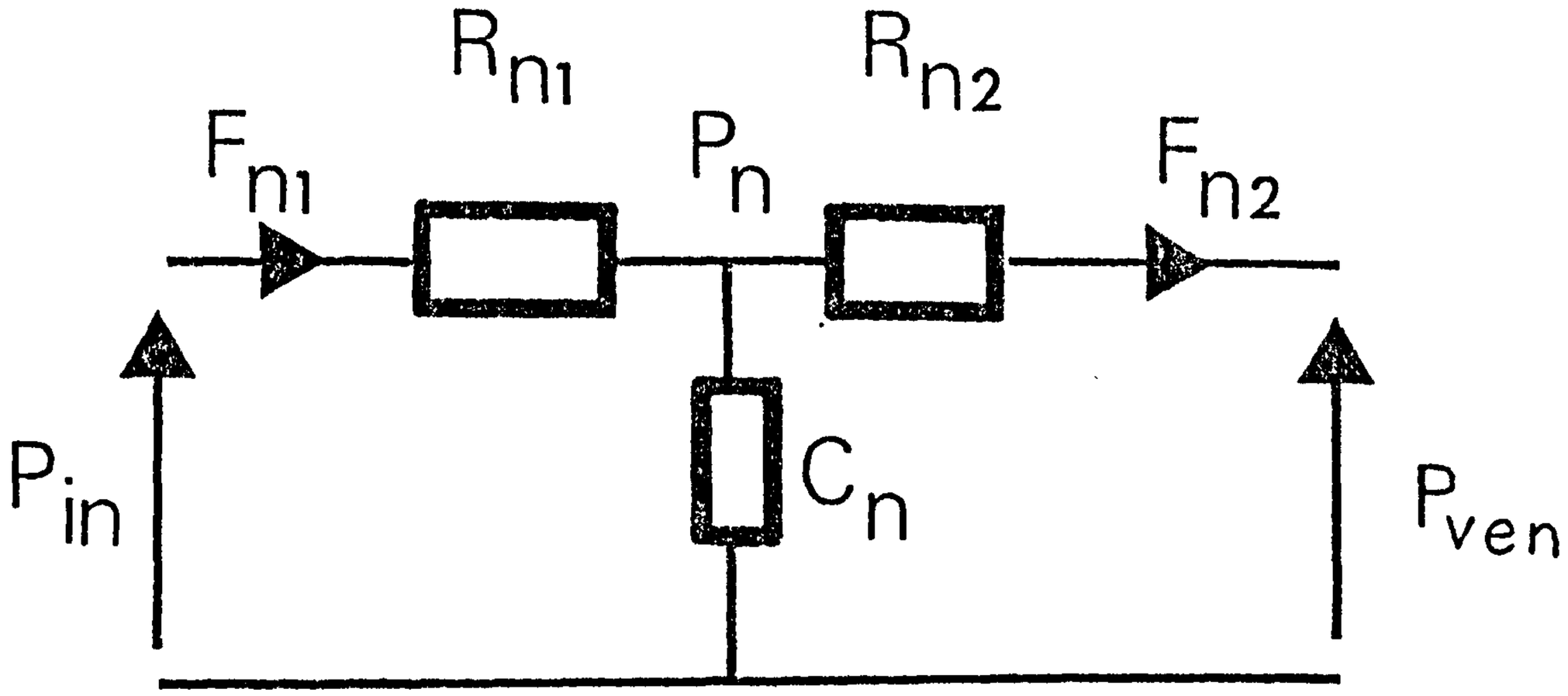

$$C_n = \left[\tfrac{1}{2} \left(C_1 + C_2 \right) \right]_n$$

Fig 4.17 SEGMENT STRUCTURE FOR BRANCHES
IN MODEL OF SNYDER ET. AL. IN DIGITAL FORMULATION.

$$F_{n1} = \frac{P_{in} - P_n}{R_{n1}} \qquad \ldots\ldots\ldots\ldots\ldots\ldots \quad (4.3)$$

$$F_{n2} = \frac{P_n - P_{ven}}{R_{n2}} \qquad \ldots\ldots\ldots\ldots\ldots\ldots \quad (4.4)$$

$$\frac{dP_n}{dt} = \frac{F_{n1} - F_{n2}}{C_n} \qquad \ldots\ldots\ldots\ldots\ldots\ldots \quad (4.5)$$

In the program, the terms in equations 4.3 to 4.5 are represented by,

$$XB(n) = P_n$$

$$ZB(1,n) = R_{n1}$$

$$ZB(2,n) = C_n$$

$$ZB(3,n) = R_{n2}$$

The complete equation set for the model is given in Appendix 1, equations 4.3 and 4.4 are represented by the Fortran statement functions, FN1 and FN2. This model was designated HT14.

4.6 TESTING THE MODEL CONFIGURATIONS

A computer program has one important similarity with an experimental procedure, until it is tested it cannot be trusted. With structured programming languages it is possible to verify the logical paths through a program for all data input. Apart from the fact that Fortran is not such a language, complex formulae are not so readily tested. In a simulation model program with many formulae, mistakes in programming cannot be dismissed as avoidable carelessness but must

be assumed present and eliminated by careful testing. For a model where there is no tabulated output data, complete verification is not possible, ultimately it must be accepted that the results presented are those for the programs used. At least with a digital computer it is possible to make these actual programs available for use elsewhere.

The logical sequence of the models is quite simple and most errors are obvious by their catastrophic results. The most persistent errors are those resulting from scaling errors, especially in the minor parameters such as damping factors. Some errors of entering program information are revealed as syntax errors upon compilation of the program. Once each model would run in a reasonable manner, producing sensible results, the following tests were carried out. Tests on the differential equation solving algorithm are described in chapter 5.

Time Domain Behaviour

A recorded flow waveform was used as the driving function for each model. The resulting time course of arterial pressures was examined and checked to be reasonable compared with normal human circulatory behaviour.

Response to constant flow input

Each model was run with a constant flow of 100 ml/s as a driving function. The flows and pressures for each branch of the model were printed out and examined. These are shown in tables 4.7 to 4.10. The models were in each case run for 10 heartbeats, which was sufficient for the models to reach a steady state. The fact that the models

Arterial segment	Outlet pressure mmHg	Flow ml s^{-1}
intra-thoracic	114.6	98.6
extra-thoracic	104.6	

Table 4.7

Arterial segment pressures and flow for the Beneken arterial model with a constant 100ml s^{-1} flow input. Note that there is a constant 4 mmHg pressure gradient between intra-thoracic and extra-thoracic regions.

Arterial segment	Outlet pressure mmHg	Flow ml s^{-1}
2	113.1	100.0
3	113.0	78.9
4	113.0	78.9
5	112.8	78.9
6	112.5	78.9
7	112.3	8.8
8	111.5	8.8
9	108.9	8.8
10	113.0	21.1
11	104.6	21.1
12	111.6	70.1

Table 4.8

Arterial segment pressures and flows in the new model, HT11, with a constant 100 ml s^{-1} flow input.

Arterial segment	Outlet pressure mmHg	Flow ml s^{-1}
2	114.3	100.0
3	114.3	74.2
4	114.3	74.2
5	114.2	74.2
6	114.2	74.2
7	114.1	10.3
8	114.1	10.3
9	113.9	10.3
10	113.5	10.3
11	114.0	25.8
12	113.0	25.8
13	113.5	63.9

Table 4.9

Arterial segment pressures and flows in the Aaslid model, with a constant 100 ml s^{-1} flow input.

Arterial segment	Outlet pressure mmHg	Flow ml s^{-1}
1	94.5	100.0
2	94.5	77.1
3	94.5	54.2
4	94.5	54.2
5	94.5	54.2
6	94.5	54.2
7	94.5	54.2
8	94.5	54.2
9	94.5	12.4
10	94.4	12.4
11	94.4	12.4
12	94.5	22.9
13	94.1	11.7

Table 4.10

Arterial segment pressures and flows in the Snyder et al. model with a constant 100 ml s^{-1} flow input.

continued over/

Branch	Pressure mmHg
1	77.5
2	77.6
3	77.6
4	77.3
5	77.3
6	77.6
7	78.2
8	77.3

Table 4.10 continued

Arterial segment pressure and flows in the Snyder et al. model with a constant 100 ml s^{-1} flow input.

would produce constant values of pressure and flow itself indicated that they had a fundamental similarity with the real circulation. Continuity of flow was confirmed by checking that the flow along each branch, between junctions with other branches, was constant. At each junction the sum of the outlet flows was confirmed as being equal to the sum of the inlet flows.

Pressure equilibrium was checked by noting that there were no abrupt changes in pressure at junctions and that the pressure gradients along branches were no more than a few mmHg.

Input impedance

The arterial input impedances were measured using an impedance response test. The resulting amplitude and phase plots were compared with the published values for the models to ensure that there were no gross discrepancies. Figs. 4.18 and 4.19 indicate, within the limits of the published data, that the digital representation of Beneken's model accurately reproduces the behaviour of the original analogue simulation. Fig. 4.20, for Aaslid's model, shows a small peak in the amplitude response at about 6 Hz in the digital version for which the corresponding peak in the analogue model is about 10 Hz. The phase responses, fig. 4.21, have larger differences above 3 Hz. Figs. 4.22 and 4.23 show similar deviations in the digital version of the Snyder et al. model from the original analogue formulation. In general the digital computer realisations of these models appears to be accurate at the lower frequencies. The higher frequency performance may indicate the effect of component tolerances in the original analogue circuits. Fig. 4.24 shows for comparison the input impedance of the new model.

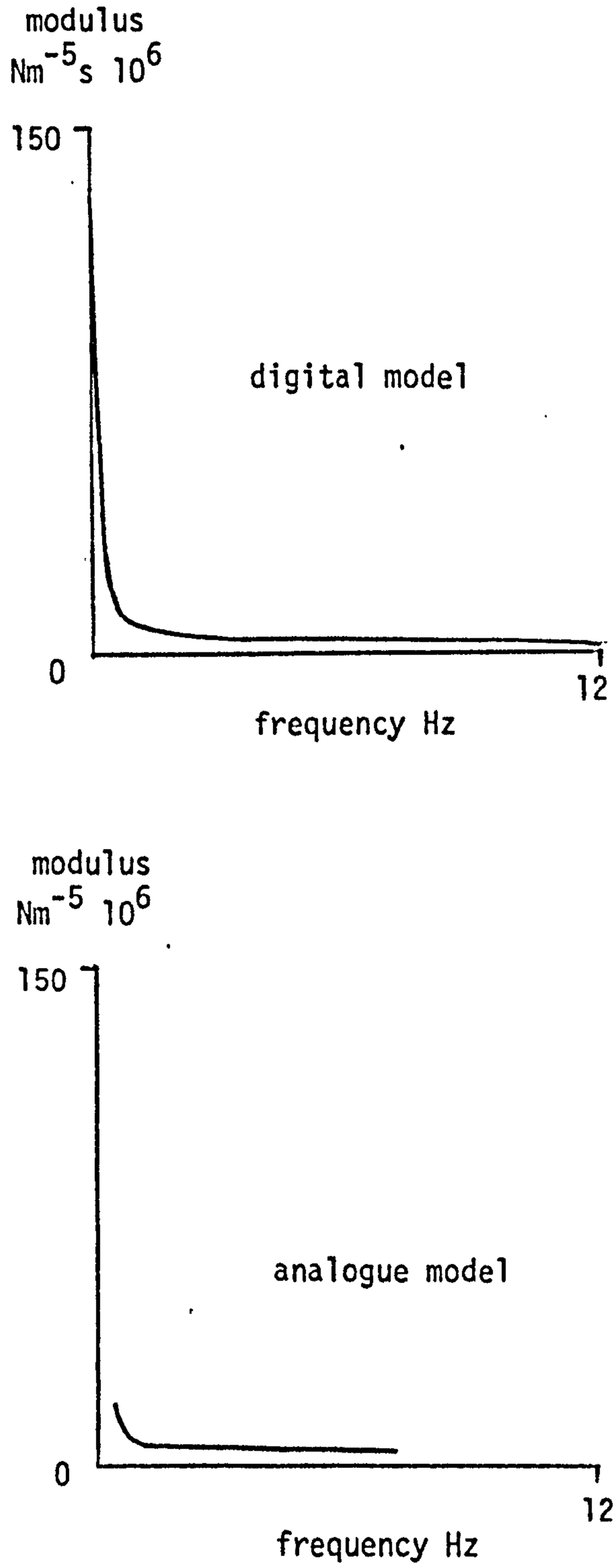

Fig. 4.18

Comparison of the input impedances of the digital version of Beneken's model, HT04, and the published response of the original analogue model.

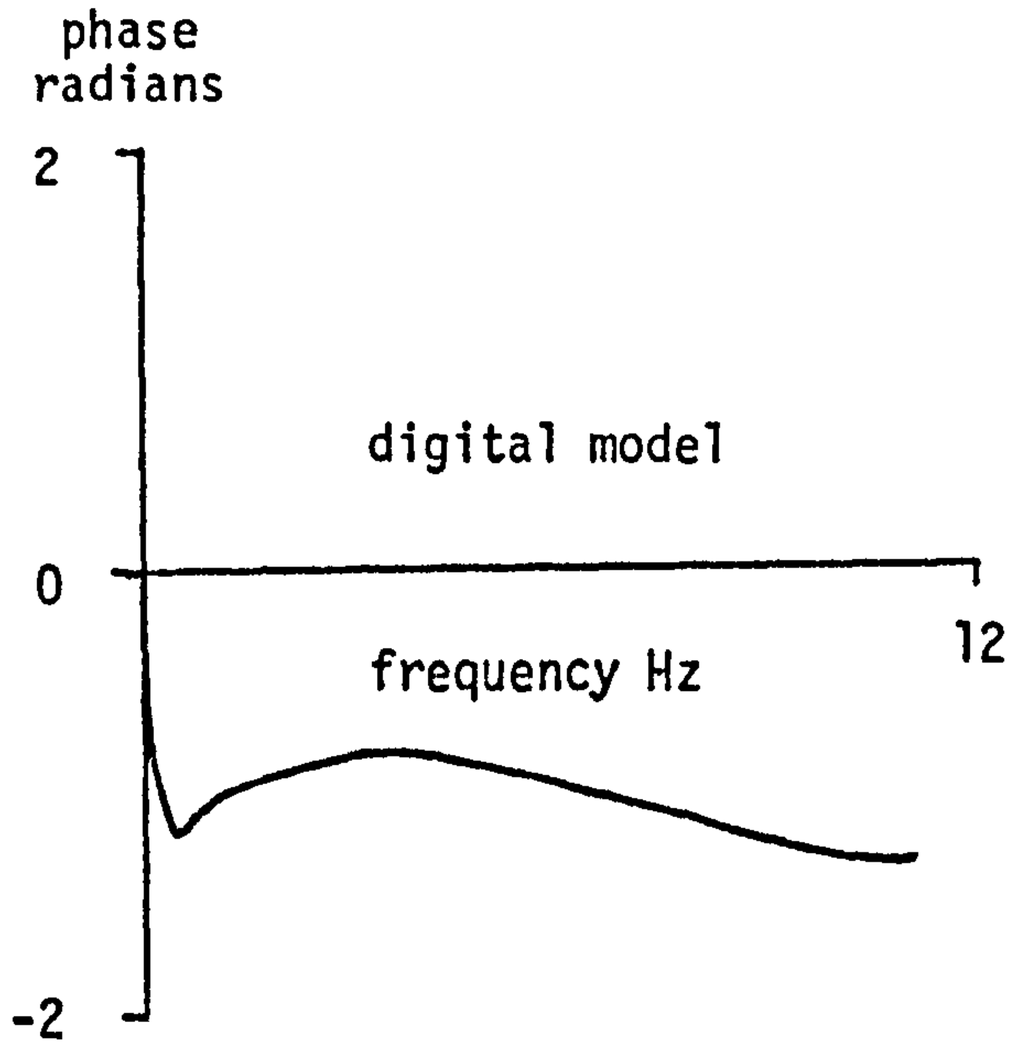

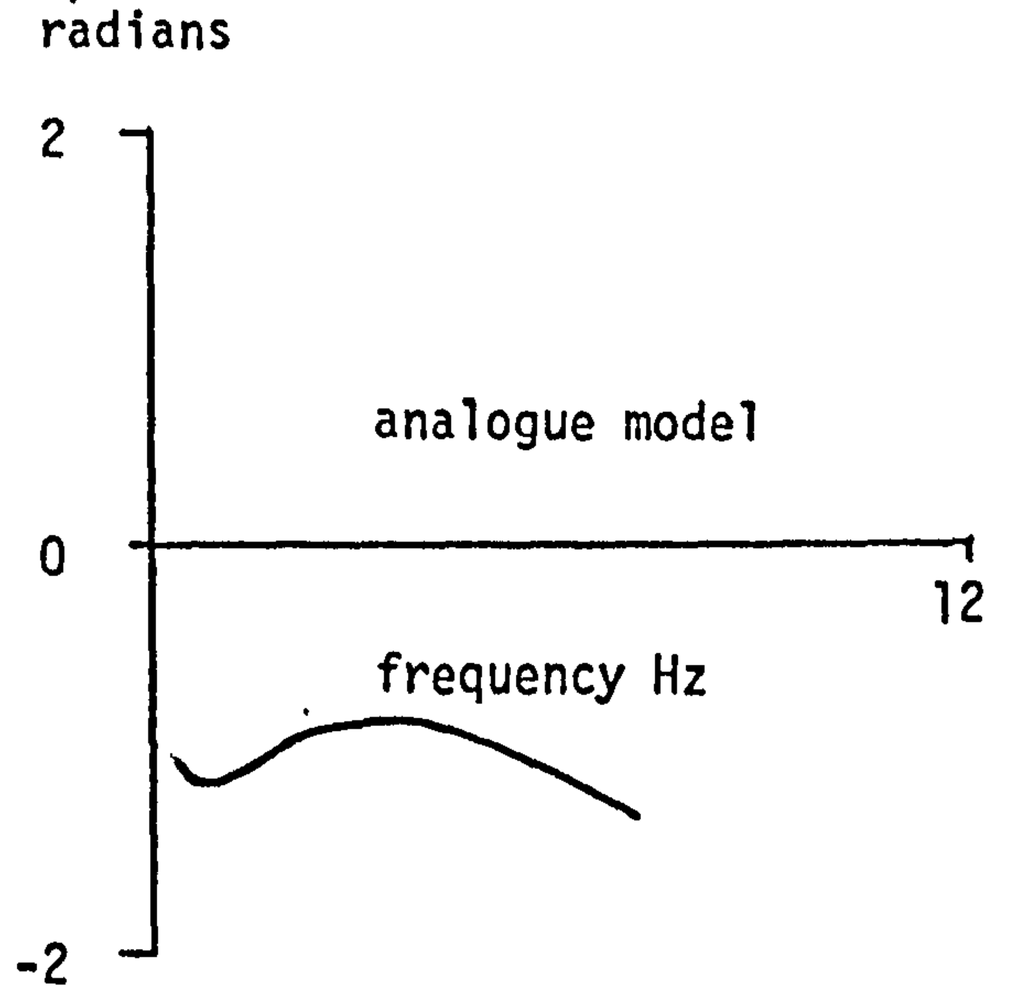

Fig. 4.19

Comparison of the input impedances of the digital version of Beneken's model, HT04, and the published response of the original analogue model.

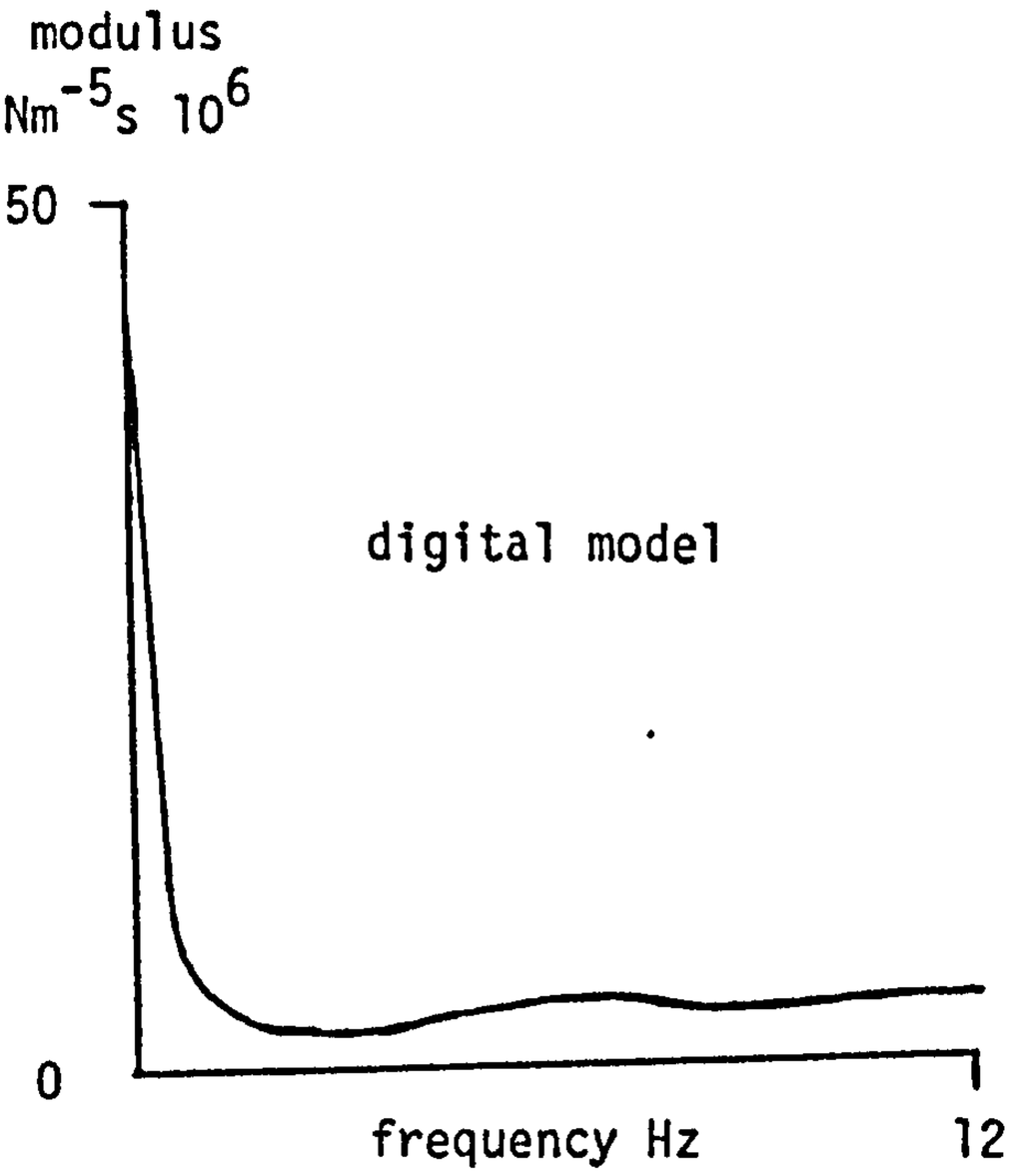

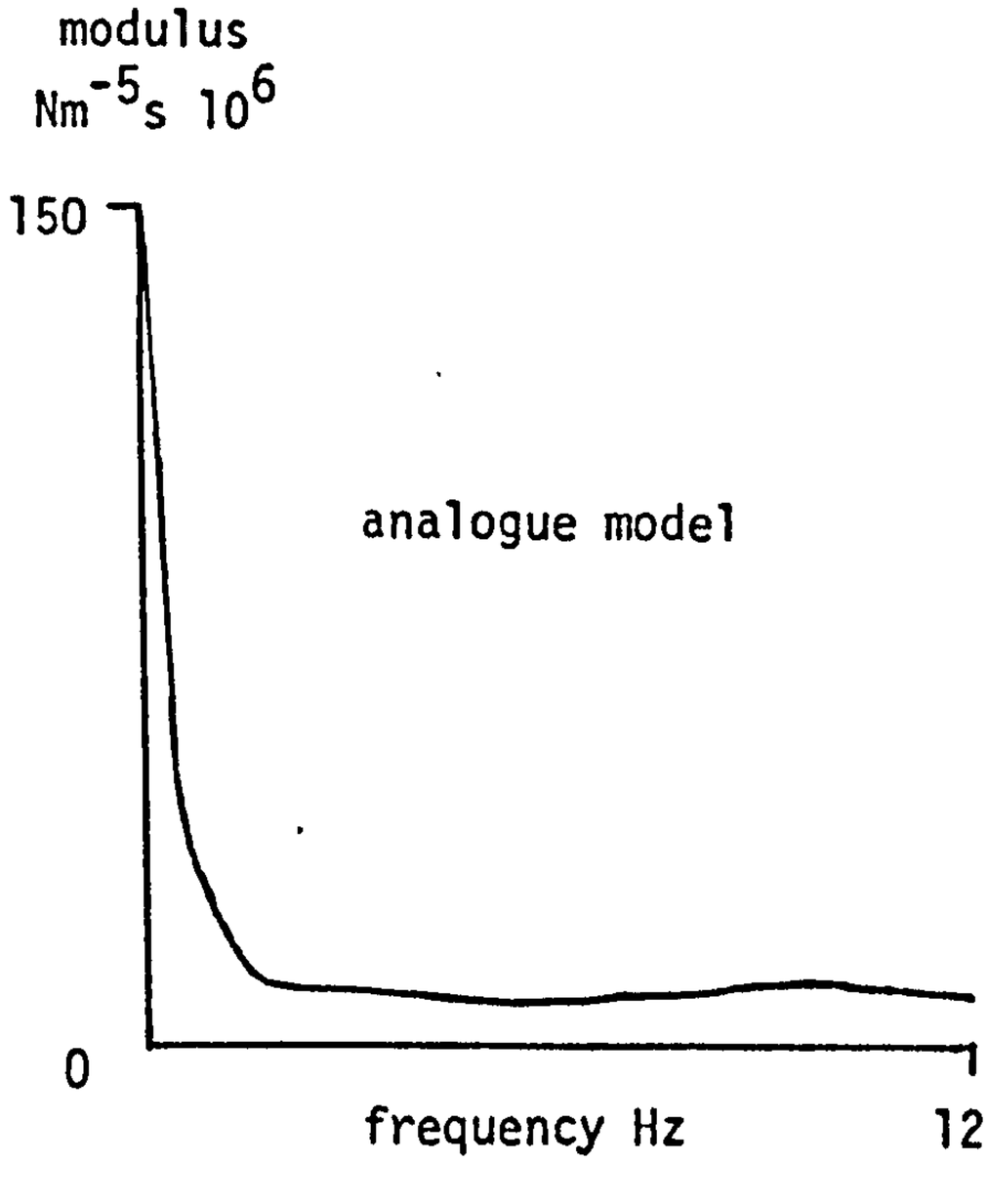

Fig. 4.20

Comparison of the input impedances of the digital version of Aaslid's model, HT13, and the published response of the original analogue model.

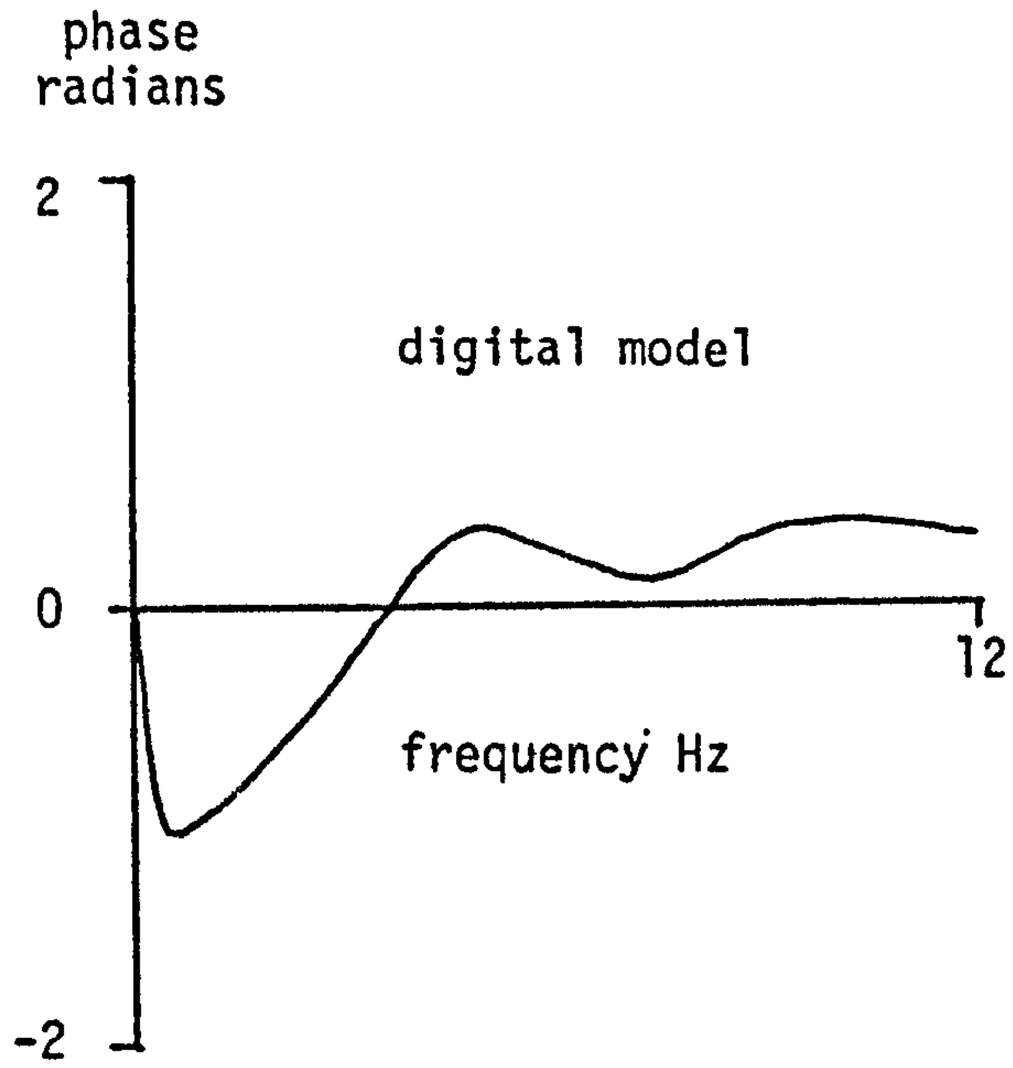

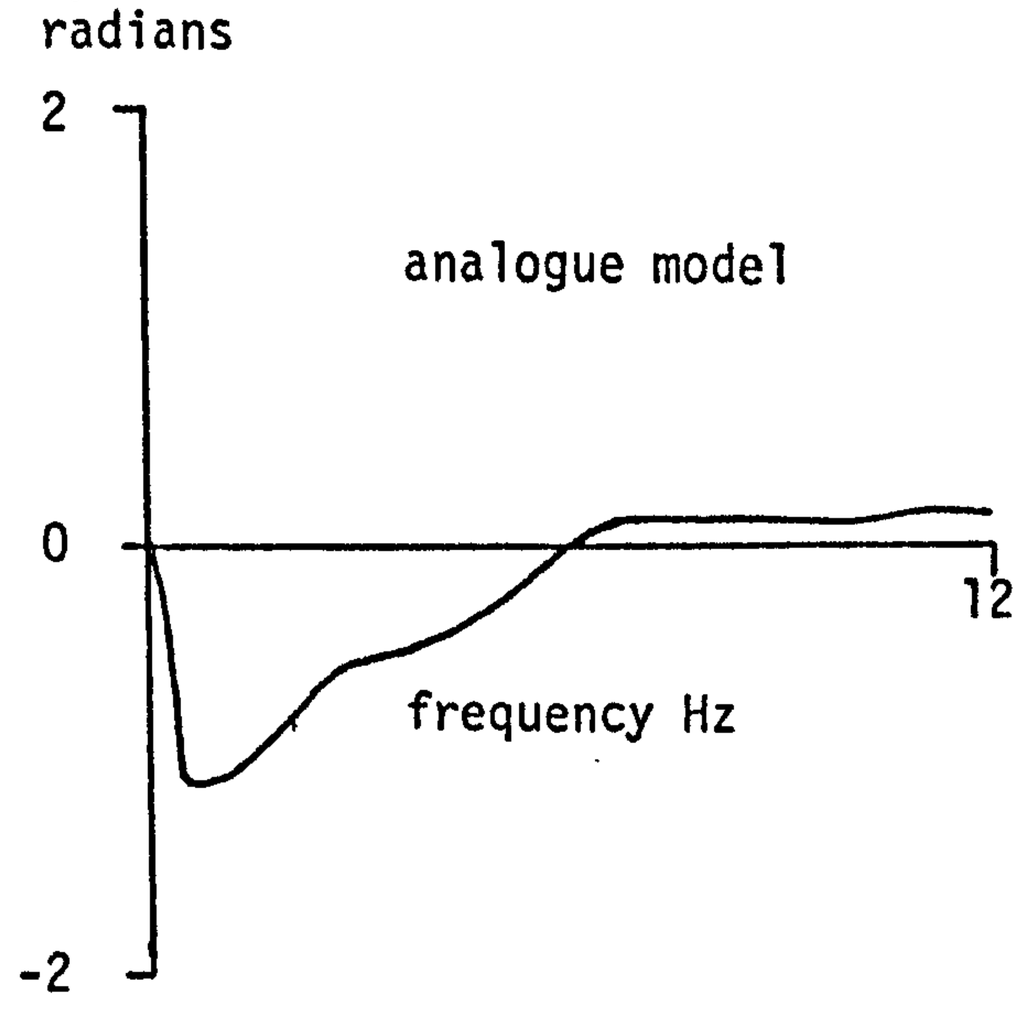

Fig. 4.21

Comparison of the input impedance of the digital version of Aaslid's model, HT13, and the published response of the original analogue model.

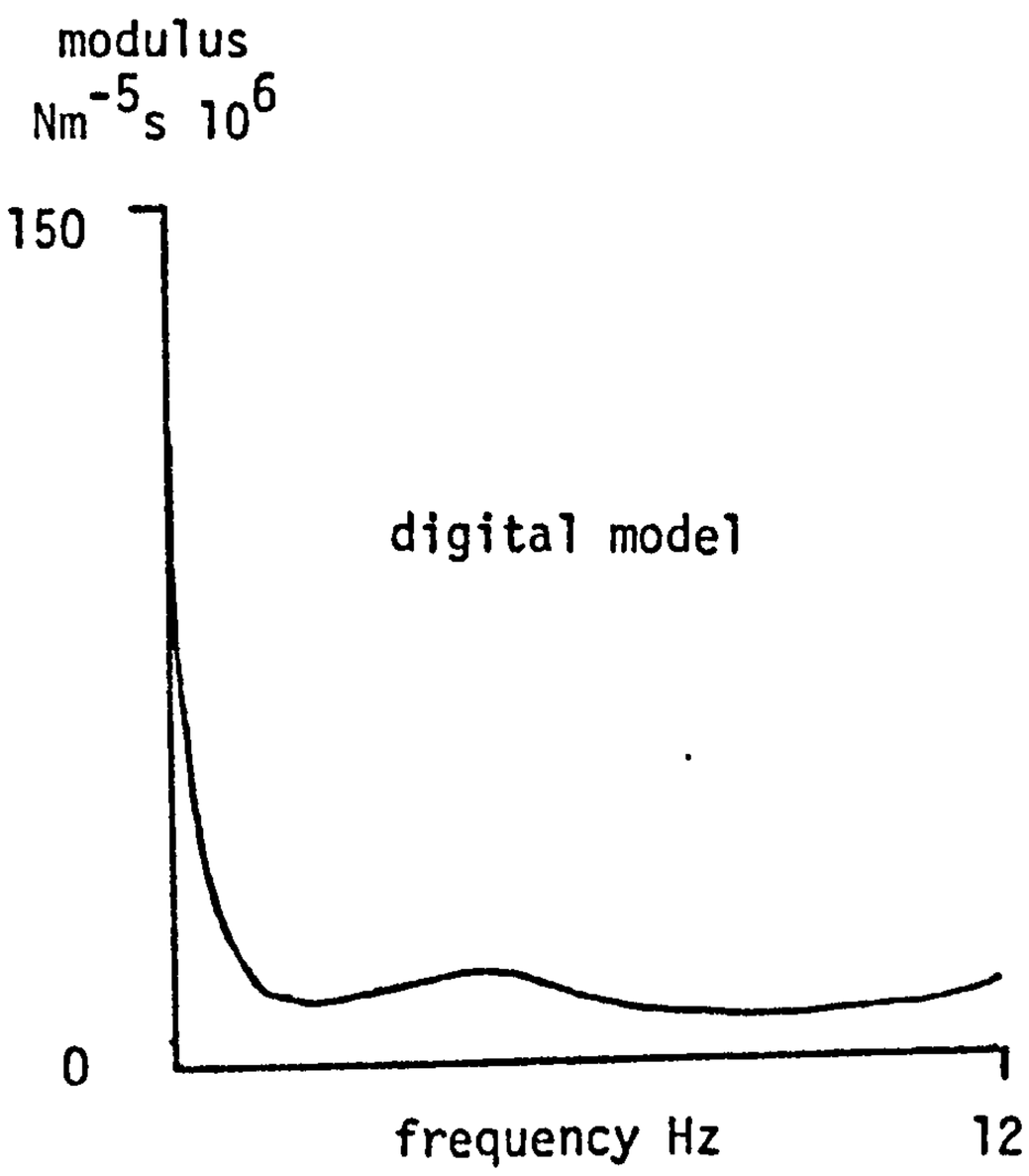

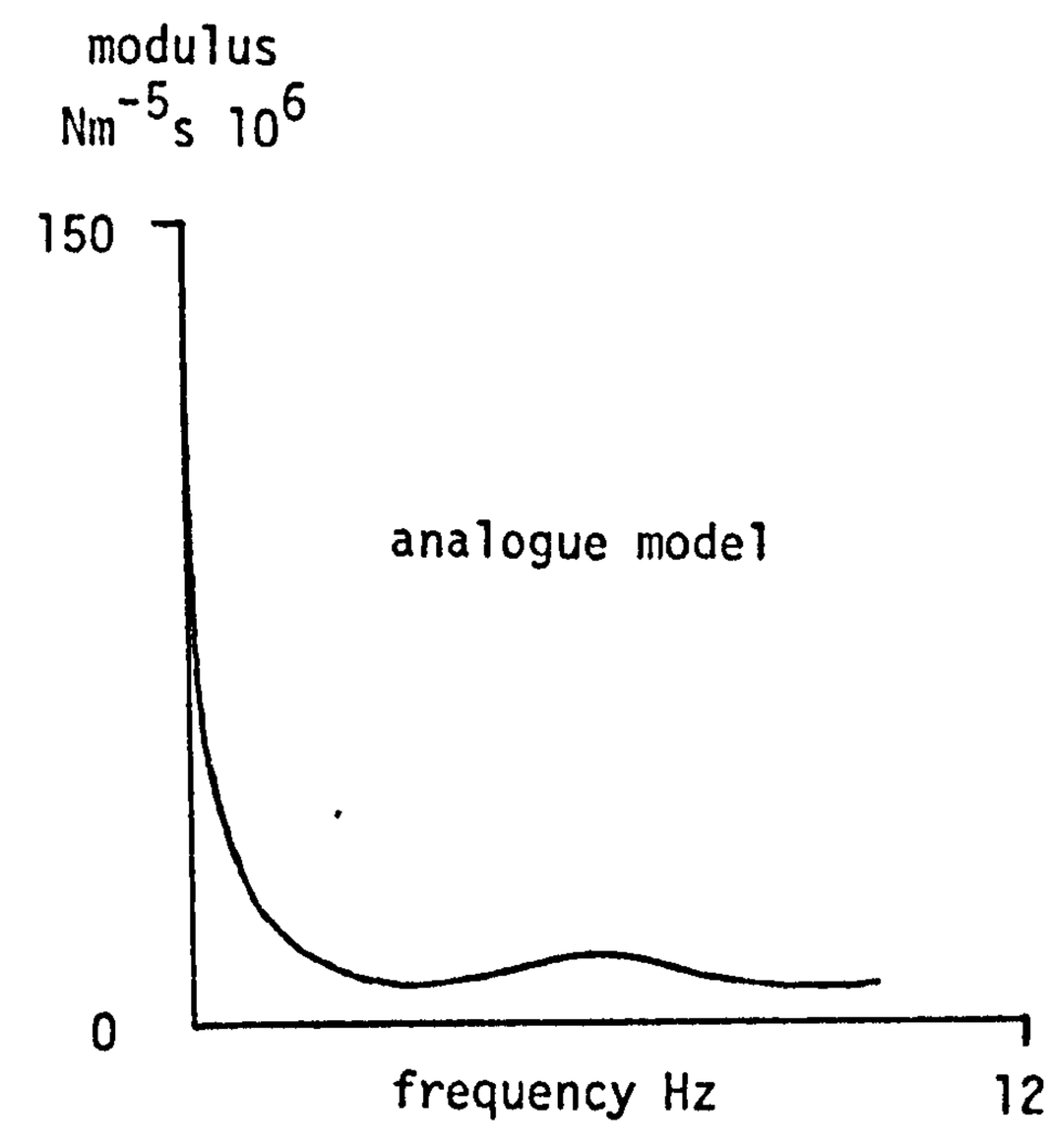

Fig. 4.22

Comparison of the input impedances of the digital version of the Snyder et. al model, HT14, and the published response of the original model.

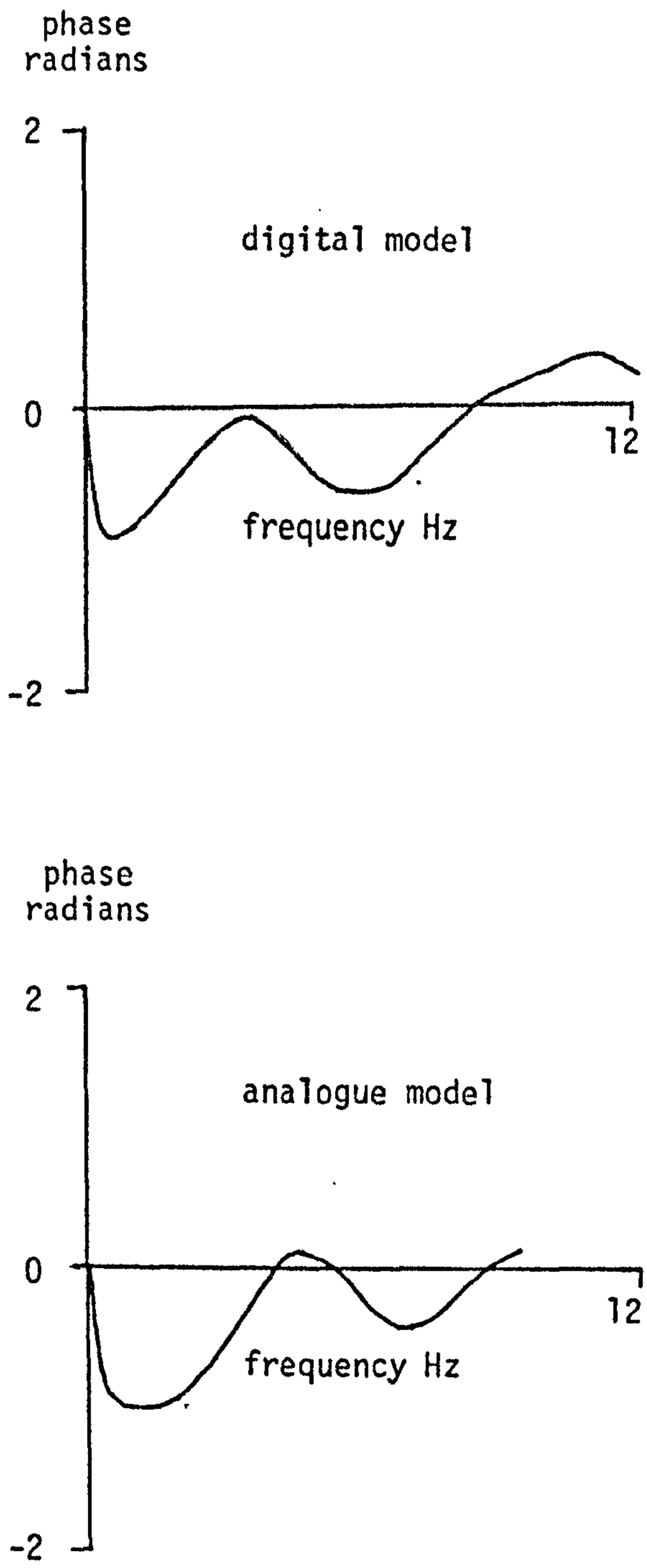

Fig. 4.23

Comparison of the input impedances of the digital version of the Snyder et. al. model, HT14, and the published response of the original analogue model.

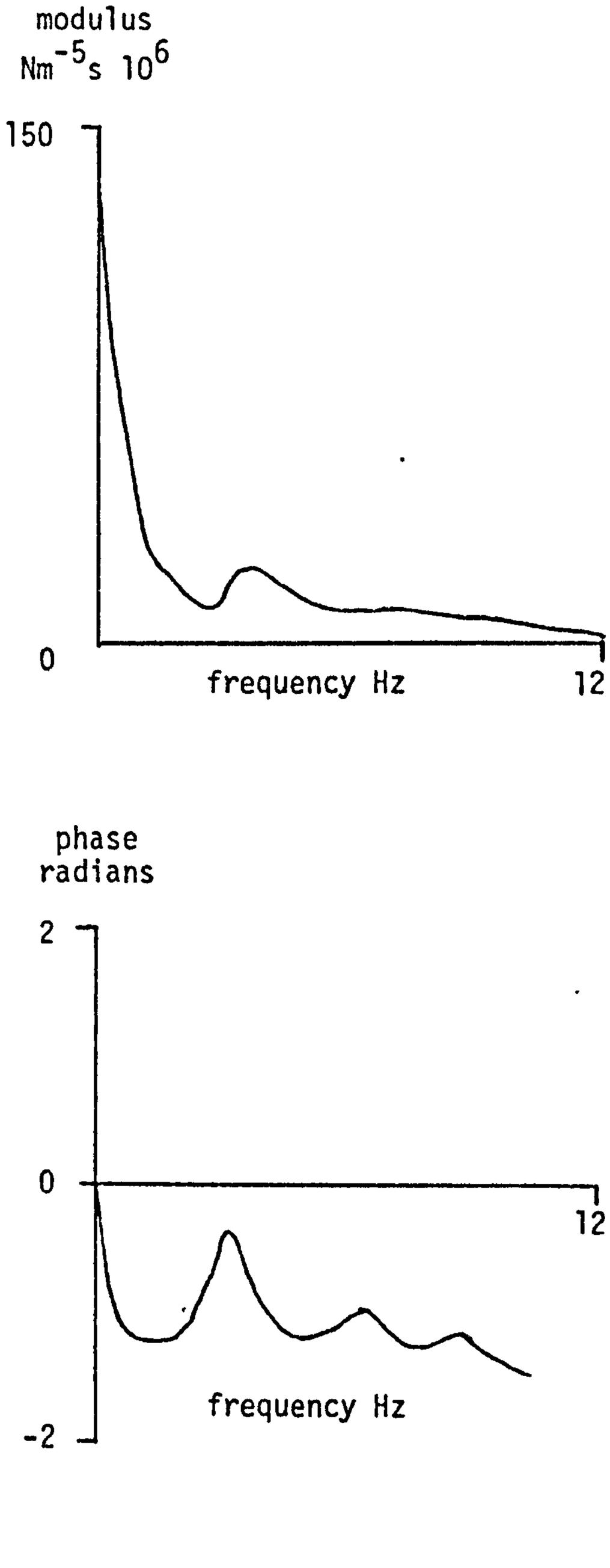

Fig. 4.24

Aortic input impedance of the new digital model, HT11.

4.7 GENERAL CONSIDERATIONS

There is little published information from which to derive an optimum design for a clinical model. The Beneken simulation was not primarily intended to simulate detailed haemodynamics but for the study of circulatory control systems. As a result it has been configured with one compartment, or segment, for each region to be controlled. More complex models, such as those of Snyder et al. and Westerhof et al. (1969) were established to examine the effect of the structure and properties of the arterial circulation. They have only been tested for their general conformity to human measurements. No attempt has been made to quantify the reduction in error of the models produced by including any detail or to relate this to the errors implicit in corresponding measurements in humans. Westerhof et al. (ibid) have in fact shown that the detailed changes considered in their model have a small effect compared with the result of altering the radii of the abdominal aorta and femoral artery in their model. Unfortunately the new radii were not tried alone in the original model. The model of Snyder et al. is considerably simpler than that of Westerhof et al. (ibid) but still appears to behave quite realistically. Its evaluation was limited to a comparison with the impedance data of Patel et al. (1964) and others and general qualitative considerations. Aaslid has matched his model with 29 patients (Brubakk and Aaslid, 1978) and justified the inclusion of peripheral damping by showing that it has a non zero value for optimum match. He has not shown that arterial wall damping, for example, is necessary or that the degree of segmentation used is optimal.

It is relatively easy to estimate optimum values for overall constants which scale parameters, such as compliance, in all the segments.

These constants are an appropriate choice for adjustment to accommodate the differences between the arterial systems of individual people. Other details of the model design are more difficult to adjust. To change the number of branches requires the alteration of some equations and the addition of others in a digital representation. In an analogue model extensive wiring changes are necessary. Increasing the degree of segmentation means adding equations and altering constants in the existing ones. All these processes would be very complicated to carry out as part of the simplest optimisation procedure. As it is not therefore practical to design a model by rigorous optimisation a comparison has been made between four models covering a range of possible configurations. The models chosen were those of Beneken, Aaslid and Snyder et al. and a simplified version of Aaslid's. Programs have been written to implement the four digital models of the circulation. They each include adjustments for compliance, blood inertia and peripheral resistance so that these parameters in the models can be changed to match patient measurements. In addition the damping terms can be altered by changing the damping time constants. These different models have been constructed in digital form to carry out a comparative study of them in terms of their ability to match patient data. This should indicate what detail is required for a model to adequately represent clinical data and provide an evaluation of the effect of the differences between the models.

CHAPTER 5

MATHEMATICAL AND COMPUTING TECHNIQUES FOR THE MODELS

Most existing simulations of the circulation are analogue models in which pressure and flow are represented by electrical voltage and current. These models usually run faster than real time, for example the model of Westerhof et al. (1969) is speeded up by a factor of 1000 times real time. This is necessary to give electronic component values in the range for which precision types are available or can be constructed. Digital simulations however, are considerably slower. On the relatively slow mini-computer used in this project the new model and that of Aaslid run at about 1/100 of real speed while the Snyder et al. model runs at 1/300 real speed. The computing processes must be as efficient as possible to produce a practical clinical method. In conflict with this requirement was the need, during the development phase, to make the methods used as flexible as possible. For example the same differential equation solving method was required to work with all the models. To make the matching accuracy comparisons valid the matching method also had to be the same for all the models tested.

The BETA operating system used on the computers permits dynamic overlay of programs. This means that on completion of one program a second one can replace it in the memory by loading from the disc with an instruction executed in the first program. This process enables long routines to be run which cannot fit into the memory as a single program. The facility has also been used to enable results printing and input

impedance programs to be used by all the models. In this respect the overlay program functions as a subroutine but with the advantage of making more memory available.

5.1 PROGRAM STRUCTURE

Two versions of each model were written, one incorporating a matching method and the other for model input impedance measurements. The first type is illustrated by the program HT1154 listed in appendix 1 and by the flow diagram in fig. 4.14, chapter 4, and is the clinical version of the model used for analysing patient data. For the impedance version the adjustable parameters are entered by hand and the input flow is an impulse function, this is described further in 5.4.

The core of the model operation is the subroutine BEAT and is best described by reference to the listing of Program HT1154. This subroutine initialises variables for mean, systolic and diastolic pressure and the matching error, CRIT. The main DO loop from lines 239 - 261 computes all the model pressures and flows at 10 ms intervals for the period of one heart beat. First finite differences around the next flow input are calculated as the variables prefixed by DEL, then calls to the differential equation solving routine, DFSOLN are made. As shown here 4 calls are made as the basic 10 ms interval is subdivided into 2.5 ms increments. The remainder of this loop is concerned with calculating mean and peak pressures and matching error and plotting the 10 ms pressure and flow values. The last part of the subroutine prints the results for the whole beat.

The call to DFSOLN includes in its argument the name of the subroutine EQNS which represents the set of first order differential equations which constitute the circulation model itself. DFSOLN, which is described in 5.2 makes calls to this subroutine under the name EXTERN passing a time, an array to contain pressures and flows and an array for the corresponding first derivatives. Within EQNS these are known as TR, X and DOT. Within EQNS and BEAT, X and DOT are structured as two dimensional arrays,

X(M,N) and DOT (M,N)

where N represents the segment number and M = 1 for flow values and 2 for pressure values. According to the Fortran convention X and DOT therefore contain alternate flow and pressure values for each of the segments in turn. The value of the aortic flow, X(1,2), at time TR is calculated by interpolating the discrete values of flow in array AOF. The first derivatives of X are then calculated for this value of the flow driving function and using the values of other flows and pressures which were passed to the subroutine in array X. EQNS solves a set of equations of the form,

$$\frac{dx}{dt} = f(X,t)$$

where x represents one element of the array X.

In the larger equation sets for the Aaslid and Snyder models, listed in appendix 1, advantage has been taken of the regular pattern for the differential equations by using general expressions for many of them within DO loops. This pattern is broken at junctions in the arterial

system. A different form of differential equation is required for the minor branches in the Snyder model. To simplify the writing of these equations the branch pressures are represented by a one dimensional array XB and the derivatives by a corresponding array DOTB. These are copied to and from the main X and DOT arrays within EQNS. In all the models DFSOLN sees two single dimensional arrays to represent X and DOT.

The main program, and the subroutine SEARCH, establish the values for the adjustable parameters. These are determined from the values of the scaling factors. The peripheral resistances are contained in the array R and the other parameters in Z(K,N) where,

K = 1 for arterial resistance
= 2 for blood inertia
= 3 for arterial compliance,

and N is again the segment number. In the Aaslid and Snyder models the damping parameters are located in Z(4,N). The Snyder model also has a further set of branch resistances stored in the array ZB.

The flow driving function is read into the main program, together with the patient pressure to be matched, from paper tape. The pressure and flow are represented by discrete values at 10 ms intervals for one complete heartbeat. The flow is then assumed to be a continuous periodic function for which the values read in represent one cycle. To enable interpolation to take place at the ends of the flow array it is extended at the ends by duplicating the appropriate values. The computed pressures are the values corresponding to the next 10 ms flow sample to that

used to predict them. The relationship between the various array samples is shown in fig. 5.1.

5.2 SOLUTION OF THE DIFFERENTIAL EQUATIONS

General Considerations

The equation set for each model is a set of first order differential equations of the form,

$$\frac{dx}{dt} = f(X,t) \quad \ldots\ldots\ldots\ldots\ldots\ldots \quad (5.1)$$

where x is one element of the Fortran array X and t is time. The basic unit of time chosen is 10 ms, hence solutions for equation 5.1 have to be found for discrete time intervals of this length. In general a solution in closed form does not exist for this set of simultaneous equations, so they are solved by numerical integration.

A simple method of solution for x would be to use the value of $\frac{dx}{dt}$ at time t_n to estimate the value of x at t_{n+1} directly by linear extrapolation,

$$x(t_{n+1}) = x(t_n) + \left(\frac{dx}{dt}\right)_{t_n} (t_{n+1} - t_n)$$

this can be conveniently written, by reference to equation 5.1 as,

$$x_{n+1} = x_n + f_n h \quad \ldots\ldots\ldots\ldots\ldots\ldots \quad (5.2)$$

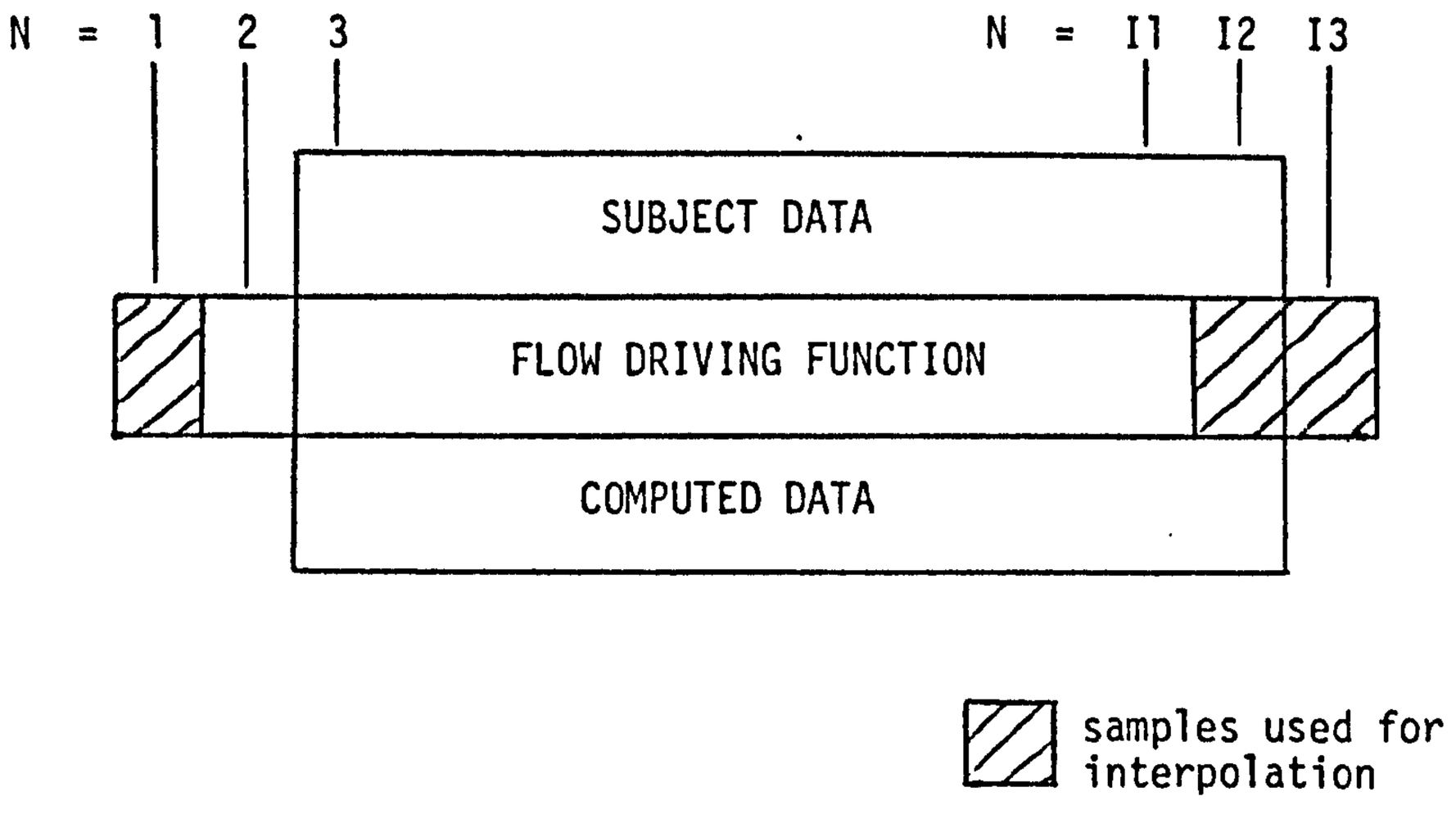

Fig. 5.1

Timing of samples of pressure and flow in model program arrays. I is the number of 10ms samples in one heartbeat, I1 is I + 1, etc. N is the sample number in the array and represents time in 10ms increments.

where h is the integration interval which can be made an integer fraction of 10 ms for greater accuracy. This is Euler's method for integrating first order differential equations and is an approximation except in the case where f is constant. It can be improved by estimating f_{n+1} using the value for x_{n+1} from equation 5.2 in equation 5.1 and then taking the average of these two values of f to estimate x_{n+1} thus,

$$x'_{n+1} = x_n + f_n h \quad \ldots\ldots\ldots\ldots\ldots\ldots \quad (5.3)$$

$$f_{n+1} = f(X'_{n+1}, t_{n+1}) \quad \ldots\ldots\ldots\ldots \quad (5.4)$$

$$x''_{n+1} = x_n + \frac{f_n + f_{n+1}}{2} h \quad \ldots\ldots\ldots \quad (5.5)$$

where x' and x" are the first and second estimates of x. This is the improved Euler or Heun's method. This approach requires two solutions of the set of differential equations in x to be found for each integration step. A series of methods of this form exist and are the Runge - Kutta methods (Dorn and McCracken, 1972, pp 366-378). The most popular of these is the fourth order method in which four solutions of the differential equation are required to find x at the end of the prescribed interval. One limitation of these methods is that no estimate of the error of the solution is produced. This is particularly relevant as the error can usually be reduced by making the integration interval smaller. Without a measure of the error this interval can only be chosen by reducing it until the solution changes by an acceptably small amount. A method which overcomes this problem is the Kutta - Merson algorithm used by Hyndman (1973) in his model. This requires five solutions of the differential equation, additional calculations in the algorithm give an estimate of the size of the error. Local alterations of the integration interval are made if the error changes from a specified value. All these methods are "one-step", that is they only

use knowledge of the solution for X at one point in time.

As a numerical solution for an equation proceeds results for a number of points before the current one will be produced which it would be reasonable to use. Predictor - Corrector methods use this information (Hamming, 1973, pp 393-411). In each case a predictor formula is used, with information from previous points, to give a first estimate for x. A corrector formula is then applied to improve this solution. By using pairs of formulae with different error characteristics it is possible, by repeated application, to converge with reasonable speed on an accurate solution.

The Milne class of predictors are described by the equation,

$$P_{m+1} = A_0 x_m + A_1 x_{m-1} + A_2 x_{m-2} + A_3 x_{m-3} + h(B_0 f_m + B_1 f_{m-1} + B_2 f_{m-2}) \quad \ldots\ldots\ldots \quad (5.6)$$

where P_{m+1} is the predicted value of x_{m+1}. A similar class of correctors is described by,

$$C_{m+1} = a_0 x_m + a_1 x_{m-1} + a_2 x_{m-2} + h(b_{-1} f_{m+1} + b_0 f_m + b_1 f_{m-1} + b_2 f_{m-2}) \quad \ldots\ldots\ldots \quad (5.7)$$

In each case there are seven coefficients for determining the estimate and by fixing two of the coefficients, A_0 and A_1 or a_0 and a_1 the equations can be made to fit fourth order polynominals. The stability and error characteristics of these formulae are determined by the

choice of the two arbitrarily chosen coefficients.

The true value of x_{m+1} is related to P_{m+1} and C_{m+1} by error functions E which are approximately the same for both predictor and corrector giving,

$$x_{m+1} = P_{m+1} + K_p E = C_{m+1} + K_c E$$

or,

$$E = \frac{P_{m+1} - C_{m+1}}{K_c - K_p} \qquad \ldots\ldots\ldots\ldots\ldots\ldots \quad (5.8)$$

This error estimate can be used to improve the value of x_{m+1} given by C_{m+1} and also to indicate the final error in x_{m+1}. It is also possible to use the estimate of E from the previous iteration to improve the value of P_{m+1}. Note that the predictor uses values in f only up to f_m while the corrector uses the predicted value of x_{m+1} to give a term in f_{m+1}.

Using previous solutions fewer iteration of the differential equation should be necessary for the same accuracy. However, the predictor and corrector formulae are generally more complicated than the Runge - Kutta formula for a similar error. So the saving in computation with a predictor - corrector method depends on the relative complexity of the equation being solved. These methods are not self starting as they require previous solutions for x, P and f to proceed. It is usual to employ a Runge - Kutta method to compute these. If the step length is to be varied during the solution then the Runge - Kutta routine will have to be used at every change in step length.

An important consideration in the choice of methods is stability. It is possible for the errors to gradually build up during the solution of some sets of equations. This is not a major problem with circulation models as they should have the property that the ultimate values of mean pressure and flow are not dependent on the starting conditions. If the circulation is disturbed the pressures and flows will eventually return to their original state because it is a closed system. Another form of instability is important in which the errors oscillate with increasing amplitude around the true solution. Both types of instability can usually be reduced and the accuracy also improved, by shortening the integration step length. The penalty for this is increased computation time. In general the stability and accuracy for a particular method of numerical integration must be found by experiment for the specific set of equations to be solved.

Specific Methods

Five methods, two "one step" and three predictor-corrector, have been tested for speed, accuracy and stability for application to the HT11 circulation model. The five algorithms were designated DFEQS1-5.

DFEQS1 is the well established fourth order Runge - Kutta method and the Fortran subroutine used was taken from the CERN 6600 computer program library, program No. D203. It uses the following equations,

$$x_{m+1} = x_m + \frac{h}{6}(K_1 + 2K_2 + 2K_3 + K_4) \quad \ldots\ldots \quad (5.9)$$

where,

$$K_1 = f(t_m, x_m) \quad \ldots\ldots\ldots\ldots\ldots\ldots \quad (5.10)$$

$$K_2 = f(t_m + \frac{h}{2}, x_m + \frac{hK_1}{2}) \quad \ldots\ldots\ldots\ldots\ldots \quad (5.11)$$

$$K_3 = f(t_m + \frac{h}{2}, x_m + \frac{hK_2}{2}) \quad \ldots\ldots\ldots\ldots\ldots \quad (5.12)$$

$$K_4 = f(t_m + h, x_m + hK_3) \quad \ldots\ldots\ldots\ldots\ldots \quad (5.13)$$

In order to evaluate equations 5.10 to 5.13, values of the differential equation have to be computed four times. The arithmetic work involved in this can be represented by 4D where D is one solution of the equations. For n differential equations this becomes 4Dn. Equations 5.11 - 5.13 also require three values of x to be calculated with a computational load of 1 multiplication and one addition in each case a total of 3 (1M + 1A)n. h/2 is a constant for the whole process and only two different times have to be calculated for any number of equations so this can be neglected if a reasonable number of equations are being solved. Equation 5.9 requires (3M + 4A)n operations so that the total work for each step of length h is (6M + 7A + 4D)n.

DFEQS2 is a predictor-corrector algorithm due to Hamming, of the Milne type, incorporating a stability factor B. When B = 1 it gives the standard Milne corrector which can be unstable, as B is reduced down to -0.6 the stability is increased with a reduction in accuracy. This routine was also from the CERN library, program No. 205. The predictor is a Milne formula,

$$P_{m+1} = A_3 x_{m-3} + \frac{4h}{3}(B_o f_m + B_1 f_{m-1} + B_2 f_{m-2}) \quad .. \quad (5.14)$$

where $A_3 = 1$, $B_o = 2$, $B_1 = -1$ and $B_2 = 2$

and the corrector,

$$C_{m+1} = a_o x_m + a_1 x_{m-1} + a_2 x_{m-2} + h(b_{-1} f_{m+1} + b_o f_m + b_1 f_{m-1}) \quad \ldots\ldots\ldots\ldots\ldots\ldots \quad (5.15)$$

where,

$$a_o = (9 - 9B)/8$$

$$a_1 = B$$

$$a_2 = (B-1)/8$$

$$b_1 = (9-B)/24$$

$$b_o = (7B+9)/12$$

$$b_1 = (17B-9)/24$$

the error is given by,

$$e_{m+1} = P_{m+1} - C_{m+1}$$

so that $x_{m+1} = C_{m+1} + \frac{9-5B}{121-5B} e_{m+1}$

and using the error for the previous iteration the estimate of x used by the corrector is given by,

$$x_{m+1} = p_{m+1} - \frac{112}{121-5B} e_m$$

The total number of operations for each iteration with this method are,

$$(11M + 11A + 2D)n$$

DFEQS3 and 4 are predictor-corrector methods which both use the Milne predictor formula of equation 5.14 but different correctors. The first of the two uses a "2/3 rule" corrector, that is $a_1 = 2/3$, $a_2 = 1/3$ which gives both greater stability and accuracy than the pure Milne corrector. DFEQS4 uses $a_1 = 0$, $a_2 = 1/16$ to give a very stable method but with increased error. Both of these methods have the same computational work per iteration as DFEQS2.

DFEQS5 is the Kutta - Merson variable step length method used by Hyndman (1973) in his version of the Beneken model. It is similar to the 4th order Runge - Kutta method but with an added solution for f to give an error estimate. It is expected that this would have very similar error and stability characteristics to DFEQS1 if the step length were fixed. The step length is in fact varied to make the estimated error equal to a constant value specified in the call to the routine. The computational load per iteration for the basic method, neglecting the step length changing routine, is (16M + 14A + 5D)n, the most for any of the methods for a given step length. But the error predicting capability could make it possible to optimise the most critical factor which is the step length. If step length changing were incorporated into the predictor-corrector methods then the additional work of a single step method would have to be done for each change.

The formulation of each program was tested using a simple equation for which an analytical solution could easily be tabulated,

$$\text{if } x = \frac{C_1}{C_2-t} \qquad \ldots\ldots\ldots\ldots\ldots\ldots \quad (5.16)$$

$$\frac{dx}{dt} = \frac{-C_1}{(C_2-t)^2} \qquad \ldots\ldots\ldots\ldots\ldots\ldots \quad (5.17)$$

this is a simple pair of equations to evaluate. To put 5.17 into the form,

$$\frac{dx}{dt} = f(X,t)$$

substitute for C_1 in 5.17 from 5.16,

$$C_1 = x(C_2-t)$$

$$\frac{dx}{dt} = \frac{-x(C_2-t)}{(C_2-t)^2}$$

$$\frac{dx}{dt} = \frac{-x}{C_2-t} \qquad \ldots\ldots\ldots\ldots\ldots\ldots \quad (5.18)$$

Equation 5.18 was solved by each of the algorithms DFEQS1-5 and the results for both x and dx/dt compared with those calculated directly from 5.16 and 5.17. All the methods produced accurate results within 0.5% for x up to 0.13 with an integration interval h = 0.001. The methods except DFEQS3 and DFEQS4 would almost achieve this accuracy for h = 0.01. The Runge - Kutta methods were in fact the most accurate with errors approaching the resolution of the computer. For this reason changing the error limit for DFEQS5 had no measurable effect over the range 5 to 0.01.

DFEQS1 was chosen, on this basis, as the method to be used for all the tests on model formulation. It was found that for model HT11 matched to femoral artery pressures from 7 patients under various conditions an integration interval of 0.0025 s was required for stability in all cases. With an interval of 0.005 or greater numerical overflows would result whereas smaller intervals made apparently no significant difference to the match. It was observed that the stability was reduced when the inertia scaling factor was reduced. One patient record was then chosen as a test flow driving function to evaluate all the algorithms; it was a beat of 0.68 s duration. In each case the model was run for 10 heartbeats and the mean, systolic and diastolic femoral artery pressures were printed for each beat and the rms difference between the patient and model pressure. The model adjustable parameters were initially fixed at their nominal value of 1.0. The integration interval for each algorithm was then changed over a range of integer subdivisions of 10 ms and the appropriate number of calls to the routine made to produce the 10 ms values required by the model. In the case of DFEQS5, where the integration subdivisions are controlled internally the error limit was adjusted over a range of 500:1. The time taken to generate one model heartbeat was calculated using the facility of the computer's internal clock. The results were classified as unstable if any computer numerical overflows were generated. It was found in all cases that no change occurred in the pressure parameters greater than 0.01 mmHg until the solutions became unstable. The stability limits and computation times are shown in table 5.1.

The computational work per iteration for each method is shown in table 5.2 using the symbols M, A and D as defined before.

Algorithm DFEQS -	Integration interval in ms	Time per beat in seconds
1	1.0	153
1	2.5	62
1	3.33333	47
1	5.0	32
1	10.0	unstable
2 (B = -0.6)	1.0	162
2 " "	2.5	unstable
3	1.0	unstable
4	1.0	151
4	2.5	unstable
	error	
5	0.1	56
5	5.0	56
5	50.0	56

Table 5.1

Stability and integration times for DFEQS1-5 with model HT11, CA = RS = I = 1.0.

Algorithm DFEQS -	Number of arithmetic steps per equation M	A	D
1	6	7	4
2	11	11	2
3	11	11	2
4	11	11	2
5	16	14	5

Table 5.2

Computational work for each integration algorithm

The average differential equation for HT11 is 1½M + 2A hence the results show, as would be expected, that DFEQS1 has a slight speed advantage over the predictor-corrector methods for the same step length. This result might be reversed for the more complex models studied. From these results it can be seen that the choice of algorithm is determined by its stability characteristics for which both Runge - Kutta type methods have clear superiority over all the predictor-corrector methods examined. To clarify any advantages of the Kutta - Merson method over the fourth order Runge - Kutta a further comparison was made with the model adjusted to give a best match to the same patient record. For this CA = 1.665, RS = 1.843 and I = 0.286 which would be expected to give reduced stability, from previous experience of the effect of the inertia term. Again, no change in the pressure parameters greater than 0.01 mmHg was detected within the limits of stability. DFEQS5 was stable for an error setting up to 50 with no significant change in computation time. The results are shown in table 5.3.

DFEQS5 sets integration intervals which are subdivisions of the overall interval by factors which are powers of 2, that is,

$$h' = h/2^n \quad \text{where } n = 1, 2, 3 \ldots\ldots$$

Table 5.3 suggests that its speed will be half that of DFEQS1 for the same interval. Table 5.1 therefore suggests that it has operated at an average of 5 ms for the first test. If the methods could be guaranteed stable for h = 2.5 ms then DFEQS1 has a significant speed advantage; if there is any uncertainty then DFEQS5 would be safer. For the experimental work with an interactive terminal DFEQS1 has been

Algorithm DFEQS -	Integration interval in ms	Time per beat s
1	1.0	154
1	2.5	62
1	3.33333	47
1	5.0	unstable
	error	
5	50.0	96

Table 5.3

Stability and integration times for DFEQS1 and DFEQS5, with model HT11, for CA = 1.665, RS = 1.843 and I = 0.286.

used. Work with a batch processing machine and a final clinical model would be best with DFEQS5 as it would then be inconvenient to have to rerun the model if it became unstable.

5.3 INTERPOLATION

The fourth-order Runge - Kutta method required solutions for the time dependant driving function at intervals of half the basic integration interval. As the latter is itself less than the tabulation interval for the driving function extensive interpolation is required. A convenient method is to use the Newton forward difference formula (Rosko, 1972). This gives values of the function f, between two times t_o and t_1, whose value at t_o is f_o,

$$f(t) = f_o + (t-t_o)\ \frac{\Delta f_o}{h}$$

$$+ (t-t_o)\ (t-t_1)\ \frac{\Delta^2 f_o}{2!\ h_2}$$

$$+ \ldots\ldots$$

$$+ (t-t_o)\ \ldots\ldots\ (t-t_{n-1})\ \frac{\Delta^n f_o}{n!\ h^n} \qquad \ldots\ldots\ldots\ldots \quad (5.19)$$

where $h = t_o - t_1$ the sampling interval for the flow and Δf_o is the forward difference. This method is convenient as for each 10 ms increment the terms of the form, $\frac{\Delta^n f_o}{n!\ h^n}$ can be calculated once. In the subroutine EQNS it is then possible to have an interpolating polynomial in

which only the coefficient involving t needs to be calculated. A third order interpolating polynomial has been used for the model, that is one with terms up to Δ^3 denoted by DELO (3). This uses differences generated from four samples of the flow waveform. The interpolating polynomial is an exact fit to these points which can be shown simply by substituting for t the times for each of the four points in turn. f_o has been chosen to be the point one before the current one so that interpolation always takes place in the middle of the points used to generate the polynomial. Equation 4.2, in section 4.4 of chapter 4, shows that the differential equation for pressure includes terms in the first derivatives of the adjacent flows when damping is added. For the input segment of the ascending aorta this requires that interpolated values of the first derivative of the driving function flow must be generated. To do this a quadratic formula has been used (Dorn and McCracken, 1972, pp 226-230),

$$\left(\frac{df}{dt}\right)_{t_o} = \frac{h_1^2\ f(t_o + h_2) + (h_2^2 - h_1^2)f(t_o) - h_2^2\ f(t_o - h_1)}{h_1 h_2 (h_1 + h_2)} \quad \ldots\ldots\ldots\ldots\ldots\ldots \quad (5.20)$$

where $x = f(t)$

$h_1 = t_o - t_{-1}$

$h_2 = t_1 - t_o$

5.4 INPUT IMPEDANCE

The measurement of aortic input impedance is a popular technique for representing the aortic flow-pressure relationship. Some clinical

studies have presented their results in this form so that it was useful to examine model characteristics in the same way. The models' input impedances are independant of the input function and only altered by changes in the adjustable parameters. It was decided to test them using an impulse function. A modified version of each model program was produced for this purpose. The input flow and resulting pressure were stored in arrays in blank COMMON and analysed by programs subsequently overlaid on the model.

A pure implulse function, in a discrete system, would consist of a single non-zero sample in an otherwise zero flow. The model frequency response is not particularly significant beyond 15 Hz, as there are only small components of pressure and flow present outside this range, in the real circulation, but an impulse would have a constant amplitude up to half the sampling frequency, that is 50 Hz. The interpolation formula, used in solving the model equations, would represent this impulse as a smooth curve. It is also possible that the integration formula, stable for any physiological flow input, might be unstable for an impulse with some parameter values.

It can be shown that for a pulse of finite width T the amplitude spectrum is of the form,

$$A(\omega) = \frac{(\mathrm{Sin}\frac{\omega T}{2})}{(\omega T/2)} \quad \ldots\ldots\ldots\ldots\ldots\ldots \quad (5.21)$$

(Lynn, 1973, p 37). The amplitude spectrum of this pulse falls by 3dB at an angular frequency ω_{3dB} given by,

$$0.707 = \frac{\text{Sin } x}{x}$$

where $$x = \frac{\omega_{3dB} T}{2}$$

Using the first two terms of a series expansion for sine x gives,

$$x - \frac{x^3}{6} = 0.707x$$

or $$x = 1.326$$

and $$\omega_{3dB} = 1.326 \ \frac{2}{T}$$

giving $$f_{3dB} = \frac{1.326}{\pi T} \quad \ldots\ldots\ldots\ldots\ldots \quad (5.22)$$

A 20 ms wide pulse would therefore, from equation 5.22, have a 3dB frequency of about 20 Hz. This represents an ample energy content at the higher frequencies for producing an impedance spectrum up to 15Hz To give maximum accuracy with the interpolation formulae used by the model, a smooth pulse, 20 ms wide at half amplitude, was generated using a cosine function sampled at 10 ms intervals,

$$F(N) = 200(1 - \cos(2\pi N/5)) \text{ ml/s} \quad \ldots\ldots\ldots \quad (5.23)$$

for $$N = 0 - 5$$

This has an amplitude of 400 ml/s and occupies 6 samples of flow input.

The measured spectrum is shown in fig. 5.2 which is consistent with the calculation for a square sided pulse.

To calculate the impedance a Fourier transform of both the flow pulse, F, and the pressure response, P, was formed. The hydraulic input impedance amplitude is then given by,

$$\sqrt{\frac{a^2 + b^2}{c^2 + d^2}} \quad \ldots\ldots\ldots\ldots\ldots\ldots \quad (5.24)$$

and the phase by,

$$\arctan b/a - \arctan d/c \quad \ldots\ldots\ldots\ldots \quad (5.25)$$

for each frequency, f where,

$$P_f = a + jb$$

$$F_f = c + jd$$

That is a and c are the real points of the two transforms for that frequency and b and d the corresponding imaginary points. Had a pure impulse been used, it would not have been necessary to transform it as the result is a constant amplitude spectrum with zero phase. Formula 5.25 can be evaluated using the Fortran function ATAN2 which is valid for angles up to $\pm \pi$. The flow input produced by formula 5.23 is a delayed pulse as it does not reach its peak for 25 ms. This is reflected in the phase spectrum of the flow, shown in fig. 5.2, as a constant phase shift with frequency of $-\pi/20$ rad/Hz. In this work, spectra have been considered up to 12 Hz. At this frequency the flow

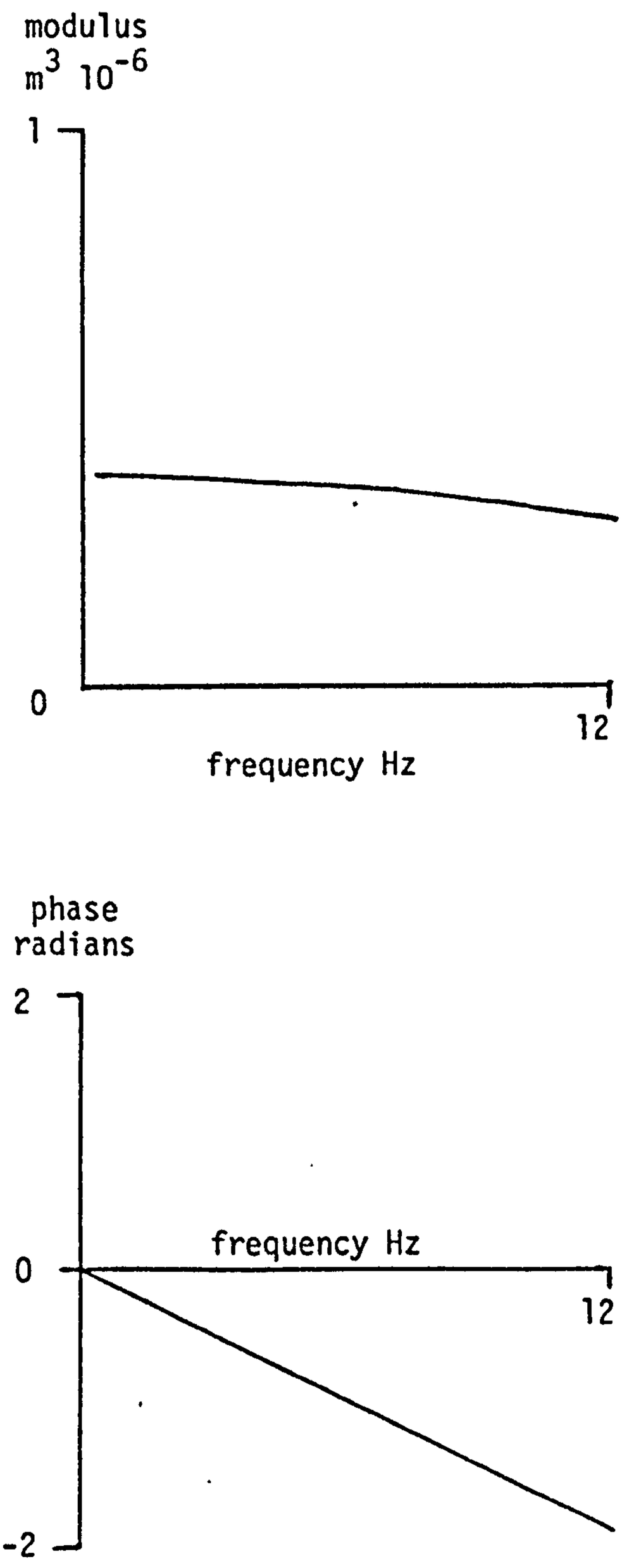

Fig. 5.2

Modulus and phase spectra of flow impulse function for model impedance determination.

pulse has a phase shift of -1.9 radians. This poses a negative limit of 1.26 radians on the pressure phase before a false sign change in the impedance phase will occur. Any additional delay of the flow pulse would be inconvenient as it would make this limit even smaller.

The fast Fourier transform used is the Fortran program developed by Monro (1976). In common with other such algorithms it only deals with record lengths which are an integer power of two long. A standard record length of 512 was therefore chosen. A transform of 256 pairs of values is produced with a maximum frequency of 50 Hz - half the sampling frequency. Of this only the first 12 Hz is used. The record length is equivalent to 5.12 s which gives a transform resolution of 1/5.12 Hz, or 0.195 Hz. As this resolution is not necessary for comparison with other published data the spectrum was smoothed with a simple recursive filter with weighting values of,

0.25, 0.5, 0.25

so that for each point X(n) the smoothed value S(n) was given by,

$$S(n) = 0.25X(n-1) + 0.5X(n) + 0.25X(n+1)$$

Clinical measurements made during cardiac catheterisation gave direct recordings of aortic pressure and flow. The data manipulation program, AOIMP, described in chapter 3, generated similar 512 point flow and pressure records which were then analysed with the same spectral analysis programs used for the models. In this case the 5.12 s record length was necessary to present a sufficient number of heart beats to give a reasonable averaged spectrum. Unlike the impulse response

these records do not start and finish near to zero. This creates a spurious spectrum due to the finite record length which looks to the transform like a 5.12 s pulse multiplying the record. The standard method of reducing this "leakage" effect is to subtract a linear trend from the record and then taper the ends (Bendat and Piersol, 1971, p 323). With the periodic functions analysed here an alternative technique was employed. A pressure and flow record was constructed from complete heartbeats only, with a length less than 512 samples. A straight line was then fitted to the first and last three points of each record and then subtracted from it. As the record started and ended at the same point on the heart cycle this line was almost one of constant pressure or flow. The record was then packed to 512 points with zero values. With the record length used it is possible to get only 4 heart beats in a record. If this record were then tapered in the conventional way there would not be many undistorted beats left.

There is no generally accepted, and theoretically sound, way of interpreting aortic input impedance spectra to give a simple physiological meaning. To get an accurate measure of characteristic impedance the analysis would have to extend well beyond 10 Hz. An estimate can be obtained by averaging the spectrum over the lower frequencies. This has been done by Nichols et al. (1977) over the range 2 - 12 Hz and this figure is calculated in the program described here. However, it should be noted that this average impedance is likely to be substantially altered by changing the frequency range and should not be described as characteristic impedance. By removing a trend line from the records the zero frequency component has been removed. This has been restored by calculating this value separately from the mean pressure and flow.

There is no general acceptance of an SI unit of pressure in clinical practice, so that mmHg has been used for all this work. However impedance is normally expressed in absolute units and for this the SI unit, Newton metre^{-5} s ($Nm^{-5}s$), has been used. Published data on impedance has been converted to these units using the following conversion factors -

$$1 \text{ dyne s cm}^{-5} = 10^5 \text{ Nm}^{-5} \text{ s}$$

$$1 \text{ mmHg s cm}^{-3} = 132.9 \times 10^6 \text{Nm}^{-5} \text{ s}$$

5.5 NOISE FUNCTIONS

In order to test the matching methods used to adjust the models it was necessary to simulate the effect of random errors or noise in the measured physiological variables. Noise in the pressure measurements can be caused by thermal noise in the transducer, accoustic noise from other body organs and externally in the room and various sources of electrical noise in the amplification and digitisation processes. A common approximation of random noise is to consider it as having a constant amplitude spectral density with frequency which is termed white noise by analogy to the visual spectrum. For computer simulation white noise can be conveniently approximated by a pseudo random binary sequence - PRBS. This is a square wave signal, of constant amplitude, whose mark and space times are pseudo random sequences. Peterson (1961) has shown that these sequences can be generated by shift registers with feedback from some outputs to the first stage input. The length of the sequences in numbers of shift register clock pulses and the outputs fed back are given in table 5.4.

No. of shift register stages	Period of sequence	Feedback the exclusive OR of following outputs
2	3	1, 2
3	7	2, 3
4	15	3, 4
5	31	3, 5
6	63	5, 6
7	127	4, 7
8	255	2, 3, 4, 8
9	511	5, 9
10	1023	7, 10
11	2047	9, 11

Table 5.4

Specification of feedback shift register configurations for various lengths of PRBS.

The amplitude spectrum of the resulting sequence is of the form,

$$A(\omega) = \left[\frac{\sin \frac{\omega \Delta t}{2}}{\frac{\omega \Delta t}{2}} \right]^2$$

(Davies, 1970, pp 67 - 68) where Δt is the period of the clock pulse and ω the angular frequency. The 3dB frequency, a convenient measure of the useful bandwidth of a noise generator, is given by,

$$0.707 = \frac{(\sin x)^2}{(x)}$$

where $x = \frac{\omega \Delta t}{2}$. Using the first two terms of a series expansion for sin x gives,

$$x - \frac{x^3}{6} = 0.84x$$

$$x = 0.98$$

i.e. $$\omega_{3dB} \approx \frac{2 \cdot 0.98}{\Delta t} \approx \frac{2}{\Delta t}$$

which gives the bandwidth $f_{3dB} \approx \frac{1}{3\Delta t}$

If the clock period is made four times the sampling interval for the data, 10 ms, then the bandwidth will be approximately 8 Hz. It is estimated that most of the pressure noise will occur in this range although electrical noise may extend to 30 Hz, the data collection filter frequency. A PRBS was used to generate "noisy" aortic and femoral

artery pressures. A typical patient flow record was shortened to 60 samples long, 0.6 s, by truncating some of the diastolic samples. Shortening the flow, by reducing the diastolic period, increases both the effective heart rate and the cardiac output. To generate corresponding pressures this flow was then used as the driving function for the model to be tested and the resulting aortic and femoral pressures recorded on paper tape. To the pressures was then added varying amounts of PRBS noise in the form of a sequence 15 clock pulses long using the four stage Fortran shift register shown in appendix 2. Note that because Fortran loops cannot use negative increments, the shift registers are arranged to shift data from the high register number to the next lower register. REG (5) is the fed back input to REG (4) and REG (2) and REG (1) represent the outputs of stages 3 and 4 in table 5.4.

The PRBS sequence is shown in fig. 5.3. The amplitude spectrum shown in fig. 5.4 was determined by analysing a record consisting of repeated cycles of the sequence. This shows the noise generator producing a series of harmonics of the frequency of the heart beat. As the patient measurements are presented to the models as repeated sequences of the same pressure and flow record, this spectrum represents reasonably the effect that noise will have on the models.

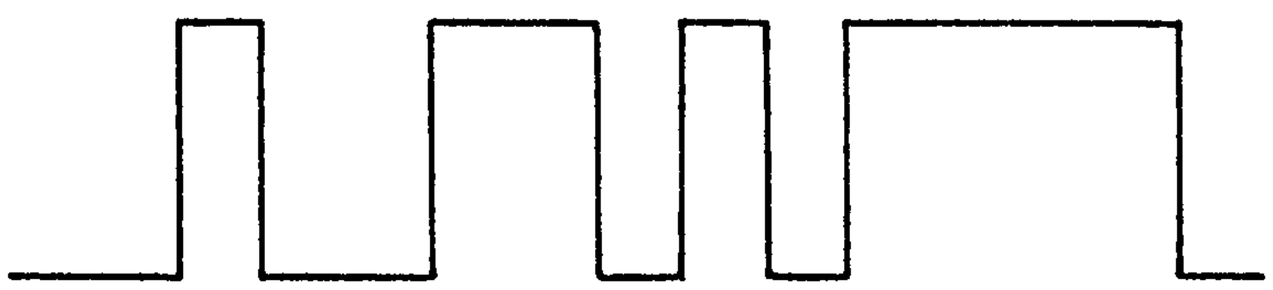

Fig. 5.3

Pseudo-random-binary-sequence of 15 clock pulses long used to simulate pressure noise.

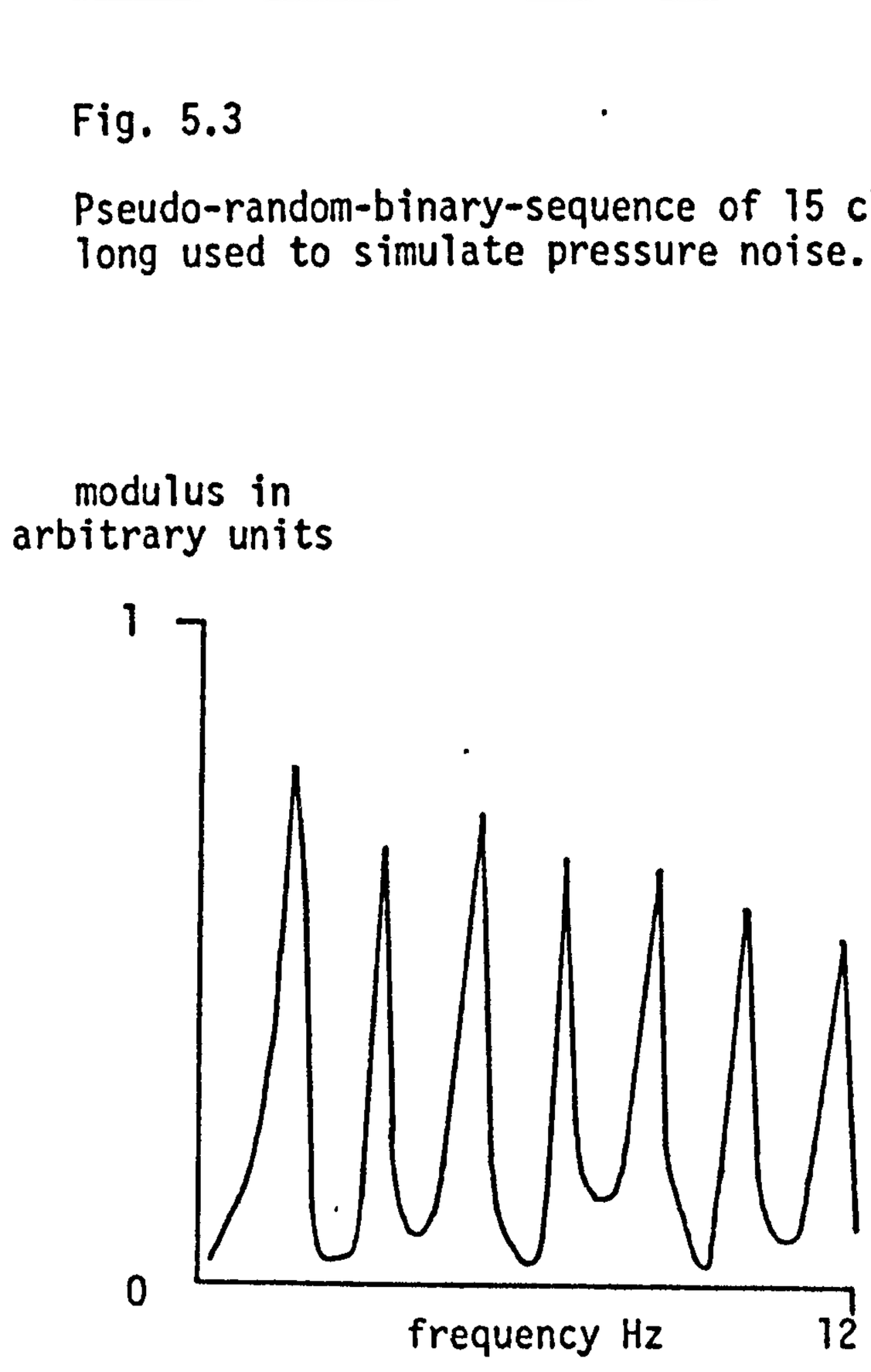

Fig. 5.4

Modulus spectrum of PRBS shown above.

CHAPTER 6

INVESTIGATION INTO THE PERFORMANCE OF FOUR CIRCULATION MODELS

6.1 OBJECTIVES AND METHODS OF STUDY

The models of Beneken, Aaslid and Snyder et al., and the new model described in chapter 4, differ considerably in both detail and parameter values. Of those published, only Aaslid's model has been compared in detail by its author with measurements on individual human subjects. The complex model of Westerhof et al. (1969), on which many other circulation models are based, was developed in order to examine the importance of various details in arterial models. However the study was made by comparing a number of input impedance measurements on humans, which themselves varied widely, with the model impedance. In this chapter a comparative study of the Beneken, Aaslid, Snyder et al. and new models is presented based on matching the models to individual patient records of arterial pressure and flow. The results give some indication of the importance of various features in arterial models when they are used to interpret clinical measurements on patients. The models were chosen to give a variety of degrees of segmentation of the arterial system and of simplification of the branch structure. These differences are shown in table 6.1.

The design of the new model was based on that of Aaslid and the segmentation is almost the same. The Snyder et al. model has some more detail in the aorta but differs mainly in having more branching near to the ascending aorta. This increased detail should give a better representation of the high frequency characteristics of the arterial system.

Model	No. of segments in main artery	No. of branches off main artery
HT04 (Beneken)	2	0
HT11 (new model)	8	2
HT13 (Aaslid)	9	2
HT14 (Snyder et al.)	11	8

Table 6.1

Detail incorporated in the models.

The simple Beneken model might be expected to deviate considerably from the performance of the others at higher frequencies with its limited arterial segmentation.

The distribution of inertia and compliance terms between the segments, or the "taper" of the vasculature, varies widely between the models. This is expected to have a substantial effect at high frequencies from the experiments of Westerhof et al. (1969) in which they changed some peripheral segments in their model.

The Aaslid and Snyder et al. models have arterial damping terms and the effect of these on matching must be determined. Damping does not increase the number of first order differential equations to be solved, but does add an extra term to every damped segment pressure equation making a significant addition to the computation. As damping is not of obvious clinical interest at present, it would need to improve the match to be worth including in a clinical model.

As more parameters are introduced into a model the better it can be matched to any data as long as these extra parameters are adjustable. This must be so if the adjustments include near zero values of the extra parameters. For the better match to be achieved in practice a good matching algorithm will have to be used which may turn out to require considerable computational effort. For data which has random errors in it, the more parameters that are estimated the less the accuracy of predicting the value of any one of them. This aspect of the problem is discussed in chapter 7 on matching techniques.

Each model, in the digital form described in chapter 4, has been ex-

amined for its ability to match measured data from human subjects. The main tests were carried out using femoral artery pressures with aortic flow as a driving function. This was a practical decision based on the availability of a considerable number of measurements at an early stage of this work. Femoral artery pressure data also has the advantage of containing time delay information along the artery. Further examination of some of the models in matching ascending aortic pressure with the same flow has been made.

6.2 ABILITY OF THE MODELS TO MATCH FEMORAL ARTERY PRESSURES

Femoral artery pressure was measured in patients after cardiac surgery, in the intensive therapy unit as described in chapter 3. A 2" long catheter was used, introduced transcutaneously in the groin, and a Gaeltec 3EA, or Millar PC350, transducer attached with a 3 way tap. Ascending aortic flow was recorded using the Carolina Medical 900 series extractible flow probe. These methods of measurement are not entirely satisfactory. The accuracy of the extractable flow probe has not been confirmed, it is certainly not rigid and is susceptible to radial distortion. The pressure measuring arrangement is good if no air bubbles are trapped, but there is no easy way of ensuring this.

Each model used the aortic flow as a driving function and was adjusted using the successive approximation algorithm described in chapter 7. For the Beneken model HT04, the outlet pressure from the systemic arteries (fig. 4.1, chapter 4) was used as the femoral pressure. In the new model, HT11, the input pressure to segment 9 (fig. 4.13) was used and for the Aaslid model, HT13, the outlet pressure from segment 9 (fig. 4.15). For the Snyder et al. model, HT14, the outlet pressure

from segment 11 (fig. 4.16) was used to represent the femoral artery pressure. Five different patient recordings were matched by the models and the resulting errors of match are shown in table 6.2. Resistance and compliance were adjusted in this process for HT04 and the inertia term in addition for the other three models. The errors are surprisingly similar for the four models, with HT11 apparently the best. Figures 6.1 to 6.4 show graphs of the model and patient pressures for record 147. The HT04 graph indicates the lack of pulse transmission and reflection properties. The pressure appears to fall linearly when the flow is zero, the "runoff" phase, which is characteristic of a single compartment system. However, the other models also show signs of not reproducing this early diastolic period as well as the late diastolic and systolic phases. The best model match was obtained for record 147. Figures 6.5 to 6.8 show graphs for record 106 which was less well simulated. The same observations apply with the diastolic period being poorly matched. There appears to be a conflict between the requirements for compliance to match the pulse pressure and the reflection properties.

Models HT13 and HT14 incorporate damping terms. To assess the effect of this on matching, HT13 was again adjusted to the same 5 records but with both arterial and peripheral damping terms set to zero. Table 6.3 shows the resulting errors of pressure match compared with those for the nominal damping values used by Aaslid. The changes are relatively small and less than the difference between this model and HT11 in most cases. Table 6.4 however shows that changing the damping has a considerable effect on the optimum values of compliance and inertia. In Aaslid's matching scheme the arterial damping, which was derived from approximate values determined by Snyder et al. (1968) and others, was

Record	Model			
	HT04	HT11	HT13	HT14
	Matching error mmHg RMS			
106	7.05	4.72	6.07	7.46
109	4.07	2.61	3.73	5.58
115	5.78	4.24	5.72	7.32
133	6.88	5.38	11.54	7.84
147	4.67	2.83	3.34	4.97

Table 6.2

Matching errors for the four models with five patient femoral artery records.

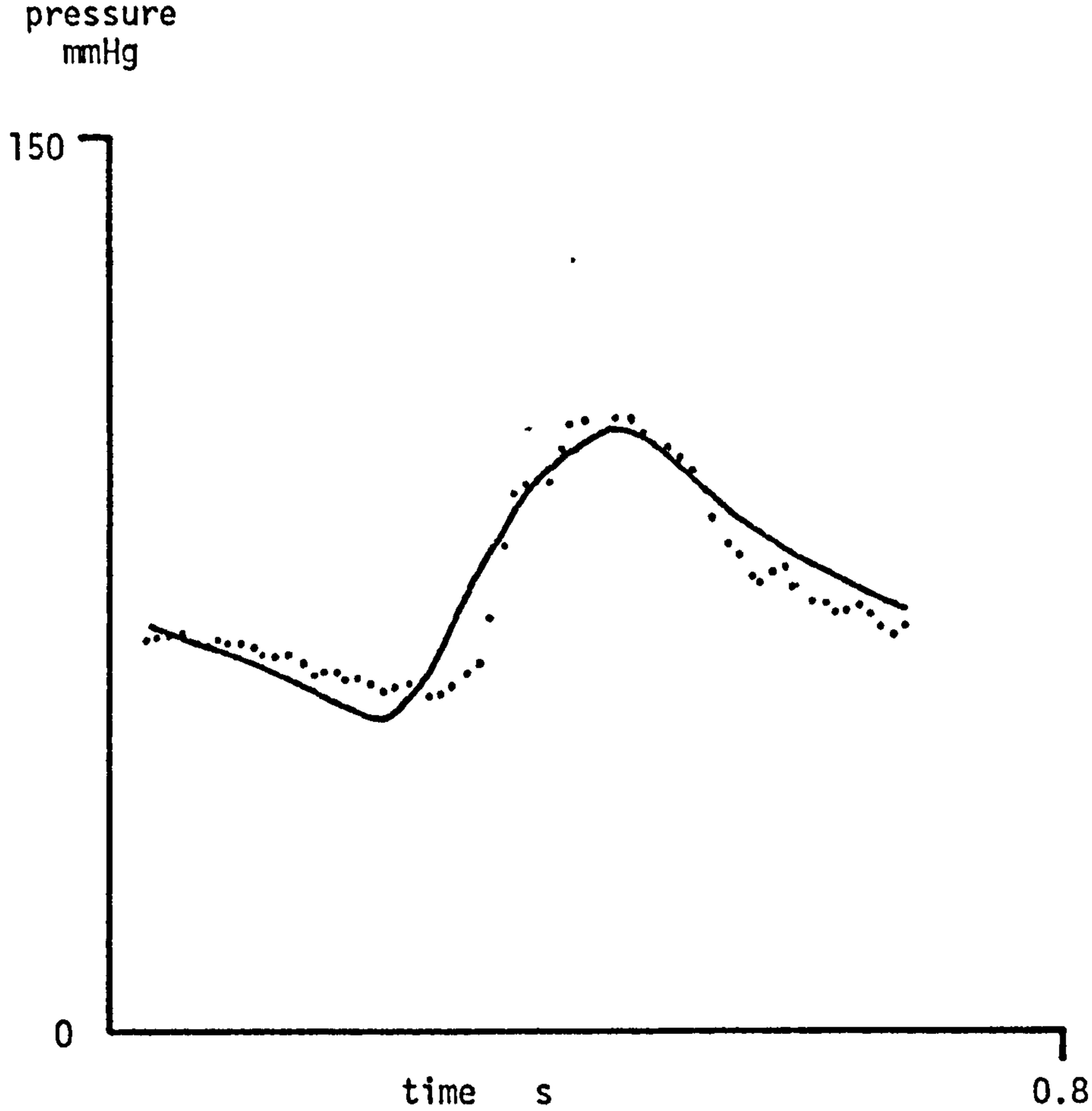

Fig. 6.1

Model femoral artery pressure, solid trace, from HT04 matched to patient record No. 147, dotted trace.

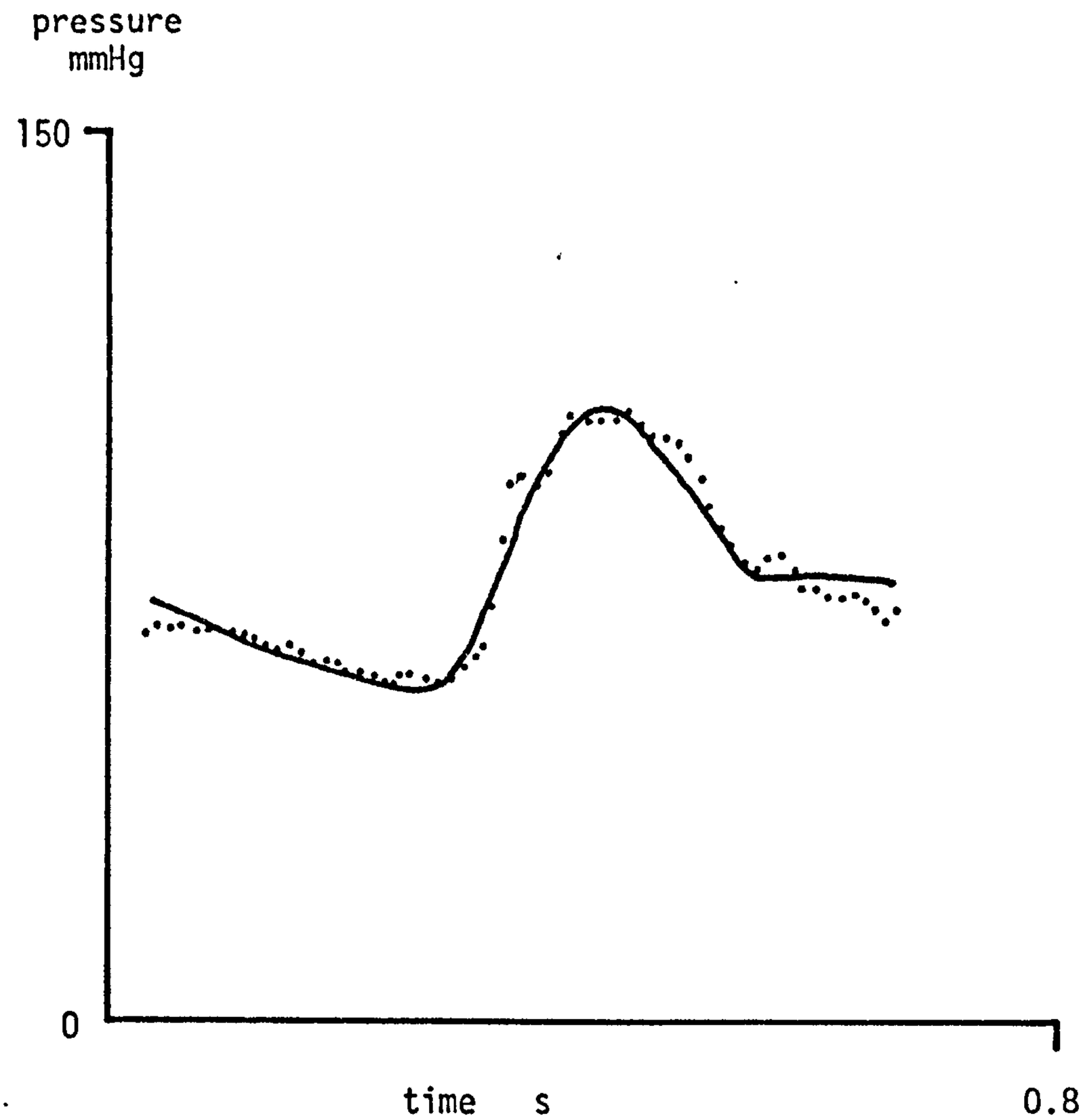

Fig. 6.2

Model femoral artery pressure, solid trace, from HT11 matched to patient record No. 147, dotted trace.

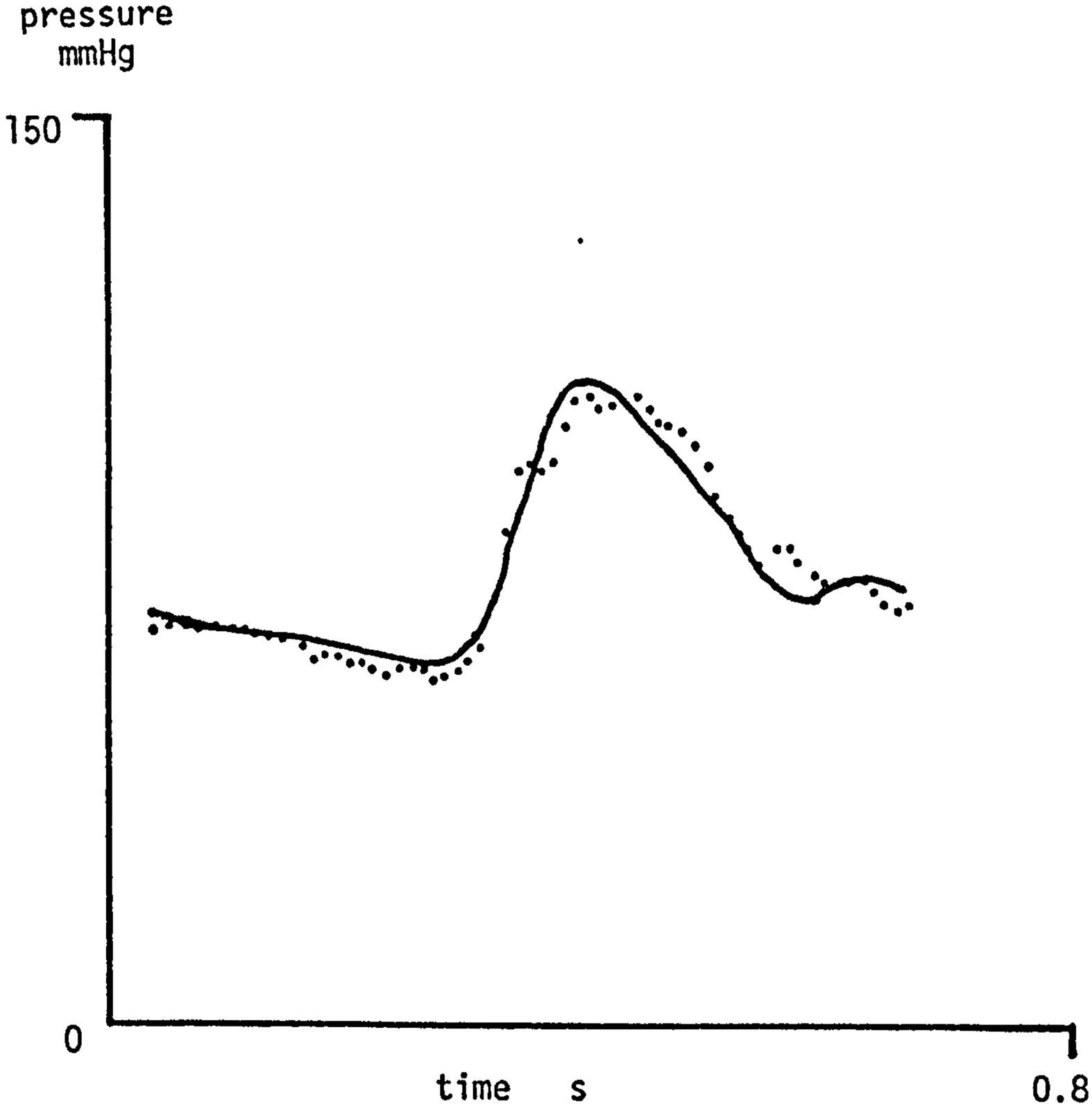

Fig. 6.3

Model femoral artery pressure, solid trace, from HT13 matched to patient record No. 147, dotted trace.

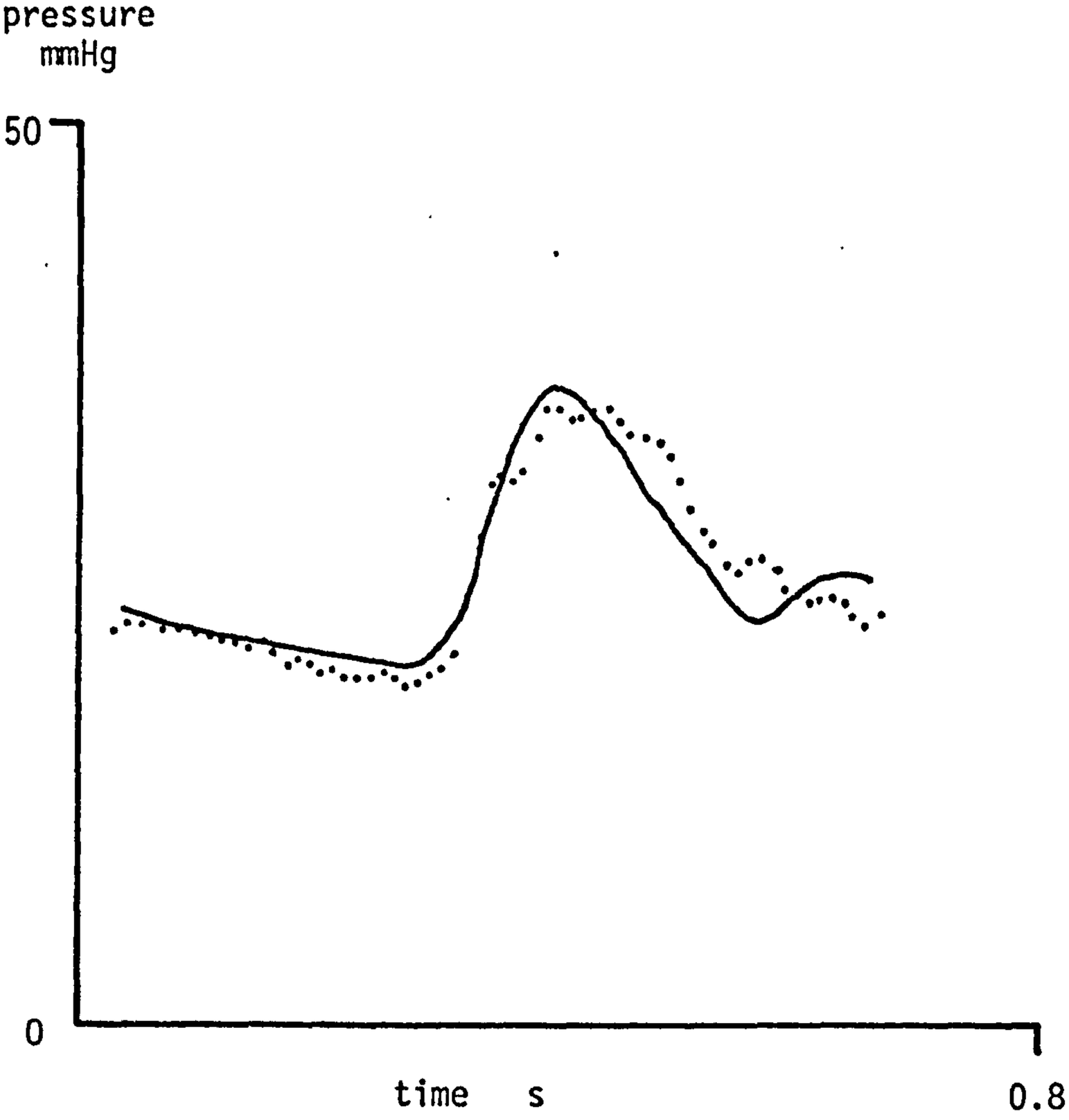

Fig. 6.4

Model femoral artery pressure, solid trace, from HT14 matched to patient record No. 147, dotted trace.

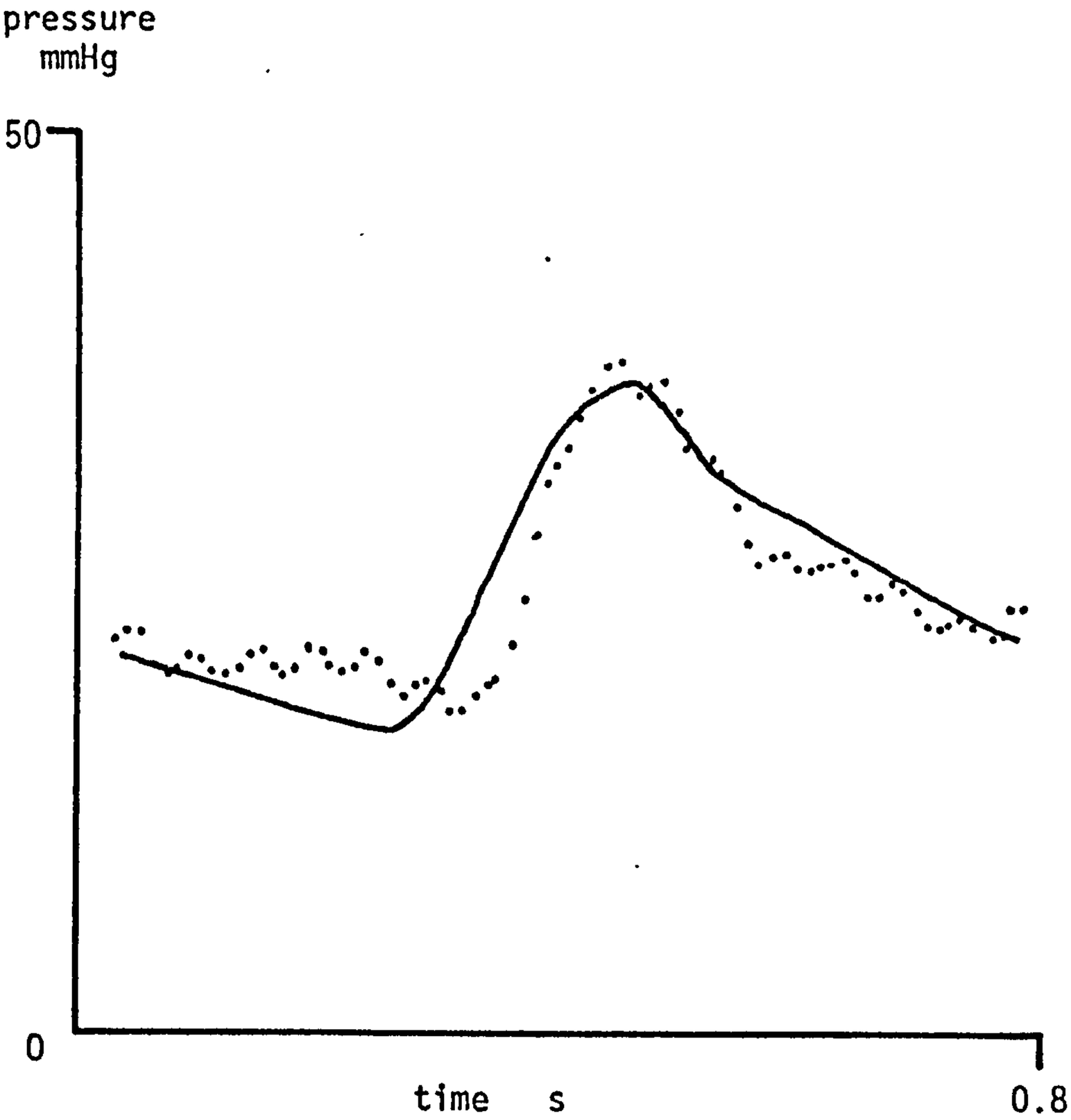

Fig. 6.5

Model femoral artery pressure, solid trace, from HT04 matched to patient record No. 106, dotted trace.

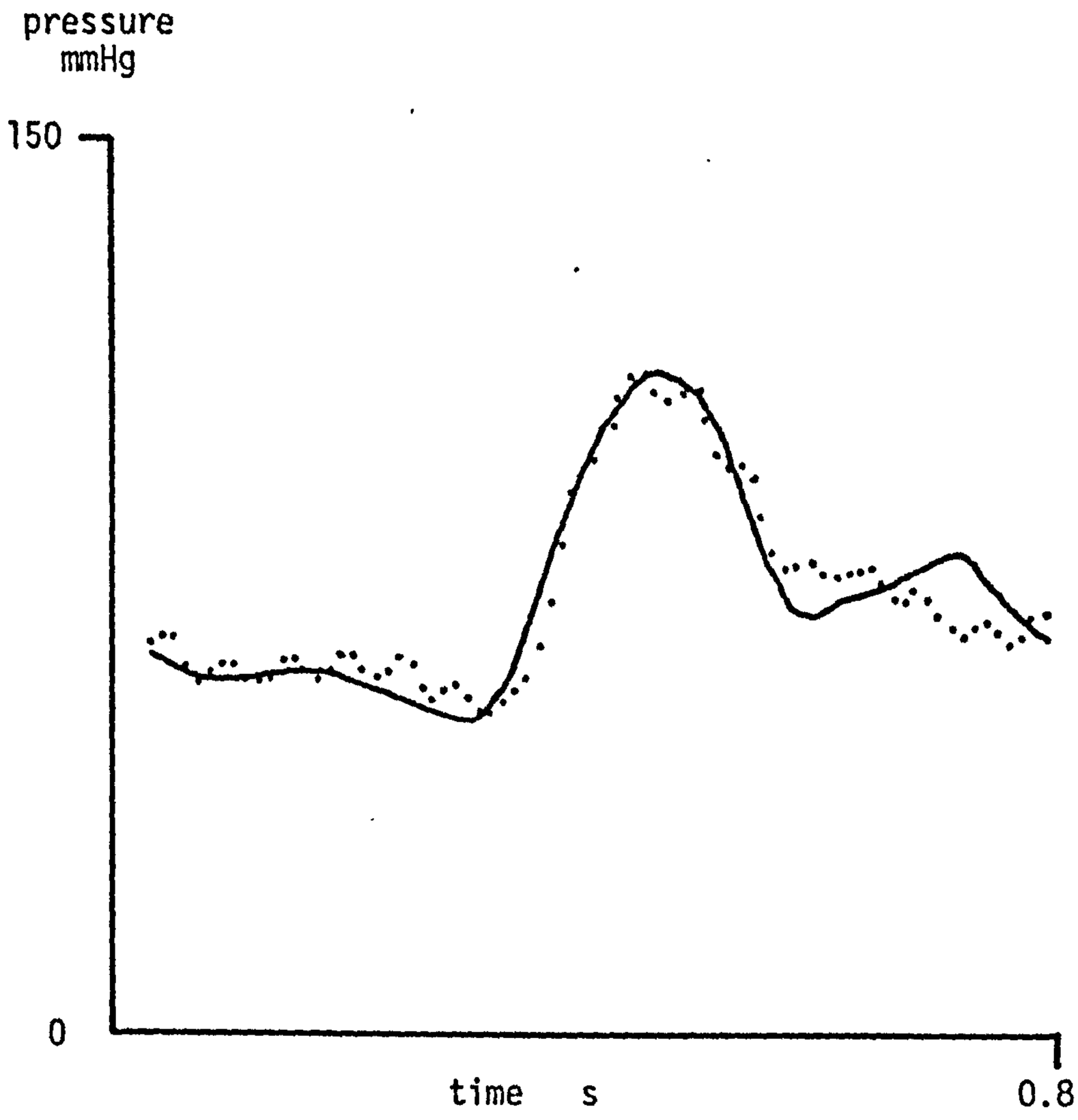

Fig. 6.6

Model femoral artery pressure, solid trace, from HT11 matched to patient record No. 106, dotted trace.

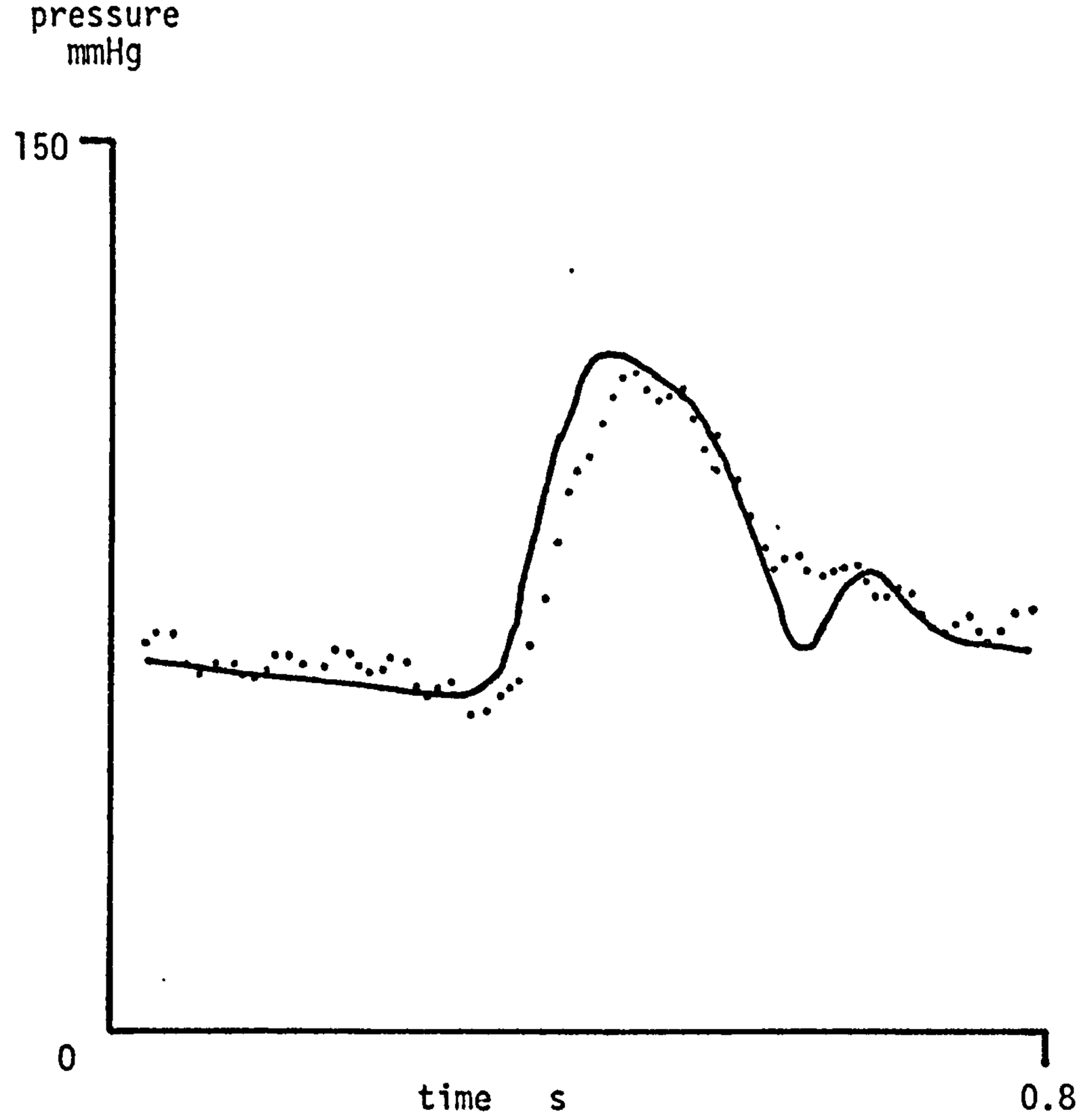

Fig. 6.7

Model femoral artery pressure, solid trace, from HT13 matched to patient record No. 106, dotted trace.

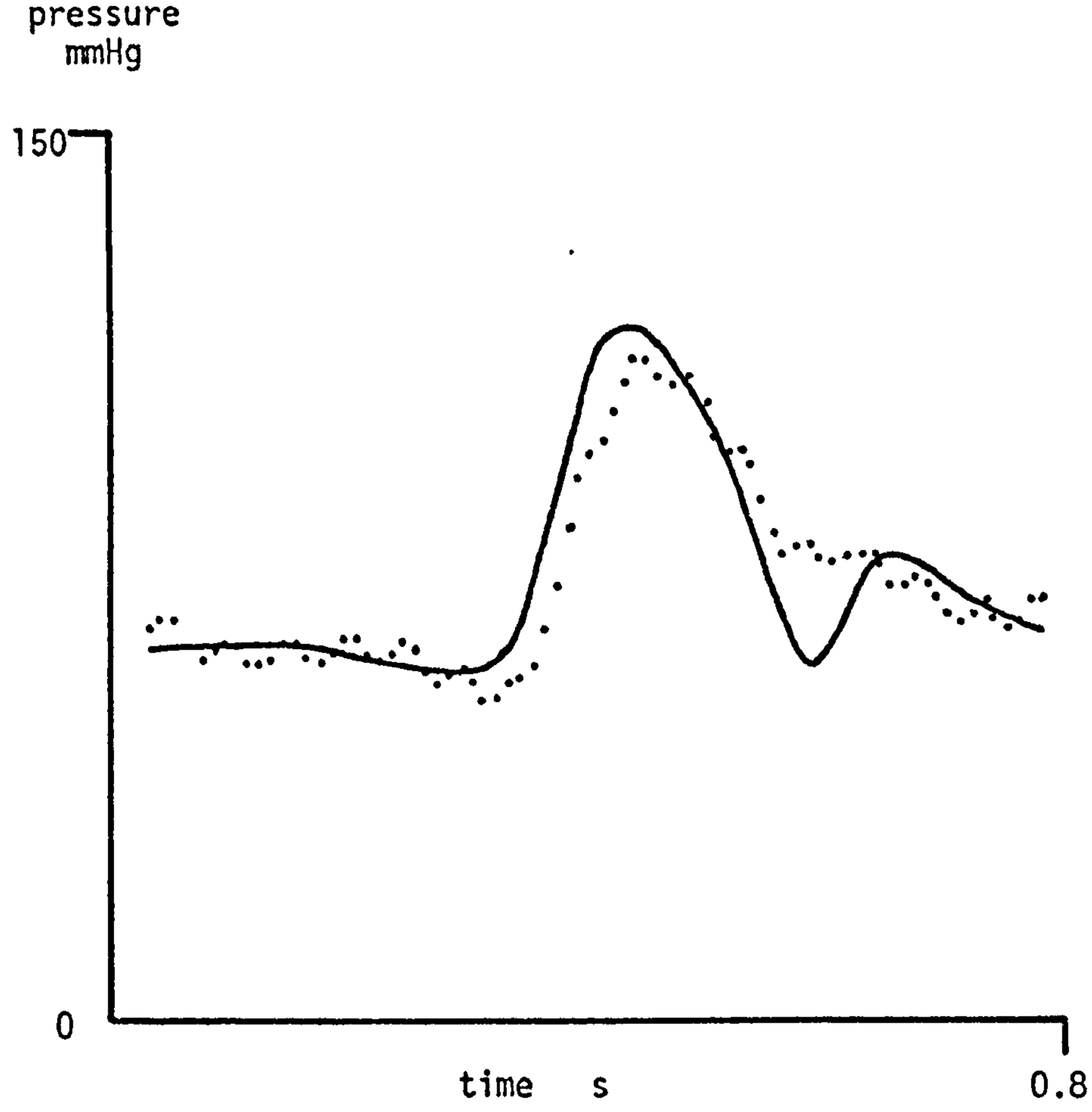

Fig. 6.8

Model femoral artery pressure, solid trace, from HT14 matched to patient record No. 106, dotted trace.

Record	With damping	Without damping
	Matching error mmHg RMS	
106	6.07	6.61
109	3.73	4.71
115	5.72	5.57
133	11.54	8.28
147	3.34	9.76

Table 6.3

The effect of damping terms in the Aaslid model on RMS pressure matching error for femoral artery pressures.

Record	With damping		Without damping	
	C	I	C	I
106	0.531	1.963	0.291	0.597
109	0.897	1.280	0.488	0.436
115	0.823	1.400	0.224	0.297
133	0.252	1.900	0.113	0.995
147	0.909	1.340	0.959	0.997

Table 6.4

The effect of damping terms on the optimum values of compliance and inertia in the Aaslid model.

not adjusted to match the individual patients. It was therefore of no diagnostic significance. The peripheral damping, which was adjusted to optimise the match of diastolic runoff, was not based on any well defined physiological measurements. As there is therefore no sound physical basis on which to assess the absolute values of peripheral damping, it is possible that the effect of these terms on the model is unphysiological. Combined with the small improvement that would seem likely to result from the optimum values of damping, this uncertainty was considered to be evidence against incorporating damping in HT11. In later work on their model Westerhof and Noordergraaf (1970) have shown that arterial wall damping does have a significant effect on arterial input impedance beyond about 5Hz. This is consistent with the findings presented here when it is considered that arterial pressure and flow have small components in this fequency range as discussed in chapter 2. The effect shown by these writers is that the frequency oscillations of impedance are reduced by damping. Considering the variability of the impedance values measured in man, it is difficult to judge whether the effect of the damping is in fact a significant improvement on their model.

Tables 6.5 and 6.6 show the compliance and inertia values determined by the four models for the same set of 5 patient records. Clearly the absolute values for these parameters are quite different. This is not surprising when it is considered that the arterial properties in each model represent an average person and are based on different interpretations of the anatomical data. However it does emphasise that these parameters are only meaningful for comparisons made between patients using the same model. A very simple statistical comparison was made between these results by carrying out a linear regression between each

Record	Model			
	HT04	HT11	HT13	HT14
106	0.220	1.383	0.531	0.99
109	0.264	1.665	0.897	1.912
115	0.239	1.466	0.823	1.693
133	0.131	0.916	0.252	0.841
147	0.281	1.716	0.909	1.675

Table 6.5

Compliance values determined by the four different models matching femoral pressures.

Record	Model		
	HT11	HT13	HT14
106	0.416	1.963	0.859
109	0.286	1.280	0.480
115	0.290	1.400	0.476
133	0.545	1.900	0.958
147	0.301	1.340	0.565

Table 6.6

Inertia values determined by the three different models matching femoral pressures.

set of model data and that for the new model, HT11. The results are shown in tables 6.7 and 6.8 where A and B are the factors in the linear fit where,

$$Y = Ax + B$$

and R is the correlation coefficient.

In general there is a good correlation with the results for the new model especially with that of Beneken where the B value is also small. The poor compliance correlation for the Snyder et al. model can be explained by the single result for record 147 being out of sequence. It seems reasonable from these correlations to conclude that compliance and inertia terms in the different models have the same significance.

6.3 ABILITY OF THE MODELS TO MATCH ASCENDING AORTIC PRESSURES

Ascending aortic pressure was measured with the Millar PC350 catheter tip pressure transducer. This gave good quality pressure recordings with no significant error in the frequency response up to 100Hz. The flow measurement was made with the Carolina Medical 1008 catheter tip flow probe. This was susceptible to catheter whip in the blood flow turbulence and the flowmeter also produced significant amounts of electrical noise. As a result the measurements were ensemble averaged with reference to the ECG as described in chapter 3.

Table 6.9 shows the matching errors for three aortic pressure records from one patient. The Snyder et al. model was not examined with this data. The inertia terms in the new model, HT11, and the Aaslid model,

Model	correlation coefficient	coefficients in linear fit A	B
HT04	0.997	0.183	-0.035
HT13	0.960	0.861	-0.548
HT14	0.854	1.275	-0.401

Table 6.7

Linear regression analysis of compliance estimated by each model, C_n, against that from the new model, HT11, for 5 patient recordings. Equation of fit is $C_n = AC_{11} + B$.

Model	correlation coefficient	coefficient in linear fit A	B
HT13	0.878	2.55	0.640
HT14	0.961	1.920	-0.038

Table 6.8

Linear regression analysis of inertia estimated by each model, I_n, against that from the new model, HT11, for 5 patient recordings. Equation of fit is $I_n = AI_{11} + B$.

Record	Matching error mmHg RMS		
	HT04	HT11	HT13
201	3.92	4.53	8.54
202	4.64	5.30	8.25
203	7.50	8.03	5.30

Table 6.9

Matching errors for three models with ascending aortic pressure. The inertia terms in all models were fixed.

HT13, were fixed. It is shown in chapter 7 that the aortic data does not lead to a unique value of inertia. A representative value of 0.3 was used for inertia in HT11 deduced from the femoral pressure matching, excluding any poorly matched records. This value is close to that of 0.31 found when the femoral pressure for the patient considered here was matched. This pressure was measured by withdrawing the pressure catheter with the flow catheter left in place. A similar average value of 1.35 was used for the Aaslid model. These results show that the simple Beneken model performs marginally better and the Aaslid model significantly worse than the others. The good match with the simplest model may indicate that there is less information present in the aortic pressure than the femoral.

6.4 MODEL ARTERIAL INPUT IMPEDANCES

The models have been tested by matching them to patient pressure measurements and determining an RMS matching error. This gives a quantitative basis for comparing the models with each other and with the measurement errors. There is some published data on the arterial input impedance in man and it is useful also to compare the models with this. The model input impedances were determined using an impulse function test as described in chapter 5.

Fig. 6.9 shows the input impedance moduli of the four models with the adjustable parameters set to the original design values. The values for man are those measured by Nichols et al. (1977) as the average for 5 normal subjects. It should be noted that the standard deviation for the human measurements was approximately 3 $Nm^{-5}10^{6}s$ which is comparable with the differences shown between the models. The smooth nature of

Key: 4 ——— Beneken

11 — — — New model

13 - - - - - Aaslid

14 —•—• Snyder et. al.

• • • • • • man

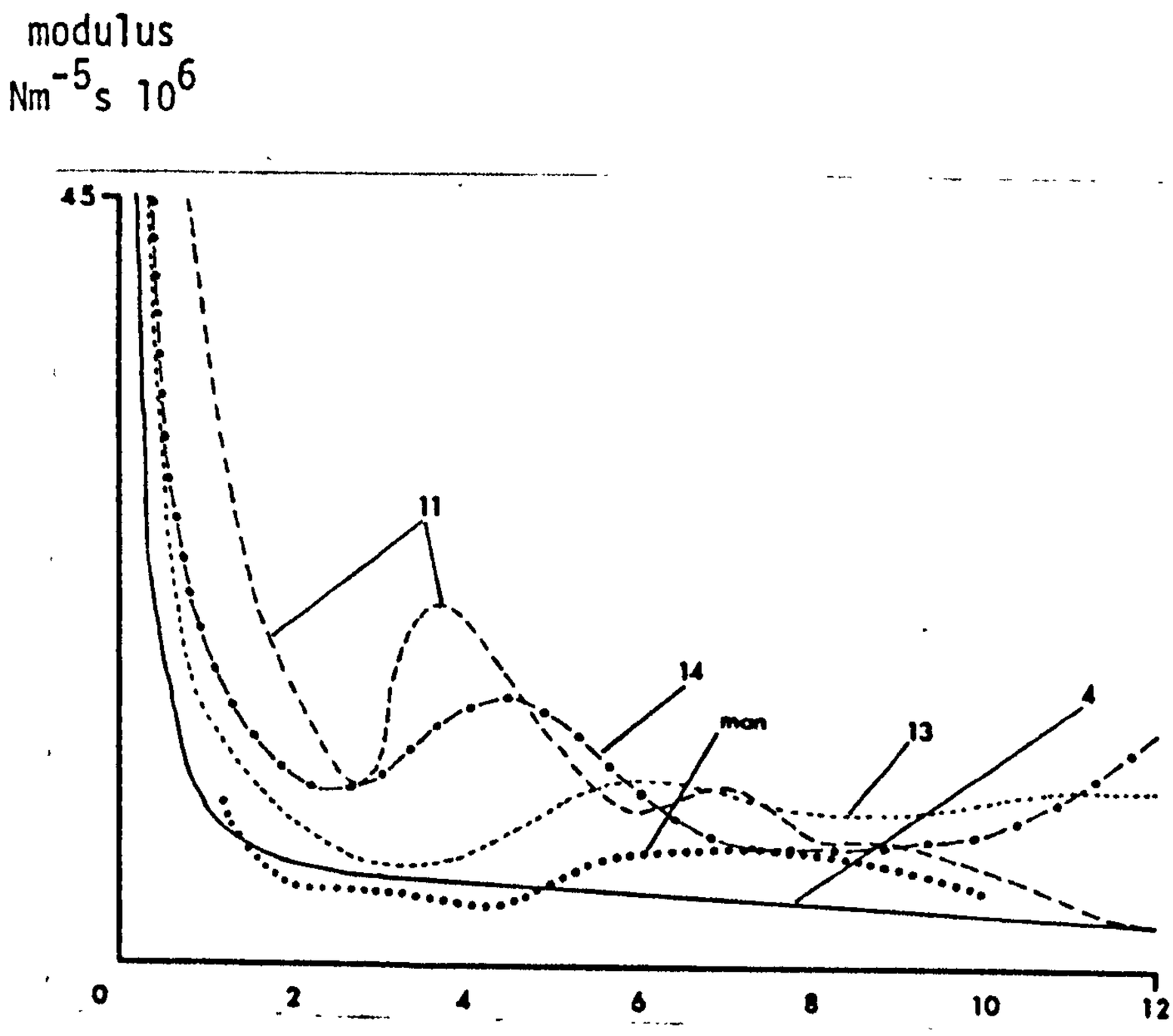

Fig. 6.9

Aortic input impedances of the four models with their nominal parameter values compared with the average impedance in man from Nichols et. al. (1977).

the curve does not necessarily represent the nature of the impedance for any one subject. It may simply reflect the fact that the oscillations in impedance differ widely between subjects and are removed by averaging. Fig. 6.10 shows the model impedances for the models when they were matched to patient record No. 147. As the models are matched to the same data it is not surprising that the impedances became more similar. What is striking is the change in the oscillatory characteristics of the impedance. HT11 changes from having the most oscillations to being one having the least. If the scale of changes is representative of the differences between subjects then it would emphasise the dangers of making detailed general comments about arterial impedance at higher frequencies. However, it is reasonable to note that the simple Beneken model, HT04, lacks what is fairly generally accepted as normal, a minimum impedance in the 2 - 5Hz region. Table 6.2 shows that all the models match the patient record No. 147 in the time domain to a similar degree. It is noticeable that the model impedances however differ quite considerably beyond 4Hz. This indicates that the components at the higher frequencies are too small to have a substantial effect on the aortic pressure and flow waveforms. Of the three multicompartment models Aaslid's appears the least satisfactory at the higher frequencies in as far as it deviates from the other models and the average human results.

6.5 GENERAL EXAMINATION OF THE NEW MODEL

There is no generally accepted and reliable method of measuring the compliance of the large arteries in living humans. The accuracy of compliance values deduced by the model can therefore only be examined indirectly. The same applies to the inertia which is determined by

Key: 4 ——— Beneken

11 — — — New model

13 - - - - - Aaslid

14 —•—• Snyder et al.

••••• man

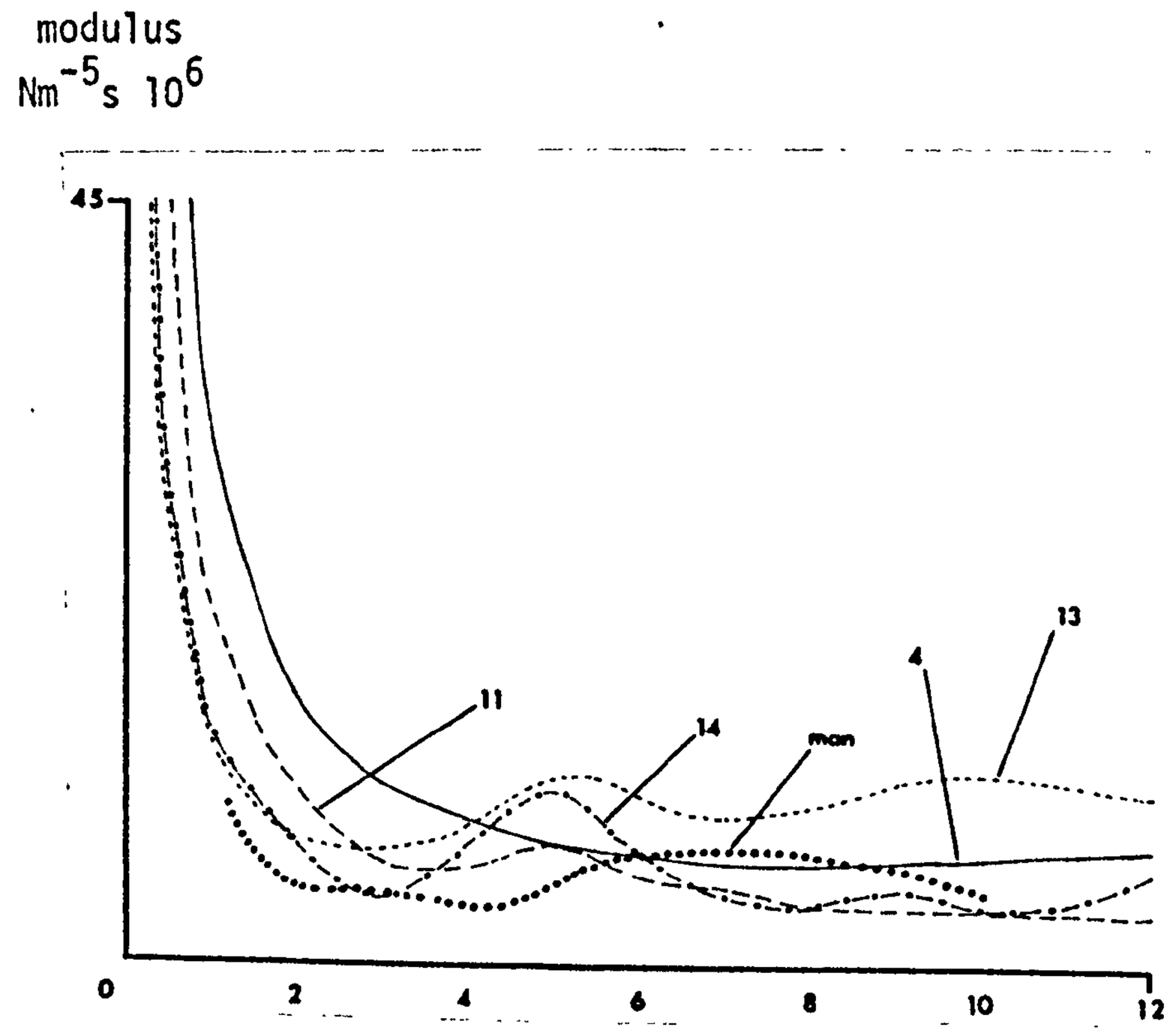

Fig. 6.10

Aortic input impedances of the four models with their parameter values adjusted to match patient record No. 147. The average impedance for man is based on the results of Nichols et. al. (1977)

arterial dimensions that cannot be measured precisely on patients. By examining the compliance and inertia values derived with a model for a number of patients it is possible to make some general observations about their likely significance. The new model HT11 has been investigated in this way using pairs of control measurements of aortic flow and femoral artery pressure on several patients. As far as possible each of the two control measurements were made with the patient under the same conditions.

Table 6.10 shows the estimated parameters from HT11 for the pairs of measurements on 5 patients. These measurements were made within a few minutes of each other in general and with no external changes in the patients' environment or drug state. The exception was the pair of records 108/111 where the second control measurement was made after recovery from a morphine injection. The last two columns summarise the pressure and flow measurements giving mean pressure and cardiac output. In the model the venous pressure has been taken as 10 mmHg in the absence of a measurement. The estimated peripheral resistance has been correlated with (P-10)/C where P is the mean femoral pressure and C the cardiac output for the five pairs of measurements. A correlation coefficient of 1.0 for peripheral resistance was calculated confirming that the matching algorithm has adjusted R to match mean pressure. R in table 6.10 can therefore be taken to be an accurate measure of peripheral resistance and shows that resistance varies in these records by a factor of more than 2:1. Only in the case of 101/102 can a variation of compliance between patients of this order be seen and the matching error for this result is large. The variation in compliance for the same patient is less than that between the patients but, with the exception of 101/102, not much more. From these limited data it cannot be

record No.	parameters estimated by model			matching error mmHg RMS	mean pressure mmHg	cardiac output l/min
	C	I	R			
101	0.55	0.768	2.06	10.1	99.5	2.6
102	0.523	1.012	1.768	9.6	101.6	3.1
106	1.383	0.416	1.185	4.7	75.4	3.3
107	1.313	0.542	1.130	5.0	78.4	3.6
108	1.665	0.280	2.197	3.1	94.6	2.3
111	1.523	0.365	1.659	2.6	90.8	2.9
139	1.382	0.425	2.063	4.0	100.1	2.6
140	1.500	0.435	1.821	3.7	98.7	2.9
146	1.645	0.301	1.035	3.3	77.8	3.9
147	1.716	0.301	0.955	2.8	76.1	4.1

Table 6.10

Parameters estimated by the new model for 5 pairs of control measurements of aortic flow and femoral artery pressure.

demonstrated that the variation in compliance between patients is clearly distinguished from the variations in the estimates produced by measurement errors and inadequacies of the matching technique. If the compliance result for one other patient record of 0.916 with an error of 5.4 mmHg rms, is included, then the compliance variations for each patient are more reasonable. A similar situation exists when considering inertia except that in this case the values of inertia exceeding 0.5 in table 6.10 are associated with large matching errors. These may then represent either limitations of the model or measurement errors.

6.6 SUMMARY AND CONCLUSIONS

Four models have been compared for their ability to represent the human circulation. It has been shown that for the femoral artery pressure measurements there is no great difference between the models on the basis of RMS matching error. During the "runoff" phase there is a noticeable deficiency in the simple Beneken model. Similarly, the addition of fixed damping terms does not significantly improve the match of the Aaslid model. Overall the new model was slightly better than the others for these data. Aortic pressure matching gave a similar result with, in this case, the Beneken model the best. This result suggests that the Beneken model is a good simulation of the input properties of the arterial system but cannot reproduce the changes in pressure that take place along the aorta so well. This is quite clearly shown by its inability to produce pulse pressure amplification as discussed in chapter 4.

Comparing the models on the basis of input impedance has shown the in-

herent weakness of this technique applied to circulation models. There are very substantial errors of measurement especially of flow in the human subject. These errors increase with frequency. This makes any general observations about the location of maxima and minima in the spectra unreliable.

Examination of the inertia and compliance parameters estimated by the different models shows that they are related although the absolute values are strongly dependent on the model formulation. Damping terms, while not improving the match, can cause considerable variation in the parameters if their values are altered.

CHAPTER 7

MATCHING TECHNIQUES

7.1 BASIC PRINCIPLES OF MINIMISATION

Matching a model to patient measurements involves adjusting the model to minimise an error function. In the clinical investigations described there are only two sets of measurements made, the aortic flow and an arterial pressure. The flow has been chosen as the driving function for the model, so the error is the difference between the model and the measured pressures. The error function to be minimised has been chosen as the sum over one heartbeat, E, where,

$$E = \sqrt{\Sigma(P_m - P)^2}$$

P = patient arterial pressure

P_m = model arterial pressure.

This matching error is a function of the adjustable parameters. In general terms it is a surface in n dimensions where n is the number of parameters and the desired solution is the minimum point on the surface.

Techniques for minimising functions of several parameters, where there is no analytical solution, can conveniently be classified as direct search or gradient methods (Box, Davies and Swann, 1969). These will be considered in relation to the problem of minimising a matching error for a model.

Direct Search

In linear direct search algorithms orthogonal direction vectors on the error function surface are specified and the parameters adjusted along each of these vectors in turn. The simplest method is the alternating variable search where the vectors are aligned with the parameters, in other words the parameters are independently adjusted. This is illustrated for the case of two parameters X_1 and X_2 in fig. 7.1 where M is the minimum error and the contours are lines of equal error. Each search is examined to see if the error has been reduced, if so the point reached is the new starting position. The path shown represents the successful searches. However, if there is a valley in the function surface, represented in the figure by Y - Y, then this strategy will continually recross the valley finding only local minima for each parameter. In this case it would be better to attempt to redefine one of the vectors along the valley after the initial search leaving the other vector to provide "course corrections" as shown in fig. 7.2. This can be done in general by establishing a size of change along each direction which is an approximation to the optimum. The vector sum of these changes is an estimate of the valley direction and the remaining orthogonal search vectors allow further adjustments to this optimum direction to be made during the progress of the search.

The method of Rosenbrock (1960) is a popular algorithm of the type which redefines the search vectors, in future it will be referred to as the Rosenbrock method. Starting from some initial point excursions are made along each search direction in turn. If an excursion proves a success, that is a reduction in the error, then this trial point replaces the current point and the step length associated with this vector

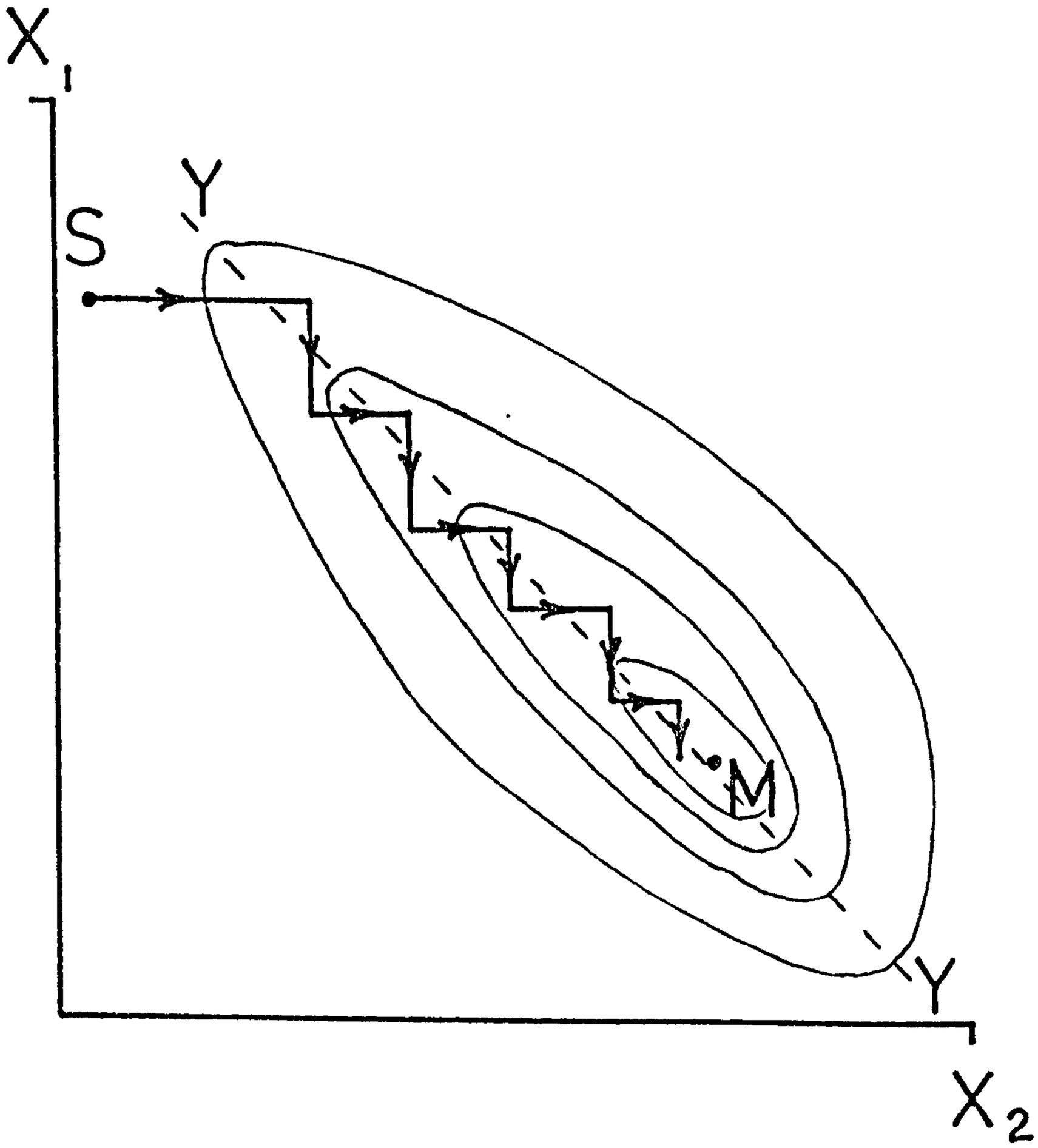

Fig. 7.1

Illustration of a matching error surface for two adjustable parameters X_1 and X_2. M is the minimum error and Y-Y a valley causing local error minima. An alternating variable search is shown starting from S.

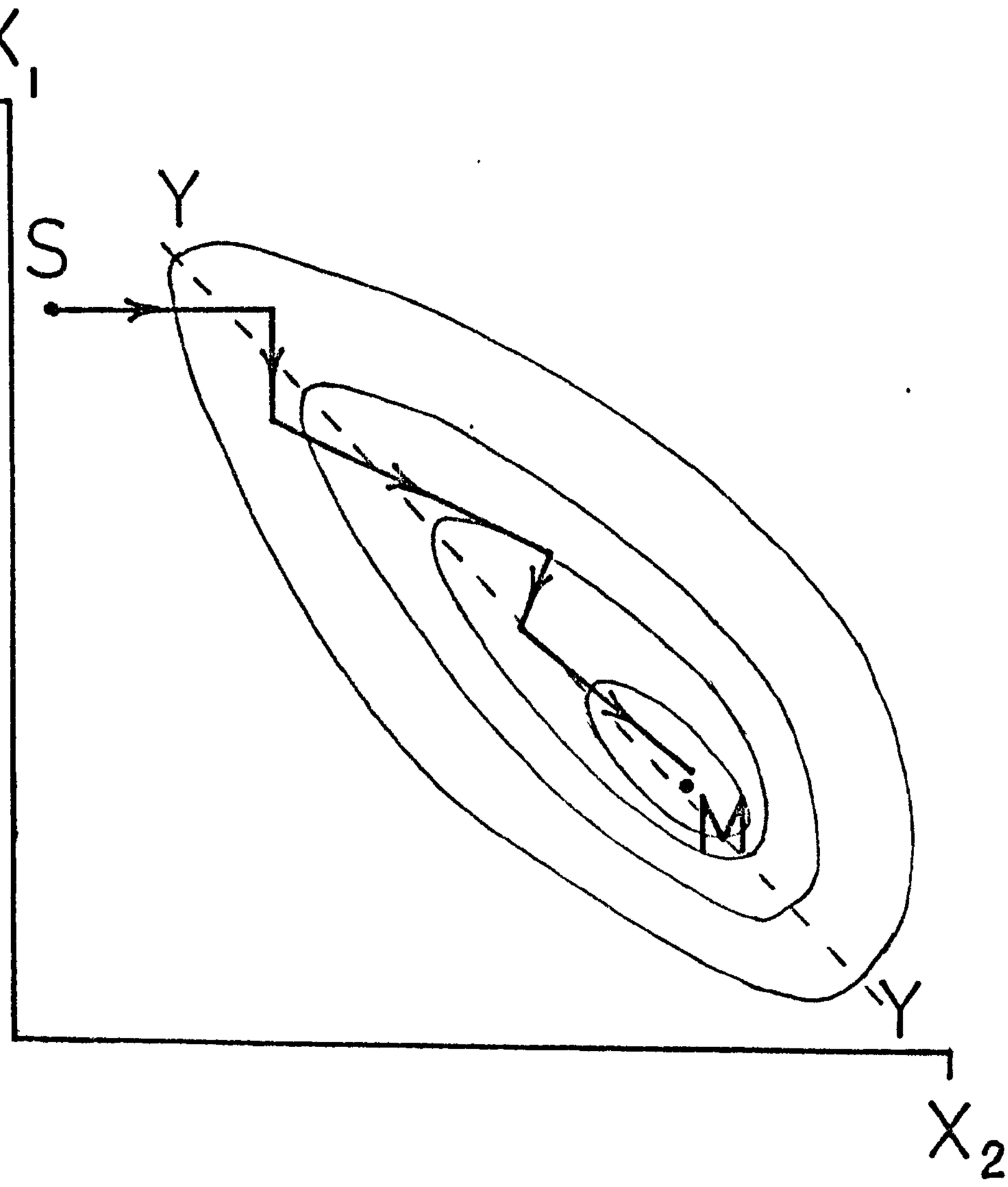

Fig. 7.2

The minimisation problem shown in fig. 7.1 solved using a search algorithm which adjusts one direction of search to be the direction of maximum progress so far.

is multiplied by 3. If the error increases the current point remains unchanged and the associated step length is multiplied by -0.5. This process is continued for all the n direction vectors and the first direction is explored again until every direction has recorded a success followed by a failure. This gives for each vector a magnitude of successful search which is an approximation to the optimum magnitude to minimise the error in that direction. The vector sum of these search vectors is the current estimate of the direction of the minimum error form the previous point. The next search cycle is commenced using this new vector as one search direction and n-1 other orthogonal vectors. The search proceeds as before until success followed by failure makes the derivation of a new search direction possible. The process is continued until some criterion of adequate match is met. It is essential that a method of this type always ensures that the n search vectors are orthogonal, that is that no vector is the linear sum of any of the others; if it were one direction in the error space is not being searched. Other methods are available which attempt to define the search vectors to find the minimum of a specific function in a definite number of steps. The method of Powell (1964) minimises a quadratic function efficiently and as in many problems the error is a quadratic function in each search direction near the minimum, this approach can be useful. If the initial search vectors are badly scaled Powell's (ibid.) method can reduce to an alternating variable search. With methods like the Rosenbrock, bad scaling only makes the first stage of search inefficient.

Gradient Methods

The direct search methods make no use of information relating to the

way in which the fitting error changes with model adjustments other than to note improvements. At any point in the search they do not attempt to estimate where the most likely position for the minimum is. The Rosenbrock method, and others which redefine the direction of search, do so only on the basis of a direction which has been successful without regard to the size of the changes in error. However, if the error contours are spherical then the direction to the minimum is also the direction of steepest error gradient. It can be shown (Box et al. 1969, pp 32,33), that the direction of steepest descent is given by,

$$\frac{\delta X_n}{K} = \frac{\partial E}{\partial X_n} \qquad \ldots\ldots\ldots\ldots\ldots\ldots \quad (7.1)$$

where δX_n is the change in parameter X_n

$\frac{\partial E}{\partial X}$ is the error gradient in the direction of X_n

and K is a constant defining the magnitude of the move down the direction of steepest descent.

This criterion for optimum search direction is the basis of gradient methods, that is schemes which require the determination of the error gradient. Various methods have been developed which attempt to overcome the restriction of spherical error contours including the classical Newton's method (Box et al. 1969, pp 36, 37) and that of Davidon (1959). If the final fitting errors for a model are the result of normally distributed random measurement errors then Marquardt's (1963) method may be used which minimises the squared fitting errors.

7.2 THE CHOICE OF FITTING METHODS

A dynamic model, like the circulation simulations described, is usually formulated as a set of first order differential equations, the state equations, time being the independent variable. Model matching is the process of fitting one or more of the model variables to data measured at a specified interval after a known initial state. The problem described here is more complicated in two important respects. An initial state of the variables, pressure and flow, is not known except for the driving function and indeed most of the variables are not measured at all. Secondly, the measurements are made at a number of points in time. The lack of initial condition data is only acceptable because the system, with a specified driving function, converges to a stationary state independent of the initial condition of all the other variables. This is clearly a fundamental property of the circulation for it to be stable. This means that the state equations must be integrated over several heart cycles before a fitting error can be determined. Secondly, the error must be computed as the difference between the measurements and the model variables over the whole interval of measurement. With a heart rate of sixty beats per minute and a sampling rate of 100Hz, each beat requires 100 solutions of the state equations to be determined. If several beats of stabilisation are required the computation for one determination of fitting error with a set of say 20 equations is considerable. Many of the minimisation techniques described in the literature imply several hundred fitting error determinations. This would be too slow a process for routine use with small computers. Even with a large machine it would represent an expensive procedure. With only two or three adjustable terms in the model simpler methods should be able to achieve the desired result.

Many authors (Box et al. 1969, Noton 1972, for example) consider that there is no universal fitting or minimisation technique. There is also very limited data on the application of model matching to circulation models. Aaslid (1974) uses a mixture of manual adjustment and automatic estimation. The latter is effected by minimising the error in each variable during a time interval in which it is particularly sensitive to the parameter being adjusted. The process is carried out using analogue techniques. Rothe and Nash (1968) designed an analogue model of the canine renal artery containing five adjustable parameters, two of which were set manually. The other parameters were controlled by a form of steepest descent strategy in which the rate of adjustment of the parameter is proportional to an error directly ascribed to it. The model became unstable if all five parameters were adjusted automatically. Sims (1972) estimated 13 parameters in an analogue model of the canine left-heart circulation using five measurements on a dog. He used Marquardt's (1963) method with a digital computer to adjust the model. Despite the inherent speed of an analogue simulation, the computer time involved was large, but this work demonstrated the power of a generalised method for dealing with a substantial number of adjustable parameters. In contrast, Burrus, Parks and Watt (1971) have used an approach based on Z transforms for a third order arterial model. This technique is appropriate when the model is simple and its transfer function can be readily determined. Dennison, Christian and Dick (1972) have used a method similar to the Newton-Raphson interpolation for finding roots of a polynomial. While this was successful, with a 7 compartment circulation model, in matching model derived data, it failed with real patient data. One of the few comparative studies of different methods for matching a circulation model has been made by Donders, Zuidervaart, Robijn and Beneken (1973). The model of these

authors was of the left heart and arterial circulation with the emphasis on the detail of the left ventricle. In this study six heart function parameters were estimated and all the vascular parameters fixed. The error function minimised by the method was computed from the weighted sum of the errors in the various model outputs. Three search methods were tried: an alternating variable search, a simple steepest descent method and a development of this due to Davidon. No clear advantage between the methods was found and no one method was particularly accurate.

A matching method has to be chosen to suit the specific problem. Box et al. (1969) consider that gradient methods are best when the gradients can be calculated analytically, approximate solutions can make the methods inefficient. For this reason direct search methods have been employed. Experience with these suggests that solutions can be obtained with fewer solutions of the state equations than would be necessary if gradients were to be determined.

7.3 PRINCIPLES OF TESTING MATCHING ALGORITHMS

Before a specific algorithm can be developed, it is necessary to establish the means by which a method or variation on it can be evaluated. The general objectives of a method will always be to match a model as fast and accurately as possible to measured data. Speed is conveniently measured in terms of the number of state equation solutions required to satisfy the accuracy criterion. If there is a basic similarity in methods it may be appropriate to use the number of matching cycles as a basis for speed comparison, where one cycle of error minimisation requires the same number of solutions.

The accuracy of matching is complicated by two factors, first the measured data will contain some errors, secondly a practical model is likely to be an approximation to the real system behaviour. For both reasons a perfect match is not likely to exist and the acceptable error of match must be related to the data measurement errors and the error in the best match possible from the model. As the latter is not known in advance, one reasonable criterion for stopping the adjustment process is to finish when the improvement in match from a further trial is less than the errors due to the input data. The testing process must then establish that this small change in error is a reasonable measure of the likely further improvements and not the result of a slowly converging minimisation procedure. Similarly it must be shown that the matching error function has no local minima that stop the matching process before the true minimum is found. Often there is no unique solution to the minimisation process because there are several minima which are equal within the error due to data measurement. A reasonable way of examining all these situations is to repeat the procedures several times, with different initial conditions for the adjustable parameters. In this way the minimum is approached along different paths in the error space.

The primary object of the models is to estimate arterial parameters, not to simulate the circulation, so that the important errors are those in the parameters themselves. The effect of errors in the measured data can be determined by adding an error function to the data and observing the change in the estimated parameter values which result. These errors represent the inherent errors which cannot be reduced by changing the minimisation procedure. They will be the criteria by which other sources of error caused by defects in the minimisation pro-

cedure described so far can be evaluated.

Measured data is not always satisfactory for testing as the optimum values for the parameters and the minimum possible matching error cannot be accurately determined. Data can be generated from the model itself run with a suitable driving function and fixed parameter values. If this data is then matched with the model using different starting conditions the matching method can be examined with the best values for the parameters known. The minimum matching error will be zero. This form of model-model testing should be treated with some caution. The error function may behave differently with model data than with real data that cannot be exactly matched by the model. This will influence tests on the failure of methods to find the true minimum and will also affect the speed of match.

7.4 DEVELOPMENT OF A MATCHING TECHNIQUE FOR THE MODELS

The model produced during this work was intended to have a general application to circulatory measurements made at different locations in the arterial system. The new model has been applied to data obtained from the ascending aorta and the femoral artery and the matching methods have been developed for these two situations (Bourne and Kitney, 1978). The most obvious use of the model is to examine the input characteristics of the aorta using the ascending aortic pressure. Clinically these measurements are difficult to make. In the catheter laboratory they require either a specialised flow-pressure catheter or two separate catheters. In the post open-chest-surgery situation an aortic catheter is needed for the pressure which is not clinically necessary. It is for this reason that femoral artery pressure measure-

ments are of interest.

First the matching technique was developed using model-generated ascending aortic pressure and adjusting compliance and peripheral resistance terms. Then the method was extended to deal with femoral artery pressures. Patient femoral measurements showed that an adjustment of the inertia term would be required and this was incorporated. Both the aortic and femoral matching procedures were then tested for their effectiveness using both model-generated and patient data.

Initial Study with Simulated Aortic Pressure

A version of the Beneken (1965) model, modified to include Aaslid's (1974) systemic arterial simulation, was used for the preliminary investigation of matching algorithms. This model had only arterial compliance, C_A and peripheral resistance, R_S adjustments, it used left ventricular pressure as its driving function and matched ascending aortic pressure. The RMS pressure matching error and the parameter values were printed out for each stage of matching to allow an examination of the adjustment path taken. This model has the advantage of short computation time while still exhibiting the basic relationships between arterial pressure and compliance and resistance. Data for the match was obtained by running the model, with Beneken's (ibid.) original ventricular simulation. Left ventricular pressure and ascending aortic pressure were punched onto paper tape for two settings of the compliance and resistance adjustments for the model as shown in table 7.1. The left ventricular pressure on the tape was then used to drive the model with its matching algorithm so that the conditions for an exact match of aortic pressure were known. First an alternating

Test	Compliance scaling factor	Resistance scaling factor
A	0.87	1.2
B	0.7	1.5

Table 7.1

Parameter settings for model generated aortic test pressures using the Beneken (1965) model, with the systemic arterial simulation of Aaslid (1974).

Algorithm	Number of Searches	
	A	B
Alternating variable search	18	20
Basic Rosenbrock	14	17

Table 7.2

Number of searches to match the Beneken circulation model, with Aaslid's arterial simulation, to model generated aortic pressure records.

variable search was used in which the compliance and peripheral resistance, C and R, are adjusted according to the formulae,

$$C_{K+1} = C_K(1 + S_1) \quad \ldots\ldots\ldots\ldots\ldots\ldots \quad (7.2)$$

$$R_{K+1} = R_K(1 + S_2) \quad \ldots\ldots\ldots\ldots\ldots\ldots \quad (7.3)$$

where S_1 and S_2 are the step lengths for the search.

The parameters were adjusted in turn and if a change resulted in an improvement then S was multiplied by 3, if the trial was a failure then S was multiplied by -0.5. Successive searches of each parameter were made starting from the best value found so far and using the current value of the corresponding S. Knowing the true values of C and R it was clear that a better value of C could be rejected because it produced a worse match with the current value of R. This was explained by the fact that the resistance determines the rate of flow of blood out of the aorta and the compliance the corresponding rate of fall of pressure. The diastolic contribution to the pulse pressure of the model is therefore roughly proportional to 1/(CR) for a given mean flow. So for any matching operation there will be local minima or a valley in the error surface along a curve defined by 1/(CR) is constant. For this reason the Rosenbrock method was next examined, as it attempts to redefine one of the directions of search along any such valley. New search vectors, for a two variable system, can be simply defined as,

$$\bar{D}_1 = S_1 (A\bar{U}_C + B\bar{U}_R) \quad \ldots\ldots\ldots\ldots\ldots\ldots \quad (7.4)$$

$$\bar{D}_2 = S_2 (B\bar{U}_C - A\bar{U}_R) \quad \ldots\ldots\ldots\ldots\ldots\ldots \quad (7.5)$$

where $\bar{U}_C$ is a unit aortic compliance vector and $\bar{U}_R$ a unit peripheral resistance vector. If A = 1 and B = 0 these search formulae reduce to the alternating variable search in which compliance and resistance are adjusted separately in turn. This is the starting condition for the Rosenbrock method. Searches are made in the directions $\bar{D}_1$ and $\bar{D}_2$ alternately with S_1 and S_2 adjusted according to a success or failure as before. When a failure has been reported in both directions $\bar{D}_1$ is redefined by adjusting A and B so that $\bar{D}_1$ is in the direction of the total success so far in both C and R, $\bar{D}_2$ will then be orthogonal to $\bar{D}_1$.

The alternating variable search and the Rosenbrock method were compared using two model generated test records. The results are shown in table 7.2. The lengths of the initial searches, which are arbitrary, were made the same for both methods. Although the Rosenbrock method shows some advantage, from this limited comparison, the problem with both methods is the arbitrary choice of search lengths. It was decided not to carry out an extensive comparison of the two methods as different results could be obtained depending on the choice of lengths used. The Rosenbrock algorithm determines the direction of the most likely future success, but it cannot predict whether the current searches have gone past the minimum or not. The best sign and magnitude for S_1 and S_2 for the next move, after redefining the vector directions, cannot be estimated with the method. Similarly, the best initial search length cannot be calculated. With a circulation model it is

possible to estimate values for S_1 and S_2 from the known gross effect of arterial compliance and resistance and a modified Rosenbrock method has been designed on this basis (Bourne and Kitney, 1978).

An initial run of the model is made to establish base values of the mean pressure, and in the overall root mean square error E_{RMS}. The changes in compliance, δC and resistance, δR that are required to improve the match are estimated as follows, assuming the relationship between pulse pressure P_p and compliance C,

$$P_p = \frac{K_1}{C} \qquad \text{where } K_1 \text{ is constant,}$$

then a change in compliance to C' will produce a pulse pressure P'_p given by,

$$P_p - P'_p = K_1 \left(\frac{1}{C} - \frac{1}{C'} \right) = K_1 \left(\frac{C' - C}{C'C} \right)$$

$$\text{now } K_1 = C' P'_p$$

$$\text{so } P_p - P'_p = P'_p \left(\frac{C' - C}{C} \right)$$

If P_p is the current model pulse pressure and P'_p the required pulse pressure then the change in compliance required, δC, is given by,

$$\delta C = C' - C = C \left(\frac{P_p - P'_p}{P'_p} \right) \qquad \ldots\ldots\ldots\ldots \quad (7.6)$$

Similarly for resistance and mean pressure P_M,

$$P_M = K_2 R$$

$$P_M - P'_M = K_2 (R - R')$$

$$K_2 = P_M / R$$

$$\delta R = R' - R = R \left(\frac{P'_M - P_M}{P_M}\right) \quad \ldots\ldots\ldots\ldots\ldots\ldots \quad (7.7)$$

For the initial search A and B in equations 7.4 and 7.5 are set to δC and δR respectively and S_1 is set to unity. This makes the initial value of $\bar{D}_1$ the estimated change required to match the model. S_2 is set to 0.1 to make $\bar{D}_2$ a trial search of 10% in the orthogonal direction.

A normal Rosenbrock search cycle is then carried out with the usual re-scaling of S_1 and S_2 for success or failure, until both vectors have produced a failed search. The standard method would then redefine $\bar{D}_1$ as the direction in which overall improvement has been made in C and R by making A and B in equations 7.4, 7.5 equal to the overall magnitude of the successful changes in C and R respectively. S_1 and S_2, which are not defined by the standard method, are calculated for the modified method as,

$$S_1 = (\delta RB + \delta CA) / (B^2 + A^2) \quad \ldots\ldots\ldots \quad (7.8)$$

$$S_2 = (\delta C - S_1 A) \ / B \qquad \ldots\ldots\ldots\ldots\ldots\ldots \quad (7.9)$$

where δC and δR are the estimated changes from equations 7.6 and 7.7. These values give $\bar{D}_1 + \bar{D}_2$ equal to the estimated changes required to match the model. This modification to the method does not affect the normal search directions of the Rosenbrock method, but it makes the sum of the first two steps of each search cycle the estimated minimum. All subsequent cycles calculate the initial values of S_1 and S_2 from equations 7.8 and 7.9.

A comparison between this method and the basic Rosenbrock method has been carried out on the new arterial model, HT11. To make the comparison fair the basic method starts with A and B also equal to δC and δR calculated from equations 7.6 and 7.7. S_1 and S_2 are kept constant throughout at 0.3, a value around the size of S_1 calculated in the modified method for the second search cycle.

The models were tested using tapes of aortic flow and aortic pressure generated by a suitable version of the new model in the same way as before. For these test functions aortic flow, measured from a patient, was used as a driving function with the model settings shown in table 7.3. With an error limit of 1.0 mmHg RMS the results of the comparison are shown in table 7.4. This shows a significant advantage for the modified method. Again the standard method has arbitrary values of S_1 and S_2, while the modified method still obeys the rules of the standard one so there is no real basis for a strict comparison.

The next logical step is to examine a successive approximation method using equations 7.6 and 7.7 to calculate the changes required in C and

Test No.	C_A	R_S	I_A
1	1.7	1.7	1.0
2	1.7	0.7	1.0
3	0.7	1.7	1.0
4	0.7	0.7	1.0
5	0.7	1.7	0.5
6	1.7	0.7	0.3
7	0.7	1.7	1.2

Table 7.3

Parameter settings for model generated aortic test pressures.

Algorithm	Number of Searches Test No.			
	1	2	3	4
Basic Rosenbrock	14	17	26	14
Modified Rosenbrock	10	9	14	4
Successive approximation	4	2	3	2

Table 7.4

Number of searches to adjust model HT11 to match model generated aortic pressure data. The search terminated when the change in error was less than 1 mmHg RMS.

R repeatedly with no search process in between. Table 7.4 shows the results of a comparison of this method with the modified Rosenbrock, a striking improvement can be seen. The danger of the modified method and successive approximations is that they may find significantly different optimum settings from those determined by minimising the chosen function of RMS pressure error by searching. Equations 7.6 and 7.7 determine that no further change in C and R will be made when the mean and pulse pressures have been matched. This would probably not arise in model-model matches where the two sets of criteria can be satisfied simultaneously. This is investigated further in section 7.5.

The arterial model HT11 has a fairly long time constant so that stationary conditions are not reached after parameter changes for several beats. This can lead to errors in the matching strategy whatever form this takes. Some improvement has been obtained by scaling all the pressures in the model, after a matching attempt by P_0/P where P_0 is a pressure measured from the patient and P the corresponding model pressure. These values then serve as the initial conditions for the next search. With the Rosenbrock methods this results in the error function increasing with each beat towards the true matching error after a parameter change. There is a reduced danger then of a good matching move being rejected because the model has not settled sufficiently, the error is more directly a measure of the result of the proposed parameter settings and less dependent on the previous ones which may have been rejected anyway. The number of heartbeats allowed for the model to settle is a compromise, too many beats will use a large computing effort without the appropriate increase in accuracy. Too few beats will make the number of searches required increase. During these comparative tests it was decided that three heart beats should be allowed after each

parameter change and six for the initial run. This was modified later when inertia adjustment was added.

In the Rosenbrock methods, searches are often made which involve large changes in the parameters. If a search was a failure it was found to be useful to reset all the flow and pressure variables to the values achieved after the most recent successful search.

Application of Successive Approximation to Femoral Artery Pressures

The initial study showed that there was a considerable advantage in using a successive approximation method for matching the arterial model. When a number of patient recordings of femoral artery pressure and aortic flow were examined it was found that adjustment of the inertia terms in the model was necessary to match the time relationship between the flow and pressure. An improvement in the matching of the pressure waveform shape also resulted from this adjustment. On the basis of the original experience a successive approximation estimate of the inertia was used to adjust the inertia scaling factor, I. The time delay between the model femoral artery pressure and the patient measurement was found by shifting the model pressure one 10 ms sample interval at a time and computing the RMS error of match which resulted. The time shift which produced the minimum error was taken as the best estimate of the delay. An empirical formula was produced to compute the estimated change required in the inertia factor I as follows,

$$\delta I = -8t$$

where t = time delay in seconds.

Table 7.5 indicates the accuracy of this estimate for recordings from 6 different patients. It can be seen from the table that the first estimate of I using this formula is a useful approximation to the value finally selected after several cycles of matching. The initial value of I was 1.

As there are some shape changes in the pressure also produced by the inertia adjustment a further stage of searching was incorporated in the method. This is carried out either when no improvement could be found by shifting the pressure, or if an estimate from the time delay did not improve the match. With only one parameter to adjust, there is only one search direction so the search is carried out as in the alternating variable search used previously. The initial search is made from the previous best estimate of I with a vector - 0.5 times the last time delay estimated, δI. The effect of this search is shown in table 7.6 for the same six patients. It can be seen that the search does not significantly improve the match and takes a disproportionate number of function evaluations. Table 7.7 shows the results for model-model tests using the test functions of table 7.8. In all four cases a reasonable match was obtained in only two successive approximations of inertia adjustment. In the two cases, 22 and 24, where a significant error is reduced by the search, it should be noted that a relatively large number of searches is required.

In the model-model test there is known to be at least one solution giving a zero error. In the tests on aortic pressure matching that have been described, where C and R only were adjusted, it was concluded that successive approximation of C and R gave accurate results. The adjustment of R was based on mean pressure which is unaffected, in a

Patient record	estimated change in I_A	final overall change in I_A	final error mmHg RMS
105	-0.24	-0.447	8.59
106	-0.48	-0.584	4.72
109	-0.56	-0.714	2.61
126	+0.08	+0.12	8.19
140	-0.56	-0.569	3.65
147	-0.64	-0.699	2.83

Table 7.5

Change in inertia scaling factor for model HT11 estimated from time delay compared with overall change after successive approximation. The pressure records being matched are femoral artery pressures from six patients.

Patient record	Successive approximation using time delay		Search	
	error mmHg RMS	No. of cycles	error mmHg RMS	No. of cycles
105	10.87	3	8.59	6
106	4.82	2	4.72	7
109	3.40	2	2.61	8
126	8.19	3	8.19	1
140	3.67	1	3.65	6
147	3.14	1	2.83	8

Table 7.6

Matching error and number of cycles for the estimate of inertia using pressure time delay compared with the result of subsequent cycles of search. The records matched are femoral artery pressures from six patients.

Test No.	Initial I_A	Successive approximation		Search	
		error mmHgRMS	No. of cycles	error mmHgRMS	No. of cycles
21	0.5	0.45	2	0.09	2
22	1.0	2.77	2	0.12	9
23	1.0	0.78	2	0.65	1
24	1.0	3.96	2	0.95	7

Table 7.7

Matching error and number of cycles for inertia estimate to match model generated pressures.

Test No.	C_A	R_S	I_A
21	1.7	1.7	1.0
22	0.7	1.7	0.5
23	1.7	0.7	0.3
24	0.7	1.7	1.2

Table 7.8

Parameter settings for model generated femoral artery test pressures.

linear model, by the compliance C. As a result the optimum R value, at any stage of match, was independent of C. So there are no local error minima in this case. When inertia adjustment is introduced into the model there is no independent criteria for its adjustment. Time delay of the pressure wave, and pulse pressure, are functions of both inertia and compliance. While R can still be adjusted satisfactorily by approximation, pulse pressure and time delay errors can be reduced to zero for non optimum values of C and I. This is why the results show some possibility of reducing the matching error by search for a better value of I after the time delay has been reduced to zero. The overall adjustment routine chosen was as follows -

1. Four beats of the model to stabilise it.
2. Determine the initial pulse, mean and RMS errors.
3. Three cycles, each of two beats, in which C and R are adjusted.
4. Estimate inertia by time delay or search and adjust compliance.
5. Using this value of inertia run three cycles, each of two beats, adjusting C and R.
6. Repeat 4 and 5 until matching error changes by less than 0.5 mmHg RMS.

This procedure of optimising C and R for each value of inertia was chosen for two reasons. The time delay estimation of inertia takes some time as all the values for model and patient pressure are compared for each of 15 values of time shift to find the optimum. This is fairly slow, so that it is preferable to keep this process to a minimum. During the search algorithm for inertia adjustment, which has been

shown to be a slowly convergent process, this procedure ensures that the best match possible with the current value of inertia is the one examined.

A further refinement is mentioned in point 4 of the adjustment routine above to compensate for the effect of inertia changes on pulse pressure. By examining the change in C which is found necessary to restore the pulse pressure with changes in inertia the following compliance change can be estimated,

$$\delta C = C((1 + \delta I/I)^{0.58} - 1)$$

7.5 EVALUATION OF THE SUCCESSIVE APPROXIMATION METHOD

General considerations

It has been shown in the last section that a successive approximation method can be considerably faster for matching the models designed for analysing patient data than a more generalised technique. A method has been developed for a model with three adjustable factors, compliance, inertia and peripheral resistance, with ascending aortic flow as a driving function. Two types of pressure have been matched with the model, femoral artery and ascending aortic pressure. For the former a successive approximation was possible for all three parameters with a subsequent phase of search for the final inertia value. For the aortic pressure no arterial time delay was available from the measurements and inertia was adjusted only by searching. It has yet to be shown that an inertia adjustment is necessary for a good match with aortic pressure. The tests on the aortic pressure matching algorithm

have therefore been carried out both with and without inertia adjustment routines. This also gives some useful information about the effect of changing the number of parameters on matching efficiency.

Some of the evaluation was carried out with model to model tests and some with real patient data. Studies were made of the effect of errors in the measured data, differences in the data itself, changes in the initial values of the adjustable parameters and the sensitivity of the matching error to the parameters.

Effect of errors in the measured data

Errors in the measurements will result from imperfections in the amplifiers, movement of the catheters and electrical interference. It was decided to simulate the errors by a pseudo-random-binary sequence added to the pressure being matched, as described in chapter 5. For this it was necessary to use a record length of $(2^n - 1)$ clock periods for the sequence and n was chosen as 4 giving a length of 15. By sampling each clock period four times a length of 60 samples, equivalent to 0.6 s was produced. A patient aortic flow recording of 66 samples was chosen, truncated to 60 samples and used as the driving function to produce a model generated pressure. The aortic pressure had a pulse amplitude of 42 mmHg and the femoral pressure 74 mmHg. To these were then added 1, 3 and 5 mmHg RMS PRBS functions having peak to peak amplitudes of 2, 6 and 10 mmHg. Tables 7.9 and 7.10 show the results for aortic pressure matching, with and without inertia adjustment, which are similar. The matching errors are significantly greater than the noise added, perhaps an indication of the effect of the algorithm minimising pulse and mean pressure errors.

Noise added mmHg RMS	amplitude % of pulse pressure	% error in C_A	R_S	Matching error mmHg RMS
0	0	+1.7	-0.1	0.3
1	4.8	-10.9	+0.1	2.1
3	14.3	-32.6	+0.6	6.2
5	23.8	-36.7	+0.9	7.8

Table 7.9

Effect of PRBS noise added to aortic pressure on model matching with constant inertia terms.

Noise added mmHg RMS	amplitude % of pulse pressure	C_A	% error in R_S	I_A	matching error mmHg RMS
0	0	+2.0	+0.1	+1.2	0.55
1	4.8	-0.9	+0.3	+6.7	1.60
3	14.3	-3.6	+0.6	+15.4	3.90
5	23.8	-38.5	+0.9	+13.0	7.45

Table 7.10

Effect of PRBS noise added to aortic pressure on model matching with an adjustable inertia term.

The compliance term is shown to be very sensitive to the noise with errors of the order of twice the percentage error in the pulse pressure. Surprisingly the addition of an extra adjustment term, inertia, does not appear to increase the error in the compliance but rather reduce it. As this term is adjusted to minimise matching error it might have been expected to reduce the matching error to less than the added noise while changing the errors in the other parameters. Apparently this term is not able to make the model match the noise to any extent. With no mean component in the noise the peripheral resistance is largely unaffected. The femoral artery matching results, table 7.11, are similar but with smaller errors in compliance, inertia and pressure match. Overall the matching errors are of the same order as the added noise indicating that the technique is effective in dealing with data it cannot accurately match.

Effect of different measured data

A very basic test of the matching technique is to establish that it can produce the correct match for a variety of different measurements. This was done with model generated data, tables 7.12 - 7.14, so that the parameter values for a perfect match were known. In each of the three cases the matching procedure was terminated when the pressure matching error changed by less than 0.5 mmHg RMS. Comparing table 7.12 with table 7.13 gives an indication that the two parameter case has a more steeply convergent minimisation strategy than that for the three parameter case , giving smaller parameter errors. There is no sign of a false minimum being found which would be indicated by large compensating errors in two or three parameters. The inertia errors are noticeably larger than those in the other parameters. It appears

Noise added mmHg RMS	Noise added amplitude % of pulse pressure	% error in parameter C_A	% error in parameter R_S	% error in parameter I_A	matching error mmHg RMS
0	0	+0.3	0.0	-0.6	0.18
1	2.7	-0.1	+0.1	-0.6	0.99
3	8.1	-5.9	+0.3	+2.6	2.90
5	13.5	-13.1	+0.7	+7.0	5.05

Table 7.11

Effect of PRBS noise added to femoral artery pressure on model matching.

Test No.	% error C_A	% error R_S	matching error mmHg RMS
1	-0.5	0.0	<0.3
2	+0.5	+0.4	<0.3
3	+0.3	-0.1	<0.3
4	-0.4	+0.3	<0.3

Table 7.12

Errors produced by matching the model to the aortic pressure test data shown in table 7.3. The inertia term is kept constant.

Test No.	% error in C_A	% error in R_S	% error in I_A	matching error mmHg RMS
1	-1.3	+0.3	-5.9	0.33
2	+0.3	+0.1	-5.9	0.19
5	-1.1	-0.2	+5.8	0.33
6	-1.4	+0.1	-16	0.42
7	-0.4	+0.1	+1.2	0.98

Table 7.13

Errors produced by matching the model to the aortic pressure test data shown in table 7.3.

Test No.	% error in C_A	% error in R_S	% error in I_A	matching error mmHg RMS
21	+0.4	+0.1	0.0	0.09
22	-0.6	+0.1	+0.2	0.12
23	+0.8	+0.0	+6.7	0.65
24	+0.7	-0.1	-2.3	0.95

Table 7.14

Errors produced by matching the model to the femoral artery test pressures shown in table 7.8.

Patient record	Initial value	% change in parameters C_A	R_S	I_A	change in error mmHg
202	0.5	+7.1	+0.2	-46.3	+2.73
	1.5	+2.0	0.0	+3.6	+2.64
203	0.5	-9.9	-0.4	+78.3	+0.35
	1.5	-3.2	-0.7	+19.2	+0.06

7.15

Effect of initial parameter values on the final values and on the matching error. The changes shown are relative to the values obtained with initial values of 1. The patient records matched were ascending aortic pressure.

that either the match is less sensitive to inertia than to compliance and resistance or that inertia is not adjusted enough in comparison to the other two.

Uniqueness of the solution

With real patient measurements, which the model may not be able to match exactly, there is increased likelihood that the method will not find the global minimum error but a local minimum. It is also possible that there is not a unique minimum within the accuracy to which the error is determined. This has been investigated by matching two patient records, one of which gives a good match and the other a poor one when the parameters are started with values of 1.0. The adjustable model parameters were initially set at 0.5 or 1.5 and the results compared with those for initial conditions of 1.0. Table 7.15 shows the changes in compliance, resistance and inertia estimated when the model matched a patient aortic pressure with the different starting conditions. The changes in the inertia term show that the optimum value for this parameter is very poorly estimated. Examination of the steps in the estimation revealed that the error changed by small amounts for large changes in the inertia. Much of the effect of an inertia change could be compensated for by a small change in compliance. However the final matching error is significantly affected as the result of large changes in inertia being tried by the search procedure as no preliminary approximation was possible for aortic pressures. These changes caused the model to take a long time to settle so that the error measurements were being taken while the error was still changing. With the low sensitivity of the error to inertia the optimum value of the latter was poorly defined. Table 7.16 shows the

Patient record	Initial value	% change in parameters C_A	R_S	change in error mmHg
202	0.5	-0.4	-0.5	-0.03
	1.5	<0.2	0.0	0.00
203	0.5	-0.5	0.0	+0.03
	1.5	<0.2	0.0	0.00

Table 7.16

Effect of initial parameter values on the final values and on the matching error. Changes shown are relative to those obtained using initial values of 1. The patient records matched are of ascending aortic pressure. Inertia values are fixed with $I_A = 0.3$.

Patient record	Initial value	% change in parameter C_A	R_S	I_A	change in error mmHg
126	0.5	0.0	0.0	+3.8	-0.01
	1.5	0.0	-0.1	+2.9	-0.01
147	0.5	+1.5	0.0	+4.7	+0.02
	1.5	+1.3	0.0	+3.6	-0.01

Table 7.17

Effect of initial parameter values on final values and on matching error. The changes are relative to estimates made with initial values of 1. Patient measured femoral artery pressures were used in this test.

result of fixing the inertia at 0.3. This was chosen as a representative value of the results obtained from the femoral artery pressure matching for several patients. It is also close to the value of 0.31 determined for this patient from the femoral pressure measured when the pressure catheter was withdrawn. The results show that in this case the minimum is well defined in terms of the parameters. Table 7.17 shows a similar result for the femoral artery pressure match, with inertia not introducing errors in the other terms.

Sensitivity of the matching error

To interpret the results presented so far it is necessary to establish the sensitivity of the matching error to changes in each of the parameters. This was done using model generated data with a measured flow as driving function. The aortic and femoral matching versions of the model with inertia adjustment were then adjusted to match the data. Plus and minus 10% changes were than made in each of the parameters in turn and the resulting matching error measured. The average error for the change in each parameter is shown in table 7.18. For the femoral pressure match this shows that the error has approximately the same sensitivity to all the parameters. The previous results therefore indicate that the matching method might be made faster by adjusting the inertia term more frequently. However the computing load for inertia adjustment is higher during the successive approximation phase than for the other parameters, so the improvement in speed will not be great. The aortic pressure match is less sensitive to both compliance and inertia, particularly the latter. The previous results still indicate that inertia may not be adjusted enough for optimum matching speed.

Model matches	Matching error for 10% change in C	R	I
		mmHg RMS	
Aortic pressure	1.68	1.9	0.68
Femoral pressure	2.60	1.93	2.33

Table 7.18

Sensitivity of the matching of model HT11 to changes in the parameters.
The test data is generated by a model with C = 0.7, R = 1, I = 0.5.

Overall Parameter Accuracy

The objective of this model matching is to estimate arterial parameters. The results in chapter 6 show that for femoral pressures a match within 2 - 5 mmHg RMS may normally be expected. These errors would correspond to parameter errors of about 10%. This represents an indication of the effect of the validity of the model in representing the patient. Errors produced by matching the model are essentially controlled by the limit chosen for terminating the search. With the present algorithm the inertia term has a greater terminal error than the other parameters. Measurement inaccuracies affect estimations using the aortic pressure more than those using femoral pressure. In other words aortic flow and femoral pressure measurements define the arterial system better. If the inaccuracies represent more than about 1 - 2 mmHg RMS after the appropriate filtering then significant parameter errors may result. It may be necessary to produce average representative single beats for matching. Of necessity the overall estimation accuracy will be limited by the calibration of the flow and pressure measuring systems. If the matching technique does not find the best match for the model there will be additional errors in the parameters. It has been shown that these errors are unacceptably high for aortic pressure matching if inertia adjustment is incorporated. Otherwise the indications are that the parameter errors from this cause are substantially less than 10%. The parameter which is likely to be most in error is the inertia term in the femoral pressure matching situation. The small matching errors in the initial condition test for femoral pressure, table 7.17, indicates that these inertia errors will not be reduced by improving the matching process, the minimum is not uniquely defined within these limits of inertia variation.

The results for aortic pressure matching with inertia adjustment (Tables 7.13 and 7.15) show that some caution must be exercised over both model-model tests and the PRBS noise test. When the model cannot match the measurement exactly, as with patient data, it is seen that the matching algorithm can produce large errors which would not be expected from the model-model case. The addition of PRBS noise to model generated data, as shown in table 7.10, is not the same as the effect of human data which the model does not match. It should be noted that a PRBS has the properties of random noise only in terms of its frequency spectrum. However the matching process adjusts according to pulse and mean pressure criteria, not by comparing frequency spectra. So the PRBS may not simulate the true effect of random noise on the process, an obvious discrepancy is that it has a constant amplitude.

In addition to these inaccuracies in determining arterial parameters from the model the overall estimation accuracy will be limited by the calibration of the flow and pressure measuring systems. Of these the errors are likely to be greatest for flow measurement. This will of course apply to any form of analysis of pressure and flow including impedance determination.

CHAPTER 8

CLINICAL APPLICATIONS

In this chapter the clinical significance of the analysis of arterial pressure-flow data using the new model described in the thesis is discussed.

Simultaneous measurements of aortic pressure and flow have been widely reported as research studies but they are not yet made as part of routine clinical investigation. Combined catheter tip pressure-flow transducers are becoming available but are still expensive and fragile. The alternative of using two separate catheters is an additional hazard to the patient and adds complication to the surgical procedures for catheter insertion. None the less there is increasing interest in pressure-flow measurement to characterise the arterial system.

Webb-Peploe (1979) proposes that the treatment of chronic heart failure requires further investigation. Surgical techniques can often alleviate valve defects, shunts and obstructed coronary arteries but when the heart muscle itself is permanently damaged means must be sought to adjust the operating conditions of the heart to optimise its performance. In this form of treatment the load on the left ventricle needs to be defined. For this the model method of estimating arterial parameters which has been described complements the calculation of hydraulic input impedance.

8.1 INTERPRETATION OF INPUT IMPEDANCE

This thesis has been mainly concerned with using models to estimate arterial parameters. They can also be used to examine the results of other methods of analysis. Published input impedance data, and its clinical interpretation, have been investigated by simulating changes in arterial properties with the model and comparing the effects on the input impedance, with those described in the literature for human subjects.

Nichols et al. (1977) have published impedances for normal subjects and those with evidence of coronary artery disease; their results are summarised in fig. 8.1. They conclude that the changes in impedance are probably the result of stiffening of the arteries in the subjects with coronary disease which is associated with increasing age. Fig. 8.2 shows the effect of reducing aortic compliance in the new arterial model. The effect on the average impedance over the range 2 - 12Hz is similar to that identified by Nichols et al. (ibid.) with increased arterial stiffness. The model shows an increase in fequency of the first minimum and maximum of the impedance which is also indicated in the subjects with disease not associated with elevated pressure. The maximum and minimum impedances for the group of patients with high arterial pressure are not well defined by the data. The general form of the impedance none the less fits the model spectrum when C is 0.5 quite well. It can be inferred from the comparison of model and patient results, that the compliance changes between the groups of patients are of the order of a factor of 3.

O'Rourke (1970) similarly shows that hypertension can lead to an ele-

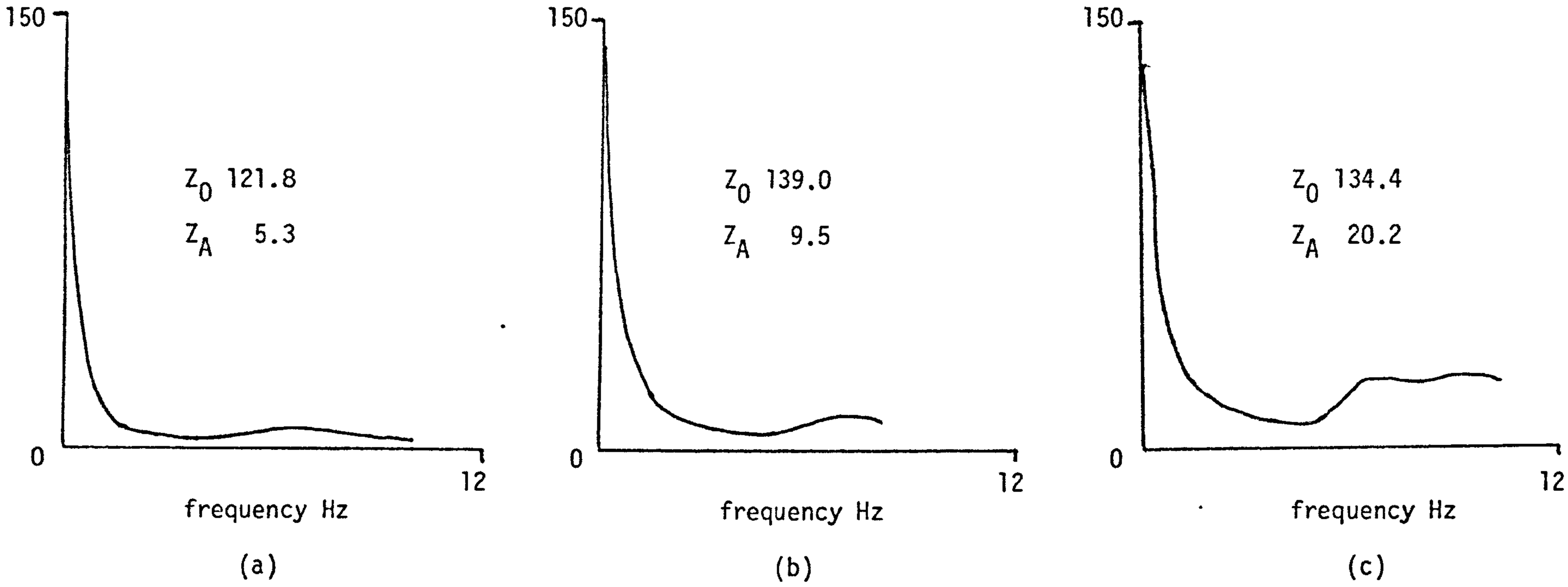

Fig. 8.1

Average arterial input impedance, in SI units, for (a) normal subjects, (b) subjects with coronary artery disease and normal arterial pressure and (c) subjects with coronary artery disease and elevated arterial pressure. Z_0 is the zero frequency impedance and Z_A the average over the range 2 - 12 Hz. Data from Nichols et al., 1977.

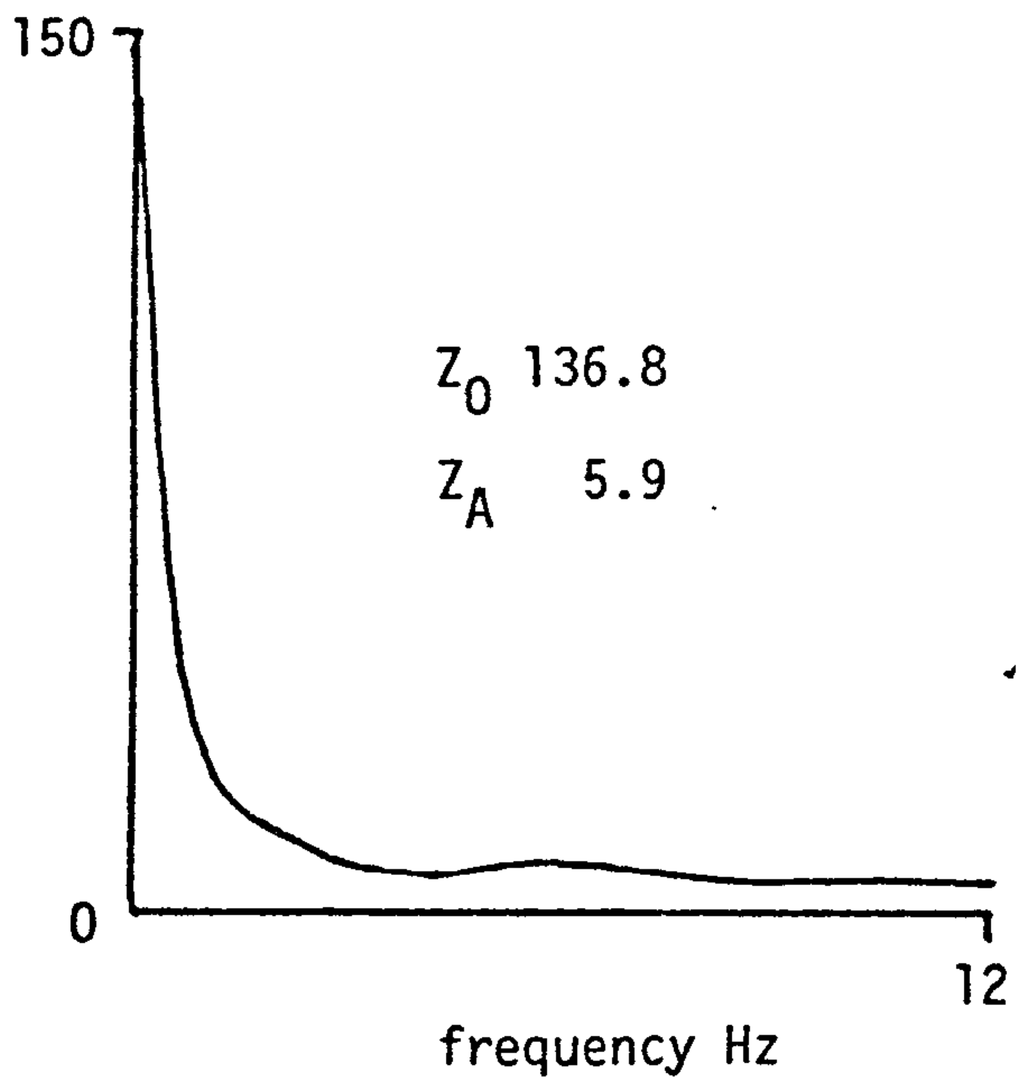

(a)

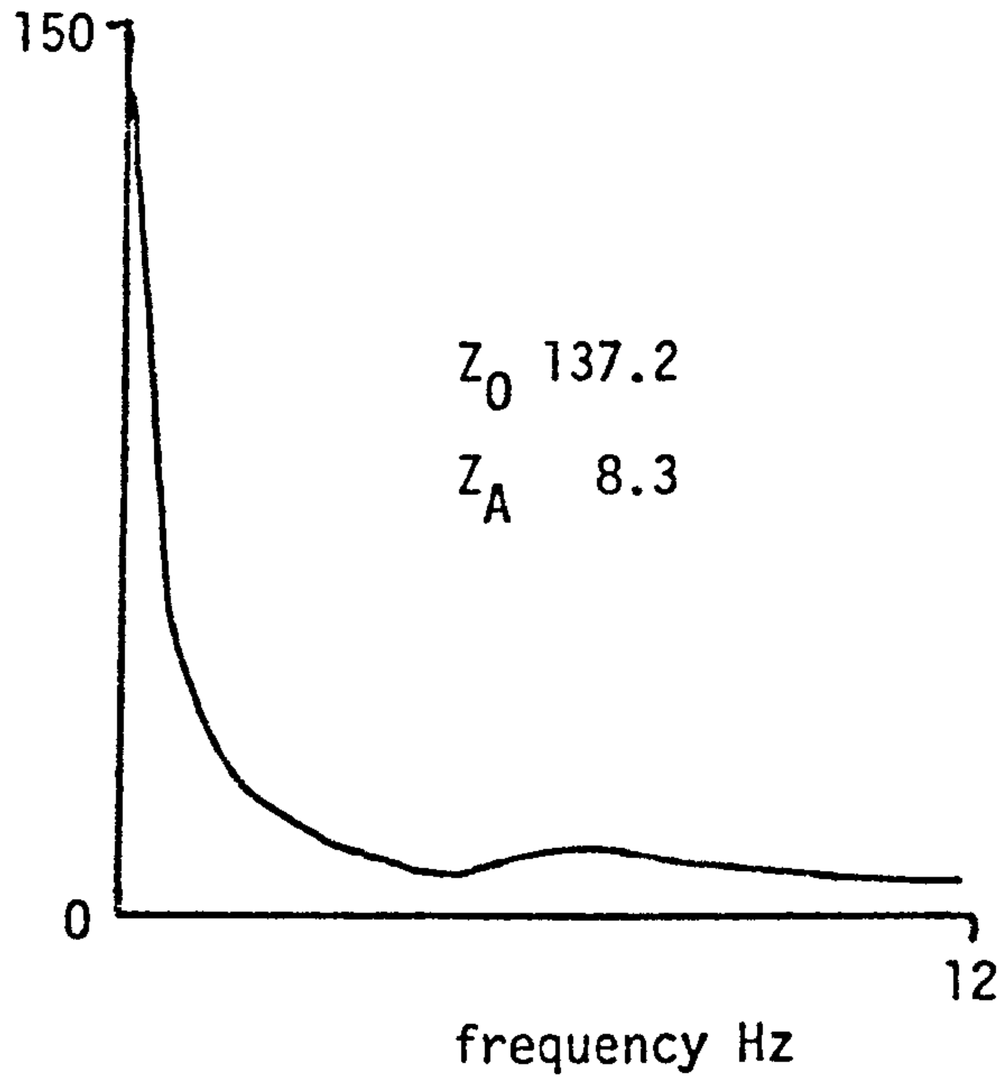

(b)

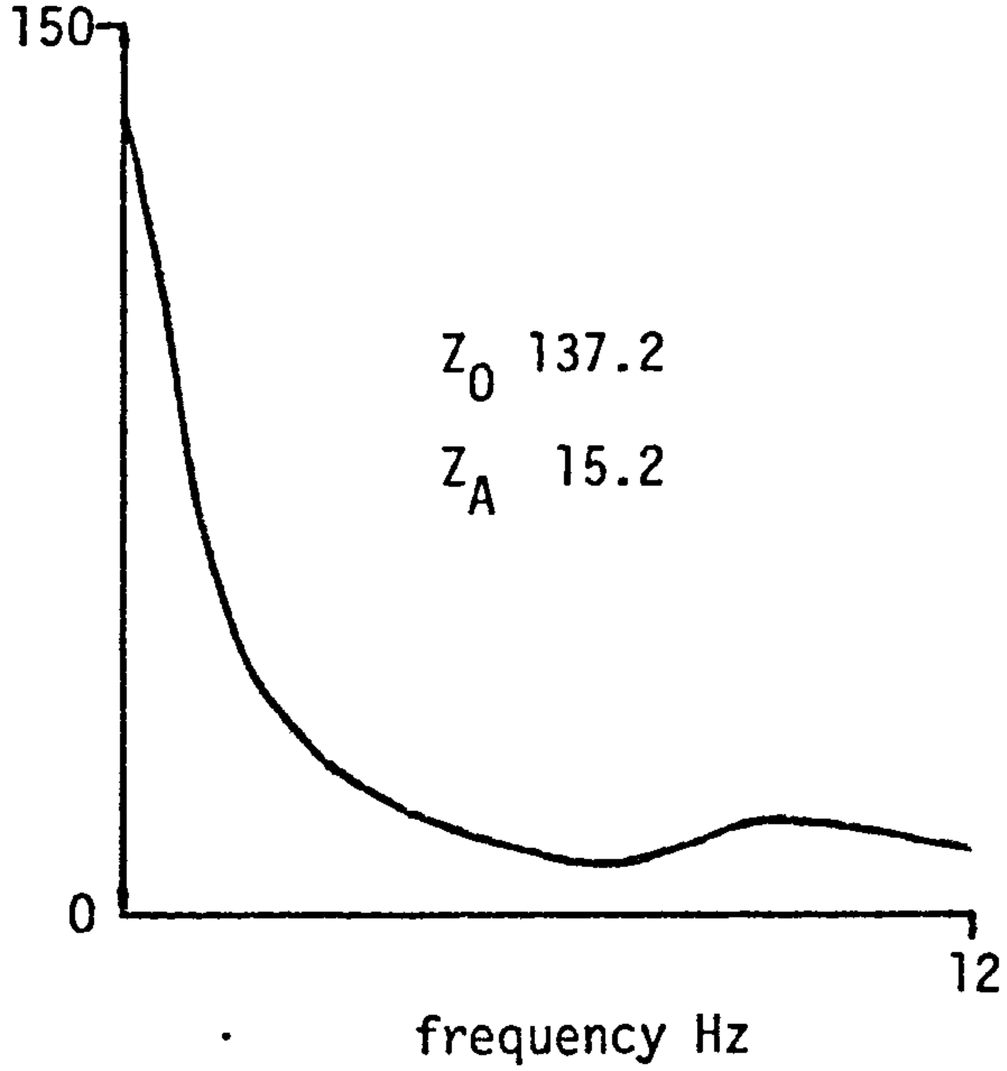

(c)

Fig. 8.2

Changes in the input impedance of the new model, in SI units, with compliance (a) 1.5, (b) 1.0, (c) 0.5. The inertia term is 0.3 and peripheral resistance 1.0 in each case. Z_0 is the zero frequency impedance and Z_A the average over the range 2 - 12 Hz.

vation of arterial impedance and a shift to higher frequencies. In this case the increased arterial stiffness is thought to be due to the dilation of the vessels.

This simple study of in vivo impedance data using the model confirms that the experimental results are consistent with changes in arterial distensibility. Other changes may result from the clinical conditions examined but the experimental results can be explained by changes in compliance alone.

Regional blood flow distribution varies considerably and the model has been used to test the effect of this on input impedance. Each of the model resistances, for the head, legs and abdomen was doubled in turn with the other resistances kept normal. The overall resistance factor was then adjusted to restore the total peripheral resistance to normal. It was found that the average impedance from 2 - 12Hz only altered over the range 5.8 to 5.9 $Nm^{-5}s\ 10^{6}$. There was no noticeable change in the frequencies of the maxima or minima of the impedance. The total peripheral resistance scaling factor was then changed from 1 to 0.5. The zero frequency impedance was reduced by a factor of 2 but no other changes in impedance beyond 1Hz were discernible. It therefore seems reasonable that impedance measurements above 2Hz are independant of peripheral resistance and that changes in regional blood flow distribution have no effect within the accuracy of normal measurements.

8.2 ANALYSIS OF FEMORAL ARTERY PRESSURES

A number of recordings of ascending aortic flow and femoral artery

pressure have been made during the administration of various drugs to one patient, called W, who had a normal left ventricular function. This patient had suffered from coronary artery disease and the measurements were made after surgery to replace sections of these arteries with saphenous vein grafts. The model matching method allows these data to be analysed to provide parameters comparable with those obtained using aortic pressure. Tables 8.1 to 8.4 show the response to the four drugs, noradrenaline, isoprenaline, morphine and omnopon. These results must be regarded as a preliminary trial. The accuracy of the flow measurement is uncertain, the cardiac outputs seem in all cases to be abnormally low. Each compliance determination was made from a single selected heartbeat. It is likely that more representative results could be obtained by averaging several beats.

The results with noradrenaline, table 8.1, probably indicate the variability of haemodynamic state more than a true drug response. Heart rate is seen to fall although this drug would normally increase it. There is a rise in arterial pressure indicating an increase in peripheral resistance which is a normal reaction to noradrenaline. The compliance variations are large but irregular.

Table 8.2 shows a more consistent pattern for isoprenaline. This drug would normally raise heart rate and cardiac output. The compliance only changes by less than 20% which could not be considered significant.

Morphine and omnopon have similar effects usually reducing blood pressure and heart rate. The results shown in tables 8.3 and 8.4 do not demonstrate this effect.

Noradrenaline infusion rate mg min^{-1}	heart rate min^{-1}	mean arterial pressure mmHg	cardiac output l min^{-1}	arterial compliance
0	90.9	90.8	2.9	1.523
2.6	82.2	80.0	2.4	1.846
5.7	80.0	99.4	2.5	2.208
11.3	80.0	95.0	2.7	1.394
16.6	76.9	101.3	2.8	1.466

Table 8.1

Effect of noradrenaline infusion on patient W. The arterial compliance was determined, from the femoral artery pressure, using the new model HT11.

Isoprenaline infusion rate mg min^{-1}	heart rate min^{-1}	mean arterial pressure mmHg	cardiac output l min^{-1}	arterial compliance
0	87.0	79.8	1.9	1.739
0.87	87.0	91.2	2.8	1.737
1.9	122.4	89.7	3.5	2.011

Table 8.2

Effect of isoprenaline infusion on patient W. The arterial compliance was determined, from the femoral artery pressure, using the new model HT11.

time after 10mg morphine injection min	heart rate min^{-1}	mean arterial pressure mmHg	cardiac output $l\ min^{-1}$	arterial compliance
0	88.2	94.6	2.3	1.665
5	89.6	97.5	2.8	1.671

Table 8.3

Effect of an injection of 10mg morphine on patient W. The arterial compliance was determined, from the femoral artery pressure, using the new model HT11.

time after 10mg omnopon injection min	heart rate min^{-1}	mean arterial pressure mmHg	cardiac output $l\ min^{-1}$	arterial compliance
0	81.1	88.4	2.3	1.703
5	87.0	79.7	2.5	1.740

Table 8.4

Effect of an injection of 10mg omnopon on patient W. The arterial compliance was determined, from the femoral artery pressure, using the new model HT11.

If the four control measurements for zero drug dose are examined they do show a noteable constancy around the 1.7 level. Using this figure the other results, especially for morphine and omnopon, give some evidence that these drugs do not significantly affect arterial compliance.

8.3 FUTURE APPLICATION - VASODILATOR THERAPY

Arterial parameters are of interest in cardiology because they affect the performance of the left ventricle. It is now considered possible to assist the failing heart in some situations by altering the arterial load with drugs. The basic principle was known twenty years ago but only recently has the application of vasodilators been investigated (Mason, 1978).

Vaso-active-drug therapy is based on the different responses of the healthy and abnormal left ventricles to changes in the arterial load (Cohn, 1973, Webb-Peploe, 1979). The long term control of cardiac output and arterial blood pressure is mainly the result of two auto-regulatory responses of the left ventricle. Although these processes are not yet well understood they are apparently independant of sympathetic or other external reflex activity. Experiments with isolated muscle preparations show that the isometric tension which is developed, the afterload, is increased by stretching the muscle to a greater length before excitation - preload. The Frank-Starling effect is the application of this result to the left ventricle (Rothe, 1966). It is observed that if the myocardial preload is increased by raising the end-diastolic-volume then the vigour of contraction is increased, augmenting the stroke volume. The end diastolic volume change also produces an elevated end diastolic pressure. The second regulatory

process is the Anrep effect in which an increase in peripheral resistance leads to a greater vigour of ventricular contraction. This increase in contractility is produced without any significant change in end-diastolic-volume.

In the normal heart an increase in arterial impedance stimulates ventricular contractility by the Anrep effect. Aortic pressure is increased, maintaining the cardiac output against the greater load, while the end-diastolic-volume and pressure are substantially unchanged.
In the failing heart the ventricle is unable to increase its contractility. The venous return flow of blood therefore exceeds the cardiac output and the end-diastolic-volume increases until the Frank-Starling mechanism stimulates the generation of a higher stroke volume. These responses to increased impedance can be described by reference to the cardiac index - ventricular filling pressure relationship. For the normal heart the curve is steep (fig. 8.3) and unchanged by moderate increases in arterial impedance. In left ventricular failure the curve is flat (fig. 8.4). Increasing the impedance causes an elevation of filling pressure to achieve the same cardiac index so that the ventricular function curve is shifted down. In extreme heart failure the flat function curve means that a large increase in filling pressure may occur without a corresponding benefit in cardiac output. This increased pressure can result in pulmonary oedema. As the ventricular size increases the myocardial wall tension required to generate a given pressure also increases. The failing heart will therefore be able to produce even less pressure when it is dilated.

Severe heart failure may be associated with elevated filling pressure, reduced cardiac output and abnormally low arterial pressure. If the

$$\text{cardiac index} = \frac{\text{cardiac output}}{\text{body surface area}}$$

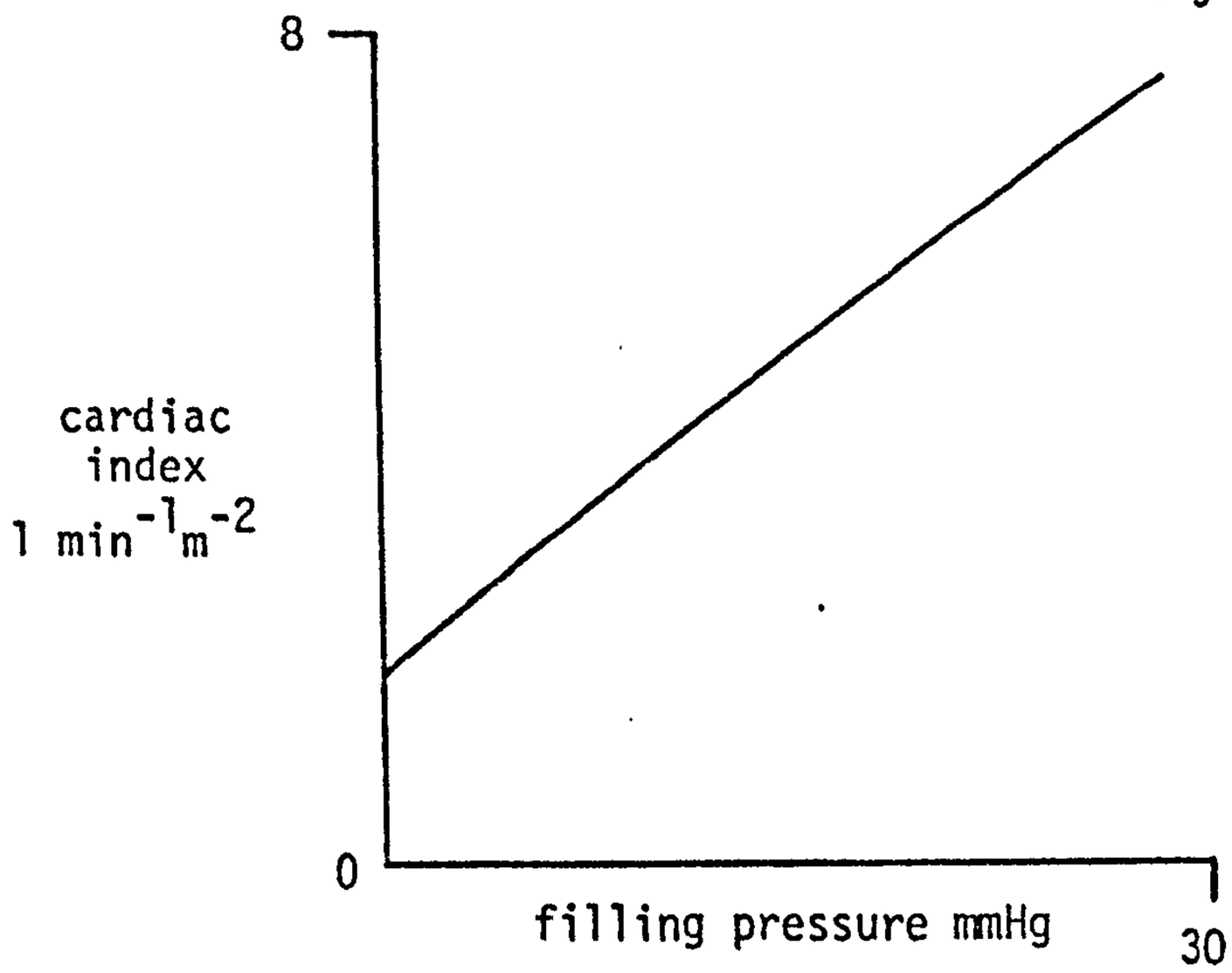

Fig. 8.3

Response of a normal heart to changes in filling pressure, changing arterial impedance has little effect.

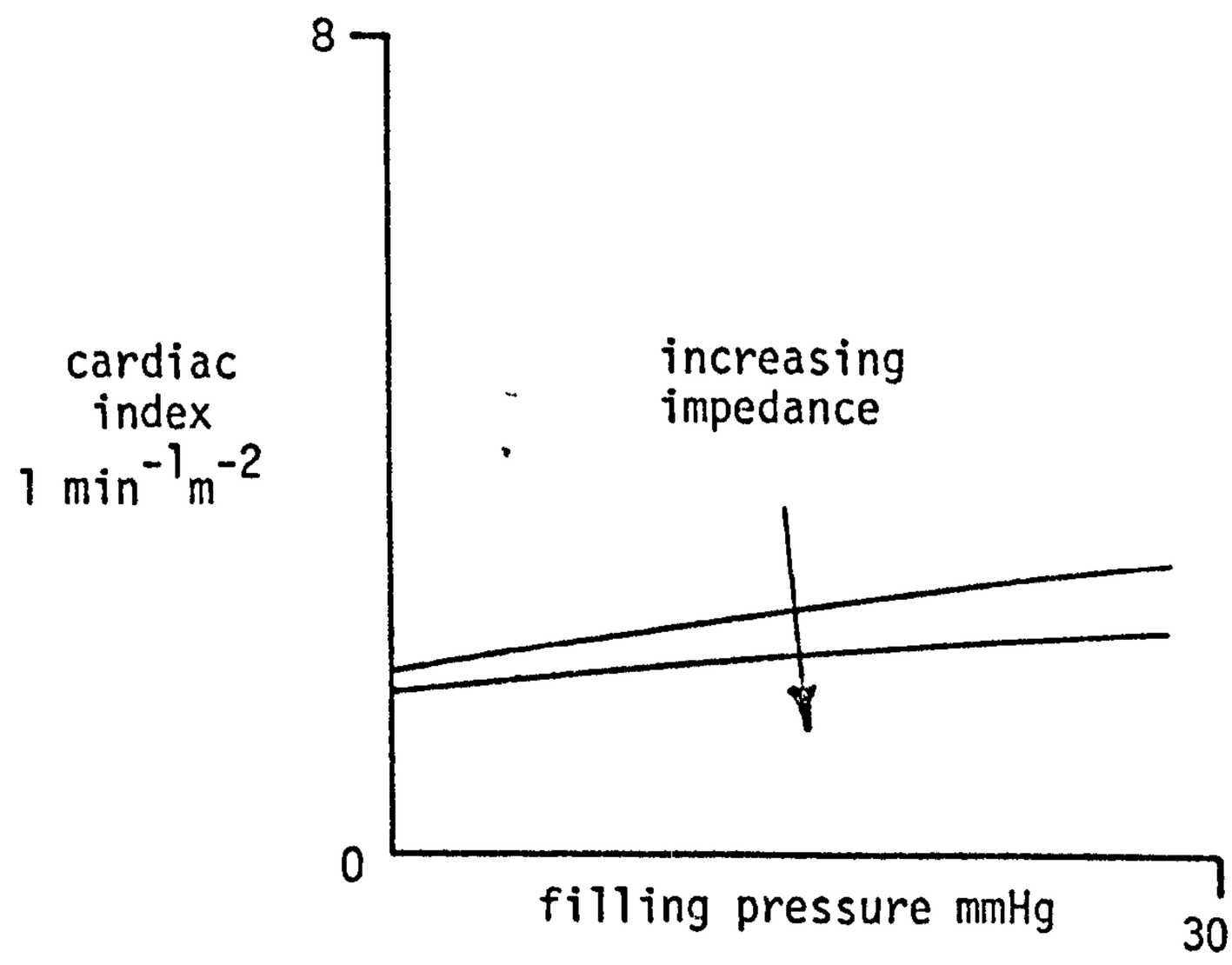

Fig. 8.4

Response of a heart with severe left ventricular failure.

arterial impedance is reduced the reverse process described above may result with the ventricular function curve being moved up and its slope increased. This may produce an increase in cardiac output and a reduction in filling pressure. There is evidence that this beneficial effect does occur in some cases and is a practical technique (Chatterjee, Massie, Rubin, Gelberg, Brundage and Ports, 1978). It is important to establish which components of impedance are changed by therapy as they have different effects on haemodynamics. There is evidence that arterial compliance is affected by the sodium content in the vessel walls (Zelis et al., 1970) and by arteriolar smooth muscle tone (Mason, Spann, Zelis and Amsterdam, 1970). These effects may provide further useful ways of manipulating the arterial system to aid the heart.

The model techniques described provide one means of obtaining an analysis of arterial changes produced by therapy. It must be noted that they cannot indicate the mechanism for any change. Arterial compliance may change because of a direct response to a drug or indirectly as the result of a change in arterial pressure.

CHAPTER 9

SUMMARY AND CONCLUSIONS

The intention of this work has been to investigate the practical application of digital models of the circulation to the analysis of clinical measurements. Many models are described in the literature and these have been tested individually but there is little data available to indicate the optimum amount of detail required for a specific use of a model. Most of the published models are analogue simulations. By using a digital computer it has been possible to produce a flexible analysis method with facilities for editing the measurements, adjusting the model and printing both numerical and graphical results.

A comparison has been carried out between four models of the systemic arterial circulation ranging from the simple two compartment model of Beneken (1965) and the 21 compartment simulation of Snyder et al. (1968). The examination was based on the ability of the simulations to match the aortic or femoral artery pressure when driven by the ascending aortic flow measured in a patient. It has been shown that there is little significant difference in the RMS error of match between these models. There is a substantial difference between the Beneken (ibid.) and other models in the change in pressure waveform shape along the main artery. In this respect the Beneken (ibid.) version is less realistic, but not necessarily less able to extract useful information from a single arterial pressure measurement. It has been shown that the incorporation of arterial or peripheral damping does not improve the overall accuracy of pressure match.

A general evaluation of arterial models by measuring their input impedance is frequently carried out and the results compared with published impedance curves for human subjects. An examination of this approach has shown that differences in the shape of the impedance curves for the models examined are most prominent above 4Hz. However, there is a relatively small component of arterial pressure in this region so that the errors in impedance measurement are large.

A useful clinical analysis technique will need to provide results in as short a period of time as possible. For this reason the methods of differential equation solving used in digital models has been investigated. It has been shown that one-step methods of the Runge-Kutta type are more efficient for the model developed for this work than predictor-corrector algorithms.

The techniques developed here for using a circulation model involve adjusting the model parameters to match patient measurements. Two algorithms for this matching process have been developed, a modified Rosenbrock method which is of general use and a simple successive approximation technique which is both fast and accurate for this particular model application.

Some preliminary clinical results have been presented which show that the method is practical with the limited measurements that can be made routinely. The model technique is a versatile one; its use for interpreting other forms of analysis has been demonstrated by a study of aortic impedance data for normal patients and those with coronary artery disease.

More clinical data must be obtained before the diagnostic usefulness of the model technique can be established. Although pressure and flow transducers for aortic measurements are available a combined probe is still not in quantity production at a realistic cost. A further comparison of the models should be made when good quality recordings of arterial pressure at several points along the aorta and femoral artery have been made. It will then be possible to examine the ability of each model to simulate the transmission properties of the systemic arteries.

APPENDIX 1

Circulation Model Program Listings

NEW MODEL PROGRAM HT11

WITH SUCCESSIVE APPROXIMATION

ADJUSTMENT ALGORITHM


```
 1 C# HT1154 09/11/78A  SUCCESSIVE APPROXIMATION H=0.0025
 2 C      AOF DRIVEN FAP MATCHED, INERTIA ADJUSTMENT,  PRINTOUT
 3 C      OF FINAL RESULTS BY HTPRNT OR IMPEDANCE PLOT.
 4        PROGRAM HT1154
 5        REAL PLV(150),NSRCH
 6        INTEGER D,TAPE,LABEL(3)
 7        COMMON TAPE(10),D(4),P(10),CRIT,AOF(150),AOPMDL(150),FAPMDL(150)
 8       +,II
 9       +,FAP(150)
10        COMMON/EQN/ N,PVEN,R(3),Z(3,12),DELO(3)
11        COMMON/BEATS/ II1,H,IFLAG,ICYCLE,X(2,12),APFA,PPFA
12        EQUIVALENCE (P(1),CA),(P(2),RS),(P(3),W),(P(4),A0),
13       +(P(5),A1),(P(6),A2),(P(7),A3),(P(8),A4),(P(9),A5),(P(10),NSRCH),
14       +(PLV(1),FAPMDL(1))
15        DATA YES/1HY/,LABEL(1)/2HHT/,LABEL(2)/2H11/,LABEL(3)/2H54/
16 C ***************
17 C      START
18 C ***************
19        WRITE(10,1000)
20  1000 FORMAT(1H1,20X,'HT1154,  AOF DRIVEN,  FAP MATCHED'///)
21        VC=0.04
22        X(1,1)=0.0
23        X(2,1)=0.0
24        DO 50 I=2,12
25        X(1,I)=100.0
26     50 X(2,I)=120.0
27        CALL DATE(D)
28        DO 7 N=1,3
29      7 TAPE(N+7)=LABEL(N)
30        DO 8 N=4,10
31      8 P(N)=0.0
32 C ****************************
33 C      READ PATIENT DATA
34 C ****************************
35      1 WRITE(1,200)
36    200 FORMAT(///'LOAD TAPE AND TYPE IDENTIFICATION')
37        READ(1,210)(TAPE(N),N=1,7)
38    210 FORMAT(7A2)
39        READ(3,2)II
40        II1=II+1
41        II2=II+2
42        READ(3,3)(PLV(N),FAP(N),AOF(N),N=3,II2)
43      2 FORMAT(I4)
44      3 FORMAT(12F6.1)
45        IF(TAPE(1).EQ.-24416)READ(3,210)(TAPE(N),N=1,7)
46        WRITE(1,6)(TAPE(N),N=1,7)
47      6 FORMAT('TAPE ',7A2,' LOADED'/)
48        AOF(1)=AOF(II1)
49        AOF(2)=AOF(II2)
50        AOF(II2+1)=AOF(3)
51      4 WRITE(1,10)
52     10 FORMAT('INPUT PVEN,  CA,  RS,W')
53        READ(1,*)PVEN,CA,RS,W
54        APFAS=0.0
55        SPFAS=0.0
56        DPFAS=1000.0
```

```
      DO 5 N=3,II2
      IF(FAP(N).GT.SPFAS)SPFAS=FAP(N)
      IF(FAP(N).LT.DPFAS)DPFAS=FAP(N)
    5 APFAS=APFAS+FAP(N)
      APFAS=APFAS/FLOAT(II)
      PPFAS=SPFAS-DPFAS
      DC=0.0
      DR=0.0
      DW=0.0
      S=1
      M=2
      NADJ=4
      CRITN=1000.0
      INERFG=1
C *********************
C       SEARCH
C *********************
      H=0.0025
  300 NSRCH=NSRCH+1.0
      WRITE(10,11)
   11 FORMAT(1H1,6X,4HCRIT,7X,4HAPFA,7X,4HDPFA,7X,4HSPFA)
      WRITE(10,12)APFAS,DPFAS,SPFAS,DW
   12 FORMAT(/4X,'PATIENT',3(2X,F9.3)//1X,3HDW=,F7.3)
      Z(2,1)=W*1E-3*0.2093
      Z(2,2)=W*1E-3*0.964
      Z(2,3)=W*1E-3*0.942
      Z(2,4)=W*1E-3*1.438
      Z(2,5)=W*1E-3*3.156
      Z(2,6)=W*1E-3*3.457
      Z(2,7)=W*1E-3*13.179
      Z(2,8)=W*1E-3*19.573
      Z(2,9)=W*1E-3*35.128
      Z(2,10)=W*1E-3*1.464
      Z(2,11)=W*1E-3*29.5
      Z(2,12)=W*1E-3*3.503
      DO 100 IFLAG=1,NADJ
      WRITE(10,30)DC,DR
   30 FORMAT(4H DC=,F7.3,4X,3HDR=,F7.3)
      CA=CA+DC
      RS=RS+DR
      WRITE(10,35)CA,RS,W
   35 FORMAT(4H CA=,F7.3,3X,3HRS=,F7.3,3X,2HW=,F7.3)
      CALL SEARCH(Z,R,M,CA,RS,APFAS,CRIT)
      DC=CA*(PPFA-PPFAS)/PPFAS
      DR=RS*(APFAS-APFA)/APFA
  100 CONTINUE
      NADJ=3
      CALL SIZE(2)
      CALL POS(-500,370,0)
      WRITE(7,40)D,TAPE,(P(N),N=1,3)
   40 FORMAT(2X,4A2,3X,'TAPE ',10A2,5X,' C ',F5.2,3X,'R ',F5.2,3X,'I ',
     +F5.2)
      CALL POS(-140,-399,0)
      ERROR=SQRT(CRIT/(0.00015*FLOAT(II)))
      WRITE(7,60)ERROR
   60 FORMAT('ERROR ',F6.2,' MMHG RMS')
```

```
113 C ******************************
114 C     CHECK IF FINISHED
115 C ******************************
116       IF(CRITN-CRIT. GT. 0. 002. OR. CRIT. GT. CRITN+0. 002)GO TO 560
117 C FINISH IF ERROR HAS NOT IMPROVED OR WORSENED SIGNIFICANTLY
118       IFLAG=3
119       DO 95 ICYCLE=1,2
120    95 CALL BEAT
121       ERROR=SQRT(CRIT/(0. 00015*FLOAT(II)))
122       CALL POS(-500, 370, 0)
123       WRITE(7, 40)D, TAPE, (P(N), N=1, 3)
124       CALL POS(-140, -399, 0)
125       WRITE(7, 60)ERROR
126    70 WRITE(1, 80)
127    80 FORMAT(/'####### PRINT RESULTS ? #######')
128       READ(1, 90)ANS
129    90 FORMAT(A1)
130       IF(ANS. NE. YES)GO TO 400
131       CALL GOTO(6HHTPRNT)
132   400 WRITE(1, 410)
133   410 FORMAT(/'####### IMPEDANCE PLOT ? #######')
134       READ(1, 90)ANS
135       IF(ANS. NE. YES)GO TO 560
136       DO 420 ICYCLE=1, 2
137   420 CALL BEAT
138       CALL GOTO(6HHTIMPD)
139 C ****************************************
140 C       ESTIMATE INERTIA WEIGHTING
141 C ****************************************
142   560 IF(CRIT. GE. CRITN)GO TO 530
143       IF(INERFG. EQ. 1)GO TO 550
144 C IMPROVEMENT IN W
145       CRITN=CRIT
146       WNEW=W
147       DW=3. 0*DW
148       GO TO 540
149 C W WORSE
150   530 INERFG=0
151       W=WNEW
152       DW=-0. 5*DW
153 C SET UP PARAMETERS
154   540 DC=CA*((1. 0+DW/W)**0. 5814-1. 0)
155       DR=0. 0
156       W=W+DW
157       IF(W. GT. 2. 0. OR. W. LT. 0. 2)GOTO 530
158       GO TO 300
159 C INITIAL ESTIMATE OF W
160   550 CRITN=CRIT
161       WNEW=W
162       NT=0
163       EMIN=1E05
164       DO 500 J=-5, 10
165       ERROR=0. 0
166       DO 510 N=3, II2
167       K=N+J
168       IF(K. LT. 3)K=K+II
```

```
169         IF(K. GT. II2)K=K-II
170      510 ERROR=ERROR+(FAPMDL(K)-FAP(N))*(FAPMDL(K)-FAP(N))
171         IF(ERROR. GE. EMIN)GO TO 500
172         EMIN=ERROR
173         NT=J
174      500 CONTINUE
175         IF(NT. EQ. 0)GOTO 570
176         DW=-0. 08*FLOAT(NT)
177         GOTO 540
178    C TIME SHIFT FAILS
179      570 IF(DW. EQ. 0. 0)DW=0. 2
180         GOTO 530
181         END
182    C ***************************
183         BLOCK DATA FRED
184    C ***************************
185         COMMON/EQN/ N, PVEN, R(3), Z(3, 12), DELO(3)
186         DATA (Z(1, N), N=1, 12)/0. 566E-6, 0. 000302, 0. 000365,
187        1   0. 000638, 0. 003071, 0. 003684, 0. 01764, 0. 091322, 0. 28976,
188        2   0. 002187, 0. 3994, 0. 011805/
189         END
190    C ***************************************************
191         SUBROUTINE SEARCH(Z, R, M, CA, RS, APFAS, CRIT)
192    C ***************************************************
193         COMMON/BEATS/ III, H, IFLAG, ICYCLE, X(2, 12), APFA, PPFA
194         DIMENSION Z(3, 12), R(3)
195         DATA CRITN/1000. 0/
196         Z(3, 1)=0. 089*CA
197         Z(3, 2)=0. 133*CA
198         Z(3, 3)=0. 0743*CA
199         Z(3, 4)=0. 00564*CA
200         Z(3, 5)=0. 0317*CA
201         Z(3, 6)=0. 0378*CA
202         Z(3, 7)=0. 0302*CA
203         Z(3, 8)=0. 0373*CA
204         Z(3, 9)=0. 0207*CA
205         Z(3, 10)=0. 0999*CA
206         Z(3, 11)=0. 0909*CA
207         Z(3, 12)=0. 00932*CA
208         R(1)=11. 2*RS
209         R(2)=4. 49*RS
210         R(3)=1. 45*RS
211         IF(M. LT. 2)GO TO 100
212         M=1
213         DO 200 ICYC=1, 2
214      100 DO 200 ICYCLE=1, 2
215      200 CALL BEAT
216         DO 350 J=1, 12
217      350 X(2, J)=X(2, J)*APFAS/APFA
218         RETURN
219         END
220    C ***************************
221         SUBROUTINE BEAT
222    C ***************************
223         INTEGER D, TAPE
224         COMMON TAPE(10), D(4), P(10), CRIT, AOF(150), AOPMDL(150), FAPMDL(150)
```

```
225         +,II
226         +,FAP(150)
227          COMMON/EQN/ N,PVEN,R(3),Z(3,12),DELO(3)
228          COMMON/BEATS/ II1,H,IFLAG,ICYCLE,X(2,12),APFA,PPFA
229          EXTERNAL EQNS
230          CRIT=0.0
231          W1=0.00015
232          W2=0.00002
233          NS=3
234          NF=24
235          K=1
236          DPFA=1000.0
237          SPFA=0.0
238          APFA=0.0
239          DO1 N=2,II1
240          N1=N+1
241          DELO(1)=AOF(N)-AOF(N-1)
242          DEL11=AOF(N+1)-AOF(N)
243          DELO(2)=DEL11-DELO(1)
244          DEL21=AOF(N+2)-AOF(N+1)
245          DEL12=DEL21-DEL11
246          DELO(3)=DEL12-DELO(2)
247          DELO(1)=DELO(1)/0.01
248          DELO(2)=DELO(2)/2E-4
249          DELO(3)=DELO(3)/6E-6
250          TR=0.01*FLOAT(N-2)
251          DO 100 I=1,4
252      100 CALL DFSOLN(K,NS,NF,H,TR,X,B,EQNS)
253          FAPMDL(N1)=X(2,8)
254          AOPMDL(N1)=X(2,2)
255          IF(X(2,8).LT.DPFA)DPFA=X(2,8)
256          IF(FAPMDL(N1).GT.SPFA)SPFA=FAPMDL(N1)
257          APFA=APFA+FAPMDL(N1)
258          IF(IFLAG.EQ.3.AND.ICYCLE.EQ.2)
259         +CALL PLOTT(AOF(N1),X(2,2),X(1,8),FAPMDL(N1),N1)
260          CRIT=CRIT+W1*(FAPMDL(N1)-FAP(N1))*(FAPMDL(N1)-FAP(N1))
261        1 CONTINUE
262          APFA=APFA/FLOAT(II)
263          PPFA=SPFA-DPFA
264          WRITE(10,2)CRIT,APFA,DPFA,SPFA
265        2 FORMAT(4(2X,F9.3))
266          RETURN
267          END
268  C ***************************************
269          SUBROUTINE EQNS(TR,X,DOT)
270  C ***************************************
271          DIMENSION X(2,12),DOT(2,12)
272          INTEGER D,TAPE
273          COMMON TAPE(10),D(4),P(10),CRIT,AOF(150),AOPMDL(150),FAPMDL(150)
274         +,II
275         +,FAP(150)
276          COMMON/EQN/ N,PVEN,R(3),Z(3,12),DELO(3)
277  C INTERPOLATE DRIVING FUNCTION
278          TI=TR-0.01*FLOAT(N-2)
279          TH=TI+0.01
280          X(1,2)=AOF(N-1)+TH*DELO(1)+TH*TI*DELO(2)
```

```
      ++TH*TI*(TI-0.01)*DELO(3)
       FLEGS=(X(2,9)-PVEN)/R(1)
       FHEAD=(X(2,11)-PVEN)/R(2)
       FABD=(X(2,12)-PVEN)/R(3)
C COMPUTE DERIVATIVES
       DOT(2,2)=(X(1,2)-X(1,3)-X(1,10))/Z(3,2)
       DOT(1,3)=(X(2,2)-X(2,3)-X(1,3)*Z(1,3))/Z(2,3)
       DOT(2,3)=(X(1,3)-X(1,4))/Z(3,3)
       DOT(1,4)=(X(2,3)-X(2,4)-X(1,4)*Z(1,4))/Z(2,4)
       DOT(2,4)=(X(1,4)-X(1,5))/Z(3,4)
       DOT(1,5)=(X(2,4)-X(2,5)-X(1,5)*Z(1,5))/Z(2,5)
       DOT(2,5)=(X(1,5)-X(1,6))/Z(3,5)
       DOT(1,6)=(X(2,5)-X(2,6)-X(1,6)*Z(1,6))/Z(2,6)
       DOT(2,6)=(X(1,6)-X(1,7)-X(1,12))/Z(3,6)
       DOT(1,7)=(X(2,6)-X(2,7)-X(1,7)*Z(1,7))/Z(2,7)
       DOT(2,7)=(X(1,7)-X(1,8))/Z(3,7)
       DOT(1,8)=(X(2,7)-X(2,8)-X(1,8)*Z(1,8))/Z(2,8)
       DOT(2,8)=(X(1,8)-X(1,9))/Z(3,8)
       DOT(1,9)=(X(2,8)-X(2,9)-X(1,9)*Z(1,9))/Z(2,9)
       DOT(2,9)=(X(1,9)-FLEGS)/Z(3,9)
       DOT(1,10)=(X(2,2)-X(2,10)-X(1,10)*Z(1,10))/Z(2,10)
       DOT(2,10)=(X(1,10)-X(1,11))/Z(3,10)
       DOT(1,11)=(X(2,10)-X(2,11)-X(1,11)*Z(1,11))/Z(2,11)
       DOT(2,11)=(X(1,11)-FHEAD)/Z(3,11)
       DOT(1,12)=(X(2,6)-X(2,12)-X(1,12)*Z(1,12))/Z(2,12)
       DOT(2,12)=(X(1,12)-FABD)/Z(3,12)
       RETURN
       END
C ***********************************************************
       SUBROUTINE DFSOLN(KIM,NNS,NNF,HH,X,Y,BB,EXTERN)
C ***********************************************************
       DIMENSION Y(24),Y1(24),Y2(24),Y3(24),FO(24),F1(24),F2(24),PC(24),
      1P1(24),G(24),O(24),Z(24)
       EQUIVALENCE (G(1),FO(1)),(O(1),PC(1)),(P1(1),Z(1))
       GO TO (1,20),KIM
     1 H=HH
       NS=NNS
       NF=NNF
       H1=0.5*H
       H2=H/6.0
       KIM=2
    20 XHH=X+H1
       XH=X+H
       CALL EXTERN(X,Y,G)
       DO 22 J=NS,NF
    22 Z(J)=Y(J)+H1*G(J)
       CALL EXTERN(XHH,Z,O)
       DO 23 J=NS,NF
       G(J)=G(J)+2.0*O(J)
    23 Z(J)=Y(J)+H1*O(J)
       CALL EXTERN(XHH,Z,O)
       DO 25 J=NS,NF
       G(J)=G(J)+2.0*O(J)
    25 Z(J)=Y(J)+H*O(J)
       CALL EXTERN(XH,Z,O)
       DO 26 J=NS,NF
```

```
      26 Y(J)=Y(J)+H2*(G(J)+O(J))
         X=XH
         RETURN
         END
C ***********************************************
         SUBROUTINE PLOTT(Y1, Y2, Y3, Y4, I)
C ***********************************************
         DIMENSION YO(4), Y(4), A(4)
         INTEGER Y, YO, X, XO, YA, YP, XA
         INTEGER D, TAPE
         COMMON TAPE(10), D(4), P(10), CRIT, AOF(150), AOPMDL(150), FAPMDL(150)
        +, II
        +, FAP(150)
         DATA A/3HAOF, 3HAOP, 3HFAF, 3HFAP/
         Y(1)=Y1*0.36
         Y(2)=Y2*1.8
         Y(3)=Y3*0.36
         Y(4)=Y4*1.8
         IF(I.GT.3)GO TO 20
         II2=II+2
         CALL INITCT
         XO=3.0*2.667
         DO 1 N=1, 4
         YO(N)=Y(N)
         YA=35.0
         IF(N.EQ.2.OR.N.EQ.4)YA=-345.0
         XA=(N/3)*512-400
         CALL POS(XA, YA, 0)
         CALL VECT(0, 360, 1)
         CALL POS(-65, -70, 1)
         WRITE(7, 100)A(N)
  100 FORMAT(1X, A3)
         CALL POS(XA, YA, 0)
         CALL VECT(400, 0, 1)
         CALL POS(-200, -20, 1)
    1 WRITE(7, 200)
  200 FORMAT(5H TIME)
         CALL SIZE(1)
         DO 2 N=3, II2
         X=FLOAT(N)*2.667+102.5
         YP=FAP(N)*1.8-348.5
         CALL POS(X, YP, 0)
    2 WRITE(7, 300)
  300 FORMAT(2H +)
         CALL SIZE(2)
         RETURN
   20 X=FLOAT(I)*2.667
         DO 30 N=1, 4
         YA=35.0
         IF(N.EQ.2.OR.N.EQ.4)YA=-345.0
         XA=(N/3)*512-400
         CALL POS(XO+XA, YO(N)+YA, 0)
         CALL VECT(X+XA, Y(N)+YA, 0)
   30 YO(N)=Y(N)
         XO=X
         RETURN
         END
```

EQUATIONS FOR THE BENEKEN ARTERIAL MODEL,

HT04


```
194 C ************************************
195       SUBROUTINE EQNS(TR,X,DOT)
196 C ************************************
197       DIMENSION X(5),DOT(5),F(3)
198       INTEGER D,TAPE
199       COMMON TAPE(10),D(4),P(10),CRIT,AOF(150),AOPMDL(150),FAPMDL(150)
200      +,II
201      +,PRESS(512),FLOW(512)
202       COMMON/EQN/ N,PVEN,CA,RS,DELO(3)
203       DATA QU/1000.0/,PGRAV2,PGRAV3/2*0.0/,PTH/-4.0/
204 C INTERPOLATE DRIVING FUNCTION
205       TI=TR-0.01*FLOAT(N-2)
206       TH=TI+0.01
207       F(1)=AOF(N-1)+TH*DELO(1)+TH*TI*DELO(2)
208      ++TH*TI*(TI-0.01)*DELO(3)
209 C COMPUTE FLOWS
210       X5=(X(5)-QU)/59.0
211       IF(X5.LT.0.0)X5=0.0
212       F(2)=(X(4)+PGRAV2-X5)/RS
213       F(3)=(X5-PVEN-PTH)/.09
214       IF(PGRAV3.GT.1.0)F(3)=(X5-PGRAV3)/.36+.75*(X5-PVEN-PTH)/.09
215       IF(PVEN+PTH-PGRAV3.LT.0.0)F(3)=(X5-PGRAV3)/.09
216 C COMPUTE DERIVATIVES
217       DOT(2)=(F(1)-X(3))/(0.7*CA)
218       DOT(3)=(X(2)+PTH-.06*X(3)-X(4))/.0007
219       DOT(4)=(X(3)-F(2))/(1.8*CA)
220       DOT(5)=(F(2)-F(3))
221       RETURN
222       END
```

EQUATIONS FOR THE AASLID ARTERIAL MODEL, HT13


```
C ************************************
      SUBROUTINE EQNS(TR,X,DOT)
C ************************************
      DIMENSION X(2,13),DOT(2,13)
      INTEGER D,TAPE
      COMMON TAPE(10),D(4),P(10),CRIT,AOF(150),AOPMDL(150),FAPMDL(150)
     +,II
     +,PRESS(512),FLOW(512)
      COMMON/EQN/ N,PVEN,R(3),Z(4,13),DELO(3)
C INTERPOLATE DRIVING FUNCTION
      TI=TR-0.01*FLOAT(N-2)
      TH=TI+0.01
      X(1,2)=AOF(N-1)+TH*DELO(1)+TH*TI*DELO(2)
     ++TH*TI*(TI-0.01)*DELO(3)
      H1=TH
      H2=0.03-H1
      H11=H1*H1
      H22=H2*H2
      DOT(1,2)=(H11*AOF(N+2)+(H22-H11)*X(1,2)-H22*AOF(N-1))/
     +(H1*H2*0.01)
C COMPUTE FLOWS IN TERMINATING SEGMENTS
      FLEGS=(X(2,10)-PVEN)/R(1)
      FHEAD=(X(2,12)-PVEN)/R(2)
      FABD=(X(2,13)-PVEN)/R(3)
C COMPUTE FLOW DERIVATIVES
      DO 10 I=3,10
   10 DOT(1,I)=(X(2,I-1)-X(2,I)-X(1,I)*Z(1,I))/Z(2,I)
      DOT(1,11)=(X(2,2)-X(2,11)-X(1,11)*Z(1,11))/Z(2,11)
      DOT(1,12)=(X(2,11)-X(2,12)-X(1,12)*Z(1,12))/Z(2,12)
      DOT(1,13)=(X(2,6)-X(2,13)-X(1,13)*Z(1,13))/Z(2,13)
C COMPUTE PRESSURE DERIVATIVES
      DO 20 I=2,9
   20 DOT(2,I)=(X(1,I)-X(1,I+1))/Z(3,I)+(DOT(1,I)-DOT(1,I+1))*Z(4,I)
      DOT(2,2)=DOT(2,2)-X(1,11)/Z(3,2)-DOT(1,11)*Z(4,2)
      DOT(2,6)=DOT(2,6)-X(1,13)/Z(3,6)-DOT(1,13)*Z(4,6)
      DOT(2,10)=((X(1,10)-FLEGS)/Z(3,10)+DOT(1,10)*Z(4,10))/
     &(1.0+Z(4,10)/R(1))
      DOT(2,11)=(X(1,11)-X(1,12))/Z(3,11)+(DOT(1,11)-DOT(1,12))*Z(4,11)
      DOT(2,12)=((X(1,12)-FHEAD)/Z(3,12)+DOT(1,12)*Z(4,12))/(1.0+Z(4,12)
     +/R(2))
      DOT(2,13)=((X(1,13)-FABD)/Z(3,13)+DOT(1,13)*Z(4,13))/(1.0+Z(4,13)/
     +R(3))
      RETURN
      END
```

EQUATIONS FOR THE SNYDER ET AL. MODEL, HT14


```
313 C ************************************
314       SUBROUTINE EQNS(TR,X,DOT)
315 C ************************************
316       REAL X(2,17),XB(8),DOT(2,17),DOTB(8)
317       INTEGER D,TAPE
318       COMMON TAPE(10),D(4),P(10),CRIT,AOF(150),AOPMDL(150),FAPMDL(150)
319      +,II
320      +,FAP(150)
321       COMMON/EQN/ N,PVEN,Z(4,13),ZB(3,8),DELO(3)
322 C BRANCH FLOW FUNCTIONS
323       F1(N,IN)=(X(2,IN)-XB(N))/ZB(1,N)
324       F2(N)=(XB(N)-PVEN)/ZB(3,N)
325       DB(N,IN)=(F1(N,IN)-F2(N))/ZB(2,N)
326       I=0
327       DO 100 J=14,17
328       DO 100 K=1,2
329       I=I+1
330   100 XB(I)=X(K,J)
331 C INTERPOLATE DRIVING FUNCTION
332       TI=TR-0.01*FLOAT(N-2)
333       TH=TI+0.01
334       X(1,1)=AOF(N-1)+TH*DELO(1)+TH*TI*DELO(2)
335      ++TH*TI*(TI-0.01)*DELO(3)
336       H1=TH
337       H2=0.03-H1
338       H11=H1*H1
339       H22=H2*H2
340       DOT(1,1)=(H11*AOF(N+2)+(H22-H11)*X(1,1)-H22*AOF(N-1))/
341      +(H1*H2*0.01)
342 C COMPUTE FLOW DERIVATIVES
343       DO 10 I=2,11
344    10 DOT(1,I)=(X(2,I-1)-X(2,I)-X(1,I)*Z(1,I))/Z(2,I)
345       DOT(1,12)=(X(2,1)-X(2,12)-X(1,12)*Z(1,12))/Z(2,12)
346       DOT(1,13)=(X(2,2)-X(2,13)-X(1,13)*Z(1,13))/Z(2,13)
347 C COMPUTE BRANCH PRESSURE DERIVATIVES
348       DOTB(1)=DB(1,12)
349       DOTB(2)=DB(2,12)
350       DOTB(3)=DB(3,2)
351       DOTB(4)=DB(4;13)
352       DOTB(5)=DB(5,13)
353       DOTB(6)=DB(6,8)
354       DOTB(7)=DB(7,11)
355       DOTB(8)=DB(8,11)
356       I=0
357       DO 200 J=14,17
358       DO 200 K=1,2
359       I=I+1
360   200 DOT(K,J)=DOTB(I)
361 C COMPUTE PRESSURE DERIVATIVES
362       DOT(2,1)=(X(1,1)-X(1,2)-X(1,12))/Z(3,1)+
363      +(DOT(1,1)-DOT(1,2)-DOT(1,12))*Z(4,1)
364       DOT(2,2)=((X(1,2)-X(1,3)-X(1,13)-F1(3,2))/Z(3,2)+
365      +(DOT(1,2)-DOT(1,3)-DOT(1,13)+DOTB(3)/ZB(1,3))*Z(4,2))/
366      +(1.0+Z(4,2)/ZB(1,3))
367       DO 20 I=3,7
368    20 DOT(2,I)=(X(1,I)-X(1,I+1))/Z(3,I)+(DOT(1,I)-DOT(1,I+1))*Z(4,I)
```

```
      DOT(2,8)=(X(1,8)-X(1,9)-F1(6,8))/Z(3,8)+
     +((DOT(1,8)-DOT(1,9)+DOTB(6)/ZB(1,6))*Z(4,8))/
     +(1.0+Z(4,8)/ZB(1,6))
      DO 30 I=9,10
   30 DOT(2,I)=(X(1,I)-X(1,I+1))/Z(3,I)+(DOT(1,I)-DOT(1,I+1))*Z(4,I)
      DOT(2,11)=((X(1,11)-F1(7,11)-F1(8,11))/Z(3,11)+
     +(DOT(1,11)+DOTB(7)/ZB(1,7)+DOTB(8)/ZB(1,8))*Z(4,11))/
     +(1.0+Z(4,11)/ZB(1,7)+Z(4,11)/ZB(1,8))
      DOT(2,12)=((X(1,12)-F1(1,12)-F1(2,12))/Z(3,12)+
     +(DOT(1,12)+DOTB(1)/ZB(1,1)+DOTB(2)/ZB(1,2))*Z(4,12))/
     +(1.0+Z(4,12)/ZB(1,1)+Z(4,12)/ZB(1,2))
      DOT(2,13)=((X(1,13)-F1(4,13)-F1(5,13))/Z(3,13)+
     +(DOT(1,13)+DOTB(4)/ZB(1,4)+DOTB(5)/ZB(1,5))*Z(4,13))/
     +(1.0+Z(4,13)/ZB(1,4)+Z(4,13)/ZB(1,5))
      RETURN
      END
```

APPENDIX 2

Analysis Program Listings

ANALOGUE RECORDING ANALYSIS PROGRAM

HTDAT1


```
1 C# HTDAT1 25/07/79   DATA ACQUISITION FOR HEART MODEL. FLOW BASELINE
2 C CORRECTION & TAPE IDENTIFICATION
3       PROGRAM HTDAT1
4       COMMON INPUT(3,1000),M
5       DIMENSION FLV(150),AOP(150),AOF(150),IDENT(10)
6       DATA P/1HP/,R/1HR/,C/1HC/,Y/1HY/,AN/1HN/
7       WRITE(10,10)
8    10 FORMAT(1H1,'  CHAN 1 RWAVE MARKER, CHAN 2 ARTERIAL PRESS,
9      +'CHAN 3 FLOW')
10      WRITE(1,70)
11   70 FORMAT('INPUT AOP,AOF DELAYS IN MS')
12      READ(1,*)D2,D3
13      M=1000.0-D2
14   90 WRITE(1,30)
15   30 FORMAT(' AOP CAL IN MMHG, AOF CAL IN L/MIN')
16      READ(1,*)CAL2,CAL3
17      CAL1=100
18      CAL3=CAL3*1000.0/60.0
19      RCAL=4000
20      RZERO=0
21      CALL CALN(2,ACAL,AZERO)
22      CALL CALN(3,FCAL,FZERO)
23      WRITE(1,40)
24   40 FORMAT(7X,'RWCAL RWZERO',7X,'APCAL APZERO',7X,'AFCAL AFZERO')
25      WRITE(1,110)RCAL,RZERO,ACAL,AZERO,FCAL,FZERO
26   110 FORMAT(3(3X,F7.1,2X,F7.1))
27   120 WRITE(1,130)
28   130 FORMAT(9H CALS OK?)
29      READ(1,140)ANS
30   140 FORMAT(A1)
31      IF(ANS.EQ.AN)GO TO 90
32      WRITE(1,50)
33    50 FORMAT(13H INPUT RECORD)
34     . READ(1,60)ANS
35    60 FORMAT(A1)
36      CALL ADC(INPUT(1,1),3000,3,3333)
37      IRZERO=RZERO
38      IAZERO=AZERO
39      IFZERO=FZERO
40      DO 20 I=1,1000
41      INPUT(1,I)=INPUT(1,I)-IRZERO
42      INPUT(2,I)=INPUT(2,I)-IAZERO
43      INPUT(3,I)=INPUT(3,I)-IFZERO
44    20 CONTINUE
45     1 I1=1
46     2 CALL CLEAR
47      CALL MAX(MAX1,I1)
48      IF(I1.EQ.M)GO TO 120
49      I1=I1+5
50      I2=I1
51      CALL MAX(MAX2,I2)
52      IF(I2.EQ.M)GO TO 120
53      I2=I2+5
54      I3=I2
55      CALL MAX(MAX3,I3)
56      IF(I3.EQ.M)GO TO 120
```

```
      CALL MIN(MIN1, I1, MAX2)
      CALL MIN(MIN2, I2, MAX3)
      II=MIN2-MIN1
      IF(II. GT. 150)GO TO 2
      TII=II
      TAS=0. 09*TII+3. 0
      NAS=TAS+0. 5
      L1=MIN1-NAS
      L2=L1+II-1
      K=0
      DO 100 N= L1, L2
      K=K+1
      N2=N+IFIX(D2/10. 0+0. 5)
      N3=N+IFIX(D3/10. 0+0. 5)
      PLV(K)=FLOAT(INPUT(1, N))*CAL1/(RCAL-RZERO)
      AOP(K)=FLOAT(INPUT(2, N2))*CAL2/(ACAL-AZERO)
  100 AOF(K)=FLOAT(INPUT(3, N3))*CAL3/(FCAL-FZERO)
      CALL PLOTT(PLV, 200. 0, II)
      CALL PLOTT(AOP, -50. 0, II)
      CALL PLOTT(AOF, -300. 0, II)
  300 WRITE(1, 400)
  400 FORMAT(24H PUNCH, CONTINUE, RERUN?)
      READ(1, 500)ANS
  500 FORMAT(A1)
      IF(ANS. EQ. C)GO TO 2
      IF(ANS. EQ. R)GO TO 120
      IF(ANS. NE. P)GO TO 300
      WRITE(1, 510)
  510 FORMAT('TYPE TAPE LABEL')
      READ(1, 520)IDENT
  520 FORMAT(10A2)
      CALL BASELN(AOF, II)
      ENDFILE 3
      WRITE(3, 550)II
      WRITE(3, 560)(PLV(N), AOP(N), AOF(N), N=1, II)
      WRITE(3, 520)IDENT
      REWIND 3
      ENDFILE 3
      GO TO 2
  550 FORMAT(I4)
  560 FORMAT(12F6. 1)
      END
C *********************************
      SUBROUTINE MAX(MAXP, K)
C *********************************
      COMMON INPUT(3, 1000), M
      K=K+1
      DO 100 N=K, M
      IF(INPUT(1, N). GT. 1800)GO TO 200
  100 CONTINUE
      K=M
      RETURN
  200 K=N
      MAXP=K
      DO 300 N=K, M
      IF(INPUT(1, N). GT. INPUT(1, MAXP))MAXP=N
```

```
      IF(INPUT(1,N).LT.1200)GO TO 400
  300 CONTINUE
      K=M
      RETURN
  400 K=N
      RETURN
      END
C ************************************
      SUBROUTINE MIN(MINP,K1,K2)
C ************************************
      COMMON INPUT(3,1000),M
      H1=0.0
      DO 100 N=K1,K2
      H=FLOAT(INPUT(1,K1)-INPUT(1,N))+FLOAT(INPUT(1,K2)
     1  -INPUT(1,K1))*FLOAT(N-K1)/FLOAT(K2-K1)
      IF(H.LT.H1) GO TO 100
      H1=H
      MINP=N
  100 CONTINUE
      RETURN
      END
C ************************************
      SUBROUTINE CALN(N,CAL,ZERO)
C ************************************
      DIMENSION IZ(3,50),IC(3,50)
      WRITE(1,10)N
   10 FORMAT(20H INPUT ZERO ON CHAN ,I1)
      READ(1,20)ANS
   20 FORMAT(A1)
      CALL ADC(IZ(1,1),150,3,3000)
      WRITE(1,30)N
   30 FORMAT('INPUT CALIBRATION ON CHANNEL',I1)
      READ(1,20)ANS
      CALL ADC(IC(1,1),150,3,3000)
      ZERO=0
      DO 50 I=1,50
   50 ZERO=ZERO+FLOAT(IZ(N,I))
      ZERO=ZERO/50.0
      CAL=0
      DO 70 I=1,50
   70 CAL=CAL+FLOAT(IC(N,I))
      CAL=CAL/50.0
      RETURN
      END
C ************************************
      SUBROUTINE PLOTT(Y,YO,II)
C ************************************
      DIMENSION Y(150)
      INTEGER X,YA
      YA=Y(1)+YO
      IF(YO.EQ.-300.0)YA=Y(1)/5.0+YO
      CALL POS(-196,YA,0)
      DO 100 N=2,II
      X=4*N-200
      YA=Y(N)+YO
      IF(YO.EQ.-300.0)YA=Y(N)/5.0+YO
```

```
169    100 CALL VECT (X,YA,0)
170        RETURN
171        END
172  C *********************************
173        SUBROUTINE BASELN(Y,X)
174  C *********************************
175        DIMENSION Y(150)
176        INTEGER X
177        RX=X
178        SUMY=0.0
179        SUMXY=0.0
180        DO 4 J=1,2
181        DO 4 K=1,3
182        N=K+(J-1)*(X-3)
183        SUMY=SUMY+Y(N)
184      4 SUMXY=SUMXY+Y(N)*FLOAT(N)
185        SUMX=3.0*RX+3.0
186        SXY=SUMXY-SUMX*SUMY/6.0
187        SXX=1.5*RX*RX-9.0*RX+17.5
188        A=SXY/SXX
189        B=(SUMY-A*SUMX)/6.0
190        DO 5 N=1,X
191      5 Y(N)=Y(N)-A*FLOAT(N)-B
192        RETURN
193        END
```

DIGITAL RECORDING ANALYSIS PROGRAMS

AOIMP & AOIMP1


```
 1 C# AOIMP  30/01/79F  OFFLINE CATHLAB M-TAPE TO FLOW PRESS STARTUP
 2       PROGRAM AOIMP
 3       INTEGER D, TAPE, LABEL(3), DATA(3000), THEAD(360), IFLAG(4)
 4       COMMON TAPE(10), D(4), P(10), CRIT, AOF(150), AOFMDL(150), FAPMDL(150)
 5      +, II
 6      +, PRESS(512), FLOW(512)
 7       EQUIVALENCE (P(1), IFLAG(1)), (NOCATH, IFLAG(1)), (NOFILE, IFLAG(4))
 8      +, (THEAD(1), FAPMDL(1))
 9 C ***************
10 C     START
11 C ***************
12       P(10)=0.0
13       NOCATH=0
14       CALL CHAIN(6HAOIMP1)
15       END
```

```
1 C# AOIMP1 25/07/79E  OFFLINE CATHLAB M-TAPE TO FLOW PRESS ANALYSIS/ PRB
 2       PROGRAM AOIMP1
 3       INTEGER D, TAPE, DATA(3000), THEAD(360), IFLAG(4), NSAM(40), ANS, C, PN
 4       COMMON TAPE(10), D(4), P(10), CRIT, AOF(150), AOPMDL(150), FAPMDL(150)
 5      +, LREC
 6      +, PRESS(512), FLOW(512)
 7       EQUIVALENCE (P(1), IFLAG(1)), (NOCATH, IFLAG(1)), (NOFILE, IFLAG(4))
 8      +, (THEAD(1), FAPMDL(1)), (P(4), AOC), (P(5), IDLY)
 9       DATA NO/1HN/, C/1HC/, PN/1HP/
10 C ***************
11 C      START
12 C ***************
13  1020 WRITE(10, 1000)
14  1000 FORMAT('1', 20X, 'CATHLAB MAGTAPE DATA')
15       IF(NOCATH. NE. 0)GOTO 4
16       CALL MGTAPE(DATA, 0, 7, IFLAG(2))
17       IF(IFLAG(2). NE. -1)GOTO 5000
18       CALL MGTAPE(DATA, 27, 0, IFLAG(2))
19       IF(IFLAG(2). NE. -1)GOTO 5000
20       WRITE(1, 1030)(DATA(N), N=1, 14)
21  1030 FORMAT(//'TAPE ', 14A2)
22 C ***********************************************
23 C      FIND TAPE HEADER FOR CATHETER NUMBER
24 C ***********************************************
25     1 WRITE(1, 2)
26     2 FORMAT(//'INPUT CATHETER NUMBER IN TAPE SEQUENCE'
27      +' OR 0 TO REWIND TAPE')
28       READ(1, *)NOCATH
29       IF(NOCATH. EQ. 0)GOTO 1020
30     3 CALL GETHED(THEAD, IFLAG(2))
31       IF(IFLAG(2). NE. -1)GOTO 5000
32       IF(THEAD(1). NE. NOCATH)GOTO 3
33       NOFILE=-2
34       WRITE(1, 1040)
35  1040 FORMAT(//'INPUT FLOW TIME DELAY IN MS')
36       READ(1, *)DLY
37       IDLY=(DLY/10. 0+0. 5)
38       IDLY=IDLY*3
39       WRITE(1, 600)
40   600 FORMAT('INPUT AORTIC CROSSECTION IN SQ.  CM')
41       READ(1, *)AOC
42       AOC=AOC*100. 0
43     4 WRITE(1, 5)THEAD(1), (THEAD(I), I=21, 38)
44     5 FORMAT(/2X, 'CATH NO. ', I3, 2X, 18A2)
45 C ***********************************************
46 C      TAPE HEADER READ, NOW READ OFF FILES
47 C ***********************************************
48    10 WRITE(1, 20)
49    20 FORMAT(//'INPUT FILE NO.  IN SEQUENCE OR 0 FOR NEW CATHETER')
50       READ(1, *)N
51       IF(N. EQ. 0)GOTO 1
52       IF(N. LE. NOFILE)GOTO 10
53       NS=NOFILE+4
54       NOFILE=N
55       DO 60 NREC=NS, 45
56       N=121+(NREC-1)*4
```

```
      LENGTH=THEAD(N+1)
      IF(LENGTH.GT.3000)LENGTH=3000
      CALL MGTAPE(DATA,LENGTH,0,IFLAG(2))
      IF(IFLAG(2).NE.-1)GOTO 5000
      IF(NREC NE.NOFILE+3)GOTO 60
      IF(DATA(2).EQ.NOFILE)GOTO 500
      IFLAG(2)=40
      GOTO 5000
   60 CONTINUE
C ************************
C     UNSCRAMBLE DATA
C ************************
  500 IF(DATA(14).EQ.3)GOTO 540
      WRITE(1,50)
   50 FORMAT('###### NOT A PRESSURE/FLOW RECORDING ######')
      GOTO 5505
  540 DO 510 N=122,700,3
      IF(DATA(N+1).LT.-10000.OR.DATA(N+2).LT.-10000)GOTO 550
  510 CONTINUE
  520 WRITE(1,530)
  530 FORMAT('###### R-WAVE MARKER ERROR ######')
      GOTO 5505
  550 N1=N+3
      NSAM(1)=1
      NS=1
      NB=1
      DO 570 N=N1,2880,3
      IF(DATA(N+1).LT.-10000.OR.DATA(N+2).LT.-10000)GOTO 560
      NF=N+IDLY
      FLOW(NS)=DATA(NF)
      PRESS(NS)=(DATA(N+1)+DATA(N+2))/2
      NS=NS+1
      IF(NS.GT.512)GOTO 590
      GOTO 570
C END OF BEAT
  560 NB=NB+1
      IF(NB.GT.40)GOTO 520
      NSAM(NB)=NS
  570 CONTINUE
  590 NBEATS=NB-1
      NSAMS=NSAM(NB)-1
      WRITE(1,580)NBEATS
  580 FORMAT(5X,I2,' BEATS RECORDED')
C ************************
C     CALIBRATE
C ************************
      DO 640 NB=1,NBEATS
      NS=NSAM(NB)
      NSS=NSAM(NB+1)-NSAM(NB)
  640 CALL BASELN(FLOW(NS),NSS)
  610 DATA(9)=FLOAT(DATA(9))*FLOAT(DATA(66))/AOC
  620 CALP=FLOAT(DATA(6))/FLOAT(DATA(8))
      ZERP=DATA(10)
      CALF=30.0*1000.0/(60.0*FLOAT(DATA(9)))
      DO 630 NS=1,NSAMS
      FLOW(NS)=FLOW(NS)*CALF
```

```
113         PRESS(NS)=(PRESS(NS)-ZERP)*CALP
114    630 CONTINUE
115  C ************************
116  C       PUNCH TAPE
117  C ************************
118         WRITE(1,700)
119    700 FORMAT('PUNCH PAPER TAPE ?')
120         READ(1,5510)ANS
121         IF(ANS.EQ.NO)GOTO 800
122    710 DO 720 NB=1,NBEATS
123         NS=NSAM(NB)
124         NF=NSAM(NB+1)-1
125         NSS=NF-NS+1
126         IF(NSS.GT.150)GOTO 720
127  C CHECK RECORD OK
128    730 CALL INITCT
129         CALL POS(350,300,0)
130         WRITE(7,780)NB
131    780 FORMAT(I3)
132         CALL POS(-300,-300,0)
133         CALL VECT(300,-300,0)
134         CALL POS(-300,-300,0)
135         CALL VECT(-300,300,0)
136         CALL PLOTT(PRESS(NS),200.0,NSS)
137         CALL PLOTT(FLOW(NS),500.0,NSS)
138    731 WRITE(1,732)
139    732 FORMAT('PUNCH, CONTINUE, NEW FILE ?')
140         READ(1,5510)ANS
141         IF(ANS.EQ.C)GO TO 720
142         IF(ANS.EQ.NO)GO TO 800
143         IF(ANS.NE.PN)GO TO 731
144         WRITE(1,740)
145    740 FORMAT('TYPE TAPE NUMBER')
146         READ(1,750)(TAPE(N),N=1,2)
147    750 FORMAT(7A2)
148         DO 755 N=3,7
149         ND=N+22
150    755 TAPE(N)=DATA(ND)
151         CALL LEDR
152         WRITE(3,760)NSS
153         WRITE(3,770)(FLOW(N),PRESS(N),FLOW(N),N=NS,NF)
154         WRITE(3,750)(TAPE(N),N=1,7)
155         CALL LEDR
156    720 CONTINUE
157    760 FORMAT(I4)
158    770 FORMAT(12F6.1)
159  C ***********************
160  C       IMPEDANCE
161  C ***********************
162    800 WRITE(1,810)
163    810 FORMAT('IMPEDANCE PLOT ?')
164         READ(1,5510)ANS
165         IF(ANS.EQ.NO)GOTO 1020
166  C STORE AVERAGED BEAT IN AOF, AOPMDL
167         LREC=148
168         DO 900 N=1,150
```

```
      AOF(N)=0.0
  900 AOPMDL(N)=0.0
      DO 910 NB=1,NBEATS
      NSS=NSAM(NB+1)-NSAM(NB)
      IF(LREC.GT.NSS)LREC=NSS
      N=NSAM(NB)
      DO 910 NS=1,LREC
      AOF(NS)=AOF(NS)+FLOW(N)
      AOPMDL(NS)=AOPMDL(NS)+PRESS(N)
  910 N=N+1
      DO 920 NS=1,LREC
      AOF(NS)=AOF(NS)/FLOAT(NBEATS)
  920 AOPMDL(NS)=AOPMDL(NS)/FLOAT(NBEATS)
      DO 930 N=1,2
      NN=LREC+N
      AOF(NN)=AOF(N)
  930 AOPMDL(NN)=AOPMDL(N)
C TAILOR DATA
      CALL BASELN(PRESS,NSAMS)
      NZERO=NSAMS+1
      IF(NZERO.GT.512)GOTO 815
      DO 816 N=NZERO,512
      PRESS(N)=0.0
  816 FLOW(N)=0.0
C STORE IDENTIFICATION
  815 DO 820 N=1,4
  820 D(N)=DATA(N+20)
      TAPE(1)=DATA(1)
      TAPE(2)=DATA(2)
      DO 830 N=3,10
      ND=N+23
  830 TAPE(N)=DATA(ND)
      CALL CHAIN(&HHTIMPS)
C ************************
C     ERROR ROUTINE
C ************************
 5000 IF(IFLAG(2).EQ.30)GOTO 5100
      IF(IFLAG(2).EQ.40)GOTO 5200
      WRITE(1,5010)IFLAG(2)
 5010 FORMAT('###### MAGTAPE NOT FUNCTIONING, ERROR ',I1,'.######'
     +//'CHECK AND TRY AGAIN')
      GOTO 5500
C WRONG TYPE OF TAPE
 5100 WRITE(1,5110)
 5110 FORMAT('###### NOT A CATHLAB TAPE ######'
     +//'CHANGE TAPE')
      GOTO 5500
C END OF TAPE OR FILE NO. ERROR
 5200 WRITE(1,5210)
 5210 FORMAT('###### FILE NOT FOUND ######'
     +//'CHANGE TAPE IF NECESSARY')
 5500 NOCATH=0
 5505 READ(1,5510)ANS
 5510 FORMAT(A1)
      GOTO 1020
      END
```

```
C ***********************************
      SUBROUTINE PLOTT(Y,YS,NSS)
C ***********************************
      DIMENSION Y(150)
      INTEGER X,YA
      X0=-300.0
      Y0=-300.0
      YA=Y0+Y(1)/YS*600.0
      X=X0
      CALL POS(X,YA,0)
      DO 100 N=2,NSS
      X=X0+FLOAT(N)*6.0
      YA=Y0+Y(N)/YS*600.0
  100 CALL VECT(X,YA,0)
      RETURN
      END
C ********************************
      SUBROUTINE BASELN(Y,X)
C ********************************
      DIMENSION Y(512)
      INTEGER X
      RX=X
      SUMY=0.0
      SUMXY=0.0
      DO 4 J=1,2
      DO 4 K=1,3
      N=K+(J-1)*(X-3)
      SUMY=SUMY+Y(N)
    4 SUMXY=SUMXY+Y(N)*FLOAT(N)
      SUMX=3.0*RX+3.0
      SXY=SUMXY-SUMX*SUMY/6.0
      SXX=1.5*RX*RX-9.0*RX+17.5
      A=SXY/SXX
      B=(SUMY-A*SUMX)/6.0
      DO 5 N=1,X
    5 Y(N)=Y(N)-A*FLOAT(N)-B
      RETURN
      END
```

PRBS GENERATOR FROM HTNOIS


```
C ************************************
C    . PSEUDO-RANDOM-BINARY-SEQUENCE
C ************************************
      DO 310 N=1,4
  310 REG(N)=1
      I=1
C SEQUENCE 15 CLOCK PULSES LONG, 4 SAMPLES PER CLOCK PULSE
      DO 330 K=1,15
      REG(5)=0
      IF(REG(1)+REG(2).EQ.1)REG(5)=1
      DO 320 N=1,4
  320 REG(N)=REG(N+1)
      OUTPUT=FLOAT(2*REG(5)-1)
      DO 330 L=1,4
      ERROR(I)=OUTPUT
      I=I+1
  330 CONTINUE
```

APPENDIX 3

List of main programs and routines used

Name	Description	Originator *
HT03	Hyndman's digital version of Beneken's (1965) model. The control mechanisms have been removed	Hyndman (1973) Kitney (1974)
(various)	Versions of HT03, with different ventricular simulations and arterial models	PRB
HT041	Hyndman's (1973) arterial simulation with manual adjustments, completely rewritten to conform with the overlay structure of the analysis routines	PRB
HT045	As HT041 with a successive approximation adjustment algorithm	PRB
HT047	Impulse response version of HT045	
HT115	New model with successive approximation algorithm	PRB
HT116	New model with modified Rosenbrock algorithm	PRB
HT1161	New model with basic Rosenbrock algorithm	PRB
HT135	Digital version of Aaslid's (1974) model with a successive approximation algorithm	PRB

HT137	Impulse response version of HT135	PRB
HT145	Digital version of the Snyder et al. (1968) model	PRB
HT147	Impulse response version of HT145	PRB
HTDAT1	Analysis program described in appendix 2	PRB
AOIMP	Analysis program described in appendix 2	PRB
AOIMP1	Analysis program described in appendix 2	PRB
HTNOIS	Analysis program described in appendix 2	PRB
HTIMPS) HTIMP2)	Programs for the input impedance determination of models and for patient data	PRB
MGTAPE) GETHED)	Programs to acquire data from catheter laboratory digital tapes	Waldron & Stoate (1979)
AS97	FFT routine used in HTIMPS	Monro (1976)

* PRB indicates that the routine was written by P. R. BOURNE, the author of this thesis.

Aaslid, R (1974) Simulation of the individual cardiovascular system. PhD thesis, Div. Eng. Cybernetics, U. of Trondheim.

Bendat, J.S. & Piersol, AG. (1971) Random data: analysis and measurement procedures. Wiley-Interscience, New York.

Beneken, J.E.W. (1965) A mathematical approach to cardiovascular function. PhD thesis, Institute of Med. Phys., Utrecht.

Beneken, J.E.W. & de Wit, B. (1967) A physical approach to hemodynamic aspects of the human cardiovascular system. In: Physical bases of circulatory transport: regulation and exchange. Ed. E.B. Reeve and A.C. Guyton, Saunders, USA, pp 1-45.

Beneken, J.E.W. (1972) Some computer models in cardiovascular research. In: Cardiovascular fluid dynamics. Vol. 1, Ed. D.H. Bergel, Academic Press, London, pp 173-223.

Bloomfield, D.A.(1974) Ed. Dye curves, the theory and application of indicator dilution. University Park Press.

Blick, E.F. & Stein, P.D. (1972) A review of second-order effects on Poiseuille's equation for application to blood and other viscous fluids. Med. Res. Eng. 11, 27-31.

Bourne, P.R. & Williams, B.T. (1975) A cardiac monitor combining flow and pressure measurement. Biomed.Eng. 10, 453-455.

Bourne, P.R. & Kitney, R.I. (1978) Matching techniques for clinical models of the circulation. Med. & Biol. Eng. & Comput. 16, 689-696.

Bourne, P.R. (1979) A cardiac catheterisation monitoring system with facilities for computer control. Unpublished.

Box, M.J., Davies, D. & Swann, W.H. (1969) Non linear optimisation techniques. I.C.I. Monograph No.5, Oliver & Boyd, Edinburgh.

Braunwald, E. & Swann, H.J.C. (1968) Ed. Cooperative study on cardiac catheterisation. Circulation Supp.3, 37.

Bronzite, M. (1970) Simple active filters: design procedure. Wireless World 76, 117-119.

Brooksby, I.A.B., Swanton, R.H. Jenkins, B.S. & Webb-Peploe, M.M. (1974) Long sheath technique for the introduction of a catheter tip monometer or endomyocardial bioptone into the left or right heart. Brit. Heart J. 36-

9, 908.

Brubakk, A.O. & Aaslid, R. (1978) Use of a model for simulating individual aortic dynamics in man. Med. & Biol. Eng. & Comput. 16, 231-242.

Burrus, C.S., Parks, T.W. & Watt, T.B. (1971) A digital parameter identification technique applied to biological signals. IEEE Trans. Biomed. Eng. BME-18, 35-37.

Chatterjee, K., Massie, B., Rubin, S., Gelberg, H., Brundage, B.H. & Ports, T.A. (1978) Long term outpatient vasodilator therapy of congestive heart failure. Am. J. Med. 65, 134-145.

Cohn, J.N. (1973) Blood pressure and cardiac performance. Am. J. Med. 55, 351-361.

Davidon, W.C. (1959) Variable metric method for minimisation. AEC Research and development report, ANL-5990 (Rev.).

Davies, W.D.T. (1970) System identification for self adaptive control. Wyley-Interscience.

D'Azzo, J.J. & Houpis, C.H. (1966) Feedback control system analysis and synthesis. Mc Graw Hill, N.Y.

Defares, J.G. & Van der Waal, H.J. (1969) A method for the determination of systemic arterial compliance in man. Acta Physiol. Pharmacol. Neerl. 15, 329-343.

Dennison, J.C., Christian, J.H. & Dick D.E. (1972) Cardiovascular parameter estimation. In: Biomedical sciences instrumentation. Vol. 9, Ed. G.G. Myers, Instrument Society of America, pp 89-94.

Dobrin, P.B. & Rovick, A.A. (1969) Influence of vascular smooth muscle on contractile mechanics and elasticity of arteries. Am. J. Phys. 217, 1644-1651.

Donders, J.J.H., Zuidervaart, J.C., Robijn, J.P. & Beneken, J.E.W. (1973) Estimation of heartfunction parameters by hybrid optimisation techniques. In: Identification and system parameter estimation. Vol. 1, Ed. P. Eykhoff, North Holland-American Elsevier, Procedings of the 3rd IFAC symposium, pp 221-230.

Dorn, W.S. & McCracken, D.D. (1972) Numerical methods with Fortran 4 case studies. Wiley, N.Y.

Fry, D.L. (1959) Measurement of pulsatile blood flow by the computed pressure gradient technique. IEEE Trans. Biomed. Eng. BME-6, 259-264.

Gabe, I.T. (1972) Pressure measurement in experimental physiology. In: Cardiovascular fluid dynamics, Vol. 1, Ed. D.H. Bergel, Academic Press, London, pp 11-50.

Gauer, O.H. & Gienapp, E. (1950) Miniature pressure recording device. Science, 112, 404-405.

Greene, D.G., Carlisle, R., Grant, C. & Bunnell, I.L. (1967) Estimation of left ventricular volume by one-plane cineangiography. Circulation, 35, 61-69.

Hamming, R.W. (1973) Numerical methods for scientists and engineers. Mc Graw Hill, N.Y.

Hyndman, B.W. (1973) An example of digital computer simulation: investigation of the human cardiovascular system. In: Computer techniques in biomedicine and medicine. Ed. E. Haga, Auerbach, USA.

Kitney, R.I. (1974) Listing of the Beneken-Hyndman model computer program in Fortran. Private communication.

Kuo, B.C. (1967) Automatic control systems. Prentice Hall, USA.

Laxminarayan, S., Sipkema, P. & Westerhof, N. (1978) Characterization of the arterial system in the time domain. IEEE Trans. Biomed. Eng. BME-25, 177-184.

Lynn, P.A. (1973) An introduction to the analysis and processing of signals. Macmillan, UK.

Marquardt, D.W. (1963) An algorithm for least squares estimation of non linear parameters. J. Soc. Indust. Appl. Math. 11, 431-441.

Mason, D.T., Spann, J.F., Zelis, R. & Amsterdam, E.A. (1970) Alterations of hemodynamics and myocardial mechanics in patients with conjestive heart failure. Prog. Cardiovascular Dis. 12, 507-557.

Mason, D.T. (1978) Symposium perspective: vasodilator and inotropic therapy of heart failure. Am. J. Med. 65, 101-105.

McDonald, D.A. (1974) Blood flow in arteries. Arnold, London.

Millar, H.D. & Baker, L.E. (1973) A stable ultraminiature catheter-tip transducer. Med. & Biol. Eng. 11, 86-89.

Mills, C.J. (1966) A catheter tip electromagnetic velocity probe. Phys. Med. Biol. 11, 323-324.

Mills, C.J. (1972) Measurement of pulsatile flow and flow velocity. In: Cardiovascular fluid dynamics. Vol. 1, Ed. D.H. Bergel, Academic Press, London, pp 51-90.

Milnor, W.R. (1975) Arterial impedance as ventricular afterload. Circulation Res. 36, 565-570

Monro, D.M. (1976) Algorithm AS97, real discrete fast Fourier transform. App. Stat. 25, 166-172.

Nichols, W.W., Conti, C.R., Walker, W.E. & Milnor, W.R. (1977) Input impedance of the systemic circulation in man. Circulation Res. 40, 451-458.

Noble, M.I.M. (1979) Left ventricular load, arterial impedance and their interrelationship. Cardiovascular Res. 13, 183-198.

Noordergraaf, A. (1956) Physical basis of balistocardiography. PhD thesis, U. of Utrecht.

Noton, M. (1972) Computer algorithms for model fitting. In: I. Chem. E. symposium series no.35. Instn. Chem. Engrs., London, pp 37-42.

Ohley, W., Birtwell, W.C., Braun, L., Bicker, A. & Soroff, H.S. (1976) Computer analysis of external counterpulsation by use of a nonlinear mathematical model of the cardiovascular system. Med. Instrum. 10, 228-231.

O'Rourke, M.F. (1970) Arterial hemodynamics in hypertension. Circulation Res. Sup. 2 to 26 & 27, 123-133.

Patel, D,J., Austen, W.G. & Greenfield, J.C. (1964) Impedance of certain large blood vessels in man. Ann. N.Y. Acad. Sci. 115, 1129-1131.

Pepine, C.J., Nichols, W.W. & Conti, C.R. (1978) Aortic input impedance in heart failure. Circulation 58, 460-465.

Peterson, W.W. (1961) Error correcting codes. MIT, USA.

Powell, M.J.D. (1964) An efficient method for finding the minimum of a function of several variables without calculating derivatives. Comput. J. 7, 155-162.

Rideout, V.C. & Dick, D.E. (1967) Difference differential equations for fluid flow in distensible tubes. IEEE Trans. Biomed. Eng. BME-14, 171-177.

Rosenbrock, H.H. (1960) An automatic method for finding the greatest or least value of a function. Comput. J. 3, 175-184.

Rosko, J.S. (1972) Digital simulation of physical systems. Addison-Wesley.

Rothe, C.F. (1966) Cardiodynamics. In: Physiology. Ed. E.E. Selkurt, Little, Brown, USA, pp 316-319.

Rothe, C.F. & Nash, F.D. (1968) Renal arterial compliance and conductance measurement using online self adaptive analog computation of model parameters. Med. & Biol. Eng. 6, 53-69.

Shultz, D.L. (1972) Pressure and flow in large arteries. In: Cardiovascular fluid dynamics. Vol. 1, Ed. D.H. Bergel, Academic Press, London, pp 287-314.

Sims, J.B. (1972) Estimation of arterial system parameters from dynamic records. Comput. Biomed. Res. 5, 131-147.

Snyder, M.F., Rideout, V.C. & Hillestad, R.J. (1968) Computer modelling of the human systemic arterial tree. J. Biomech. 1, 341-353.

Spencer, M.P. & Barefoot, C.A. (1968) Sensor design for electromagnetic blood flowmeters. In: New findings in blood flowmetry. Ed. C. Cappelen, Universitetsforlaget, Oslo.

Tewari, K.P. & Sundaram, K. (1971) Digital computer simulation of pulse wave transmission in arteries. Med. & Biol. Eng. 9, 297-304.

Thompson, W.E. (1952) Networks with maximally flat delay. Wireless Engr. 29, 256-263.

Verel, D. & Grainger, R.G. (1973) Cardiac catheterisation and angiocardiography, an introductory manual. Churchill-Livingstone, Edingburgh.

Watt, T.B. & Burrus, C.S. (1976) Arterial pressure contour analysis for estimating human vascular properties. J. Appl. Physiol. 40, 171-176.

Waldron, C.B. (1974) Interactive computer analysis of cardiac cine angiogram film. Private communication.

Waldron, C.B. & Stoate, M. (1979) A system for recording and analysing routine cardiac catheterisation measurements. Private communication.

Webb-Peploe, M.M. (1979) New approaches to the treatment of heart failure. In: Topics in therapeutics. Vol. 5, Ed. D.M. Davies & M.D. Rawlins, Pitman, London, pp 137-161.

Wemple, R.R. (1972) Origin of the dicrotic notch and wave. In: Biomedical sciences instrumentation. Vol. 9, Ed. G.G. Myers, Instrument society of America, pp 45-48.

Wesseling, K.H., Purschke, R., Smith, N.T., Wust, H.J., de Wit, B. & Weber, H.A.P. (1976) A computer module for the continuous monitoring of cardiac output in the operating theatre and the ICU. Acta. Anaesthesioligica Belgica, 27, 327-341.

Westerhof, N., Bosman, F., de Vries, C.J. & Noordergraaf, A. (1969) Analog studies of the human systemic arterial tree. J. Biomech. 2, 121-143.

Westerhof, N. & Noordergraaf, A. (1970) Arterial viscoelasticity: a generalised model. J. Biomech. 3, 357-379

Westerhof, N., Elzinga, G. & Van den Bos, G.C. (1973) Influence of central and peripheral changes on the hydraulic input impedance of the systemic arterial tree. Med. & Biol. Eng. 11, 710-723.

Williams, B.T., Barefoot, C.A. & Schenk, W. (1969) A removeable electromagnetic flow probe: preliminary report. Rev. Surg. 26, 227-228

Williams, B.T., Sancho-Fornos, S., Clarke, D.B., Abrams, L.D. & Schenk, W.G. (1971) Continuous, long term measurement of cardiac output after open heart surgery. Ann. Surg. 174, 357-363.

Womersley, J.R. (1957) An elastic tube theory of pulse transmission and oscillatory flow in mammalian arteries. WADC Technical Report TR 56-614.

Zelis, R., Delea, C.S., Coleman, H.N. & Mason, D.T. (1970) Arterial sodium content in experimental congestive heart failure. Circulation, 41, 213-216.